A UNITED STATES DEPARTMENT OF COMMERCE PUBLICATION

EASTROPAC ATLAS

U.S. DEPARTMENT OF COMMERCE
National Oceanic and Atmospheric Administration
National Marine Fisheries Service

CIRCULAR
330
VOLUME 7
JULY 1973

EASTROPAC *Atlas*

Volume 1	Physical oceanographic and meteorological data from principal participating ships, first survey cruise, February-March 1967.	Published June 1972
Volume 2	Biological and nutrient chemistry data from principal participating ships, first survey cruise, February-March 1967.	Published April 1971
Volume 3	Physical oceanographic and meteorological data from principal participating ships, first and second monitor cruises, April-July 1967.	Published September 1971
Volume 4	Biological and nutrient chemistry data from principal participating ships, first and second monitor cruises, April-July 1967.	Published November 1970
Volume 5	Physical oceanographic and meteorological data from principal participating ships, second survey cruise, August-September 1967.	Published September 1972
Volume 6	Biological and nutrient chemistry data from principal participating ships, second survey cruise, August-September 1967.	Published December 1972
Volume 7	Physical oceanographic and meteorological data from principal participating ships and *Oceanographer*, third and fourth monitor cruises, October 1967-January 1968.	Published July 1973
Volume 8	Biological and nutrient chemistry data from principal participating ships and *Oceanographer*, third and fourth monitor cruises, October 1967-January 1968.	In preparation
Volume 9	Physical oceanographic and meteorological data from principal participating ships, third survey cruise, February-March 1968.	In preparation
Volume 10	Biological and nutrient chemistry data from principal participating ships, third survey cruise, February-March 1968.	In preparation
Volume 11	Data from Latin American cooperating ships and ships of opportunity, all cruises, February 1967-March 1968.	In preparation

Cover. Immature magnificent frigatebirds near Cocos Island.
Photo by John H. Taylor, Scripps Institution of Oceanography.

ABSTRACT

This atlas contains charts depicting the distribution of physical, chemical, and biological oceanographic properties and associated meteorological properties observed during EASTROPAC. EASTROPAC was an international cooperative investigation of the eastern tropical Pacific Ocean (20° N. to 20° S., and from the west coasts of the American continents to 119° W.) which was intended to provide data necessary for a more effective use of the marine resources of the area, especially tropical tunas, and also to increase knowledge of the ocean circulation, air-sea interaction, and ecology. The Bureau of Commercial Fisheries (now National Marine Fisheries Service) was the coordinating agency. The field work, from February 1967 through March 1968, was divided into seven 2-month cruise periods. During each cruise period one or more ships were operating in the study area.

On completion of the field work the data seemed too numerous for a classical data report. Instead, it was decided to produce an 11-volume atlas of the results, with 5 volumes containing physical oceanographic and meteorological data from the principal participating ships, 5 volumes containing biological and nutrient chemistry data from the same ships, and 1 volume containing all data from Latin American cooperating ships and ships of opportunity. Extensive use was made of a computer and automatic plotter in preparation of the atlas charts. Methods used to collect and process the data upon which the atlas is based are described in detail by the contributors of the following categories of charts: temperature, salinity, and derived quantities; thickness of the upper mixed layer; dissolved oxygen; meteorology; nutrient chemistry; phytoplankton standing stocks and production; zooplankton and fish larvae; micronekton; birds, fish schools, and marine mammals.

EASTROPAC Atlas

VOLUME 6

ERRATA Number 1

April 1973

FIGURE 40-FLN.
FIGURE 40-FLD.
FIGURE 40-FE.
FIGURE 40-FS.
FIGURE 40-FA.
FIGURE 40-FC.
FIGURE 40-FMN.
FIGURE 40-FMD.
FIGURE 40-FGN.
FIGURE 40-FGD.

The shading scales were omitted from these fish larvae and fish eggs charts. The shading scheme used is the same as was used on the 10-series fish larvae charts in Volume 2 and the 20- and 30-series charts in Volume 4, and is shown below:

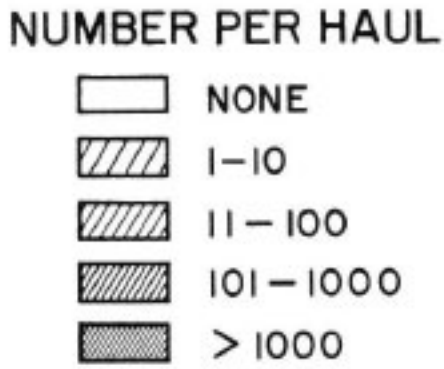

FIGURE 45-Si-v1. The small closed contour at a depth of 210 m. at station 127 should be labeled 28.

FIGURE 46-Si-v3. The small closed contour at a depth of 160 m. at station 82 should be labeled 18.

FIGURE 46-P-v4. The closed contour at a depth of 210 m. at station 183 should be labeled 2.6. The small closed contour at 210 m. at station 153 should be labeled 2.2.

EASTROPAC Atlas

VOLUME 7

ERRATA Number 1

July 1973

FIGURE 50-δ300-z. There should be a 25 m contour in the vicinity of 8°S., 85°W. The chartlet below shows its location:

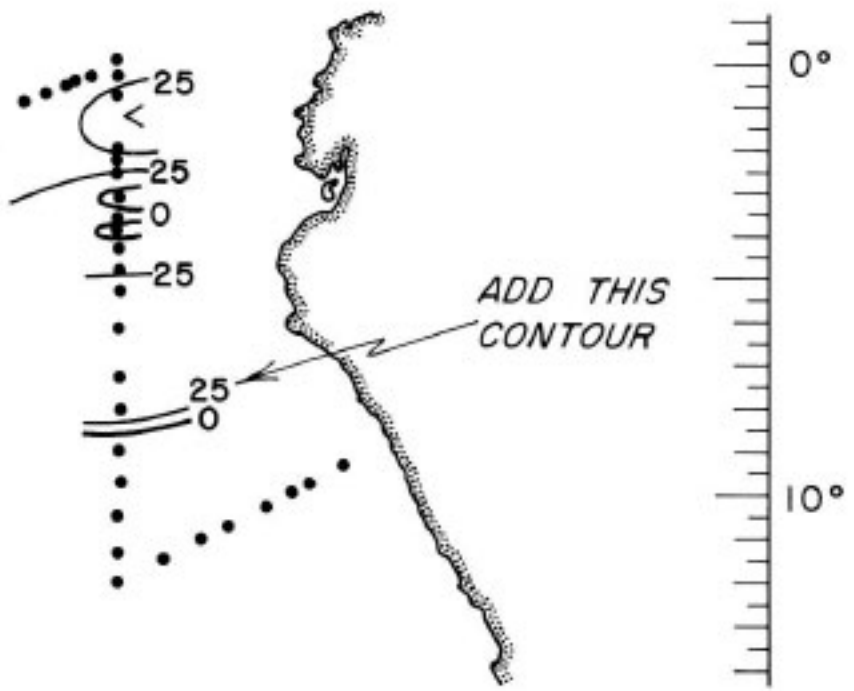

FIGURE 60-S-v5. The short unlabeled line at a depth of 170 m between stations 207 and 213 is extraneous and should be disregarded.

The heavy contour which intersects the sea surface at 8.1°N and 9.7°N should be labeled 33.5.

EASTROPAC *Atlas*

VOLUME 7

ERRATA Number 2

December 1973

FIGURE 50-S-v5. The closed heavy contour at a depth of 50-100m in the vicinity of 1°-2°S should be labeled 35.0. The heavy contour which intersects the sea surface at 2.2°N and 4.3°N should be labeled 34.0.

FIGURE 50-S-v6. The heavy contour which intersects the sea surface at 6.8°N and 7.7°N should be labeled 33.0.

FIGURE OP-S-v4. The dot at the sea surface near 10° N is not a contour and should be disregarded.

FIGURE OP-O_2-v1.
FIGURE OP-O_2-v3.
FIGURE OP-O_2-v4. The whole numbered contours (1.00, 2.00, etc.) on these charts have not been accented with heavier lines as is the case with other oxygen sections in this and other volumes.

FIGURE OP-O_2-v1. The contour at the top center of the chart should be labeled 5.50 instead of 55.0.

FIGURE OP-O_2-v3. Some of the contours near the surface are incorrectly labeled. The short contour at the very top, in the vicinity of 2°S should be labeled 5.25. The contour immediately below it should be labeled 5.00. The next contour down (the first one to extend across the whole section) should be labeled 4.75 instead of 4.50.

FIGURE 60-S-v3. The small heavy contour which intersects the sea surface twice in the vicinity of 15.6°N should be labeled 33.5.

VOLUME 1

INTRODUCTION ---- Page 9, Paragraph 2, Line 1 now reads ". . . 20 cm diameter Secchi disc.", this should read ". . . 30 cm diameter Secchi disc."

UNITED STATES DEPARTMENT OF COMMERCE
Frederick B. Dent, Secretary

NATIONAL OCEANIC AND ATMOSPHERIC ADMINISTRATION
Robert M. White, *Administrator*

NATIONAL MARINE FISHERIES SERVICE
Robert W. Schoning, *Acting Director*

EASTROPAC ATLAS

VOLUME 7

PHYSICAL OCEANOGRAPHIC AND METEOROLOGICAL DATA FROM
PRINCIPAL PARTICIPATING SHIPS AND *OCEANOGRAPHER*
THIRD AND FOURTH MONITOR CRUISES, OCTOBER 1967-JANUARY 1968

CUTHBERT M. LOVE, *Editor*

CIRCULAR 330
WASHINGTON, D.C.
JULY 1973

For sale by the Superintendent of Documents, U.S. Government Printing Office, Washington, D.C. 20402—Price $4.75 per volume

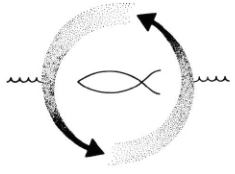

COORDINATOR, EASTROPAC PROJECT

WARREN S. WOOSTER, Scripps Institution of Oceanography, June 27, 1966-May 15, 1967
ALAN R. LONGHURST, National Marine Fisheries Service, May 15, 1967-June 30, 1970

ATLAS CONTRIBUTORS

ELBERT H. AHLSTROM—National Marine Fisheries Service, Fish Larvae
MAURICE BLACKBURN—Scripps Institution of Oceanography, Micronekton
WITOLD L. KLAWE—Inter-American Tropical Tuna Commission, Scombroid Larvae
R. MICHAEL LAURS—National Marine Fisheries Service, Zooplankton, Micronekton, Bird and Mammal Observations
FORREST R. MILLER—Inter-American Tropical Tuna Commission, Meteorology
ROBERT W. OWEN, Jr.—National Marine Fisheries Service, Phytoplankton, Oxygen, Mixed Layer Depth
BRUCE A. TAFT—Scripps Institution of Oceanography, Physical Oceanography
WILLIAM H. THOMAS—Scripps Institution of Oceanography, Nutrient Chemistry
MIZUKI TSUCHIYA—Scripps Institution of Oceanography, Physical Oceanography
BERNT ZEITZSCHEL—Scripps Institution of Oceanography, Phytoplankton

EDITORIAL COMMITTEE

CUTHBERT M. LOVE, National Marine Fisheries Service
BRUCE A. TAFT, Scripps Institution of Oceanography
R. MICHAEL LAURS, National Marine Fisheries Service

National Marine Fisheries Service
Southwest Fisheries Center
La Jolla, California 92037

Scripps Institution of Oceanography
University of California, San Diego
La Jolla, California 92037

Inter-American Tropical Tuna Commission
% Scripps Institution of Oceanography
La Jolla, California 92037

INTRODUCTION

EASTROPAC was an international cooperative investigation of the eastern tropical Pacific Ocean which was intended to provide data necessary for a more effective use of the marine resources of the area, especially tropical tunas, and also to increase knowledge of the ocean circulation, air-sea interaction, and ecology. The National Marine Fisheries Service (NMFS)—the Bureau of Commercial Fisheries (BCF) at the time of the investigations—was the coordinating agency. The field work, from February 1967 through March 1968, was divided into seven 2-month cruise periods.

At a meeting of the EASTROPAC Coordinating Committee held at La Jolla in April 1968, it was decided that the data derived from the cruises were so numerous as to render classical data reports impractical and that a comprehensive atlas of the physical and biological results of the project should be produced instead. The atlas has been divided into 11 volumes, with five volumes containing physical oceanographic and meteorological data from the principal participating ships, five volumes containing biological and nutrient chemistry data from the same ships, and one volume containing all data from Latin-American cooperating ships and ships of opportunity.

Volume 7 contains physical oceanographic and meteorological data collected mainly by the principal participating ships and *Oceanographer* during the third and fourth monitor cruise periods: cruise 50, October-November 1967, and cruise 60, December 1967-January 1968. The companion volume presenting the corresponding biological and nutrient chemistry data is volume 8. The locations of stations occupied by participating ships are shown in figure 50-TC and figure 60-TC.

Information concerning the history and organization of the EASTROPAC Project, a description of the cruises undertaken, the program of observations, the methods used for preparation of the charts, and remarks on the organization of the atlas are contained in volumes 1 and 4 with descriptions by the contributing scientists of the methods used to collect and process the data upon which the atlas charts are based.

CUTHBERT M. LOVE
Editor

Abbreviations used in figure designation system

Cruise or cruise period	Property represented	Mnemonic to explain choice of letters	Indicator for vertical sections or type of horizontal surface
Numbers 11, 12, 13, etc., indicate principal cruises. See figure 1.	T Temperature S Salinity δ Thermosteric anomaly (δ_T) G Geostrophic velocity O_2 Oxygen concentration O_2Sa Oxygen saturation ML Thickness of the mixed layer δ300 300 cl./t. thermosteric anomaly surface AP Acceleration Potential		v1, v2, etc., indicate vertical sections. Vertical sections are assigned consecutive numbers within each cruise which follow the chronological order in which the ship ran the sections.
Letters or letter-number combinations indicate cruises of Latin American cooperating ships or ships of opportunity, as follows:	P Phosphate-phosphorus Si Silicate-silicon NO_3 Nitrate-nitrogen NO_2 Nitrite-nitrogen NH_3 Ammonia-nitrogen		Number 10 or 100 following O_2Sa or horizontal P, Si, NO_3, NO_2, or NH_3 charts indicates distribution at that depth (m.).
MZ-4 *Yolanda*, MZ-4 MZ-5 *Yolanda*, MZ-5 MZ-6 *Yolanda*, MZ-6 MZ-7 *Defiance*, MZ-7 MZ-8 *Tuxpan*, MZ-8	Ch Chlorophyll-a Ph Phaeophytin PP Primary production EL Thickness of the euphotic layer		s Distribution at the sea surface δ300 Distribution on the surface where δ_T=300 cl./t. ei Distribution integrated over the euphotic layer 150i Distribution integrated to 150 m. depth z Depth of a surface
H1 *Huayaipe*-1 H2 *Huayaipe*-2 H3 *Huayaipe*-3	FCp Fish and cephalopod standing stock Cr Crustacean standing stock Nk Total micronekton standing stock		
U1 *Unanue* 6702 U2 *Unanue* 6708 U3 *Unanue* 6802	ZhN Zooplankton standing stock from 50-cm. net hauls, night	Zooplankton, half-meter, Night	Number 1 or 2 following SP or SW charts indicates one of two 6-month periods into which those observations were divided.
Y5 *Yelcho* MARCHILE V Y6 *Yelcho* MARCHILE VI Y7 *Yelcho* MARCHILE VII	Z1N Zooplankton standing stock from 1-m. net hauls, night	Zooplankton, 1-meter, Night	
E6 *Esmeralda* BE VI	ZhD Zooplankton standing stock from 50-cm. net hauls, day	Zooplankton, half-meter, Day	
OP *Oceanographer* CD *Charles H. Davis*	Z1D Zooplankton standing stock from 1-m. net hauls, day	Zooplankton, 1-meter, Day	Numbers 1 to 4 or 1 to 6 following MT or MW charts indicate one of the approximate 2-week periods into which those observations were divided. For all cruise periods except 40, the MT and MW charts were drawn for four 2-week periods. For the 40 cruise period these charts were drawn for six periods ranging from 12 to 16 days in length, but with several days overlap between some periods. Number 1 or 2 following MC charts indicates one of the monthly periods for which those charts were drawn.
T3 *Te Vega* 13 T4 *Te Vega* 14 T5 *Te Vega* 15 T6 *Te Vega* 16 T7 *Te Vega* 17	FLN Total fish larvae, night hauls FLD Total fish larvae, day hauls	Fish Larvae, Night Fish Larvae, Day	
Numbers 10, 20, 30, 40, 50, 60, 70, indicate 2-month cruise periods.	FE Total fish eggs FS Total skipjack tuna larvae FA Total *Auxis* larvae FC Total *Coryphaena* larvae	Fish, Skipjack Fish, *Auxis* Fish, *Coryphaena*	
	FMN Total myctophid larvae, night hauls FMD Total myctophid larvae, day hauls	Fish, Myctophid, Night Fish, Myctophid, Day	
	FGN Total gonostomatid and sternoptychid larvae, night hauls	Fish, Gonostomatid, Night	
	FGD Total gonostomatid and sternoptychid larvae, day hauls	Fish, Gonostomatid, Day	
	BP Relative abundance of plankton-feeding birds	Birds, Plankton-feeding	
	BF Relative abundance of fish and cephalopod-feeding birds	Birds, Fish-feeding	
	SP Porpoise sightings SW Whale sightings ST Tuna school sightings, all cruises	Sightings, Porpoise Sightings, Whales Sightings, Tuna	
	UA Upper atmosphere meteorology MW Surface meteorological analysis, winds and pressure	Meteorology, Winds	
	MC Surface meteorological analysis, clouds, dewpoint, temperature	Meteorology, Clouds	
	MT Surface meteorological analysis, sea temperature, sea-air temperature difference, sea temperature anomaly	Meteorology, Temperature	
	RM Reference map TC Track chart		

LIST OF FIGURES

FIGURE 50-MT-3.—Analysis of sea surface temperatures based on averages for 2-degree (latitude-longitude) squares from all available ship observations for the period November 1-14, 1967. Solid lines are sea surface isotherms (°C.); the isotherms are dashed where data are sparse. Dark hatching outlines areas with positive temperature anomalies (computed from mean sea surface temperatures averaged over 22 years) greater than 1° C.; light hatching shows areas with negative anomalies greater than 1° C. Sea surface temperature (°C. x 10) averaged for 5-degree squares is plotted above the mean position of the square; sea temperature minus air temperature difference (°C. x 10) is plotted below the symbol.

FIGURE 50-MT-4.—Analysis of sea surface temperatures based on averages for 2-degree (latitude-longitude) squares from all available ship observations for the period November 15-30, 1967. Solid lines are sea surface isotherms (°C.); the isotherms are dashed where data are sparse. Dark hatching outlines areas with positive temperature anomalies (computed from mean sea surface temperatures averaged over 22 years) greater than 1° C.; light hatching shows areas with negative anomalies greater than 1° C. Sea surface temperature (°C. x 10) averaged for 5-degree squares is plotted above the mean position of the square; sea temperature minus air temperature difference (°C. x 10) is plotted below the symbol.

FIGURE 50-MC-1.—Analyses of the surface dew-point temperature of the air and total cloud cover based on 2-degree (latitude-longitude) averages from all available ship observations for the month of October 1967. Solid lines depict the monthly mean total cloud cover in oktas; the lines are dashed where data are sparse. Dash-dot lines are isotherms of the mean monthly dew-point temperature at 2-degree (°C.) intervals. Areas where 15 percent or more of the ships reported rain of any type at or within sight of the ship are shaded. Dew-point temperature (°C. x 10) averaged for 5-degree squares is plotted above the mean position of the square, with total cloud cover (oktas) below and rainfall frequency (%) to the right of the symbol.

FIGURE 50-MC-2.—Analyses of the surface dew-point temperature of the air and total cloud cover based on 2-degree (latitude-longitude) averages from all available ship observations for the month of November 1967. Solid lines depict the monthly mean total cloud cover in oktas; the lines are dashed where data are sparse. Dash-dot lines are isotherms of the mean monthly dew-point temperature at 2-degree (°C.) intervals. Areas where 15 percent or more of the ships reported rain of any type at or within sight of the ship are shaded. Dew-point temperature (°C. x 10) averaged for 5-degree squares is plotted above the mean position of the square, with total cloud cover (oktas) below and rainfall frequency (%) to the right of the symbol.

Temperature and salinity—White pages

FIGURE 50-T-v1.—Vertical distribution of temperature (°C.) along 119°10′ W., October 20-29, 1967.

FIGURE 50-T-v2.—Vertical distribution of temperature (°C.) along 112°10′ W., October 30-November 4, 1967.

FIGURE 50-T-v3.—Vertical distribution of temperature (°C.) along a section from 12° N., 112°10′ W. to Manzanillo, November 4-7, 1967.

FIGURE 50-T-v4.—Vertical distribution of temperature (°C.) along a section from Acapulco to 12° N., 105°10′ W., November 11-13, 1967.

FIGURE 50-T-v5.—Vertical distribution of temperature (°C.) along 105°10′ W., November 13-18, 1967.

FIGURE 50-T-v6.—Vertical distribution of temperature (°C.) along 98°10′ W., November 20-26, 1967.

FIGURE 50-S-v1.—Vertical distribution of salinity (‰) along 119°10′ W., October 20-29, 1967.

FIGURE 50-S-v2.—Vertical distribution of salinity (‰) along 112°10′ W., October 30-November 4, 1967.

FIGURE 50-S-v3.—Vertical distribution of salinity (‰) along a section from 12° N., 112°10′ W. to Manzanillo, November 4-7, 1967.

FIGURE 50-S-v4.—Vertical distribution of salinity (‰) along a section from Acapulco to 12° N., 105°10′ W., November 11-13, 1967.

FIGURE 50-S-v5.—Vertical distribution of salinity (‰) along 105°10′ W., November 13-18, 1967.

FIGURE 50-S-v6.—Vertical distribution of salinity (‰) along 98°10′ W., November 20-26, 1967.

Thermosteric anomaly and geostrophic velocity—Yellow pages

FIGURE 50-δ-v1.—Vertical distribution of thermosteric anomaly, δ_T, (cl./t.) along 119°10′ W., October 20-29, 1967.

FIGURE 50-δ-v2.—Vertical distribution of thermosteric anomaly, δ_T, (cl./t.) along 112°10′ W., October 30-November 4, 1967.

FIGURE 50-δ-v3.—Vertical distribution of thermosteric anomaly, δ_T, (cl./t.) along a section from 12° N., 112°10′ W. to Manzanillo, November 4-7, 1967.

FIGURE 50-δ-v4.—Vertical distribution of thermosteric anomaly, δ_T, (cl./t.) along a section from Acapulco to 12° N., 105°10′ W., November 11-13, 1967.

FIGURE 50-δ-v5.—Vertical distribution of thermosteric anomaly, δ_T, (cl./t.) along 105°10′ W., November 13-18, 1967.

FIGURE 50-δ-v6.—Vertical distribution of thermosteric anomaly, δ_T, (cl./t.) along 98°10′ W., November 20-26, 1967.

FIGURE 50-G-v1.—Vertical distribution of the zonal component of geostrophic velocity (cm./sec.), relative to 500 db., along 119°10′ W., October 20-29, 1967. Dark shading indicates eastward flow with a velocity greater than 5 cm./sec.; light shading indicates westward flow with a velocity greater than 5 cm./sec.

FIGURE 50-G-v2.—Vertical distribution of the zonal component of geostrophic velocity (cm./sec.), relative to 500 db., along 112°10′ W., October 30-November 4, 1967. Dark shading indicates eastward flow with a velocity greater than 5 cm./sec.; light shading indicates westward flow with a velocity greater than 5 cm./sec.

FIGURE 50-G-v3.—Vertical distribution of the component of geostrophic velocity (cm./sec.), relative to 500 db., normal to a section from 12° N., 112°10′ W., to Manzanillo, November 4-7, 1967. Dark shading indicates flow toward the southeast with a velocity greater than 5 cm./sec.; light shading indicates flow toward the northwest with a velocity greater than 5 cm./sec.

FIGURE 50-G-v4.—Vertical distribution of the component of geostrophic velocity (cm./sec.), relative to 500 db., normal to a section from Acapulco to 12° N., 105°10′ W., November 11-13, 1967. Dark shading indicates flow toward the southeast with a velocity greater than 5 cm./sec.; light shading indicates flow toward the northwest with a velocity greater than 5 cm./sec.

FIGURE 50-G-v5.—Vertical distribution of the zonal component of geostrophic velocity (cm./sec.), relative to 500 db., along 105°10′ W., November 13-18, 1967. Dark shading indicates eastward flow with a velocity greater than 5 cm./sec.; light shading indicates westward flow with a velocity greater than 5 cm./sec.

FIGURE 50-G-v6.—Vertical distribution of the zonal component of geostrophic velocity (cm./sec.), relative to 500 db., along 98°10′ W., November 20-26, 1967. Dark shading indicates eastward flow with a velocity greater than 5 cm./sec.; light shading indicates westward flow with a velocity greater than 5 cm./sec.

Oxygen—Green pages

FIGURE 50-O_2-v1.—Vertical distribution of oxygen (ml./l.) along 119°10′ W., October 20-29, 1967.

FIGURE 50-O_2-v2.—Vertical distribution of oxygen (ml./l.) along 112°10′ W., October 30-November 4, 1967.

FIGURE 50-O_2-v3.—Vertical distribution of oxygen (ml./l.) along a section from 12° N., 112°10′ W. to Manzanillo, November 4-7, 1967.

FIGURE 50-O_2-v4.—Vertical distribution of oxygen (ml./l.) along a section from Acapulco to 12° N., 105°10′ W., November 11-13, 1967.

FIGURE 50-O_2-v5.—Vertical distribution of oxygen (ml./l.) along 105°10′ W., November 13-18, 1967.

FIGURE 50-O_2-v6.—Vertical distribution of oxygen (ml./l.) along 98°10′ W., November 20-27, 1967.

Temperature and salinity—White pages

FIGURE OP-T-v1.—Vertical distribution of temperature (°C.) along a northeast-southwest section from the coast of Peru to 12° S., 85° W., November 14-15, 1967.

FIGURE OP-T-v2.—Vertical distribution of temperature (°C.) along 85° W., November 15-19, 1967.

FIGURE OP-T-v3.—Vertical distribution of temperature (°C.) along a northeast-southwest section from the Equator at 85° W. to 3° S., 92° W., November 19-21, 1967.

FIGURE OP-T-v4.—Vertical distribution of temperature (°C.) along 92° W., November 21-26, 1967.

FIGURE OP-S-v1.—Vertical distribution of salinity (‰) along a northeast-southwest section from the coast of Peru to 12° S., 85° W., November 14-15, 1967.

FIGURE OP-S-v2.—Vertical distribution of salinity (‰) along 85° W., November 15-19, 1967.

FIGURE OP-S-v3.—Vertical distribution of salinity (‰) along a northeast-southwest section from the Equator at 85° W. to 3° S., 92° W., November 19-21, 1967.

FIGURE OP-S-v4.—Vertical distribution of salinity (‰) along 92° W., November 21-26, 1967.

Thermosteric anomaly and geostrophic velocity—Yellow pages

FIGURE OP-δ-v1.—Vertical distribution of thermosteric anomaly, δ_T, (cl./t.) along a northeast-southwest section from the coast of Peru to 12° S., 85° W., November 14-15, 1967.

FIGURE OP-δ-v2.—Vertical distribution of thermosteric anomaly, δ_T, (cl./t.) along 85° W., November 15-19, 1967.

FIGURE OP-δ-v3.—Vertical distribution of thermosteric anomaly, δ_T, (cl./t.) along a northeast-southwest section from the Equator at 85° W. to 3° S., 92° W., November 19-21, 1967.

FIGURE OP-δ-v4.—Vertical distribution of thermosteric anomaly, δ_T, (cl./t.) along 92° W., November 21-26, 1967.

FIGURE OP-G-v1.—Vertical distribution of the component of geostrophic velocity (cm./sec.), relative to 500 db., normal to a northeast-southwest section from the coast of Peru to 12° S., 85° W., November 14-15, 1967. Dark shading indicates flow toward the southeast with a velocity greater than 5 cm./sec.

FIGURE OP-G-v2.—Vertical distribution of the zonal component of geostrophic velocity (cm./sec.), relative to 500 db., along 85° W., November 15-18, 1967. Dark shading indicates eastward flow with a velocity greater than 5 cm./sec.

FIGURE OP-G-v4.—Vertical distribution of the zonal component of geostrophic velocity (cm./sec.), relative to 500 db., along 92° W., November 24-25, 1967. Since there were no geostrophic velocity components equal to or greater than 5 cm./sec. on this section, no contours are shown.

Oxygen—Green pages

FIGURE OP-O_2-v1.—Vertical distribution of oxygen (ml./l.) along a northeast-southwest section from the coast of Peru to 12° S., 85° W., November 14-15, 1967.

FIGURE OP-O_2-v2.—Vertical distribution of oxygen (ml./l.) along 85° W., November 15-19, 1967.

FIGURE OP-O_2-v3.—Vertical distribution of oxygen (ml./l.) along a northeast-southwest section from the Equator at 85° W. to 3° S., 92° W., November 19-21, 1967.

FIGURE OP-O_2-v4.—Vertical distribution of oxygen (ml./l.) along 92° W., November 21-26, 1967.

Meteorology—Blue pages

FIGURE OP-UA-v2.—Vertical section of the atmosphere along 85° W., November 16-21, 1967. Solid lines are isotherms of air temperature (°C.). Dashed lines are isopleths of mixing ratio of the air (g./kg.). Surface air temperature is plotted above surface mixing ratio and below a base line representing the surface pressure (mb.). The computed height (m.) of each standard pressure surface is plotted for the northernmost radiosonde station of the section. At other stations the difference of computed height minus the corresponding height at the northern station is shown at each standard level.

FIGURE OP-UA-v4.—Vertical section of the atmosphere along 92° W., November 21-28, 1967. Solid lines are isotherms of air temperature (°C.). Dashed lines are isopleths of mixing ratio of the air (g./kg.). Surface air temperature is plotted above surface mixing ratio and below a base line representing the surface pressure (mb.). The computed height (m.) of each standard pressure surface is plotted for the northernmost radiosonde station of the section. At other stations the difference of computed height minus the corresponding height at the northern station is shown at each standard level.

Surface and near-surface properties—Pages of various colors

FIGURE 60-T-s.—Temperature (°C.) at the sea surface, December 1967-January 1968. These contours are based on Nansen cast data.

FIGURE 60-ML.—Thickness of the mixed layer in meters, December 1967-January 1968. Dashed lines indicate portions of the cruise track where such data were collected.

FIGURE 60-S-s.—Salinity (‰) at the sea surface, December 1967-January 1968. These contours are based on Nansen cast data.

FIGURE 60-O_2Sa-10.—Oxygen saturation (%) at 10 meters, December 1967-January 1968. Areas with less than 100% saturation are shaded.

Properties on isanosteric surfaces—Pages of various colors

FIGURE 60-δ300-z.—Depth (m.) of the surface where $\delta_T = 300$ cl./t., December 1967-January 1968.

FIGURE 60-S-δ300.—Salinity (‰) on the surface where $\delta_T = 300$ cl./t., December 1967-January 1968. The table shows the temperature corresponding to each isohaline on the chart.

FIGURE 60-AP-δ300.—Acceleration potential (j./kg.), relative to 500 db., on the surface where $\delta_T = 300$ cl./t., December 1967-January 1968. For computing acceleration potential, thermosteric anomaly, δ_T, was used instead of specific volume anomaly, δ.

FIGURE 60-O_2-δ300.—Oxygen (ml./l.) on the surface where $\delta_T = 300$ cl./t., December 1967-January 1968.

FIGURE 60-δ250-z.—Depth (m.) of the surface where $\delta_T = 250$ cl./t., December 1967-January 1968.

FIGURE 60-S-δ250.—Salinity (‰) on the surface where $\delta_T = 250$ cl./t., December 1967-January 1968. The table shows the temperature corresponding to each isohaline on the chart.

FIGURE 60-AP-δ250.—Acceleration potential (j./kg.), relative to 500 db., on the surface where $\delta_T = 250$ cl./t., December 1967-January 1968. For computing acceleration potential, thermosteric anomaly, δ_T, was used instead of specific volume anomaly, δ.

FIGURE 60-O_2-δ250.—Oxygen (ml./l.) on the surface where $\delta_T = 250$ cl./t., December 1967-January 1968.

FIGURE 60-δ200-z.—Depth (m.) of the surface where $\delta_T = 200$ cl./t., December 1967-January 1968.

FIGURE 60-S-δ200.—Salinity (‰) on the surface where $\delta_T = 200$ cl./t., December 1967-January 1968. The table shows the temperature corresponding to each isohaline on the chart.

FIGURE 60-AP-δ200.—Acceleration potential (j./kg.), relative to 500 db., on the surface where $\delta_T = 200$ cl./t., December 1967-January 1968. For computing acceleration potential, thermosteric anomaly, δ_T, was used instead of specific volume anomaly, δ.

FIGURE 60-O_2-δ200.—Oxygen (ml./l.) on the surface where $\delta_T = 200$ cl./t., December 1967-January 1968.

FIGURE 60-δ160-z.—Depth (m.) of the surface where $\delta_T = 160$ cl./t., December 1967-January 1968.

FIGURE 60-S-δ160.—Salinity (‰) on the surface where $\delta_T = 160$ cl./t., December 1967-January 1968. The table shows the temperature corresponding to each isohaline on the chart.

FIGURE 60-AP-δ160.—Acceleration potential (j./kg.), relative to 500 db., on the surface where $\delta_T = 160$ cl./t., December 1967-January 1968. For computing acceleration potential, thermosteric anomaly, δ_T, was used instead of specific volume anomaly, δ.

FIGURE 60-O_2-δ160.—Oxygen (ml./l.) on the surface where $\delta_T = 160$ cl./t., December 1967-January 1968.

Meteorology—Blue pages

FIGURE 60-MW-1.—Analyses of the surface air pressure and surface winds from all available ship observations, averaged over 2-degree (latitude-longitude) squares for the period December 1-16, 1967. Heavy dashed lines are isobars. Solid lines are streamlines showing the mean resultant direction of wind flow. Light dash-dot lines are isotachs indicating mean resultant wind speed (kn.). Pressure (mb.) averaged for 5-degree squares is plotted above the mean position of the square, and resultant wind direction followed by speed (kn.) is plotted below. The monthly climatological position of the intertropical convergence zone is shown by a wide dashed band.

FIGURE 60-MW-2.—Analyses of the surface air pressure and surface winds from all available ship observations, averaged over 2-degree (latitude-longitude) squares for the period December 17-31, 1967. Heavy dashed lines are isobars. Solid lines are streamlines showing the mean resultant direction of wind flow. Light dash-dot lines are isotachs indicating mean resultant wind speed (kn.). Pressure (mb.) averaged for 5-degree squares is plotted above the mean position of the square, and resultant wind direction followed by speed (kn.) is plotted below. The monthly climatological position of the intertropical convergence zone is shown by a wide dashed band.

FIGURE 60-MW-3.—Analyses of the surface air pressure and surface winds from all available ship observations, averaged over 2-degree (latitude-longitude) squares for the period January 1-14, 1968. Heavy dashed lines are isobars. Solid lines are streamlines showing the mean resultant direction of wind flow. Light dash-dot lines are isotachs indicating mean resultant wind speed (kn.). Pressure (mb.) averaged for 5-degree squares is plotted above the mean position of the square, and resultant wind direction followed by speed (kn.) is plotted below. The monthly climatological position of the intertropical convergence zone is shown by a wide dashed band.

FIGURE 60-MW-4.—Analyses of the surface air pressure and surface winds from all available ship observations, averaged over 2-degree (latitude-longitude) squares for the period January 15-31, 1968. Heavy dashed lines are isobars. Solid lines are streamlines showing the mean resultant direction of wind flow. Light dash-dot lines are isotachs indicating mean resultant wind speed (kn.). Pressure (mb.) averaged for 5-degree squares is plotted above the mean position of the square, and resultant wind direction followed by speed (kn.) is plotted below. The monthly climatological position of the intertropical convergence zone is shown by a wide dashed band.

FIGURE 60-MT-1.—Analysis of sea surface temperatures based on averages for 2-degree (latitude-longitude) squares from all available ship observations for the period December 1-16, 1967. Solid lines are sea surface isotherms (°C.); the isotherms are dashed where data are sparse. Dark hatching outlines areas with positive temperature anomalies (computed from mean sea surface temperatures averaged over 22 years) greater than 1° C.; light hatching shows areas with negative anomalies greater than 1° C. Sea surface temperature (°C. x 10) averaged for 5-degree squares is plotted above the mean position of the square; sea temperature minus air temperature difference (°C. x 10) is plotted below the symbol.

FIGURE 60-MT-2.—Analysis of sea surface temperatures based on averages for 2-degree (latitude-longitude) squares from all available ship observations for the period December 17-31, 1967. Solid lines are sea surface isotherms (°C.); the isotherms are dashed where data are sparse. Dark hatching outlines areas with positive temperature anomalies (computed from mean sea surface temperatures averaged over 22 years) greater than 1° C.; light hatching shows areas with negative anomalies greater than 1° C. Sea surface temperature (°C. x 10) averaged for 5-degree squares is plotted above the mean position of the square; sea temperature minus air temperature difference (°C. x 10) is plotted below the symbol.

FIGURE 60-MT-3.—Analysis of sea surface temperatures based on averages for 2-degree (latitude-longitude) squares from all available ship observations for the period January 1-14, 1968. Solid lines are sea surface isotherms (°C.); the isotherms are dashed where data are sparse. Dark hatching outlines areas with positive temperature anomalies (computed from mean sea surface temperatures averaged over 22 years) greater than 1° C.; light hatching shows areas with negative anomalies greater than 1° C. Sea surface temperature (°C. x 10) averaged for 5-degree squares is plotted above the mean position of the square; sea temperature minus air temperature difference (°C. x 10) is plotted below the symbol.

FIGURE 60-MT-4.—Analysis of sea surface temperatures based on averages for 2-degree (latitude-longitude) squares from all available ship observations for the period January 15-31, 1968. Solid lines are sea surface isotherms (°C.); the isotherms are dashed where data are sparse. Dark hatching outlines areas with positive temperature anomalies (computed from mean sea surface temperatures averaged over 22 years) greater than 1° C.; light hatching shows areas with negative anomalies greater than 1° C. Sea surface temperature (°C. x 10) averaged for 5-degree squares is plotted above the mean position of the square; sea temperature minus air temperature difference (°C. x 10) is plotted below the symbol.

FIGURE 60-MC-1.—Analyses of the surface dew-point temperature of the air and total cloud cover based on 2-degree (latitude-longitude) averages from all available ship observations for the month of December 1967. Solid lines depict the monthly mean total cloud cover in oktas; the lines are dashed where data are sparse. Dash-dot lines are isotherms of the mean monthly dew-point temperature at 2-degree (°C.) intervals. Areas where 15 percent or more of the ships reported rain of any type at or within sight of the ship are shaded. Dew-point temperature (°C. x 10) averaged for 5-degree squares is plotted above the mean position of the square, with total cloud cover (oktas) below and rainfall frequency (%) to the right of the symbol.

FIGURE 60-MC-2.—Analyses of the surface dew-point temperature of the air and total cloud cover based on 2-degree (latitude-longitude) averages from all available ship observations for the month of January 1968. Solid lines depict the monthly mean total cloud cover in oktas; the lines are dashed where data are sparse. Dash-dot lines are isotherms of the mean monthly dew-point temperature at 2-degree (°C.) intervals. Areas where 15 percent or more of the ships reported rain of any type at or within sight of the ship are shaded. Dew-point temperature (°C. x 10) averaged for 5-degree squares is plotted above the mean position of the square, with total cloud cover (oktas) below and rainfall frequency (%) to the right of the symbol.

Temperature and salinity—White pages

FIGURE 60-T-v1.—Vertical distribution of temperature (°C.) along 118°45′ W., December 21-31, 1967.

FIGURE 60-T-v2.—Vertical distribution of temperature (°C.) along 111°45′ W., January 2-6, 1968.

FIGURE 60-T-v3.—Vertical distribution of temperature (°C.) along a section from 12° N., 111°45′ W. to Manzanillo, January 6-9, 1968.

FIGURE 60-T-v4.—Vertical distribution of temperature (°C.) along a section from Acapulco to 12° N., 104°45′ W., January 13-15, 1968.

FIGURE 60-T-v5.—Vertical distribution of temperature (°C.) along 104°45′ W., January 15-21, 1968.

FIGURE 60-T-v6.—Vertical distribution of temperature (°C.) along 97°45′ W., January 22-28, 1968.

FIGURE 60-S-v1.—Vertical distribution of salinity (‰) along 118°45′ W., December 21-31, 1967.

FIGURE 60-S-v2.—Vertical distribution of salinity (‰) along 111°45′ W., January 2-6, 1968.

FIGURE 60-S-v3.—Vertical distribution of salinity (‰) along a section from 12° N., 111°45′ W. to Manzanillo, January 6-9, 1968.

FIGURE 60-S-v4.—Vertical distribution of salinity (‰) along a section from Acapulco to 12° N., 105°45′ W., January 13-15, 1968.

FIGURE 60-S-v5.—Vertical distribution of salinity (‰) along 104°45′ W., January 15-21, 1968.

FIGURE 60-S-v6.—Vertical distribution of salinity (‰) along 97°45′ W., January 22-28, 1968.

Thermosteric anomaly and geostrophic velocity—Yellow pages

FIGURE 60-δ_T-v1.—Vertical distribution of thermosteric anomaly, δ_T, (cl./t.) along 118°45′ W., December 21-31, 1967.

FIGURE 60-δ_T-v2.—Vertical distribution of thermosteric anomaly, δ_T, (cl./t.) along 111°45′ W., January 2-6, 1968.

FIGURE 60-δ_T-v3.—Vertical distribution of thermosteric anomaly, δ_T, (cl./t.) along a section from 12° N., 111°45′ W. to Manzanillo, January 6-9, 1968.

FIGURE 60-δ_T-v4.—Vertical distribution of thermosteric anomaly, δ_T, (cl./t.) along a section from Acapulco to 12° N., 104°45′ W., January 13-15, 1968.

FIGURE 60-δ_T-v5.—Vertical distribution of thermosteric anomaly, δ_T, (cl./t.) along 104°45′ W., January 15-21, 1968.

FIGURE 60-δ_T-v6.—Vertical distribution of thermosteric anomaly, δ_T, (cl./t.) along 97°45′ W., January 22-28, 1968.

FIGURE 60-G-v1.—Vertical distribution of the zonal component of geostrophic velocity (cm./sec.), relative to 500 db., along 118°45′ W., December 21-31, 1967. Dark shading indicates eastward flow with a velocity greater than 5 cm./sec.; light shading indicates westward flow with a velocity greater than 5 cm./sec.

FIGURE 60-G-v2.—Vertical distribution of the zonal component of geostrophic velocity (cm./sec.), relative to 500 db., along 111°45′ W., January 2-6, 1968. Dark shading indicates eastward flow with a velocity greater than 5 cm./sec.; light shading indicates westward flow with a velocity greater than 5 cm./sec.

FIGURE 60-G-v3.—Vertical distribution of the component of geostrophic velocity (cm./sec.), relative to 500 db., normal to a section from 12° N., 111°45′ W. to Manzanillo, January 6-9, 1968. Dark shading indicates flow toward the southeast with a velocity greater than 5 cm./sec.; light shading indicates flow toward the northwest with a velocity greater than 5 cm./sec.

FIGURE 60-G-v4.—Vertical distribution of the component of geostrophic velocity (cm./sec.), relative to 500 db., normal to a section from Acapulco to 12° N., 104°45′ W., January 14-15, 1968. Dark shading indicates flow toward the southeast with a velocity greater than 5 cm./sec.

FIGURE 60-G-v5.—Vertical distribution of the zonal component of geostrophic velocity (cm./sec.), relative to 500 db., along 104°45′ W., January 15-21, 1968. Dark shading indicates eastward flow with a velocity greater than 5 cm./sec.; light shading indicates westward flow with a velocity greater than 5 cm./sec.

FIGURE 60-G-v6.—Vertical distribution of the zonal component of geostrophic velocity (cm./sec.), relative to 500 db., along 97°45′ W., January 22-28, 1968. Dark shading indicates eastward flow with a velocity greater than 5 cm./sec.; light shading indicates westward flow with a velocity greater than 5 cm./sec.

Oxygen—Green pages

FIGURE 60-O_2-v1.—Vertical distribution of oxygen (ml./l.) along 118°45′ W., December 21-31, 1967.

FIGURE 60-O_2-v2.—Vertical distribution of oxygen (ml./l.) along 111°45′ W., January 2-6, 1968.

FIGURE 60-O_2-v3.—Vertical distribution of oxygen (ml./l.) along a section from 12° N., 111°45′ W. to Manzanillo, January 6-9, 1968.

FIGURE 60-O_2-v4.—Vertical distribution of oxygen (ml./l.) along a section from Acapulco to 12° N., 104°45′ W., January 13-15, 1968.

FIGURE 60-O_2-v5.—Vertical distribution of oxygen (ml./l.) along 104°45′ W., January 15-21, 1968.

FIGURE 60-O_2-v6.—Vertical distribution of oxygen (ml./l.) along 97°45′ W., January 22-29, 1968.

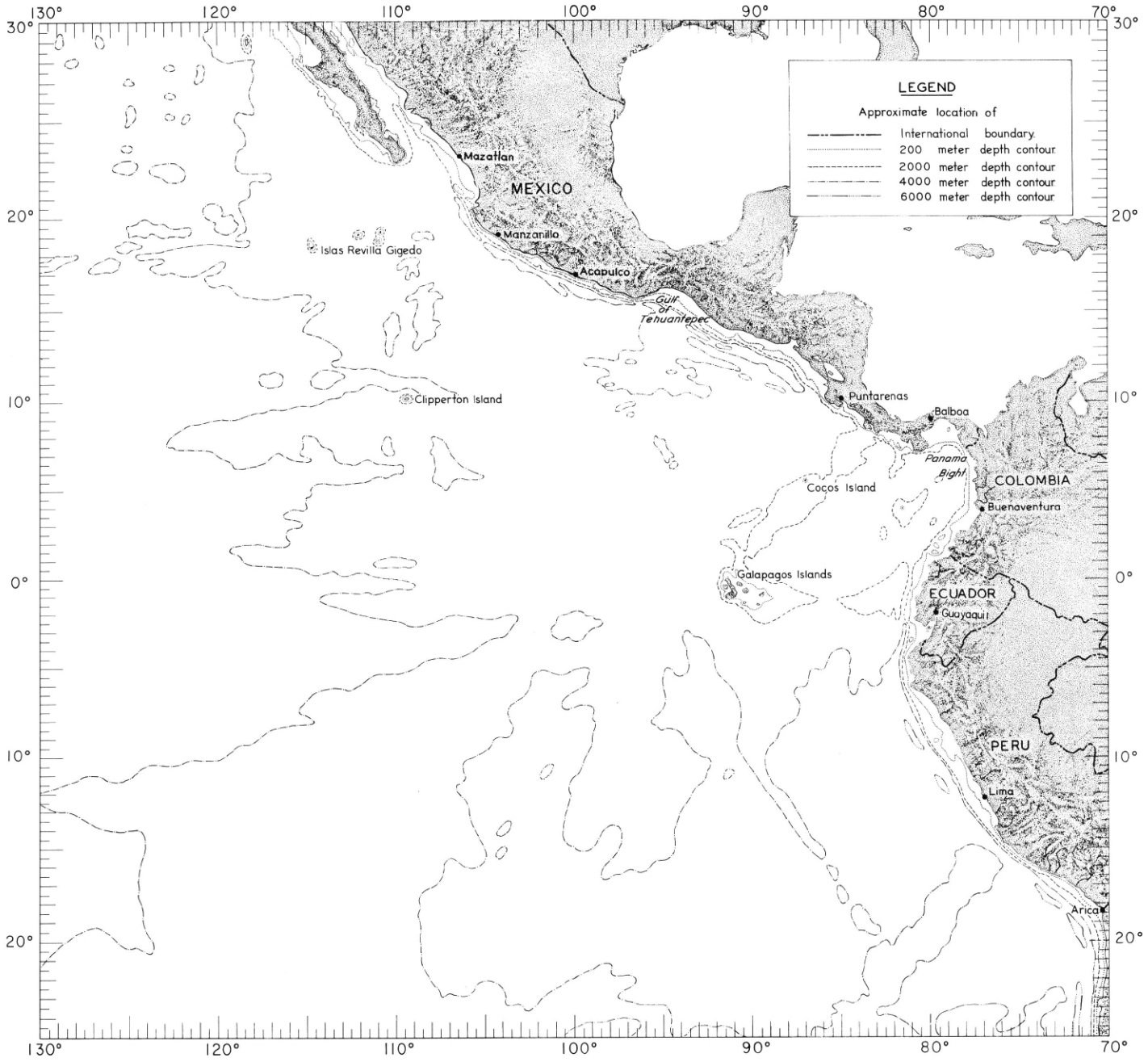

RM-a.

FIGURE RM-a. — Reference map of the main portion of the EASTROPAC area. The topographic shading and bathymetric contours are approximate only and should not be considered as portraying the latest available information.

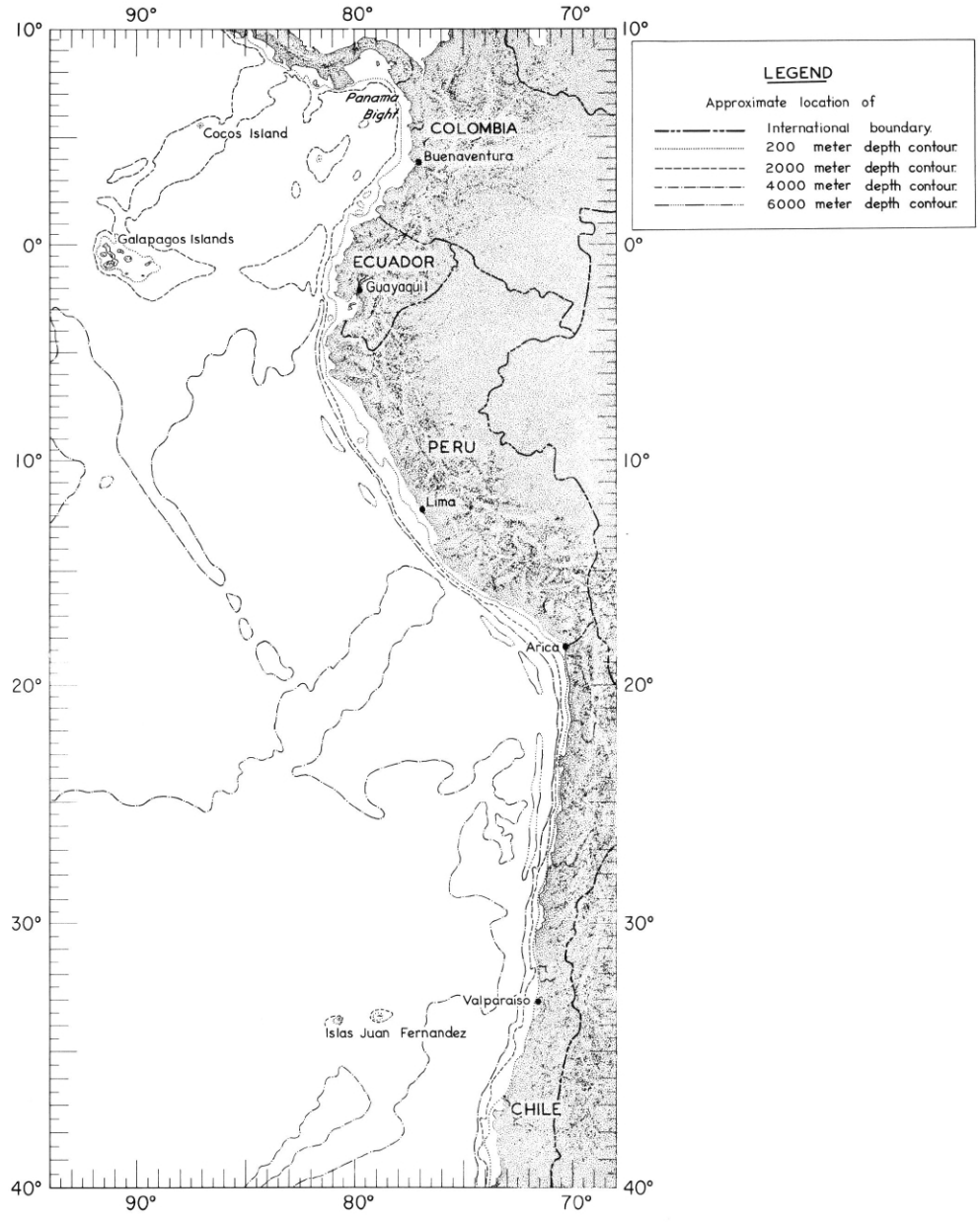

FIGURE RM-b — Reference map of the southern coastal portion of the EASTROPAC area. The topographic shading and bathymetric contours are approximate only and should not be considered as portraying the latest available information.

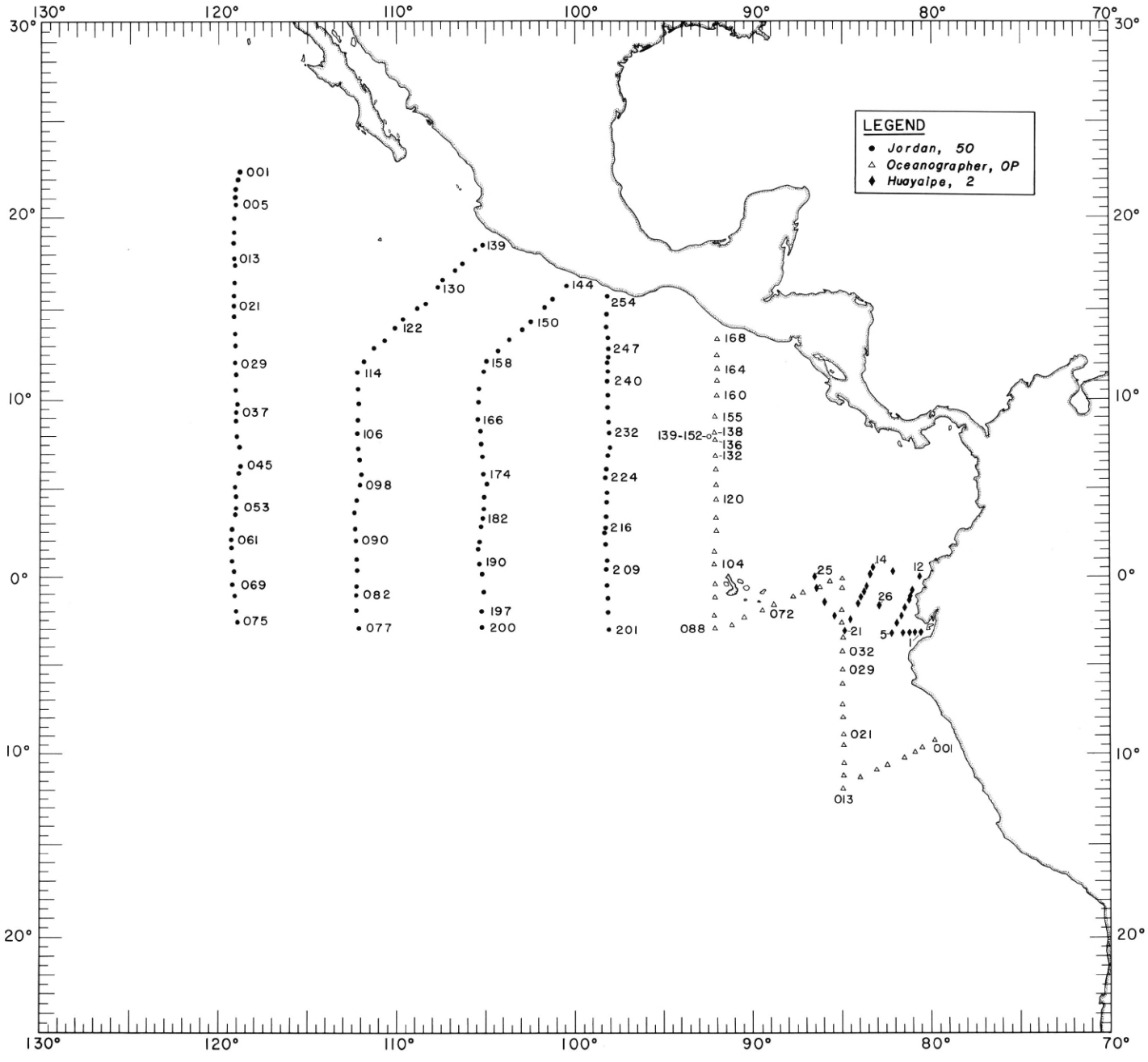

50-TC.

FIGURE 50-TC. — Locations of stations occupied by participating ships during the third monitor period, October-November 1967.

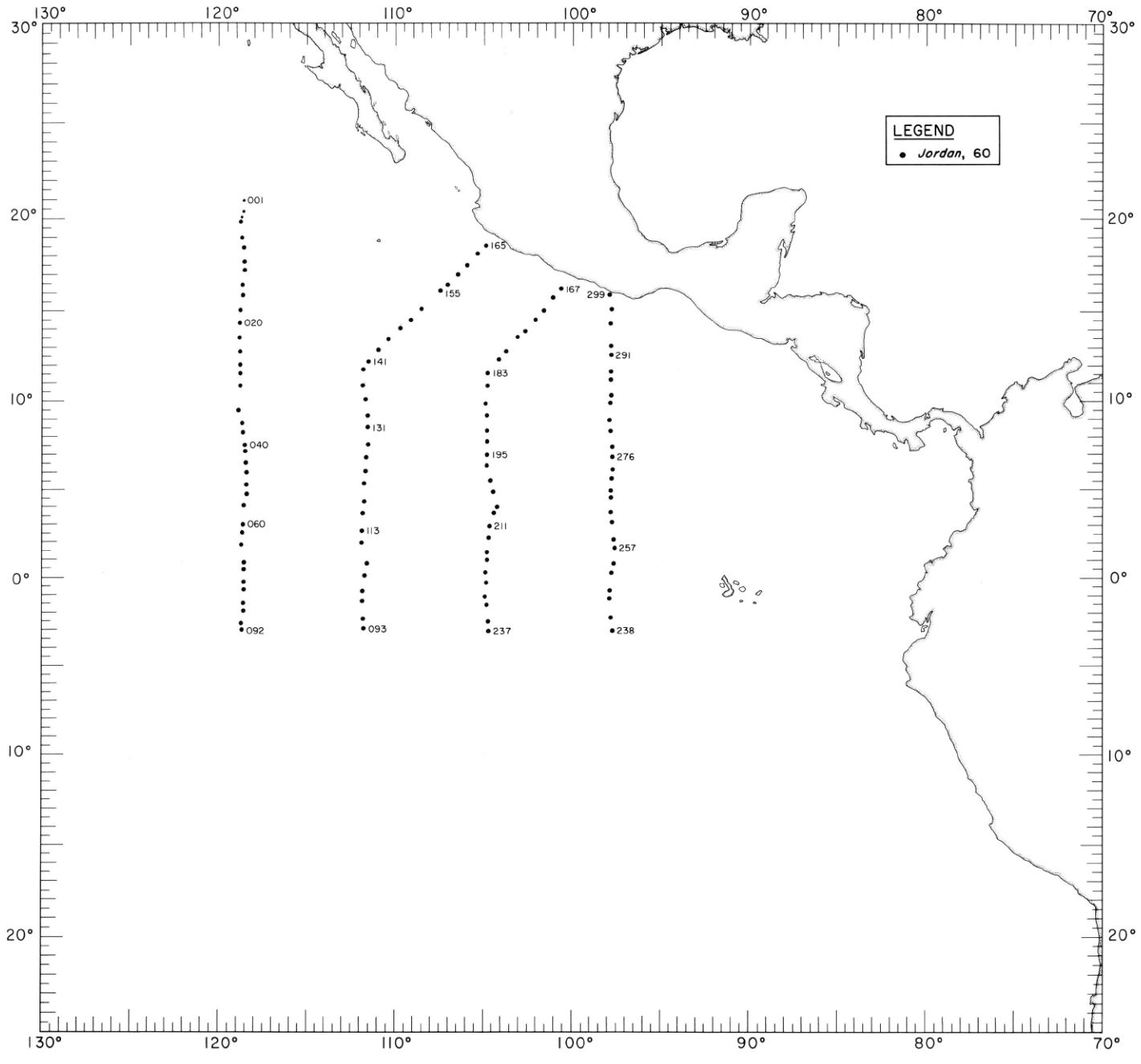

FIGURE 60-TC. — Locations of stations occupied by participating ships during the fourth monitor period, December 1967-January 1968.

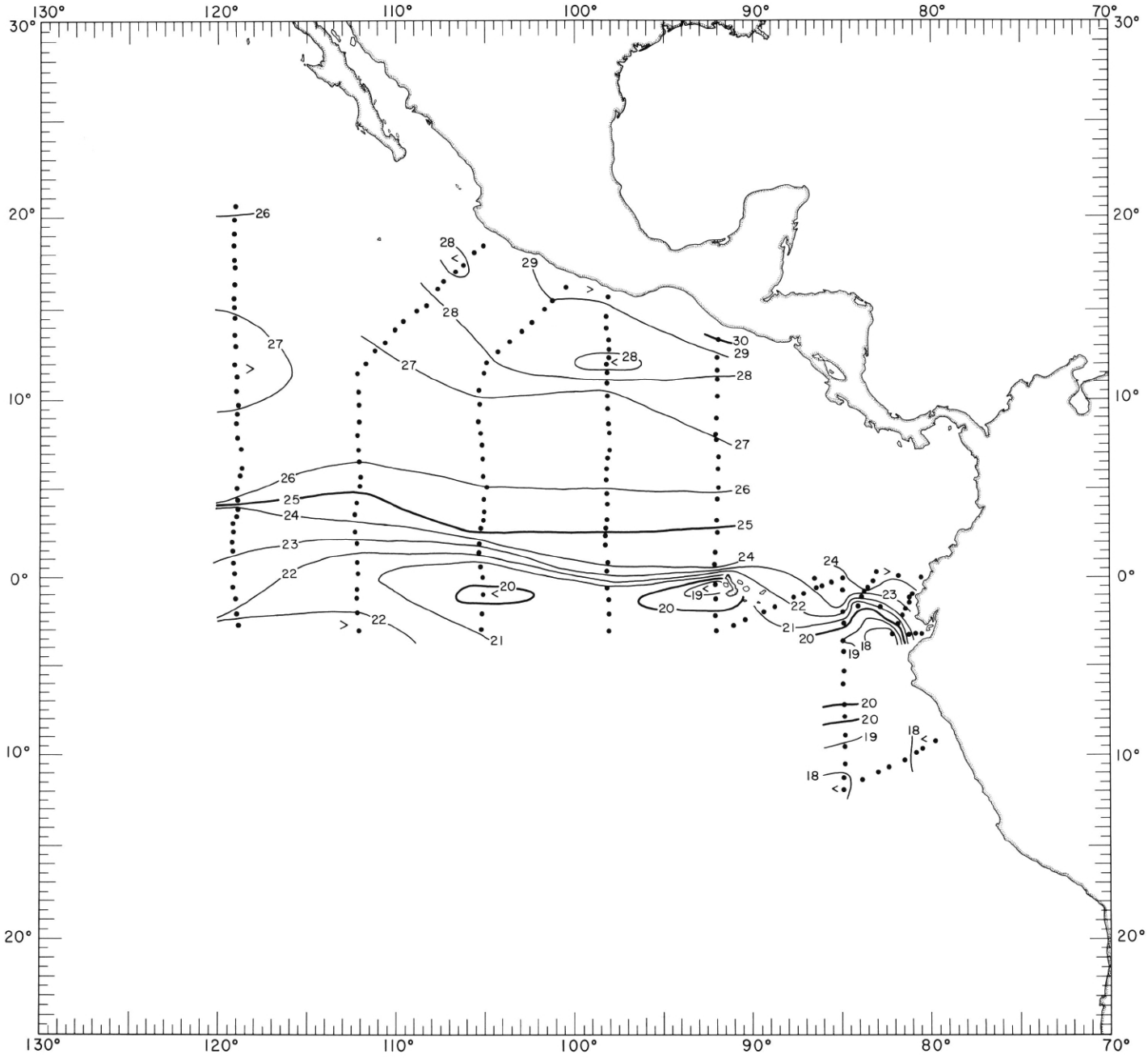

50-T-s.

FIGURE 50-T-s.—Temperature (°C.) at the sea surface, October-November 1967. These contours are based on Nansen cast data.

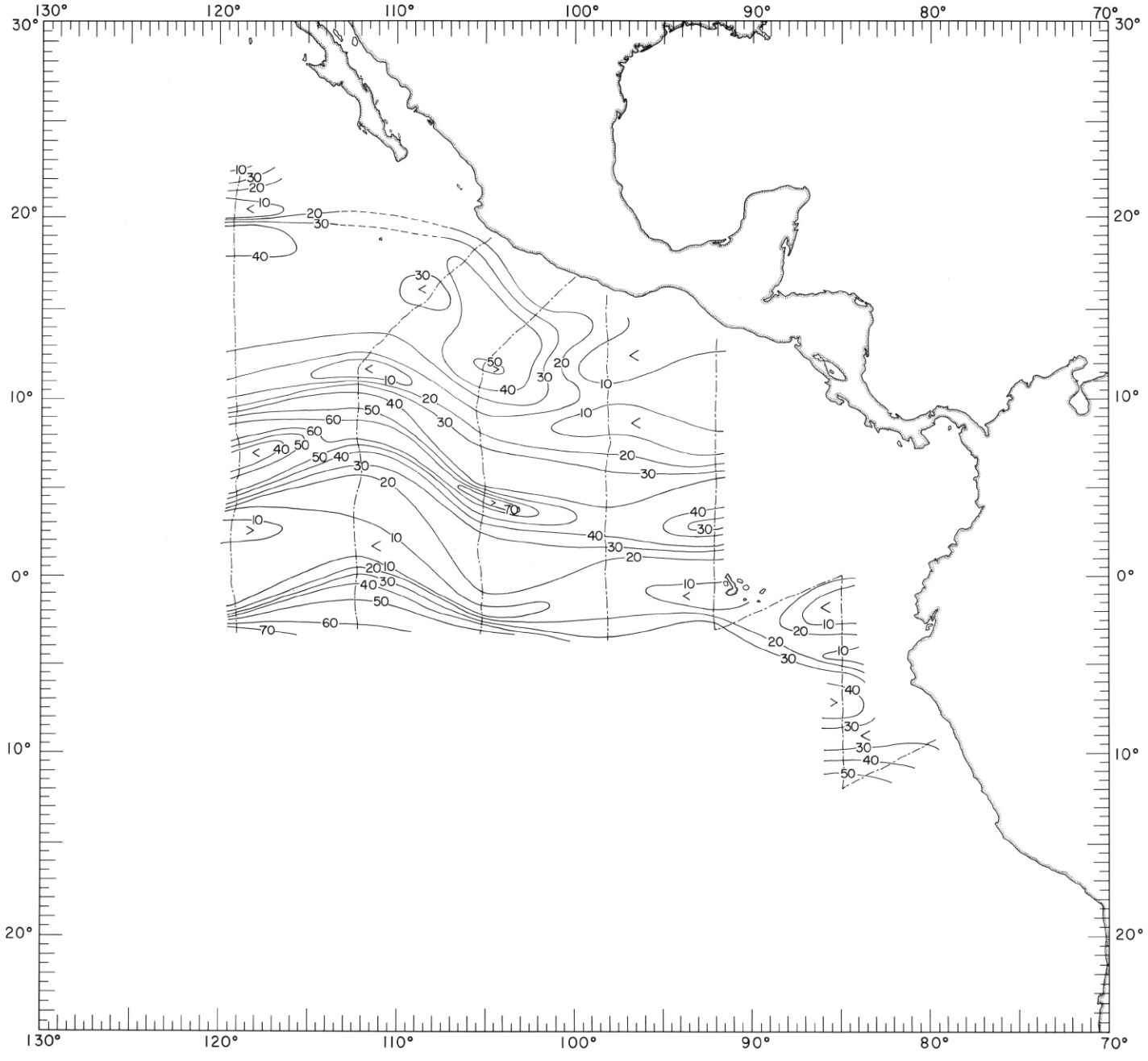

FIGURE 50-ML.—Thickness of the mixed layer in meters, October-November 1967. Dashed lines indicate portions of the cruise track where such data were collected.

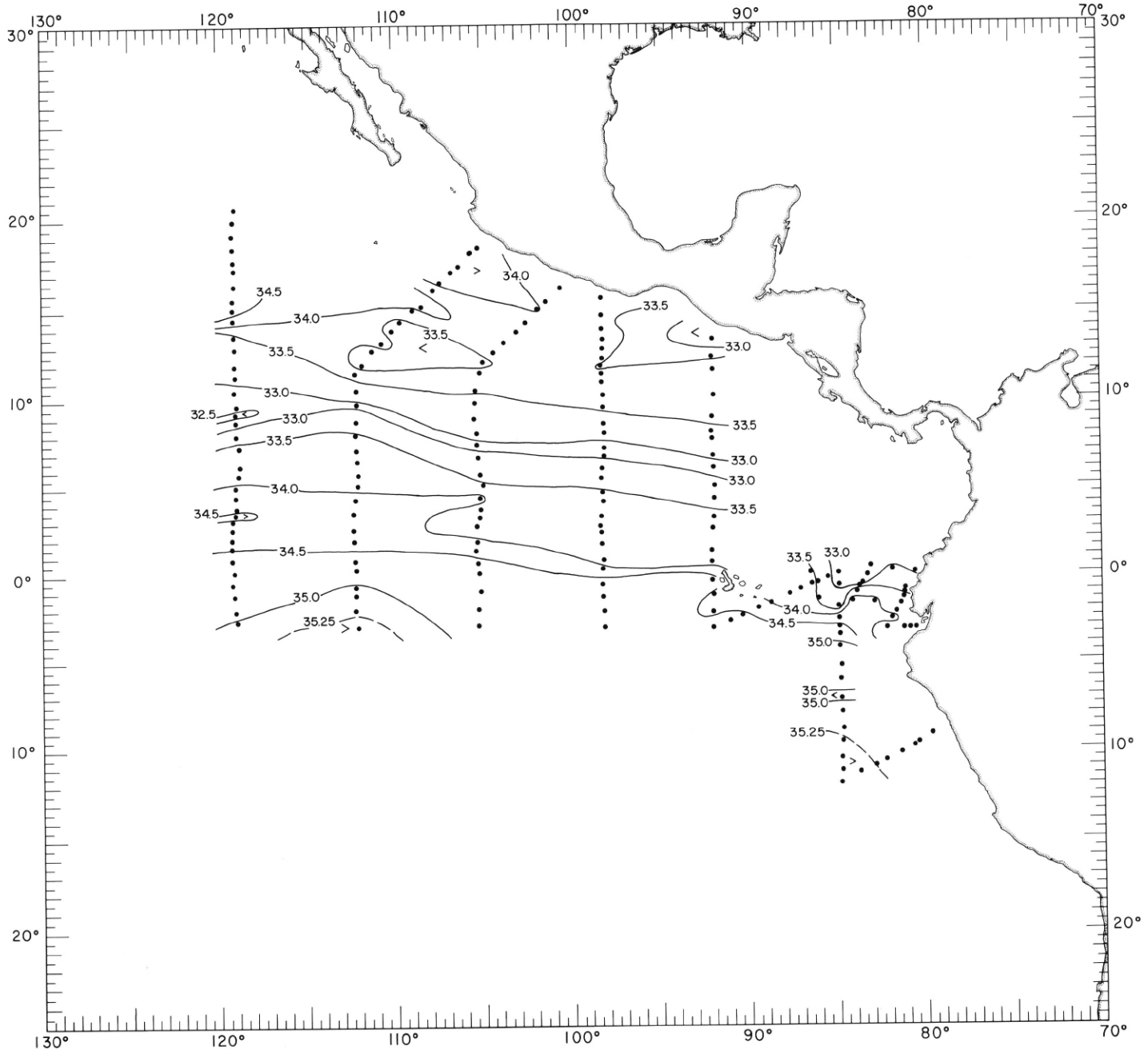

50-S-s.

FIGURE 50-S-s.—Salinity (‰) at the sea surface, October-November 1967. These contours are based on Nansen cast data.

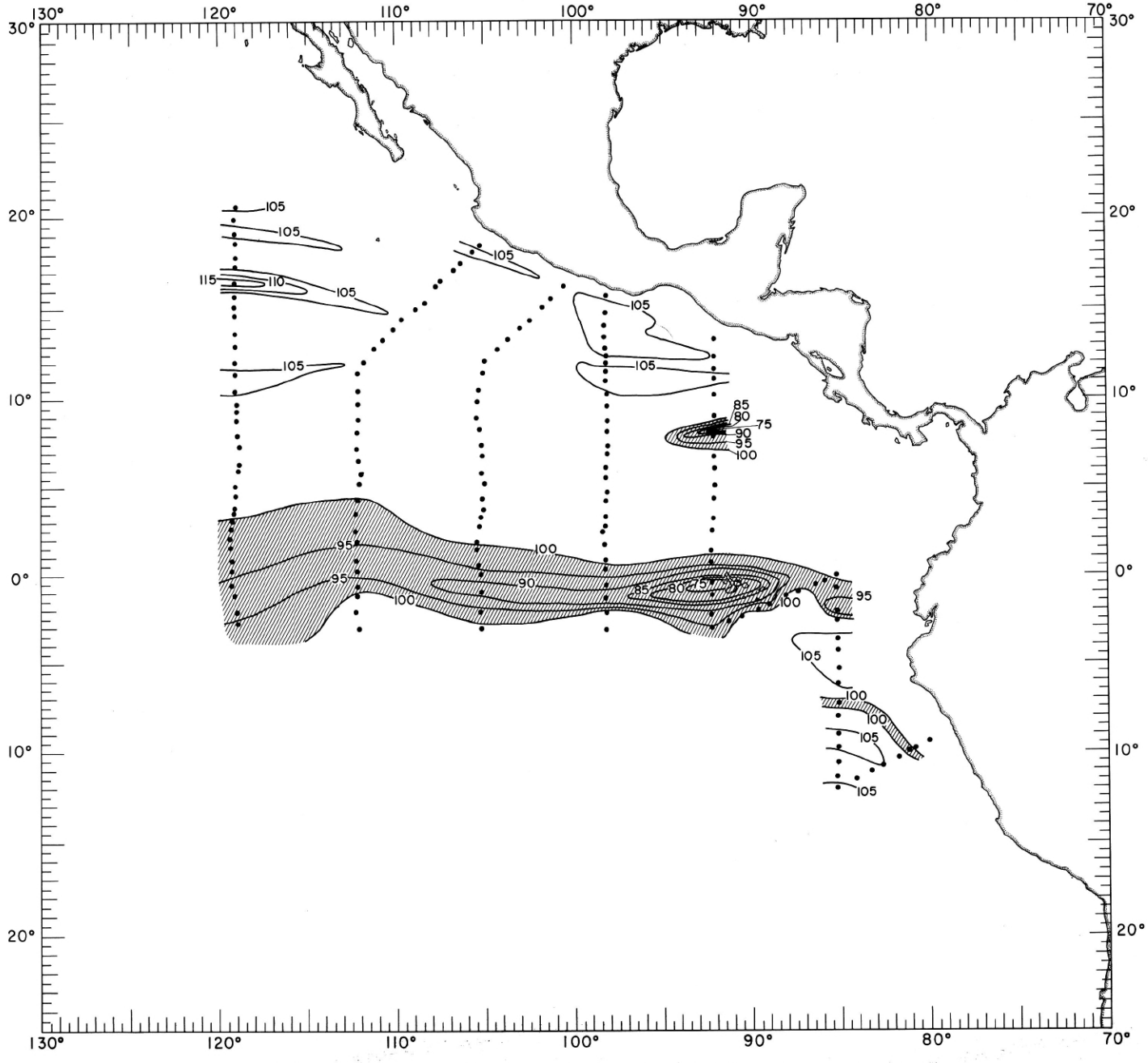

50-O₂Sa-10.

FIGURE 50-O₂Sa-10.—Oxygen saturation (%) at 10 meters, October-November 1967. Areas with less than 100% saturation are shaded.

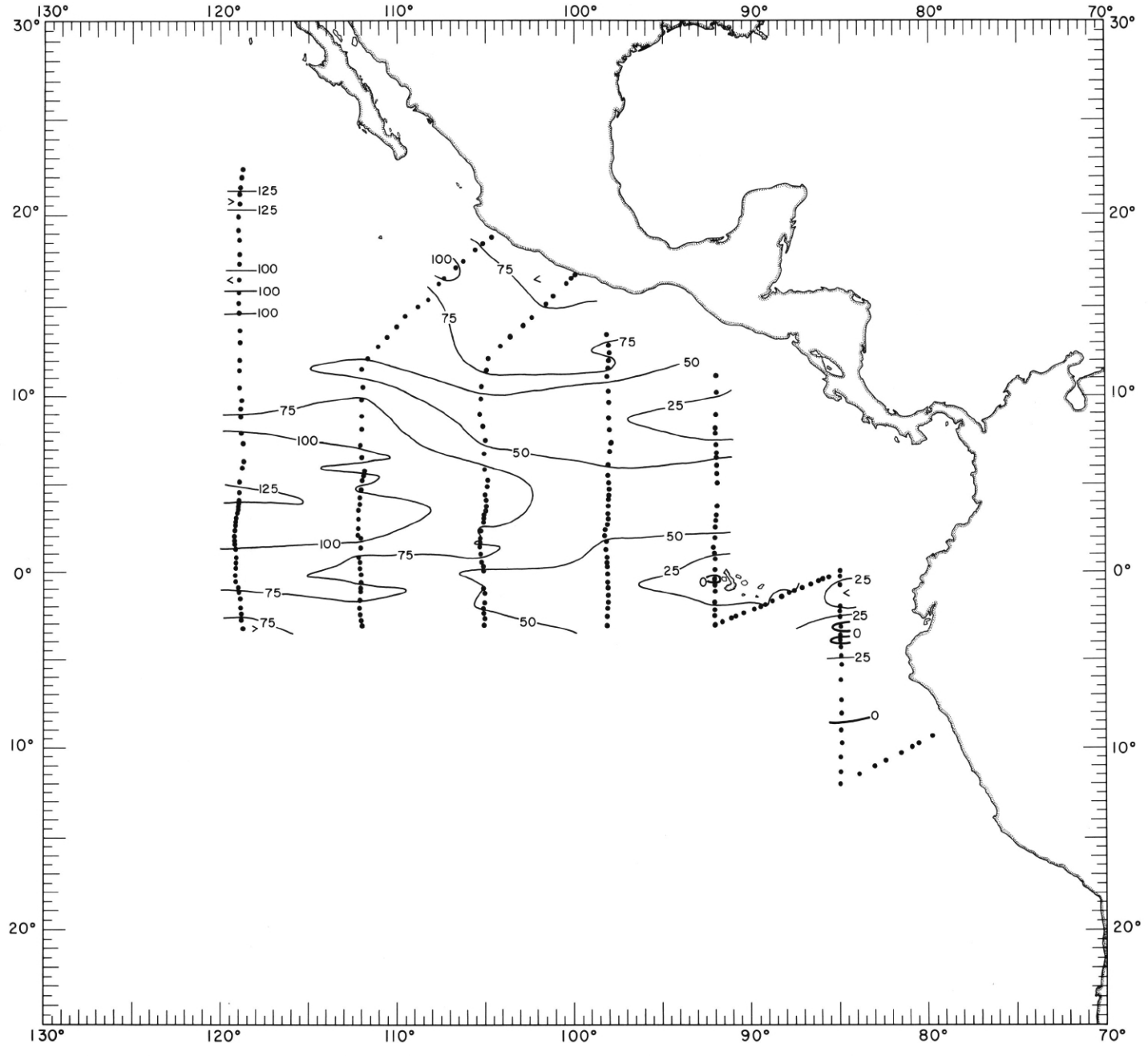

50-δ300-z.

FIGURE 50-δ300-z.—Depth (m.) of the surface where $\delta_T = 300$ cl./t., October-November 1967. The zero contours in the vicinity of 85° W. and west of the Galapagos indicate the intersections of this surface with the sea surface.

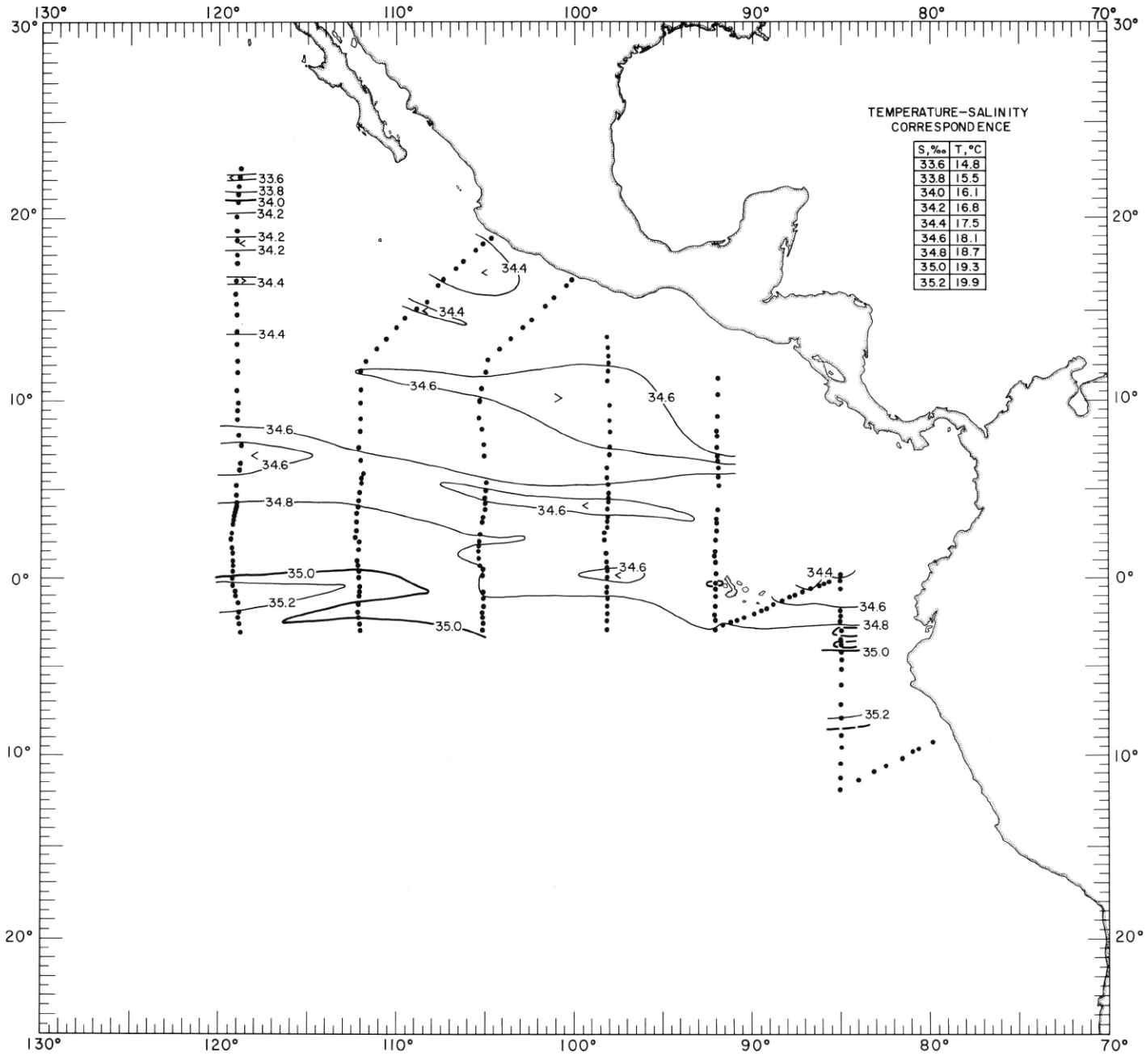

50-S-δ300.

FIGURE 50-S-δ300.—Salinity (‰) on the surface where $\delta_T = 300$ cl./t., October-November 1967. The heavy dashed lines in the vicinity of 85° W. and west of the Galapagos indicate the intersections of this surface with the sea surface. The table shows the temperature corresponding to each isohaline on the chart.

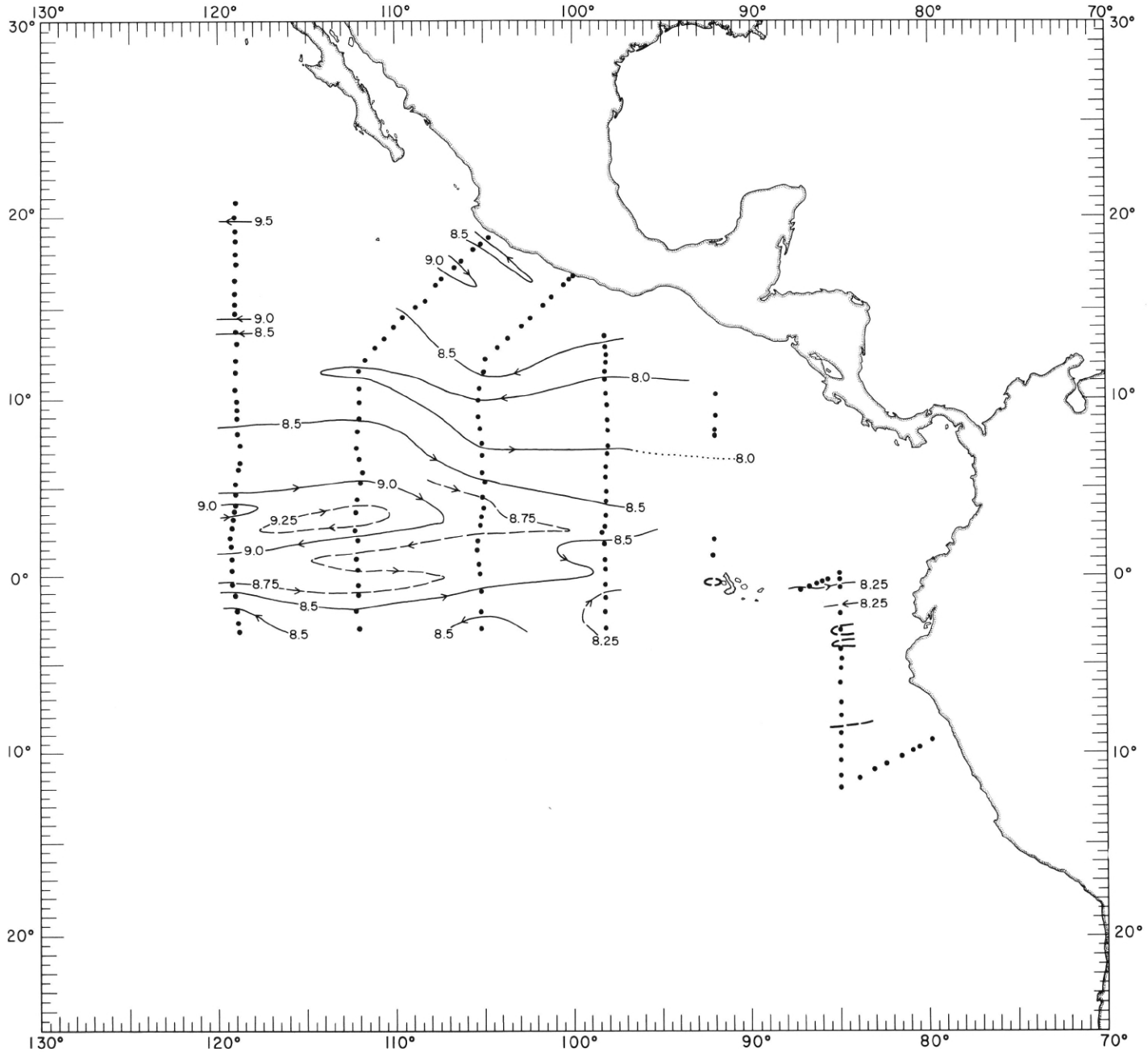

50-AP-δ300.

FIGURE 50-AP-δ300.—Acceleration potential (j./kg.), relative to 500 db., on the surface where $\delta_T = 300$ cl./t., October-November 1967. The heavy dashed lines in the vicinity of 85° W. and west of the Galapagos indicate the intersections of this surface with the sea surface. For computing acceleration potential, thermosteric anomaly, δ_T, was used instead of specific volume anomaly, δ.

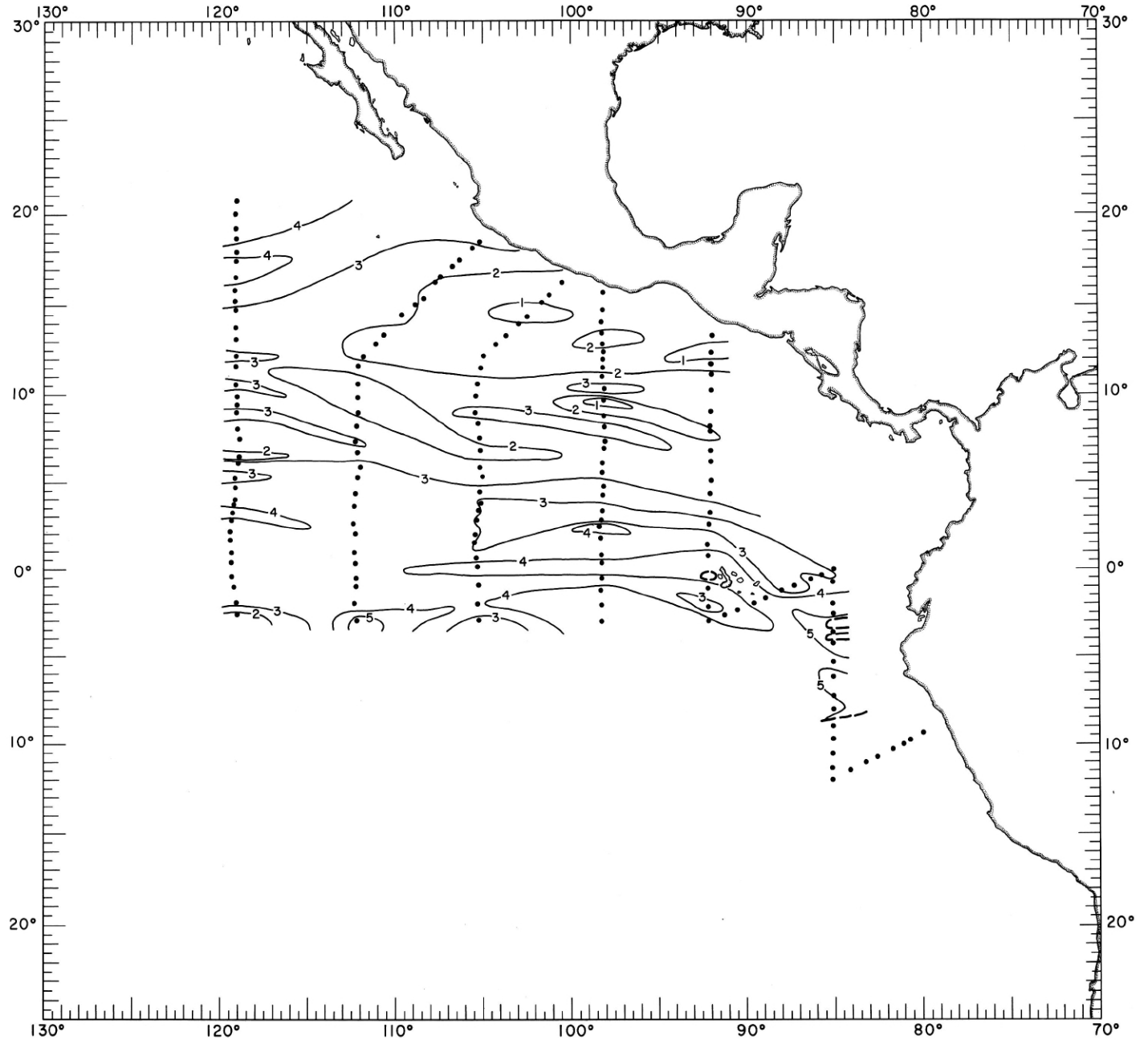

50-O₂-δ300.

FIGURE 50-O₂-δ300.—Oxygen (ml./l.) on the surface where $\delta_T = 300$ cl./t., October-November 1967. The heavy dashed lines in the vicinity of 85° W. and west of the Galapagos indicate the intersections of this surface with the sea surface.

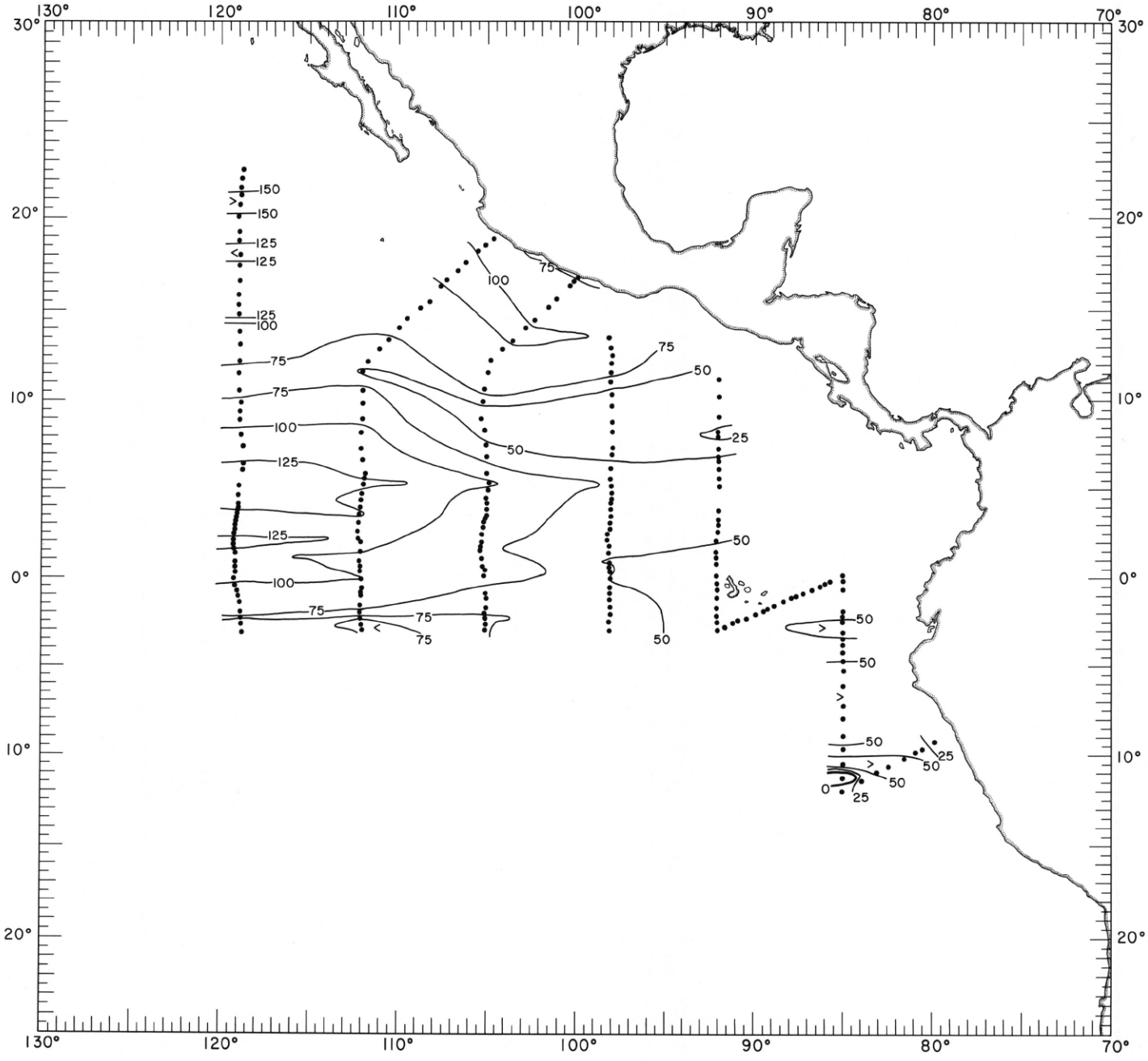

50-δ250-z.

FIGURE 50-δ250-z.—Depth (m.) of the surface where $\delta_T = 250$ cl./t., October-November 1967. The zero contour in the vicinity of 11° S., 85° W. indicates the intersection of this surface with the sea surface.

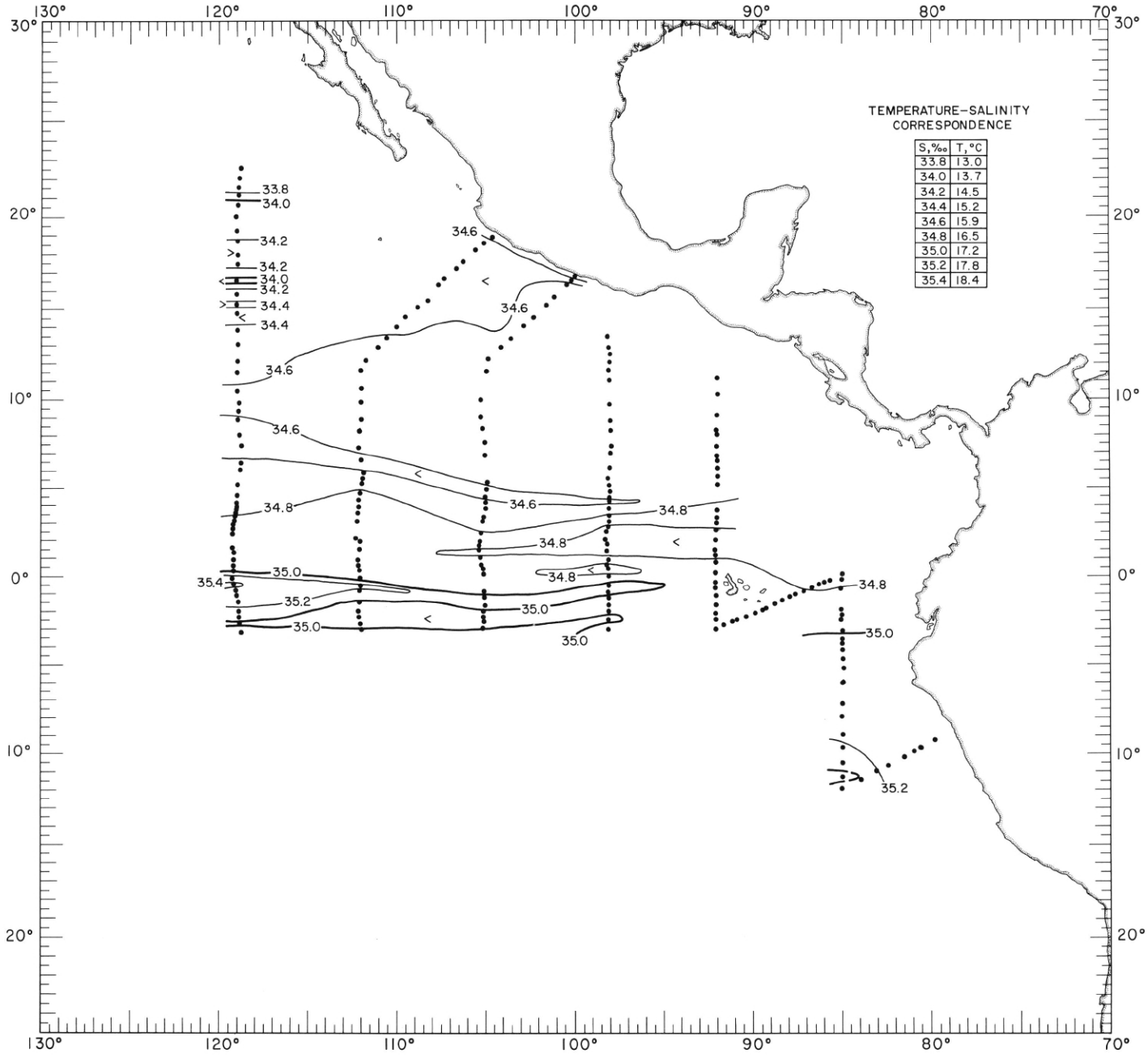

50-S-δ250.

FIGURE 50-S-δ250.—Salinity (‰) on the surface where $\delta_T = 250$ cl./t., October-November 1967. The heavy dashed line in the vicinity of 11° S., 85° W. indicates the intersection of this surface with the sea surface. The table shows the temperature corresponding to each isohaline on the chart.

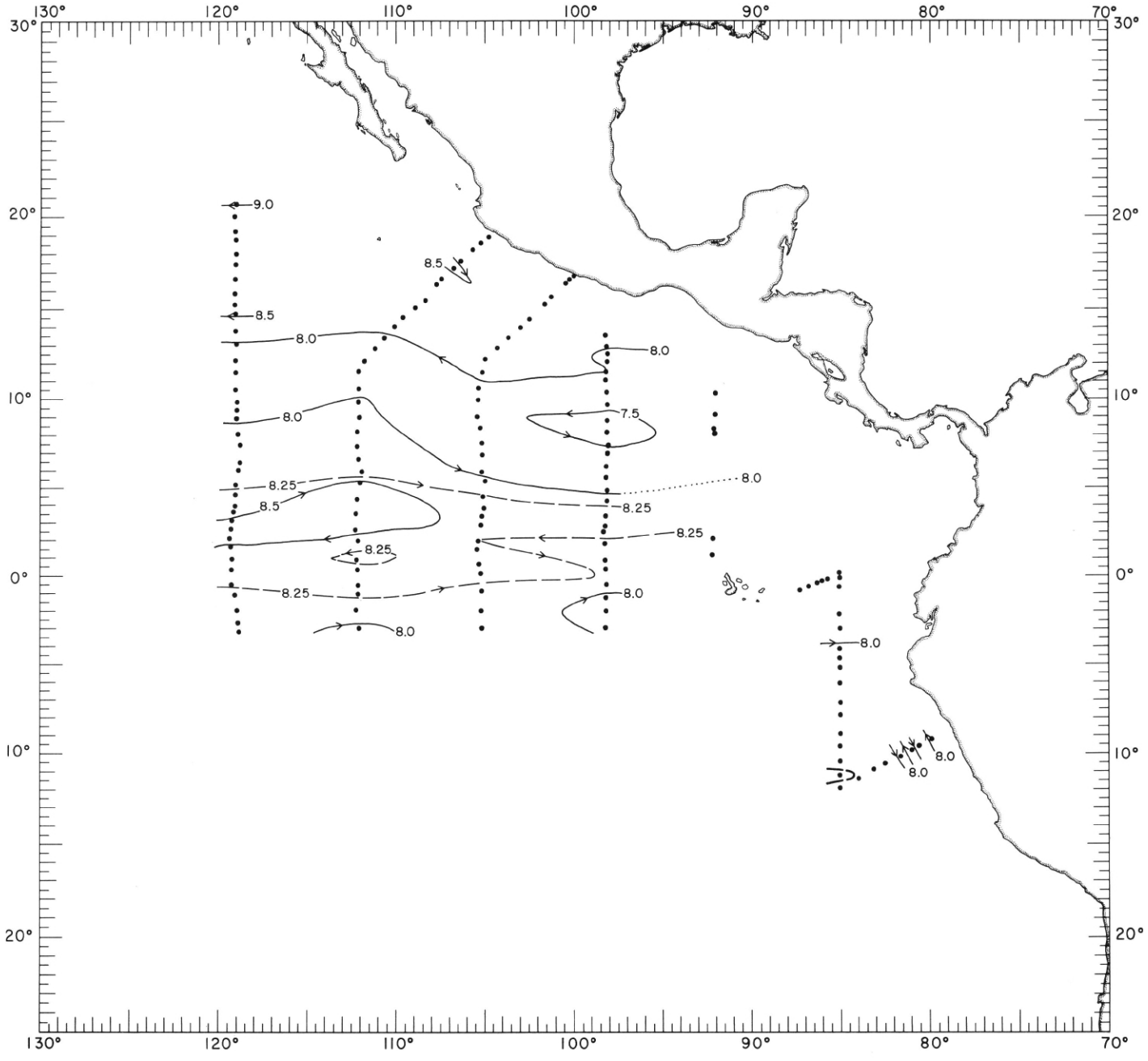

FIGURE 50-AP-δ250.—Acceleration potential (j./kg.), relative to 500 db., on the surface where $\delta_T = 250$ cl./t., October-November 1967. The heavy dashed line in the vicinity of 11° S., 85° W. indicates the intersection of this surface with the sea surface. For computing acceleration potential, thermosteric anomaly, δ_T, was used instead of specific volume anomaly, δ.

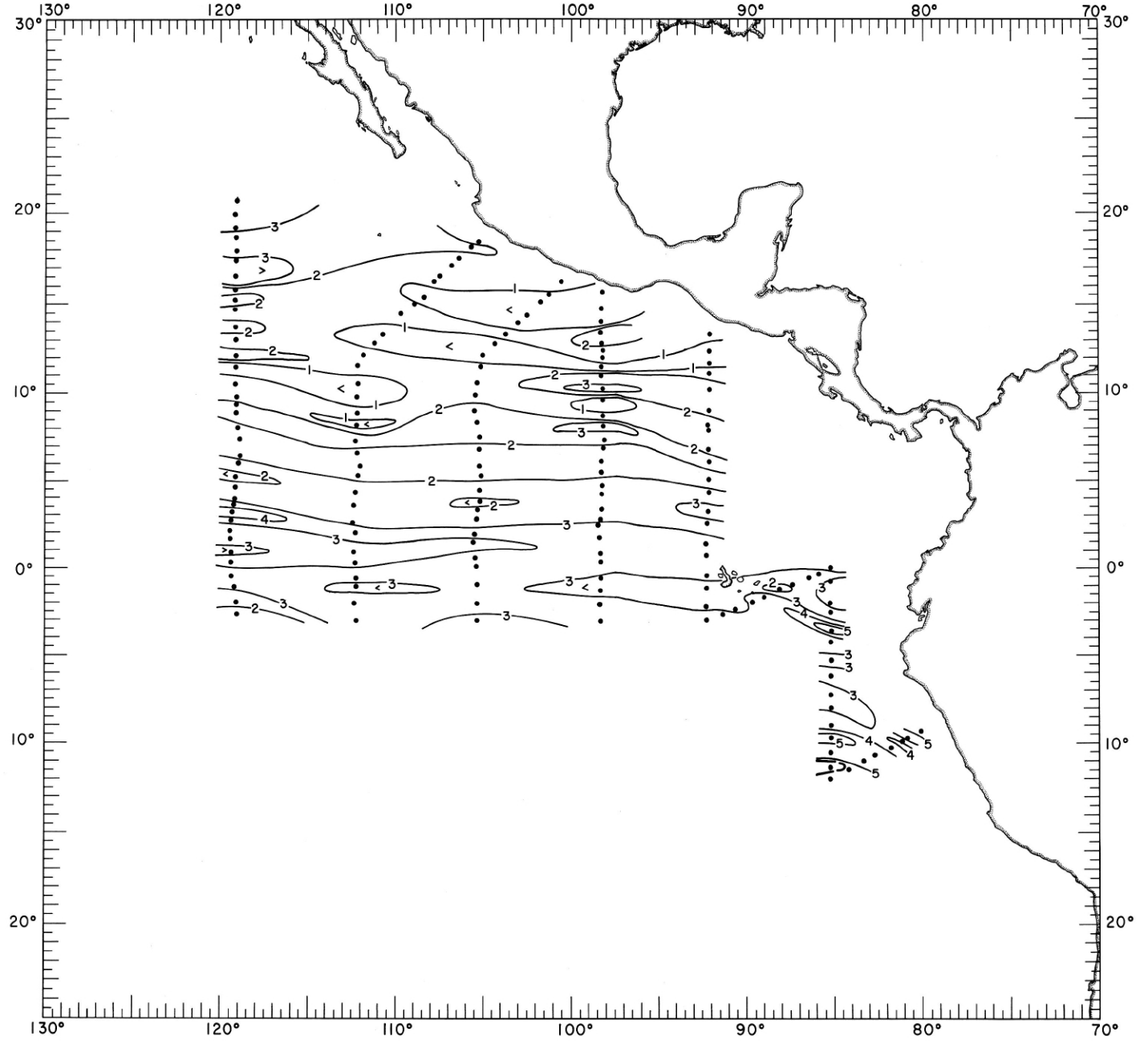

FIGURE 50-O_2-δ250.—Oxygen (ml./l.) on the surface where $\delta_T = 250$ cl./t., October-November 1967. The heavy dashed line in the vicinity of 11° S., 85° W. indicates the intersection of this surface with the sea surface.

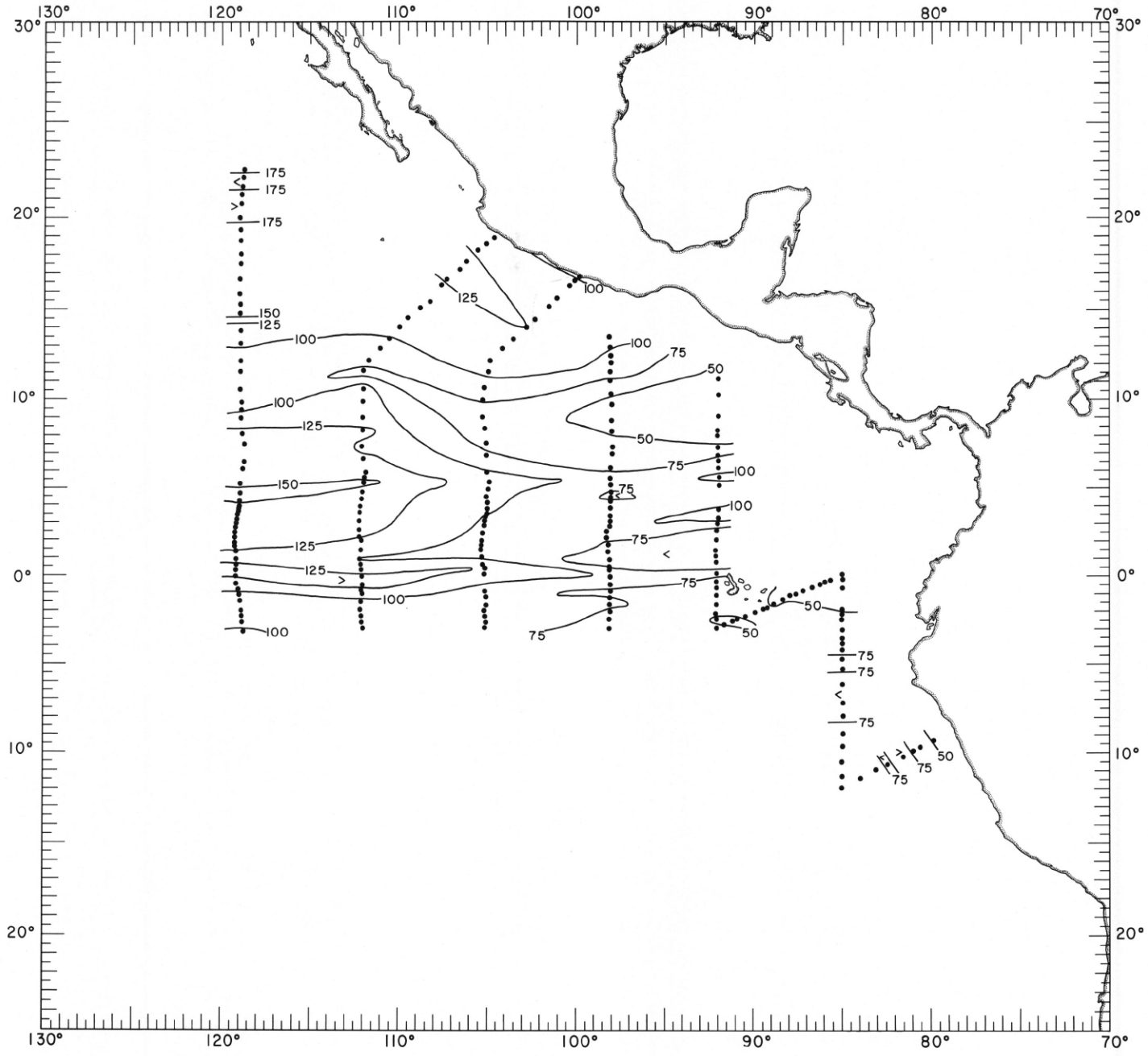

50-δ200-z.

FIGURE 50-δ200-z.—Depth (m.) of the surface where $\delta_T = 200$ cl./t., October-November 1967.

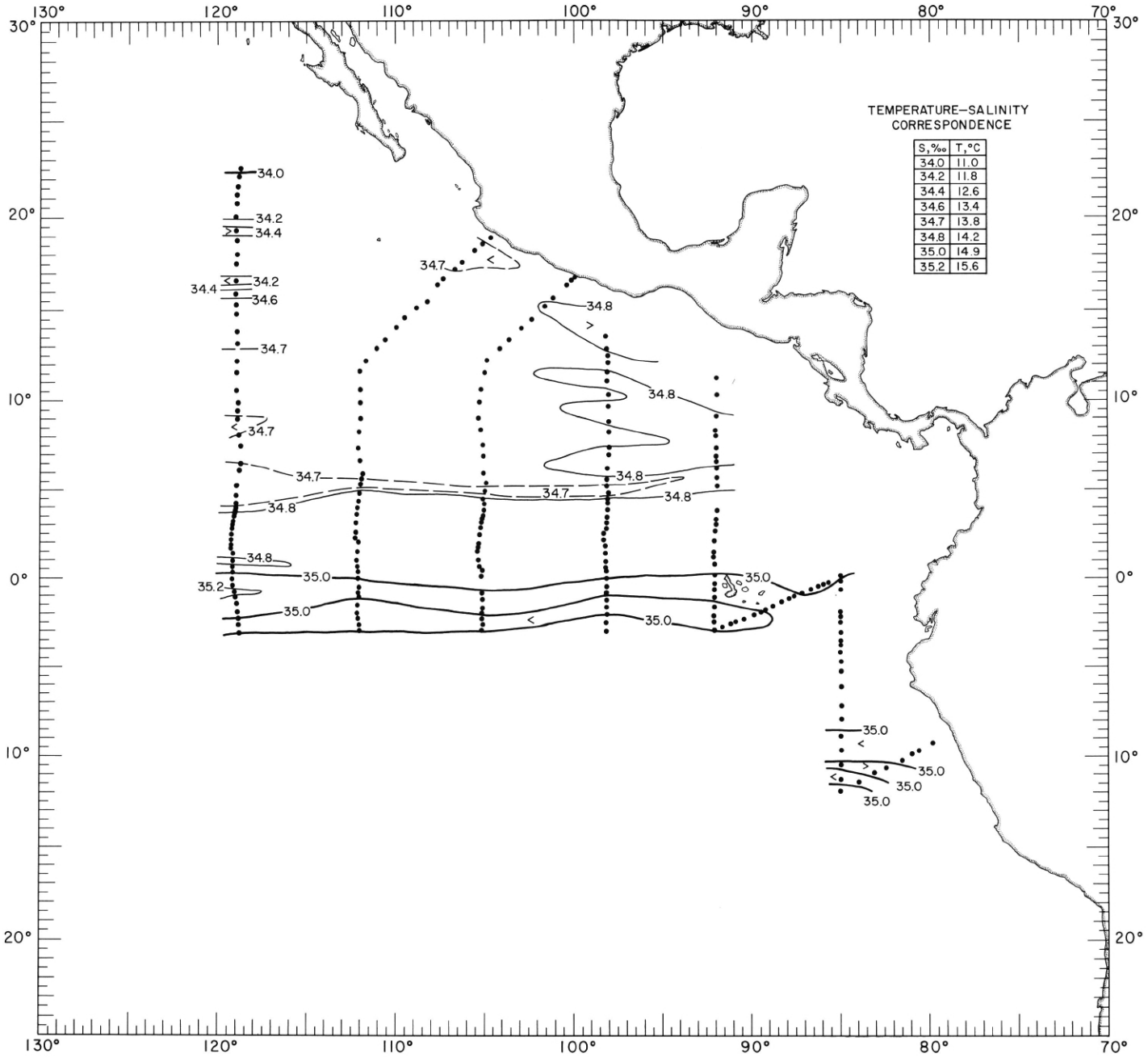

50-S-δ200.

FIGURE 50-S-δ200.—Salinity (‰) on the surface where $\delta_T = 200$ cl./t., October-November 1967. The table shows the temperature corresponding to each isohaline on the chart.

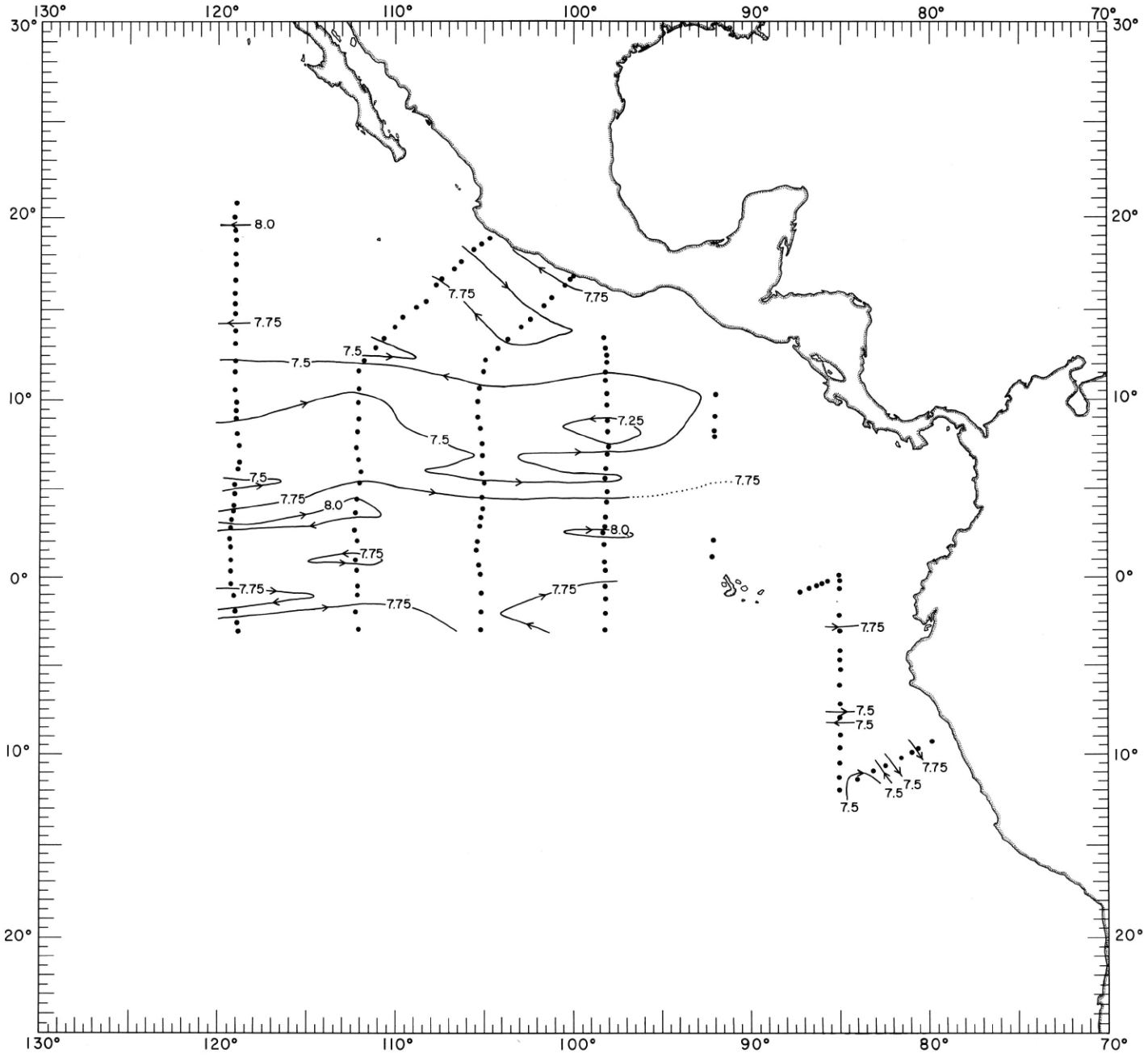

50-AP-δ200.

FIGURE 50-AP-δ200.—Acceleration potential (j./kg.), relative to 500 db., on the surface where $\delta_T = 200$ cl./t., October-November 1967. For computing acceleration potential, thermosteric anomaly, δ_T, was used instead of specific volume anomaly, δ.

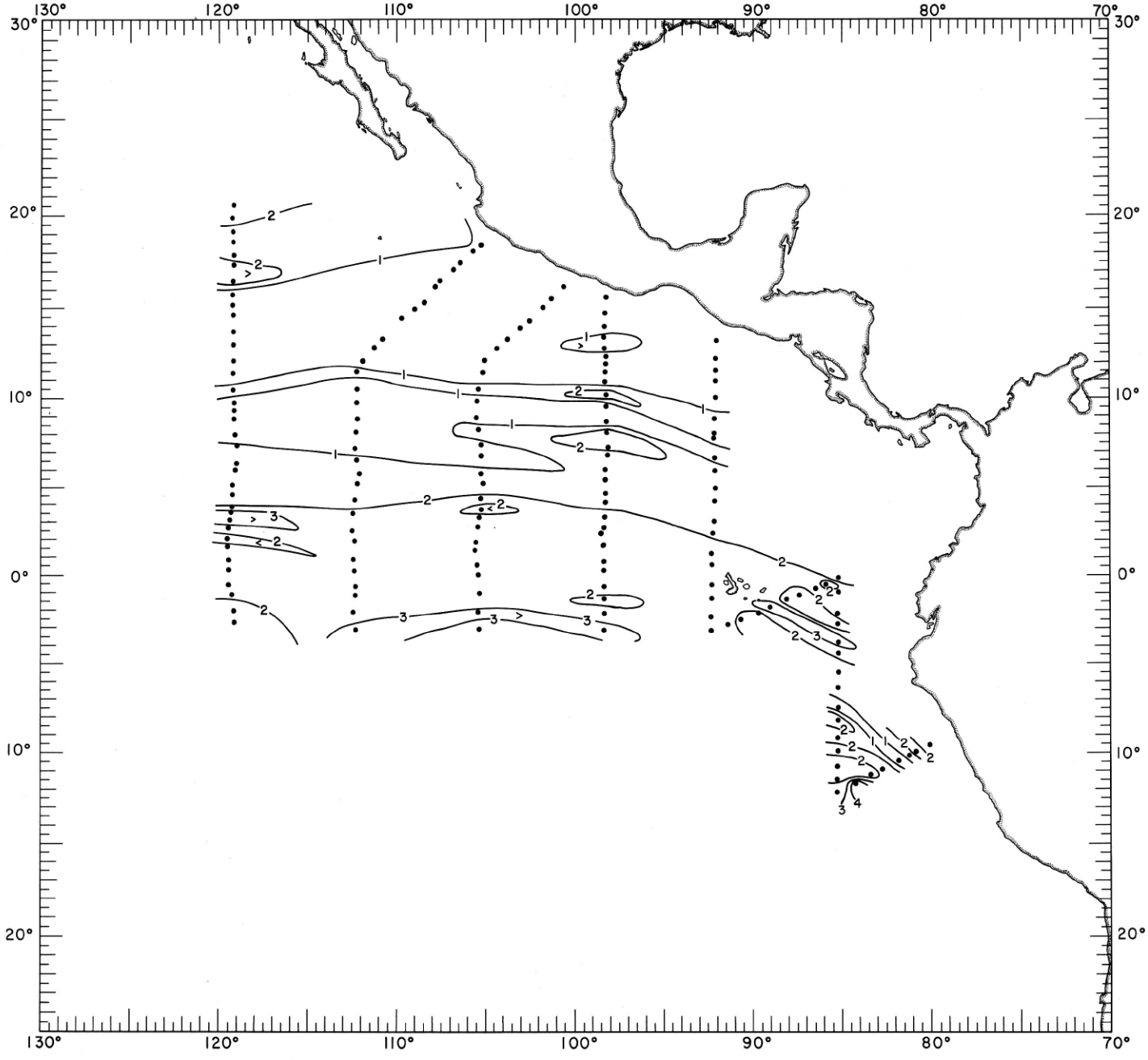

50-O_2-δ200.

FIGURE 50-O_2-δ200.—Oxygen (ml./l.) on the surface where $\delta_T = 200$ cl./t., October-November 1967.

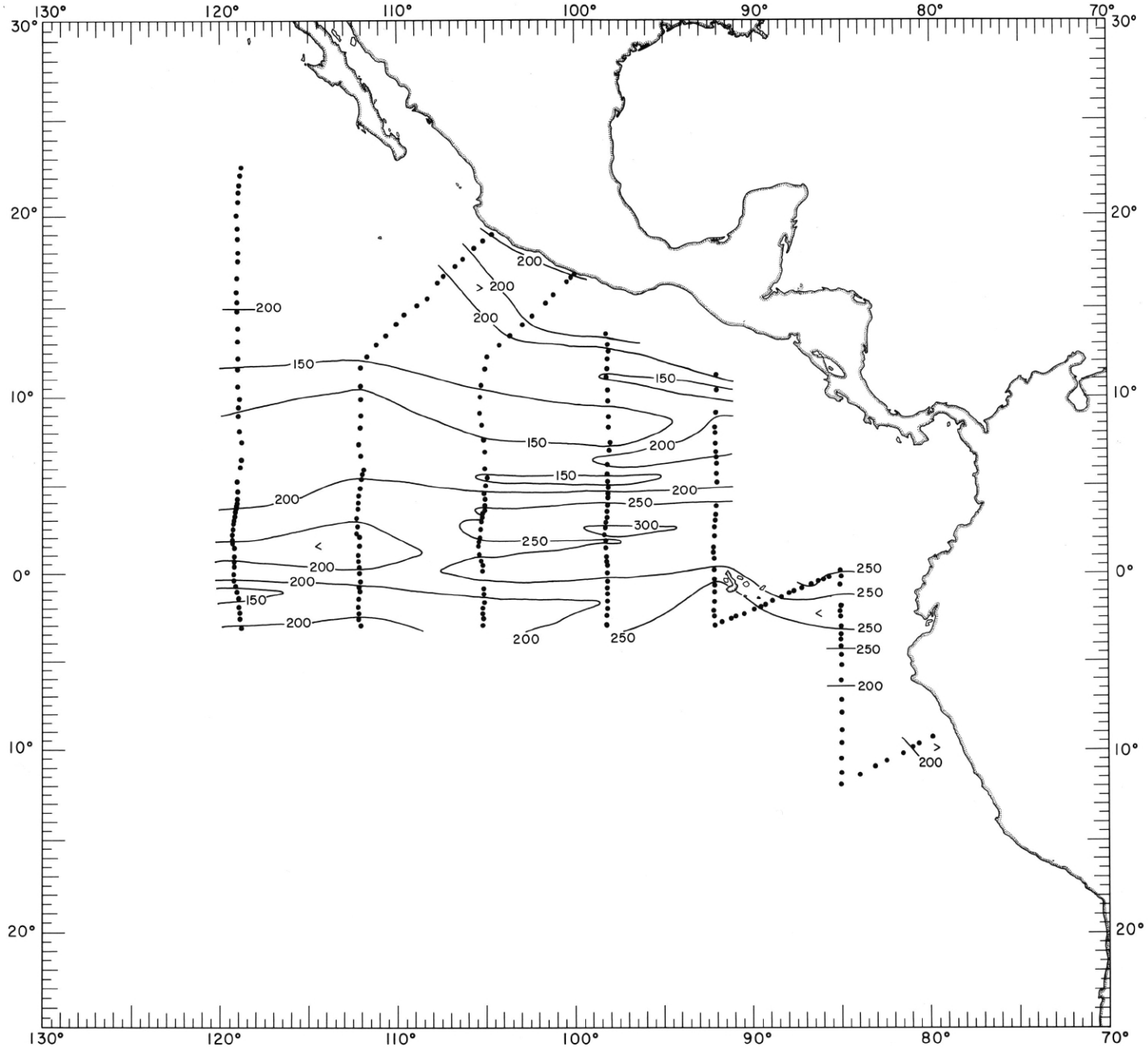

FIGURE 50-δ160-z.—Depth (m.) of the surface where δ_T = 160 cl./t., October-November 1967.

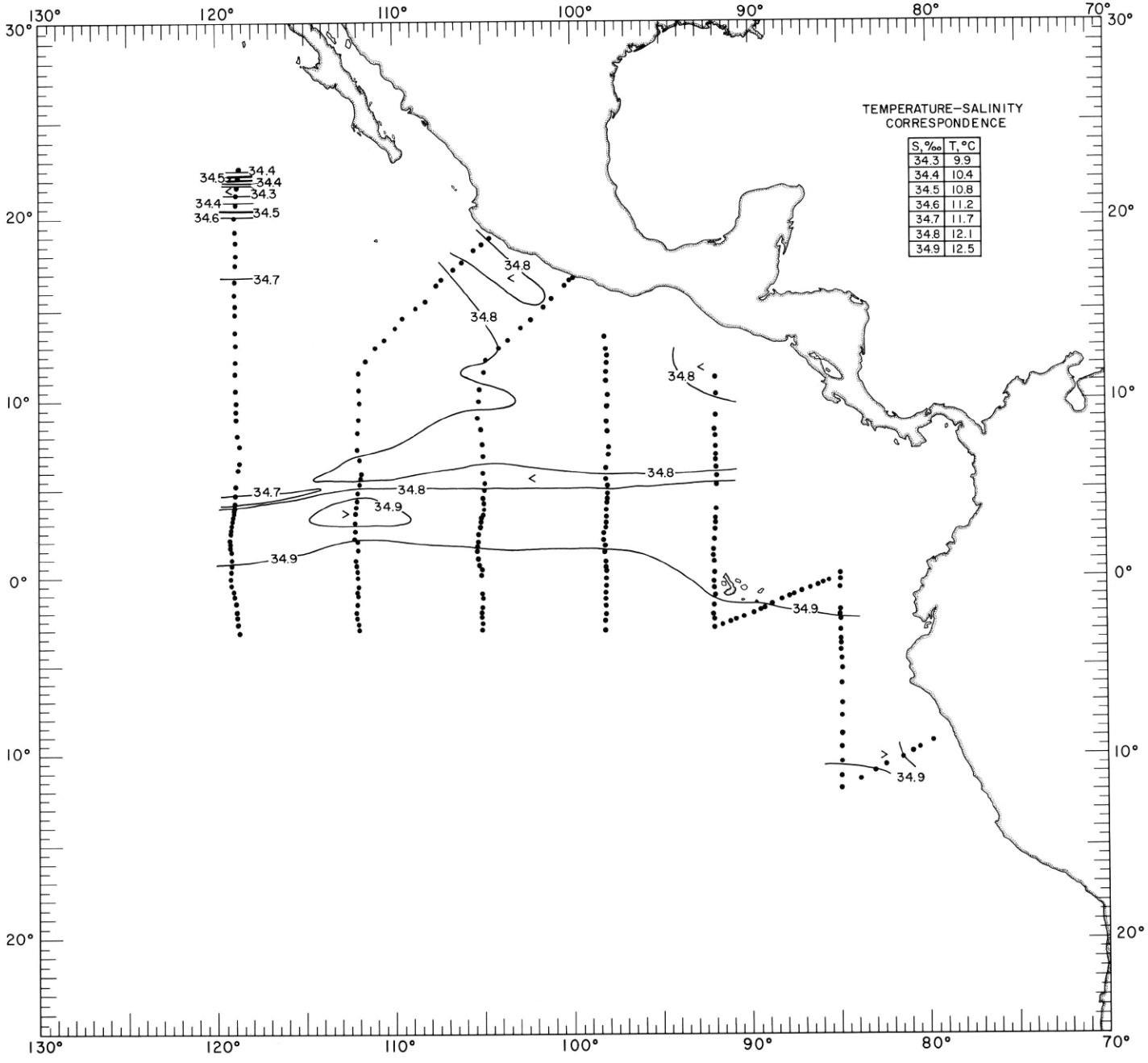

50-S-δ160.

FIGURE 50-S-δ160.—Salinity (‰) on the surface where $\delta_T = 160$ cl./t., October-November 1967. The table shows the temperature corresponding to each isohaline on the chart.

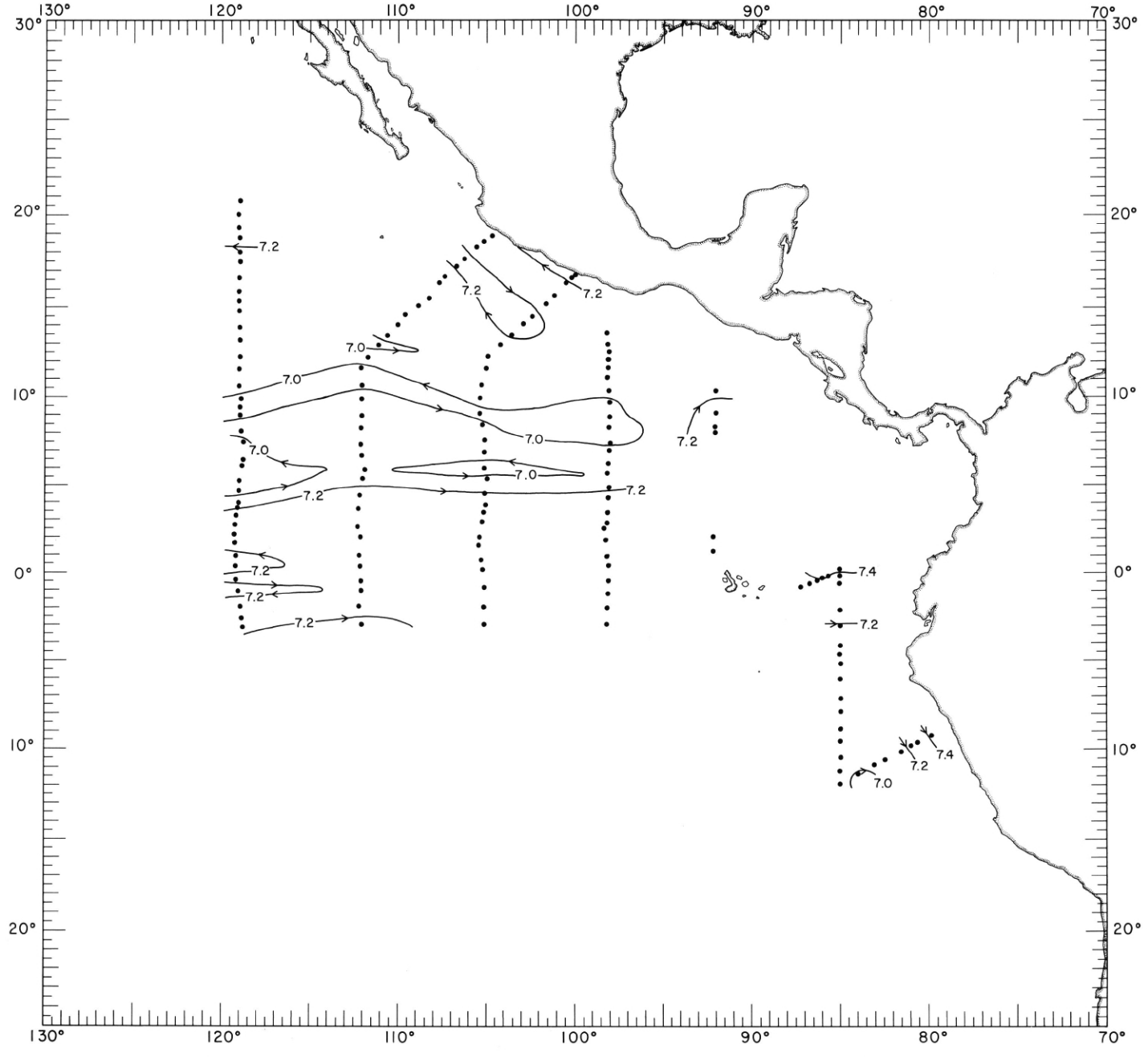

50-AP-δ160.

FIGURE 50-AP-δ160.—Acceleration potential (j./kg.), relative to 500 db., on the surface where $\delta_T = 160$ cl./t., October-November 1967. For computing acceleration potential, thermosteric anomaly, δ_T, was used instead of specific volume anomaly, δ.

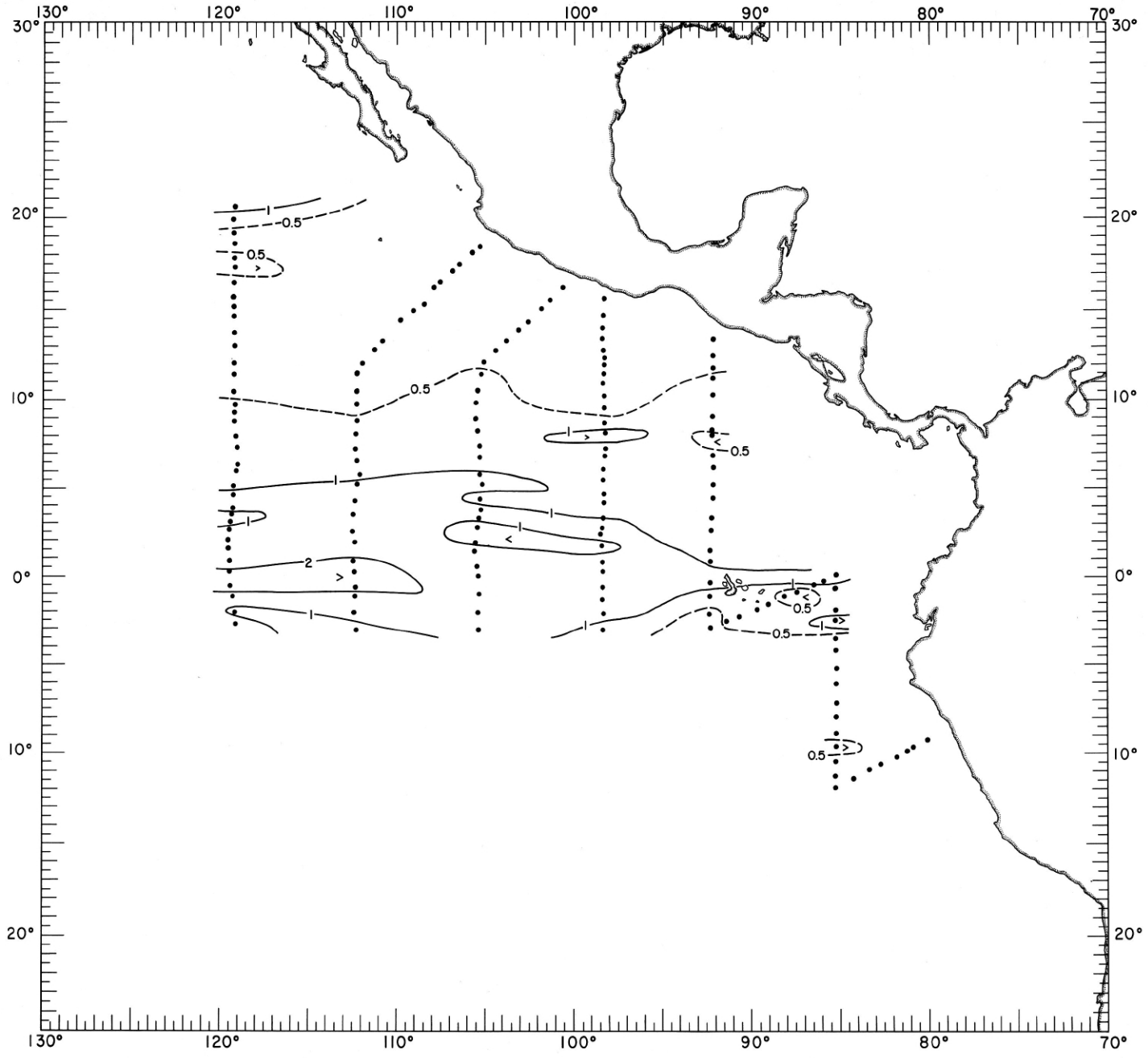

FIGURE 50-O_2-δ160.—Oxygen (ml./l.) on the surface where $\delta_T = 160$ cl./t., October-November 1967.

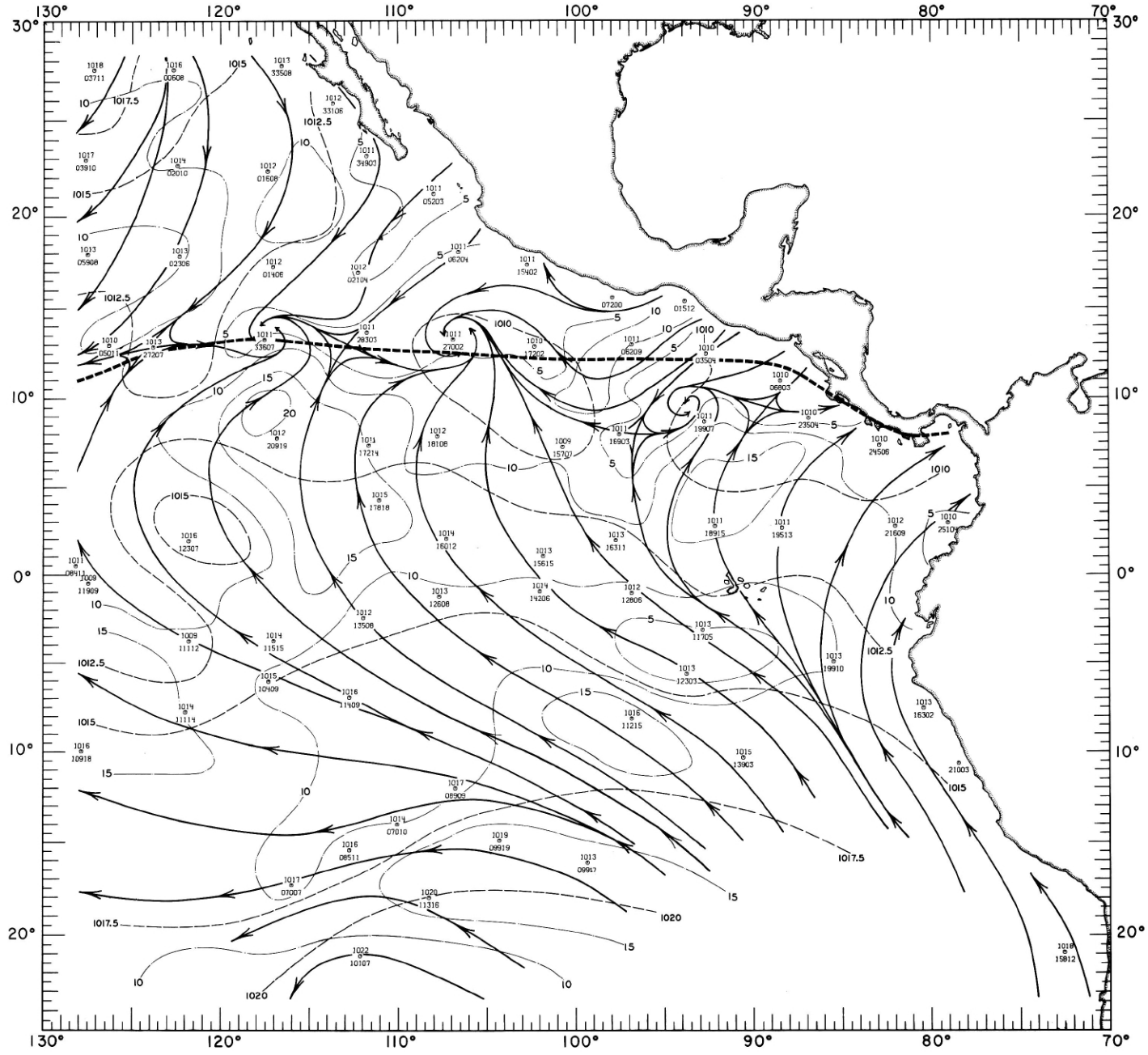

FIGURE 50-MW-1.—Analyses of the surface air pressure and surface winds from all available ship observati ons, averaged over 2-degree (latitude-longitude) squares for the period October 1-15, 1967. Heavy dashed lines are isobars. Solid lines are streamlines showing the mean resultant direction of wind flow. Light dash-dot lines are isotachs indicating mean resultant wind speed (kn.). Pressure (mb.) averaged for 5-degree squares is plotted above the mean position of the square, and resultant wind direction followed by speed (kn.) is plotted below. The monthly climatological position of the intertropical convergence zone is shown by a wide dashed band.

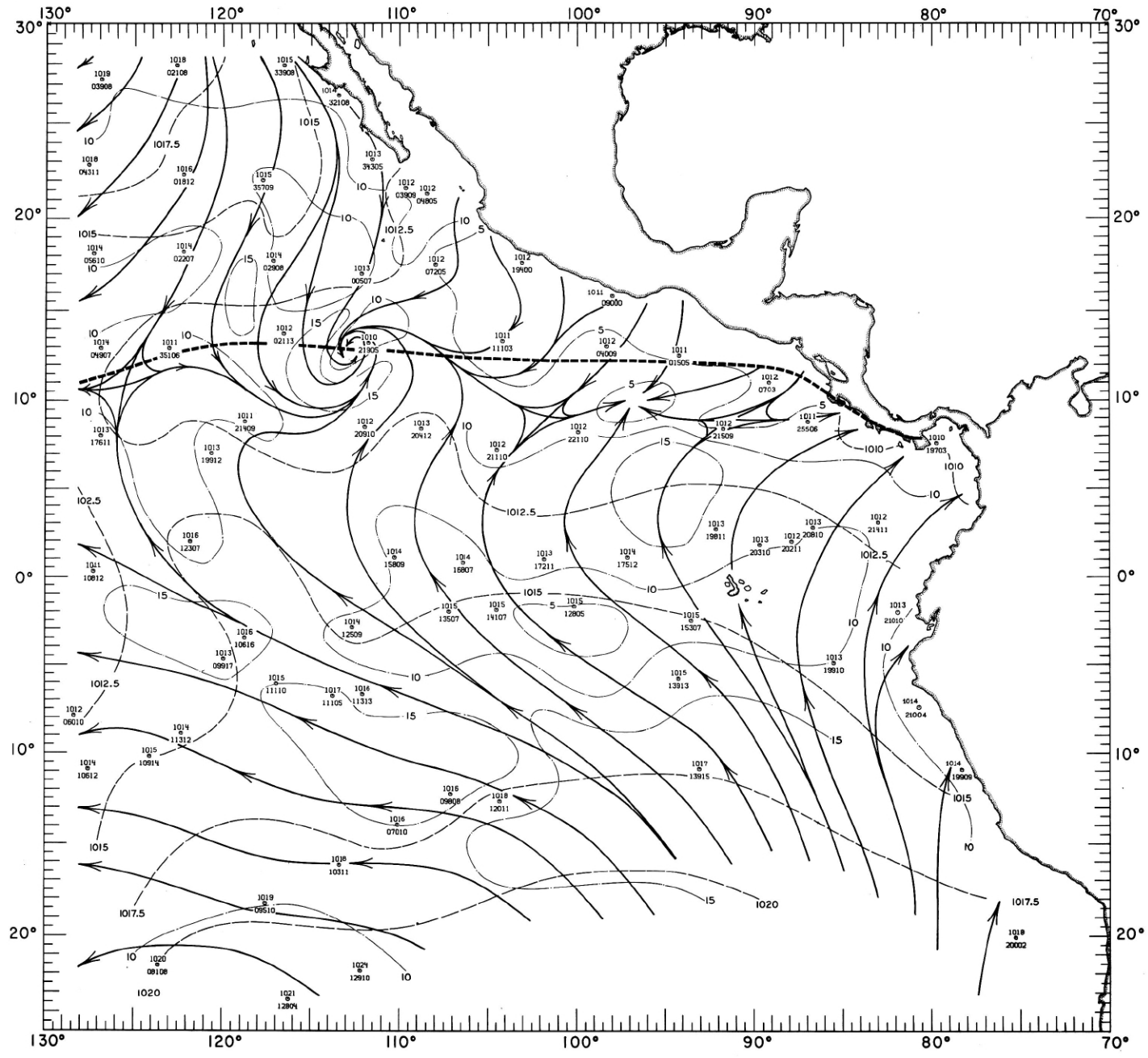

50-MW-2.

FIGURE 50-MW-2.—Analyses of the surface air pressure and surface winds from all available ship observations, averaged over 2-degree (latitude-longitude) squares for the period October 16-31, 1967. Heavy dashed lines are isobars. Solid lines are streamlines showing the mean resultant direction of wind flow. Light dash-dot lines are isotachs indicating mean resultant wind speed (kn.). Pressure (mb.) averaged for 5-degree squares is plotted above the mean position of the square, and resultant wind direction followed by speed (kn.) is plotted below. The monthly climatological position of the intertropical convergence zone is shown by a wide dashed band.

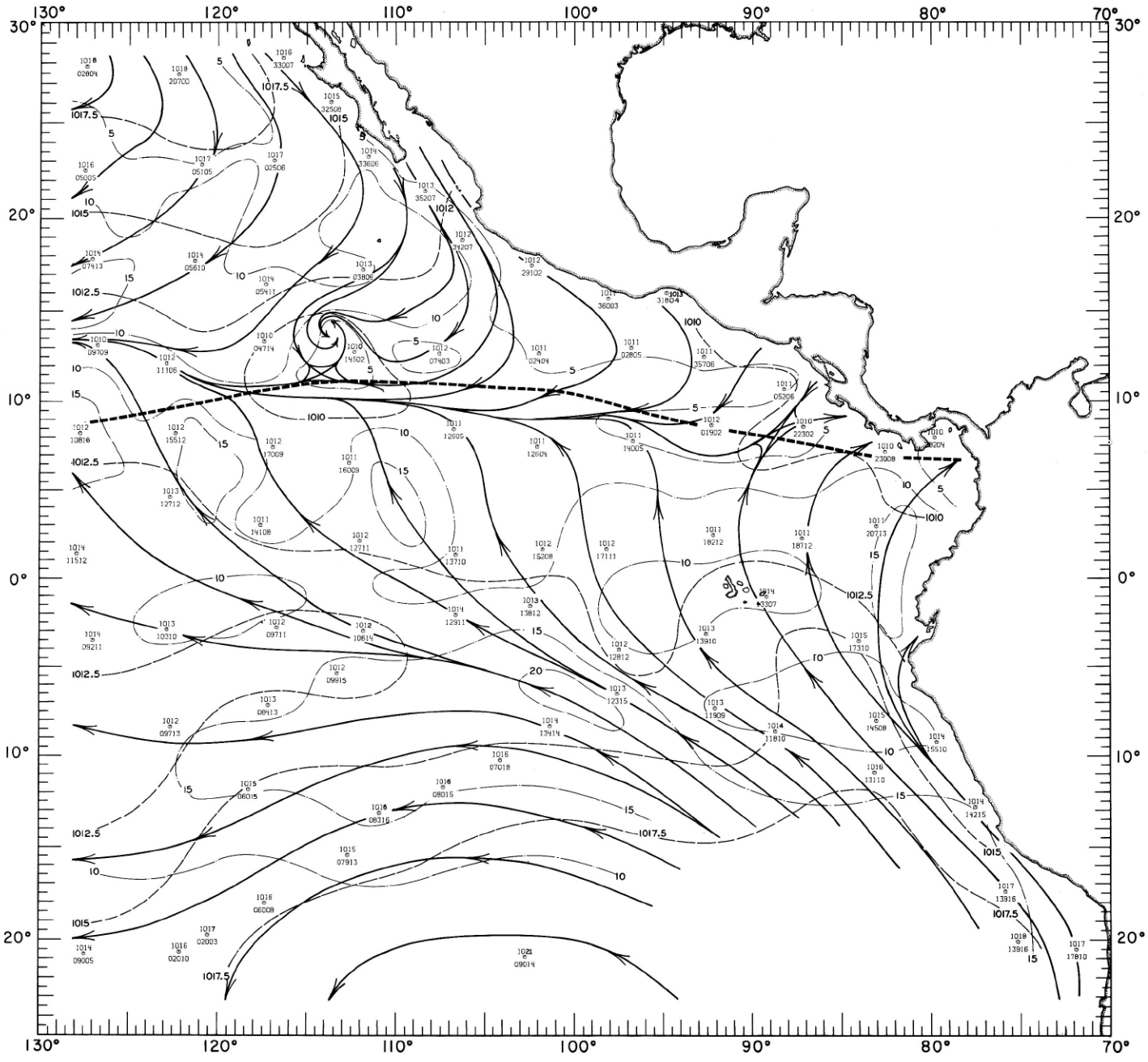

50-MW-3.

FIGURE 50-MW-3.— Analyses of the surface air pressure and surface winds from all available ship observations, averaged over 2-degree (latitude-longitude) squares for the period November 1-14, 1967. Heavy dashed lines are isobars. Solid lines are streamlines showing the mean resultant direction of wind flow. Light dash-dot lines are isotachs indicating mean resultant wind speed (kn.). Pressure (mb.) averaged for 5-degree squares is plotted above the mean position of the square, and resultant wind direction followed by speed (kn.) is plotted below. The monthly climatological position of the intertropical convergence zone is shown by a wide dashed band.

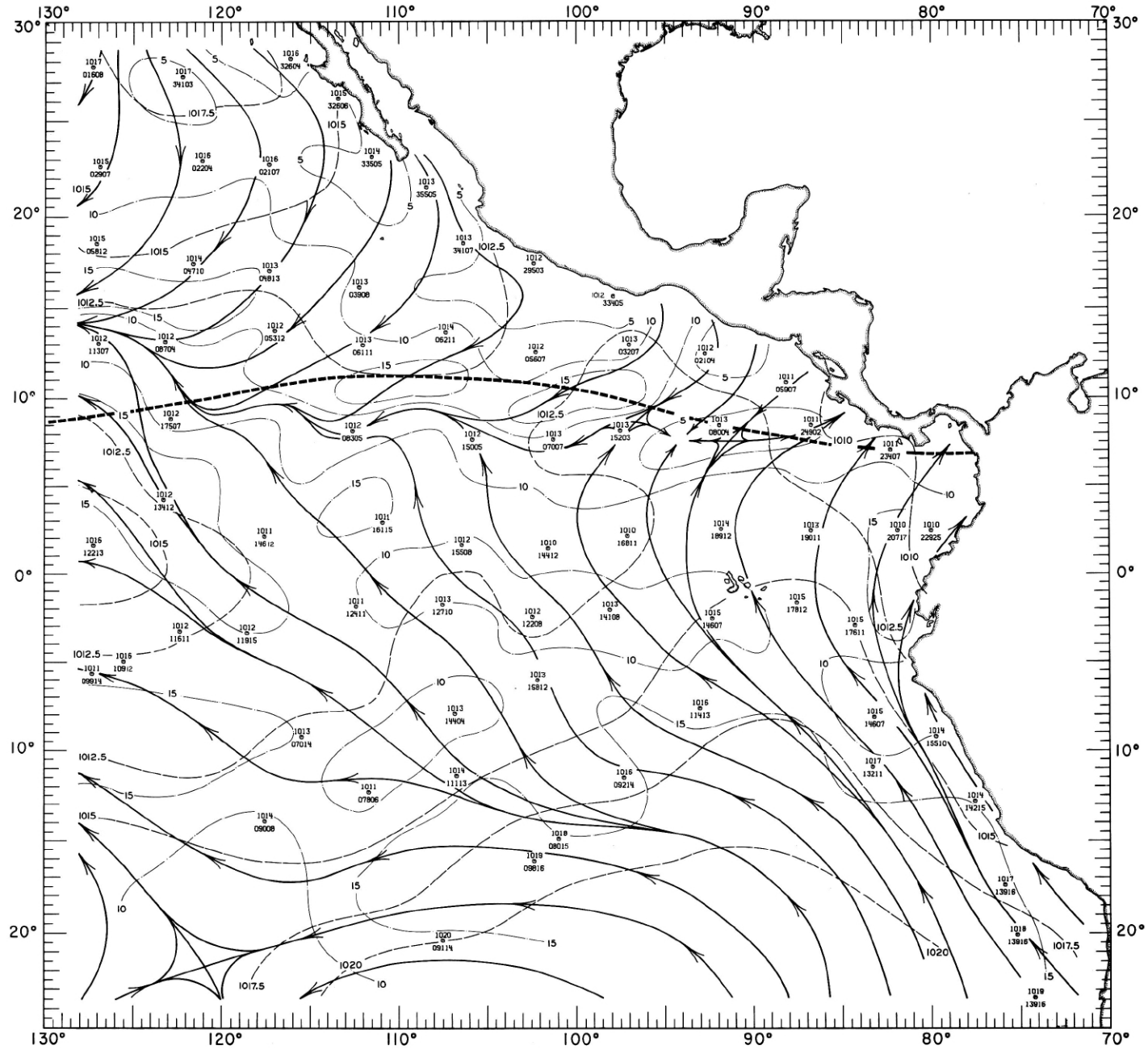

50-MW-4.

FIGURE 50-MW-4.—Analyses of the surface air pressure and surface winds from all available ship observations, averaged over 2-degree (latitude-longitude) squares for the period November 15-30, 1967. Heavy dashed lines are isobars. Solid lines are streamlines showing the mean resultant direction of wind flow. Light dash-dot lines are isotachs indicating mean resultant wind speed (kn.). Pressure (mb.) averaged for 5-degree squares is plotted above the mean position of the square, and resultant wind direction followed by speed (kn.) is plotted below. The monthly climatological position of the intertropical convergence zone is shown by a wide dashed band.

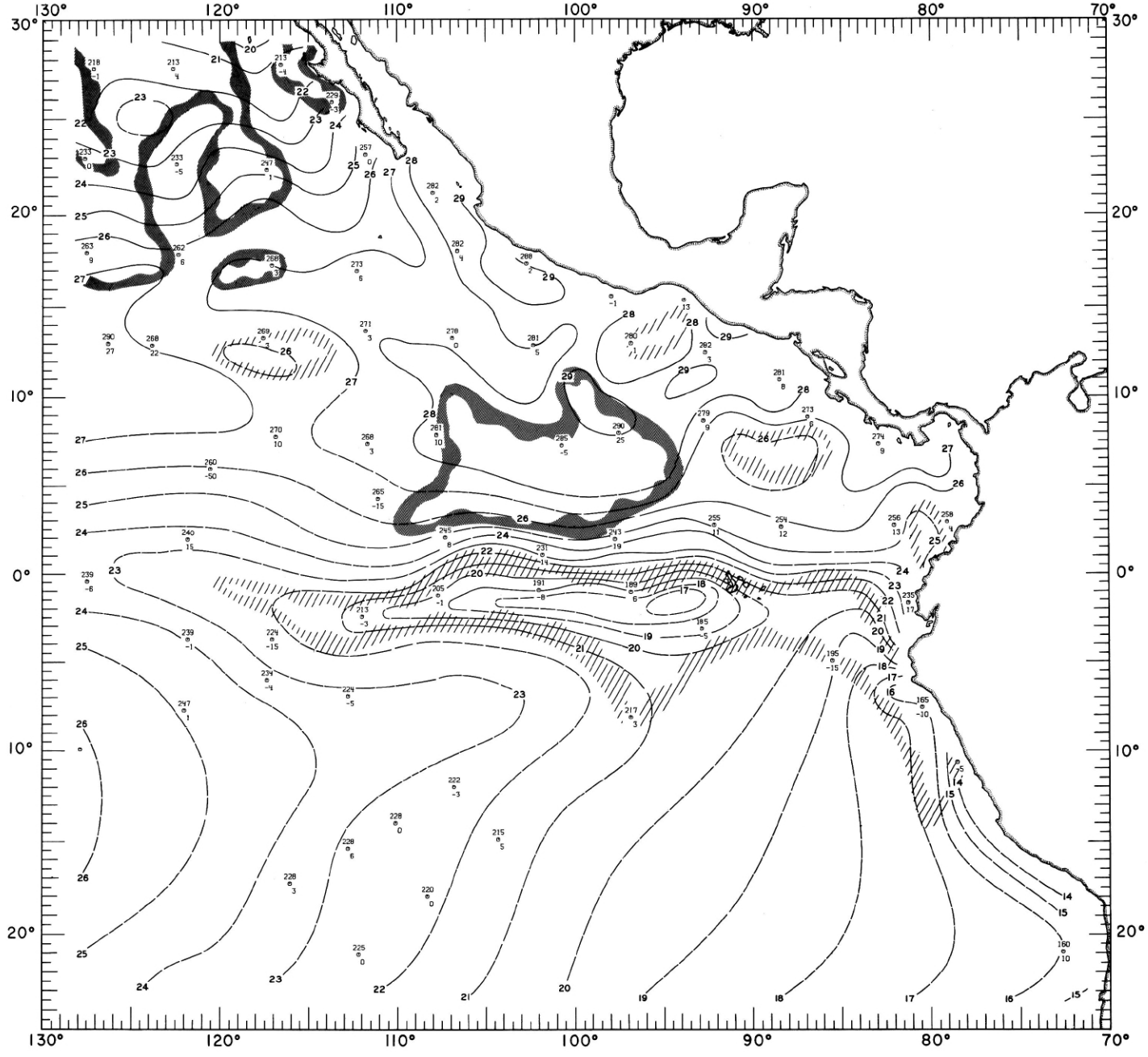

50-MT-1.

FIGURE 50-MT-1.—Analysis of sea surface temperatures based on averages for 2-degree (latitude-longitude) squares from all available ship observations for the period October 1-15, 1967. Solid lines are sea surface isotherms (°C.); the isotherms are dashed where data are sparse. Dark hatching outlines areas with positive temperature anomalies (computed from mean sea surface temperatures averaged over 22 years) greater than 1° C.; light hatching shows areas with negative anomalies greater than 1° C. Sea surface temperature (°C. x 10) averaged for 5-degree squares is plotted above the mean position of the square; sea temperature minus air temperature difference (°C. x 10) is plotted below the symbol.

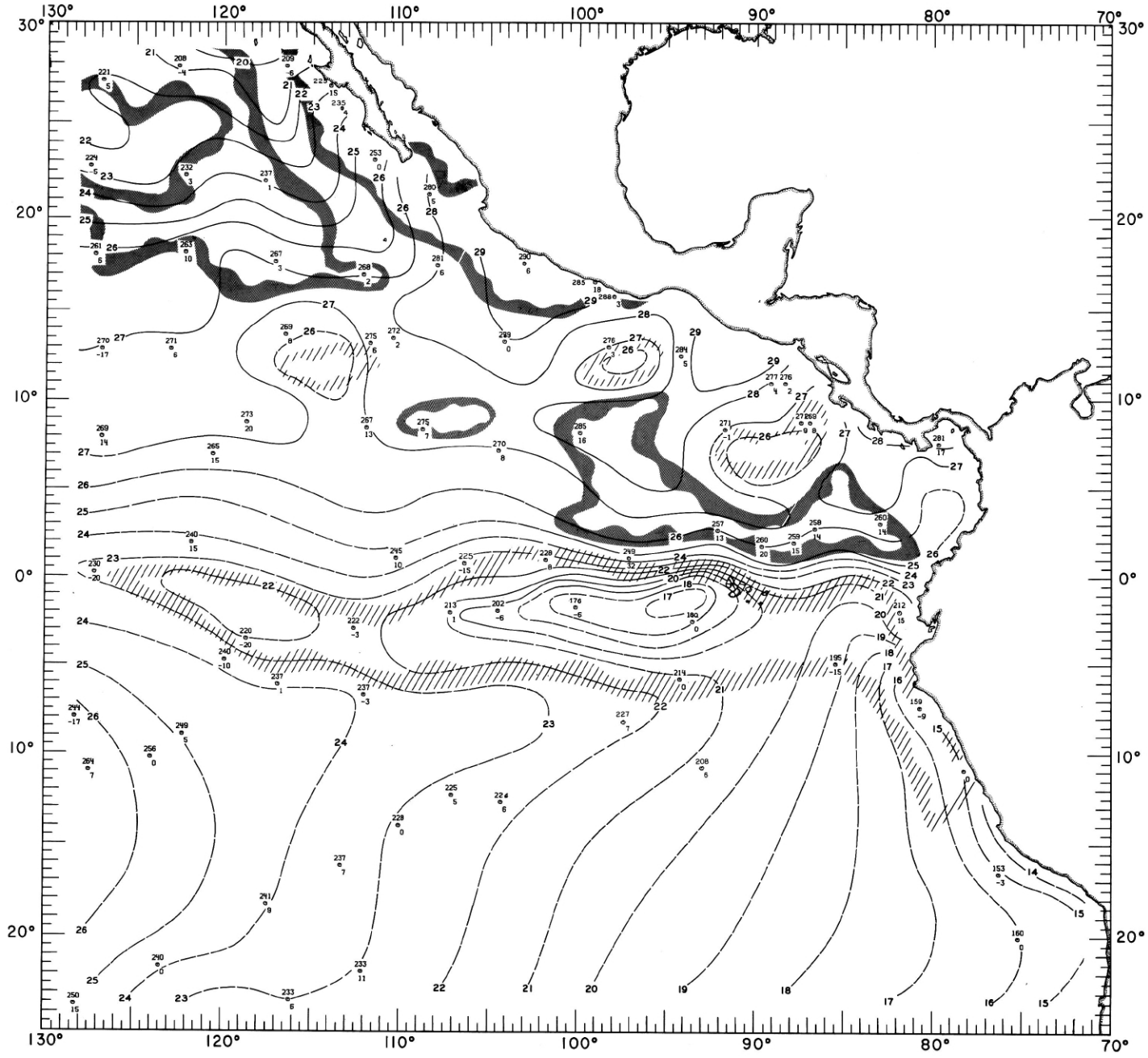

50-MT-2.

FIGURE 50-MT-2.—Analysis of sea surface temperatures based on averages for 2-degree (latitude-longitude) squares from all available ship observations for the period October 16-31, 1967. Solid lines are sea surface isotherms (°C.); the isotherms are dashed where data are sparse. Dark hatching outlines areas with positive temperature anomalies (computed from mean sea surface temperatures averaged over 22 years) greater than 1° C.; light hatching shows areas with negative anomalies greater than 1° C. Sea surface temperature (°C. x 10) averaged for 5-degree squares is plotted above the mean position of the square; sea temperature minus air temperature difference (°C. x 10) is plotted below the symbol.

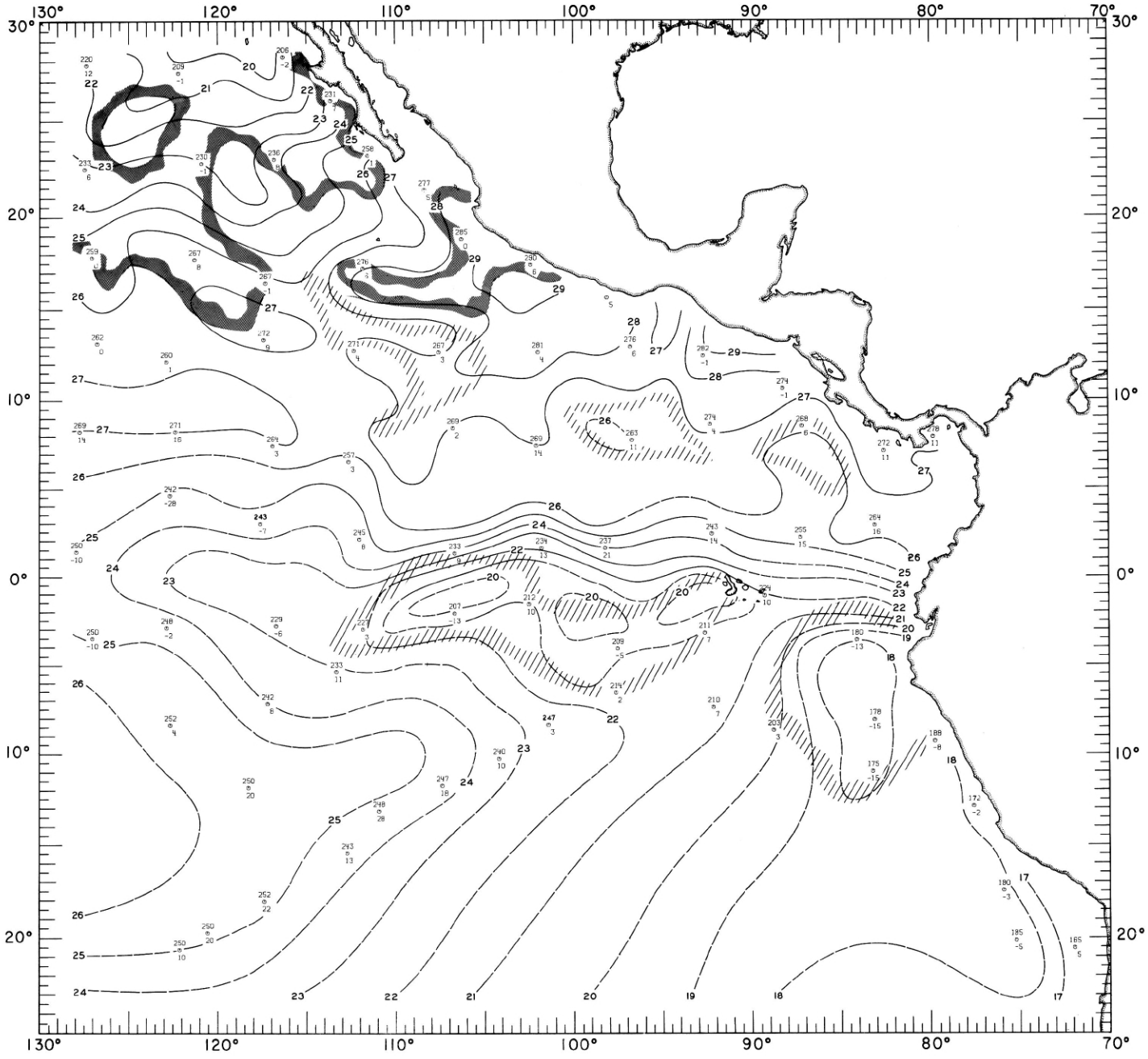

50-MT-3.

FIGURE 50-MT-3.—Analysis of sea surface temperatures based on averages for 2-degree (latitude-longitude) squares from all available ship observations for the period November 1-14, 1967. Solid lines are sea surface isotherms (°C.); the isotherms are dashed where data are sparse. Dark hatching outlines areas with positive temperature anomalies (computed from mean sea surface temperatures averaged over 22 years) greater than 1° C.; light hatching shows areas with negative anomalies greater than 1° C. Sea surface temperature (°C. x 10) averaged for 5-degree squares is plotted above the mean position of the square; sea temperature minus air temperature difference (°C. x 10) is plotted below the symbol.

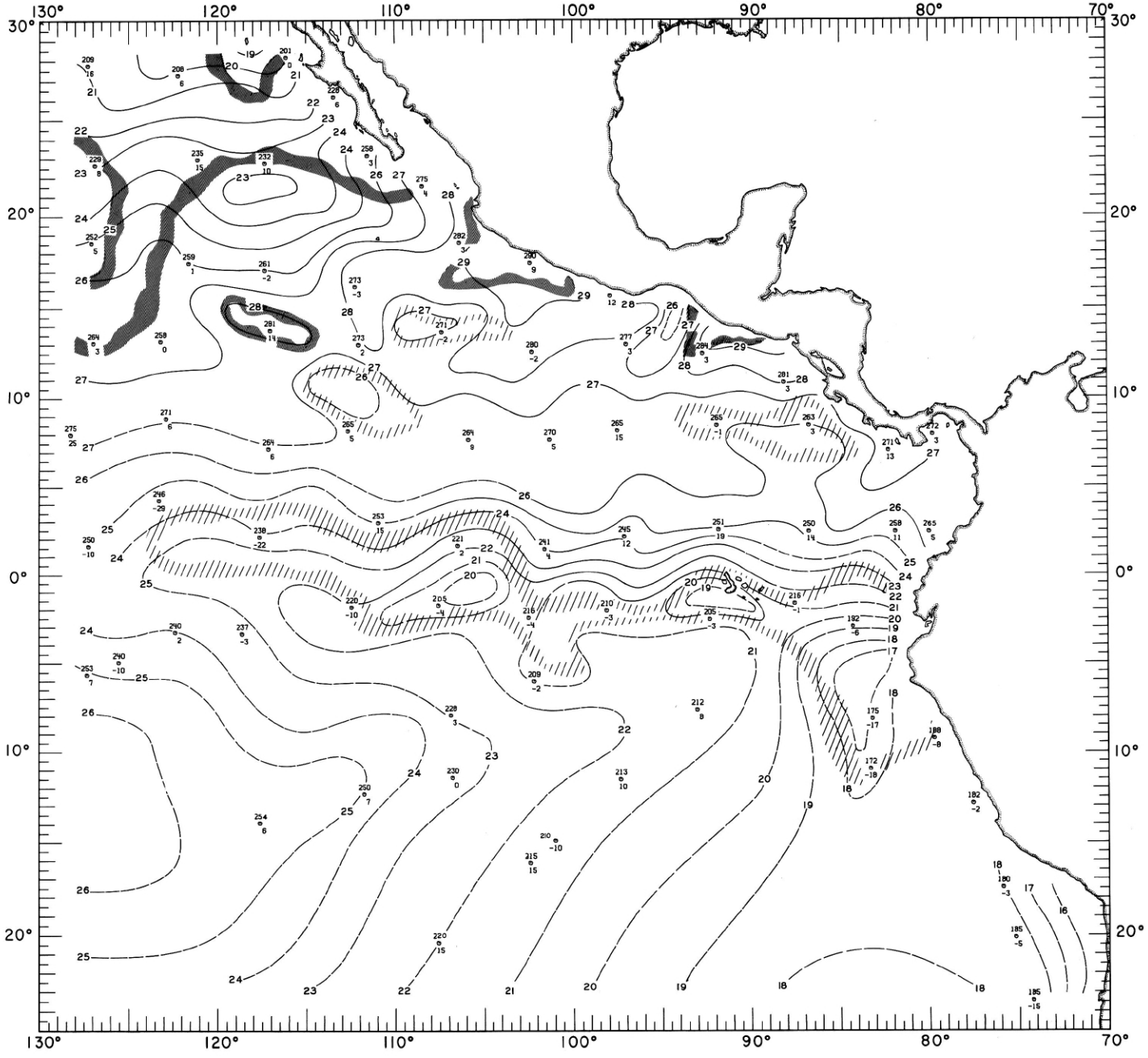

50-MT-4.

FIGURE 50-MT-4.—Analysis of sea surface temperatures based on averages for 2-degree (latitude-longitude) squares from all available ship observations for the period November 15-30, 1967. Solid lines are sea surface isotherms (°C.); the isotherms are dashed where data are sparse. Dark hatching outlines areas with positive temperature anomalies (computed from mean sea surface temperatures averaged over 22 years) greater than 1° C.; light hatching shows areas with negative anomalies greater than 1° C. Sea surface temperature (°C. x 10) averaged for 5-degree squares is plotted above the mean position of the square; sea temperature minus air temperature difference (°C. x 10) is plotted below the symbol.

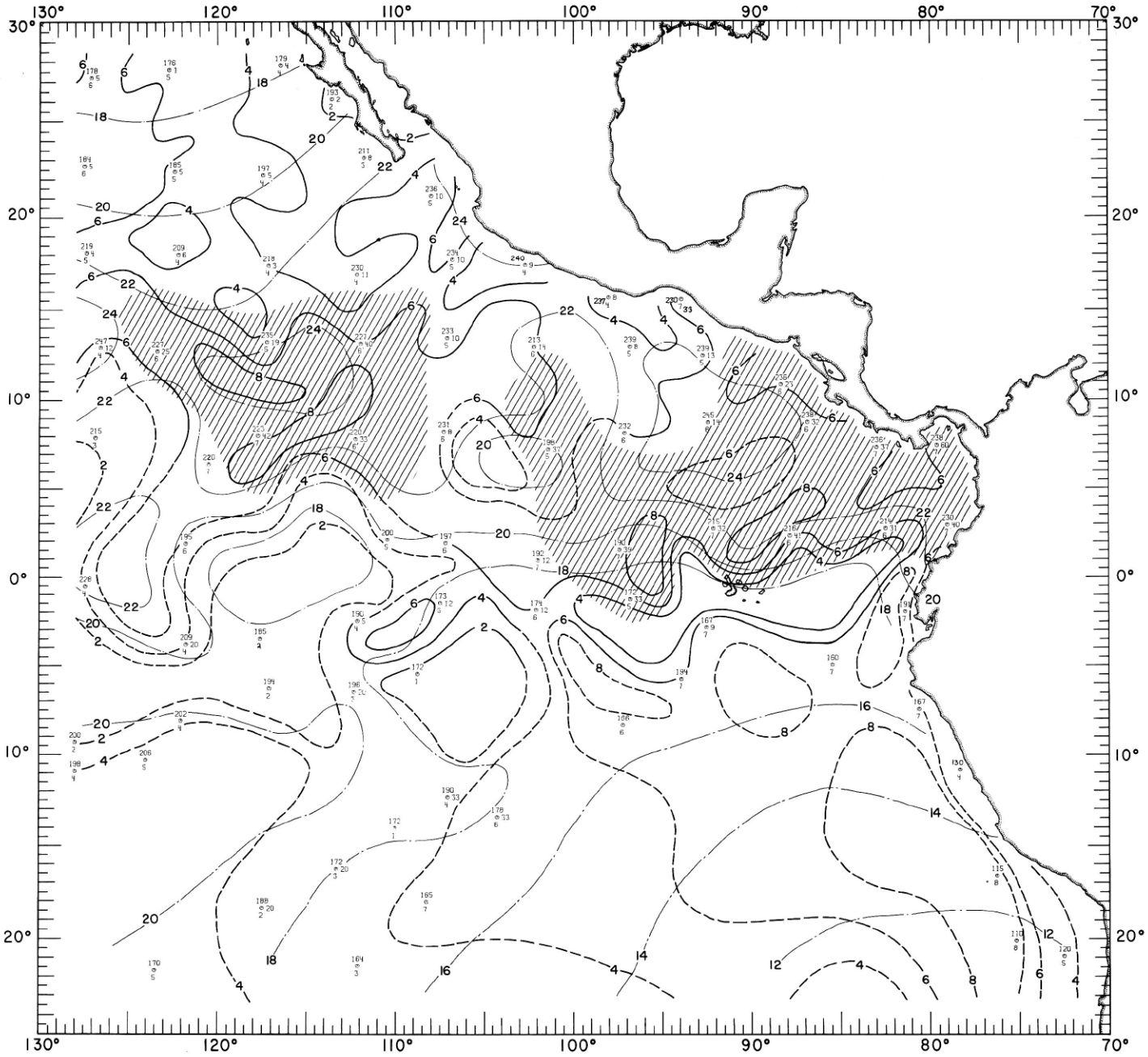

50-MC-1.

FIGURE 50-MC-1.—Analyses of the surface dew-point temperature of the air and total cloud cover based on 2-degree (latitude-longitude) averages from all available ship observations for the month of October 1967. Solid lines depict the monthly mean total cloud cover in oktas; the lines are dashed where data are sparse. Dash-dot lines are isotherms of the mean monthly dew-point temperature at 2-degree (C.) intervals. Areas where 15 percent or more of the ships reported rain of any type at or within sight of the ship are shaded. Dew-point temperature (°C. x 10) averaged for 5-degree squares is plotted above the mean position of the square, with total cloud cover (oktas) below and rainfall frequency (%) to the right of the symbol.

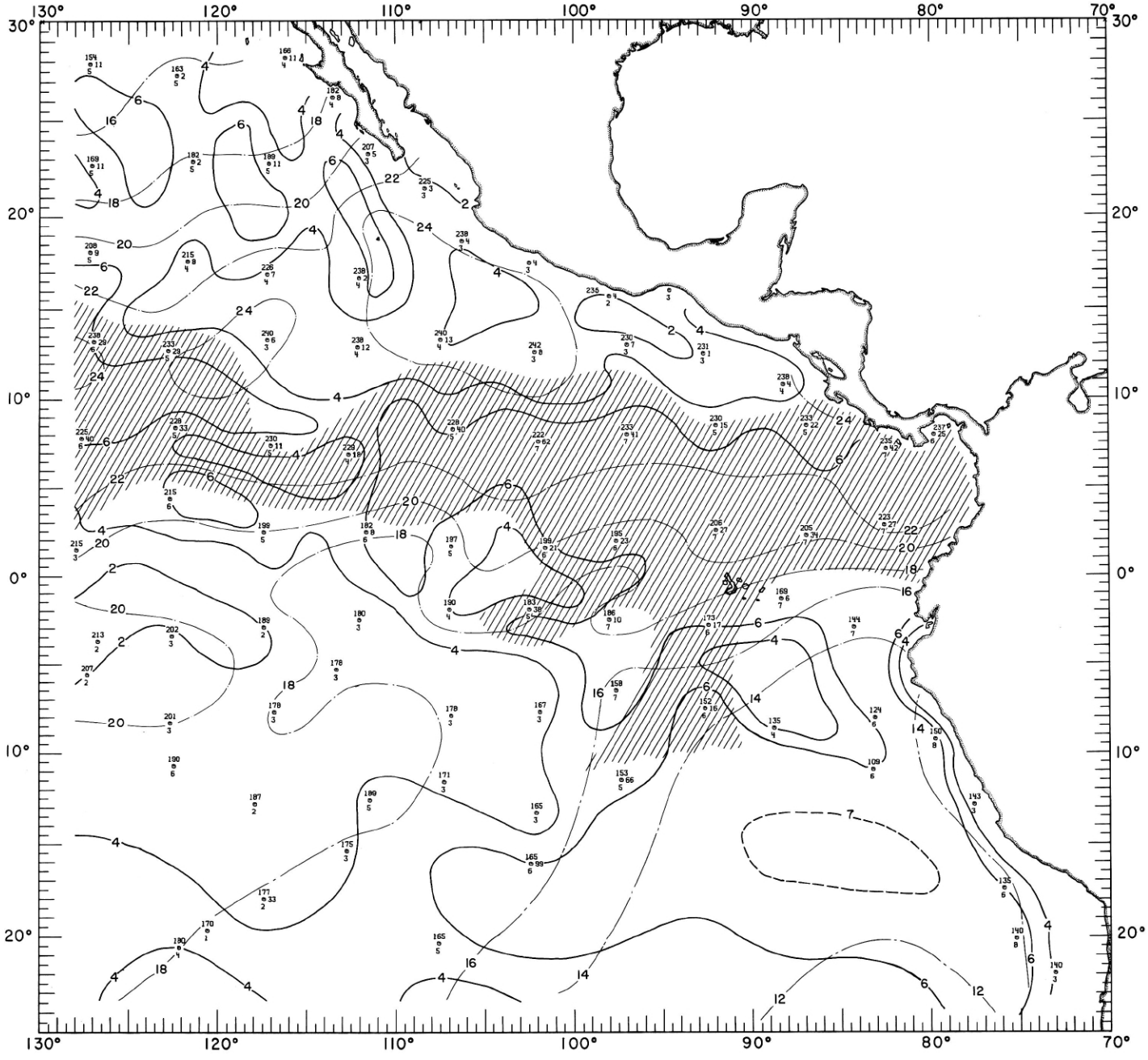

50-MC-2.

FIGURE 50-MC-2.—Analyses of the surface dew-point temperature of the air and total cloud cover based on 2-degree (latitude-longitude) averages from all available ship observations for the month of November 1967. Solid lines depict the monthly mean total cloud cover in oktas; the lines are dashed where data are sparse. Dash-dot lines are isotherms of the mean monthly dew-point temperature at 2-degree (C.) intervals. Areas where 15 percent or more of the ships reported rain of any type at or within sight of the ship are shaded. Dew-point temperature (°C. x 10) averaged for 5-degree squares is plotted above the mean position of the square, with total cloud cover (oktas) below and rainfall frequency (%) to the right of the symbol.

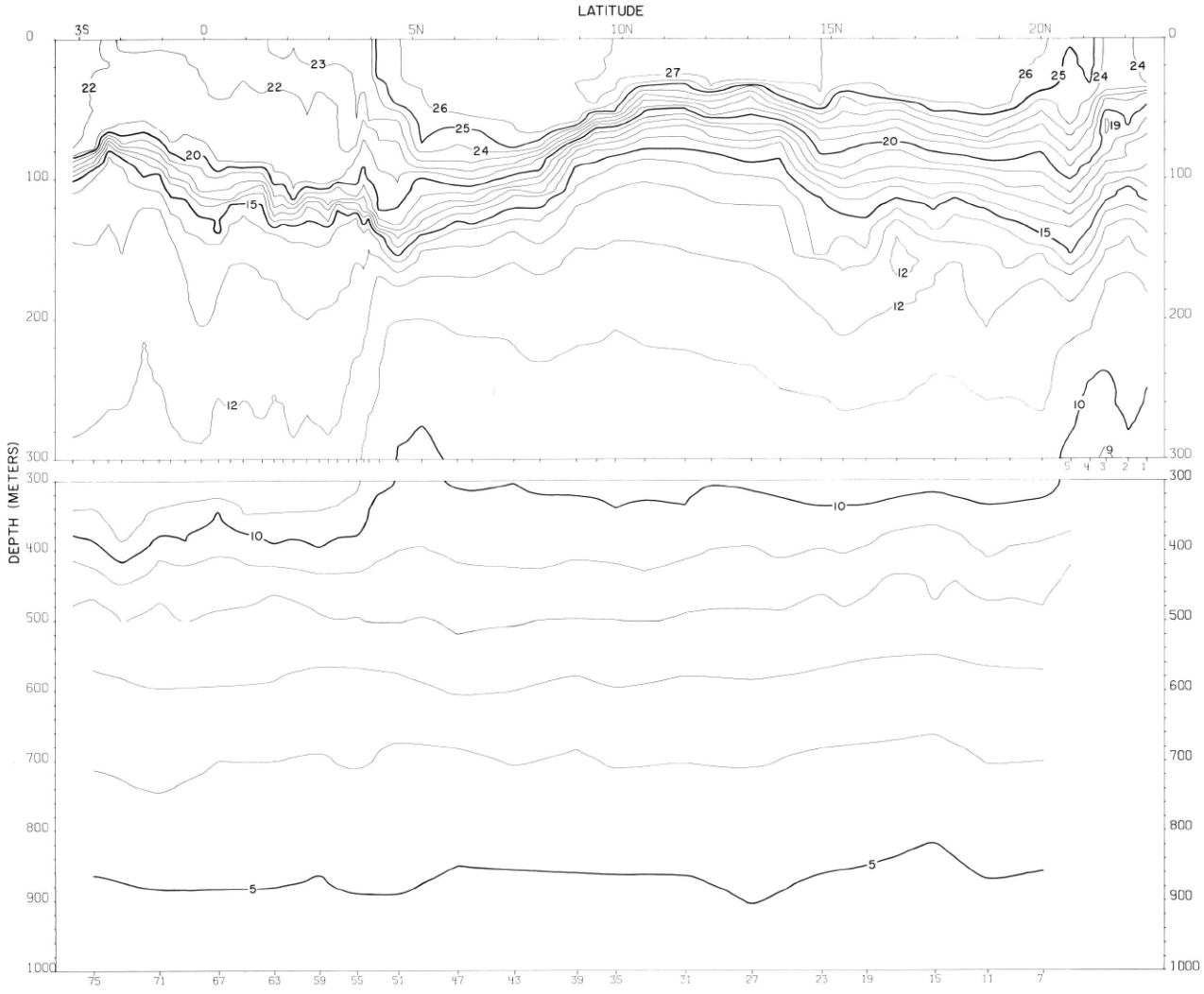

FIGURE 50-T-v1.—Vertical distribution of temperature (°C.) along 119°10′ W., October 20-29, 1967.

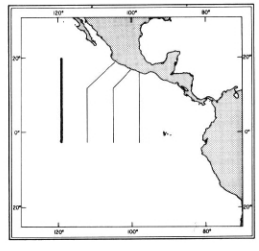

50-T-v1.

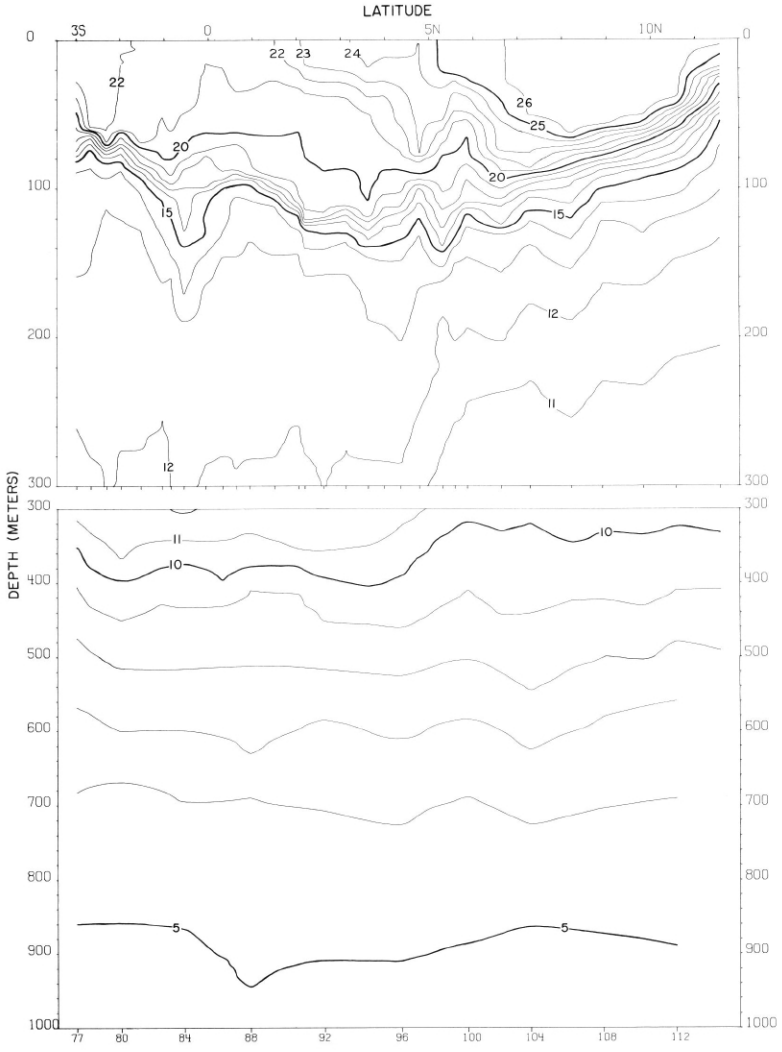

FIGURE 50-T-v2.—Vertical distribution of temperature (°C.) along 112°10′ W., October 30-November 4, 1967.

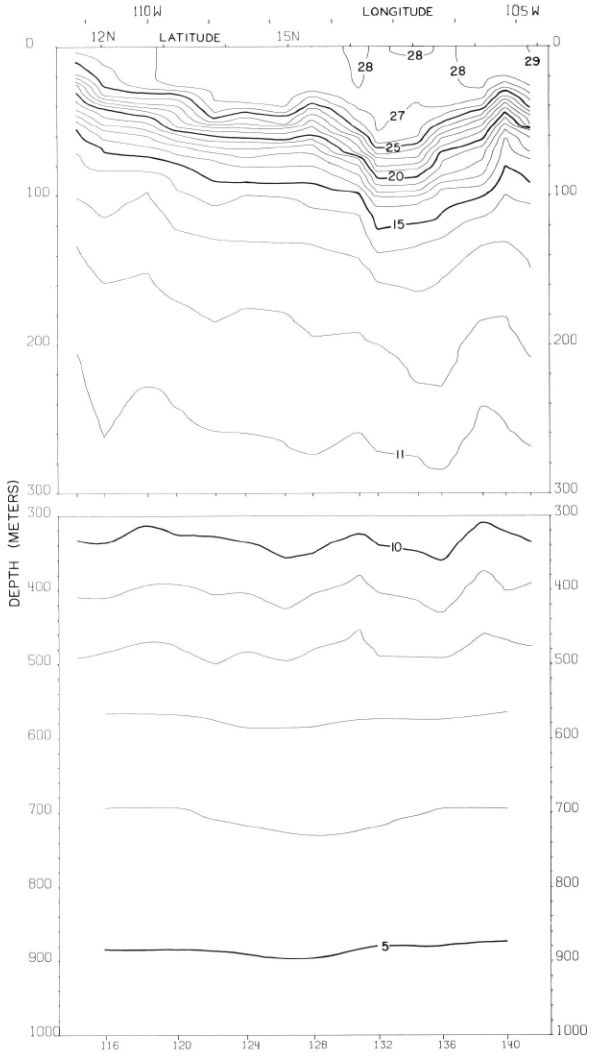

FIGURE 50-T-v3.—Vertical distribution of temperature (°C.) along a section from 12° N., 112°10′ W to Manzanillo, November 4-7, 1967.

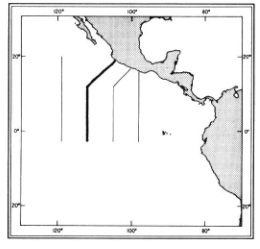

50-T-v2.

50-T-v3.

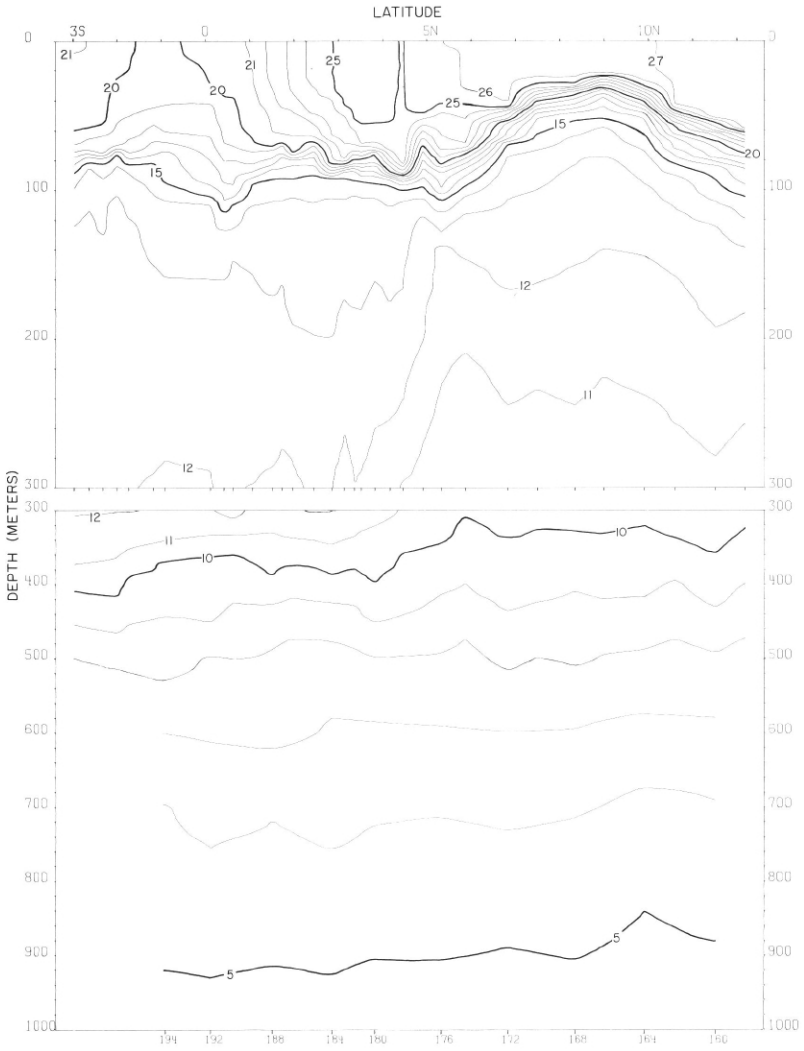

FIGURE 50-T-v5.—Vertical distribution of temperature (°C.) along 105°10′ W., November 13-18, 1967.

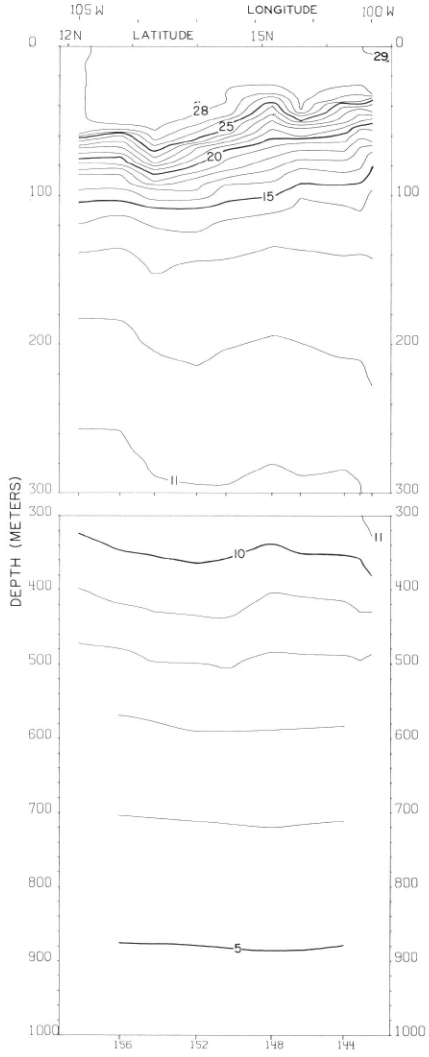

FIGURE 50-T-v4.—Vertical distribution of temperature (°C.) along a section from Acapulco to 12° N., 105°10′ W., November 11-13, 1967.

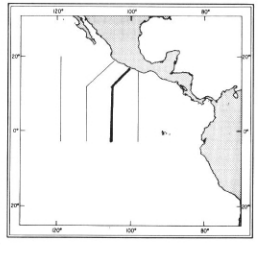

50-T-v4.

50-T-v5.

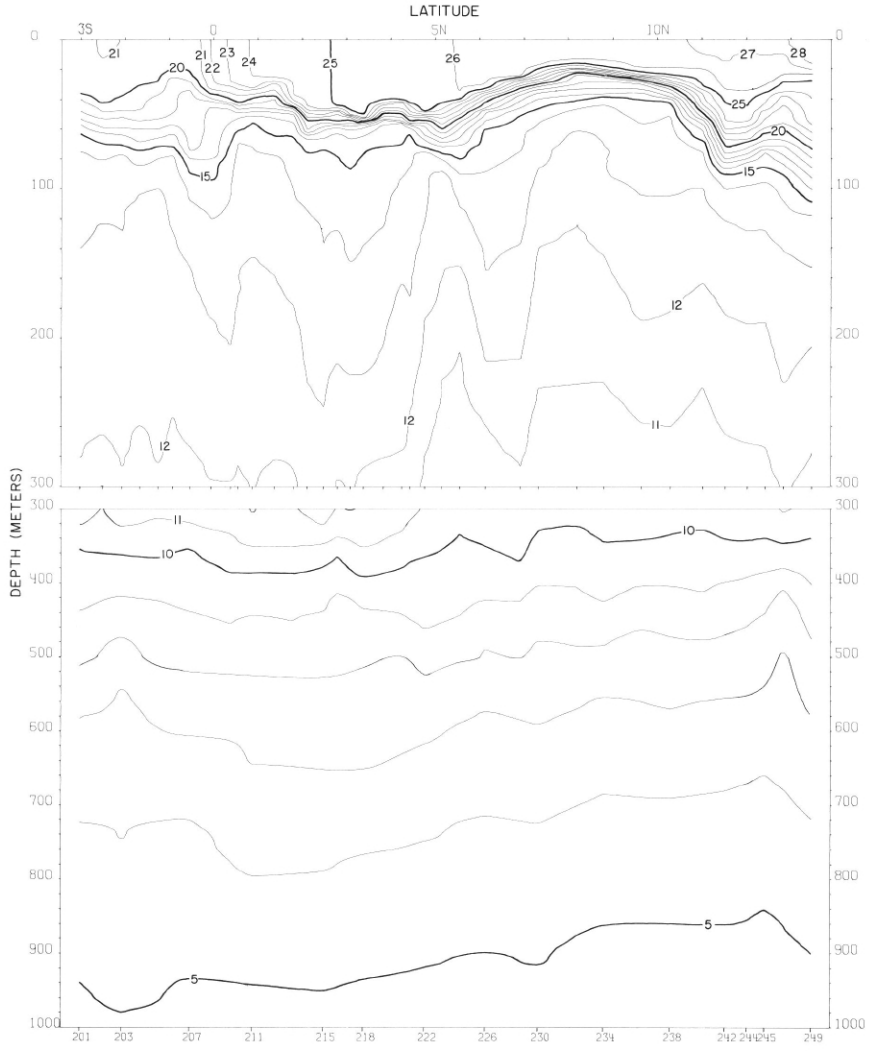

FIGURE 50-T-v6.—Vertical distribution of temperature (°C.) along 98°10′ W., November 20-26, 1967.

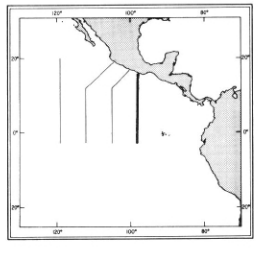

50-T-v6.

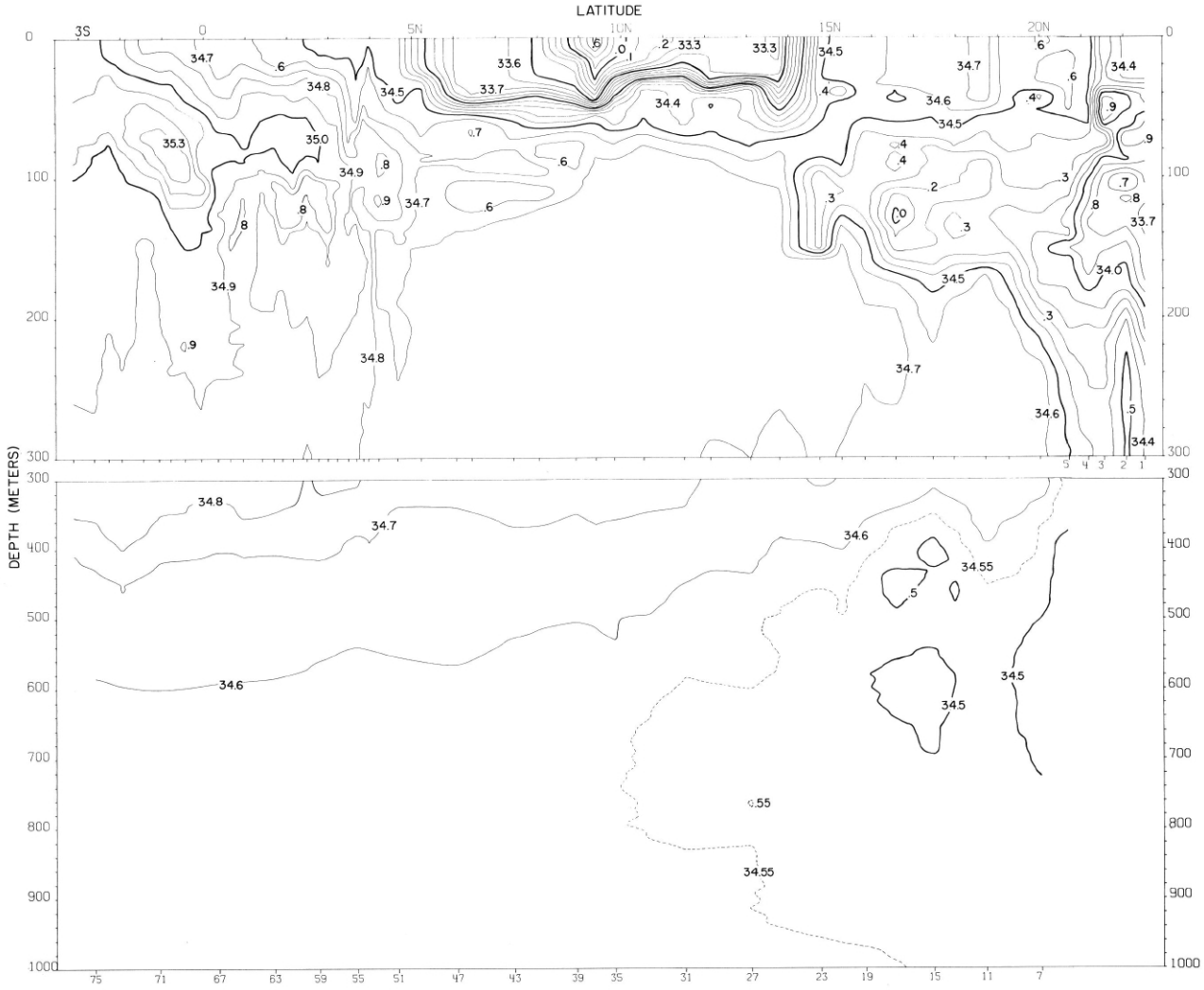

FIGURE 50-S-v1.—Vertical distribution of salinity (‰) along 119°10′ W., October 20-29, 1967.

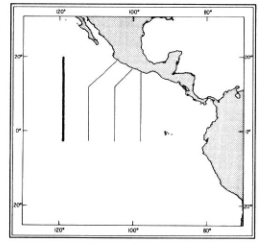

50-S-v1.

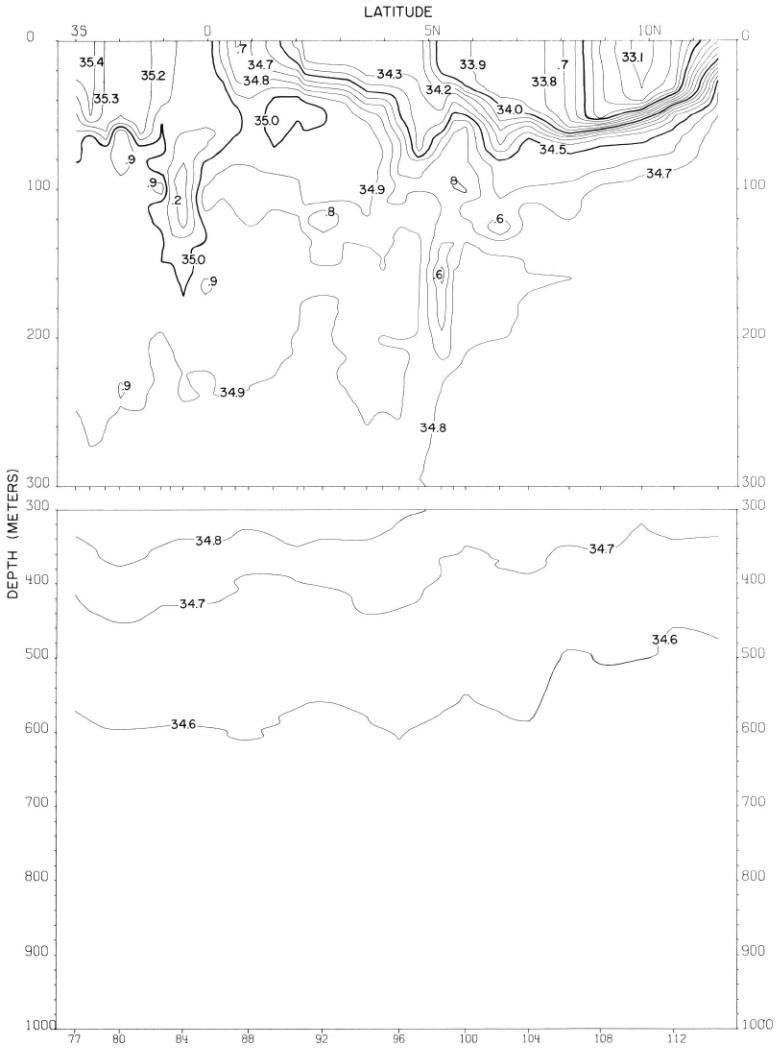

FIGURE 50-S-v2.—Vertical distribution of salinity (‰) along 112°10′ W., October 30-November 4, 1967.

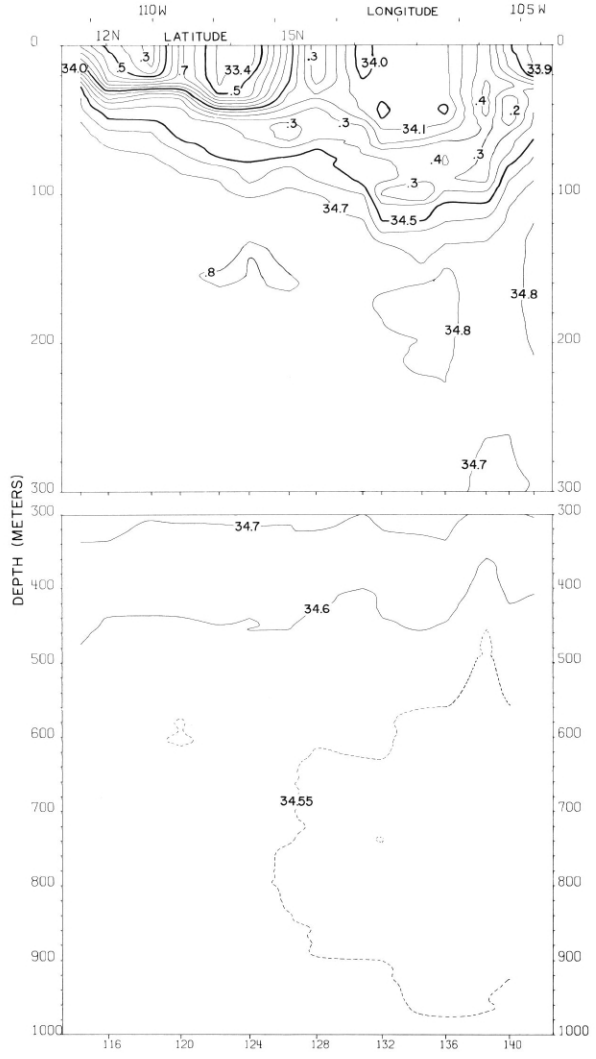

FIGURE 50-S-v3.—Vertical distribution of salinity (‰) along a section from 12° N., 112°10′ W. to Manzanillo, November 4-7, 1967.

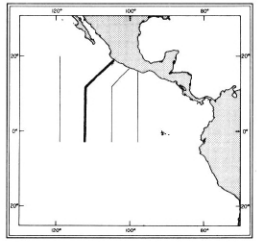

50-S-v2.

50-S-v3.

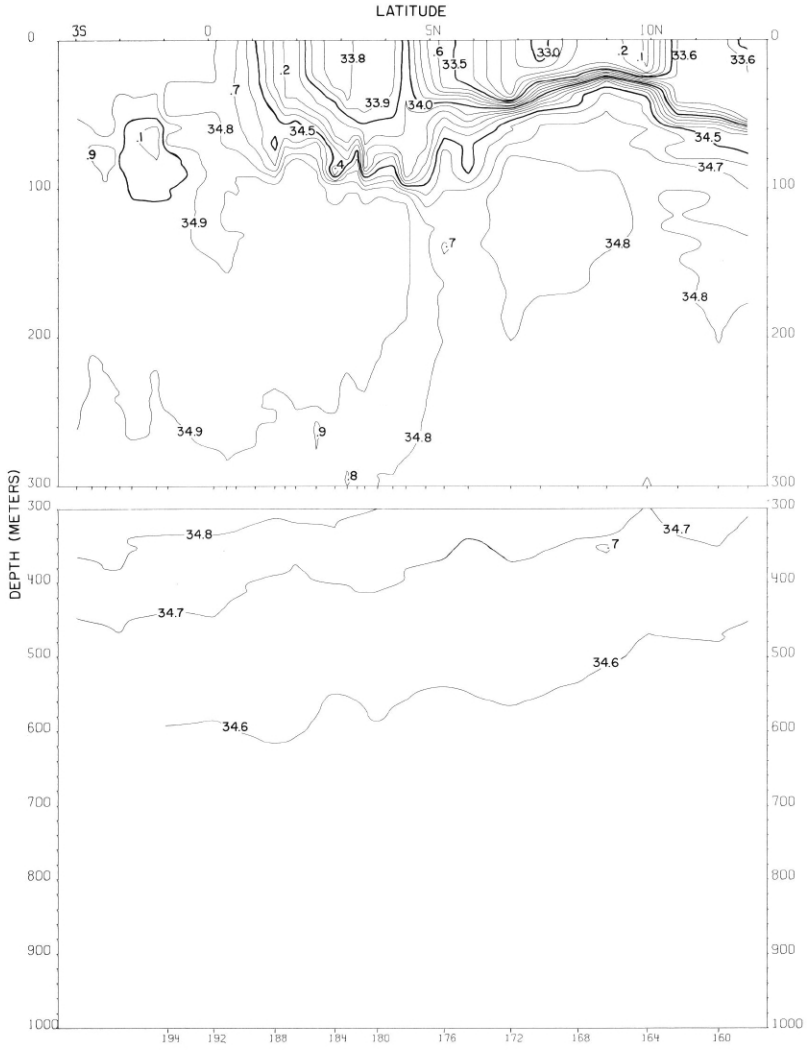

FIGURE 50-S-v5.—Vertical distribution of salinity (‰) along 105°10′ W., November 13-18, 1967.

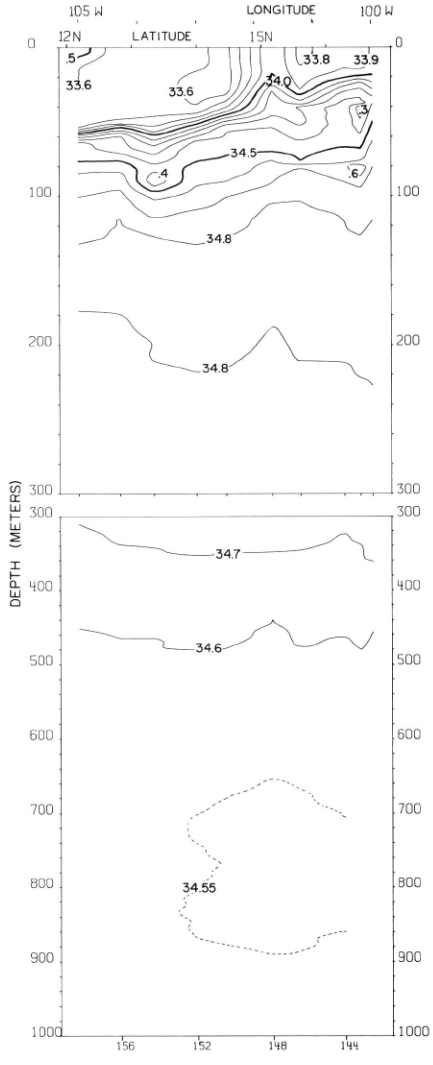

FIGURE 50-S-v4.—Vertical distribution of salinity (‰) along a section from Acapulco to 12° N., 105°10′ W., November 11-13, 1967.

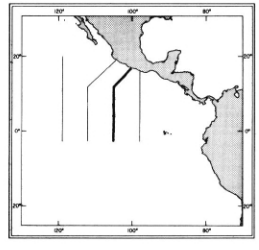

50-S-v4.

50-S-v5.

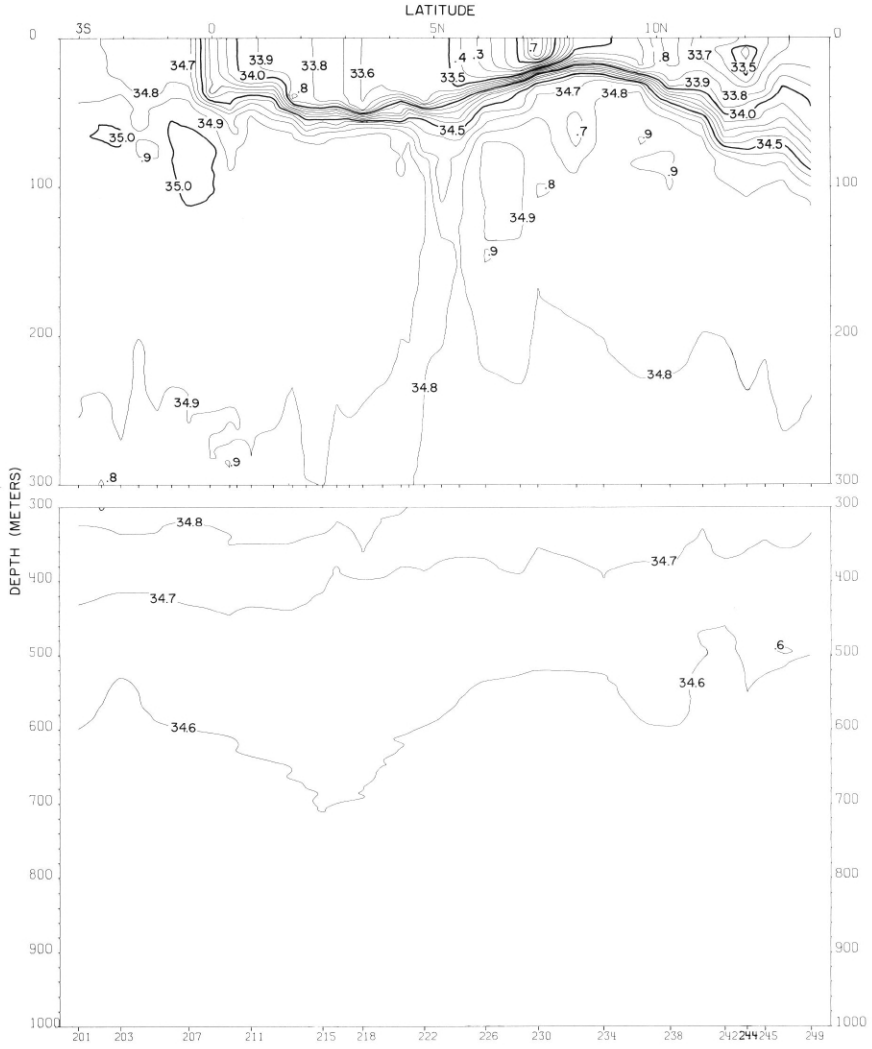

FIGURE 50-S-v6.—Vertical distribution of salinity (‰) along 98°10′ W., November 20-26, 1967.

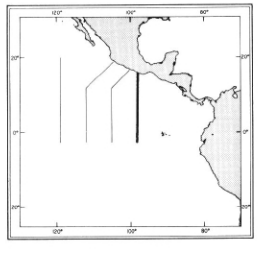

50-S-v6.

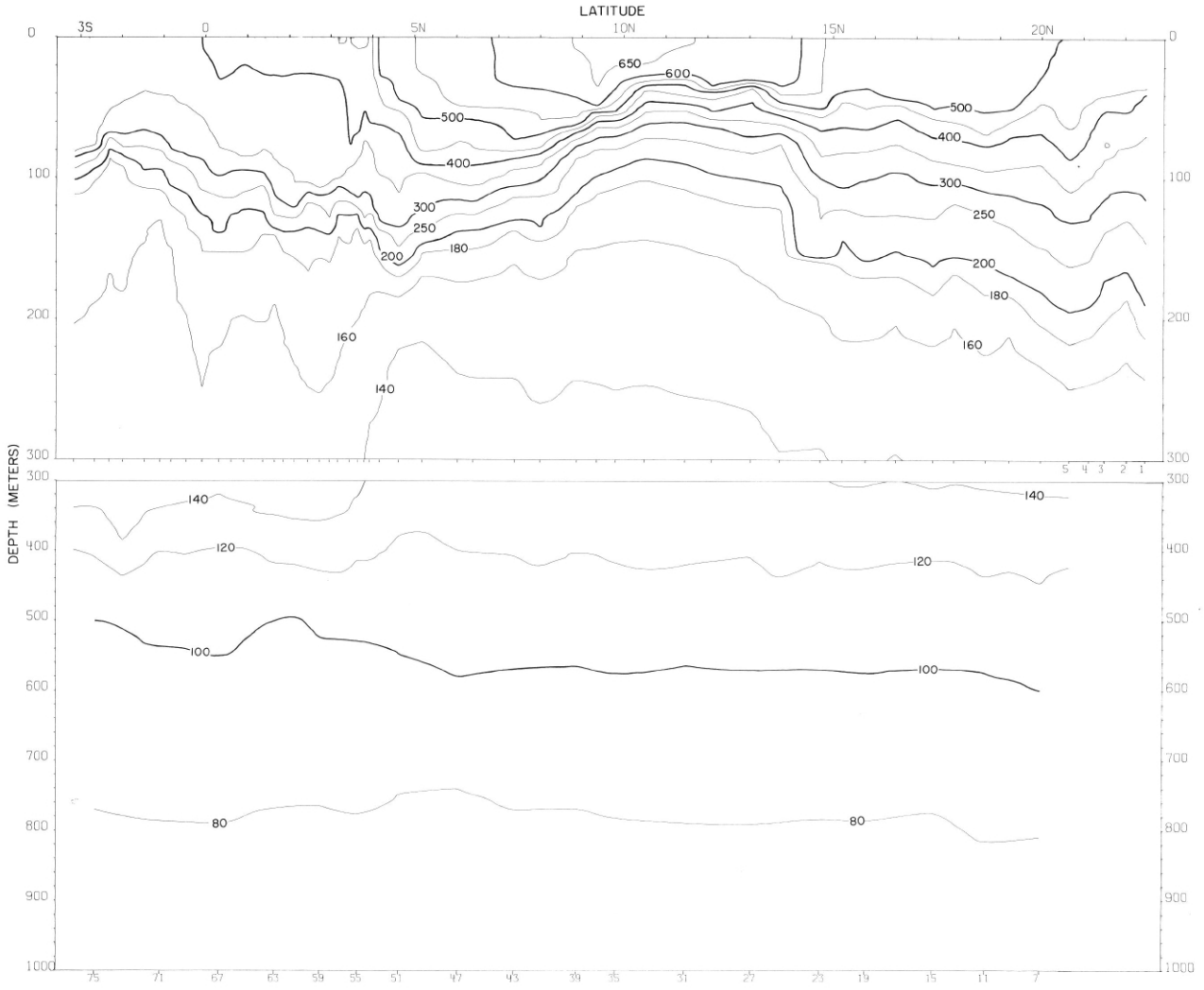

FIGURE 50-δ-v1.—Vertical distribution of thermosteric anomaly, δ_T, (cl./t.) along 119°10′ W., October 20-29, 1967.

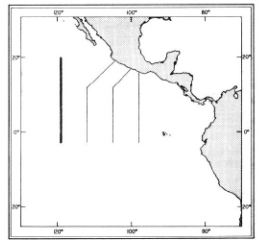

50-δ-v1.

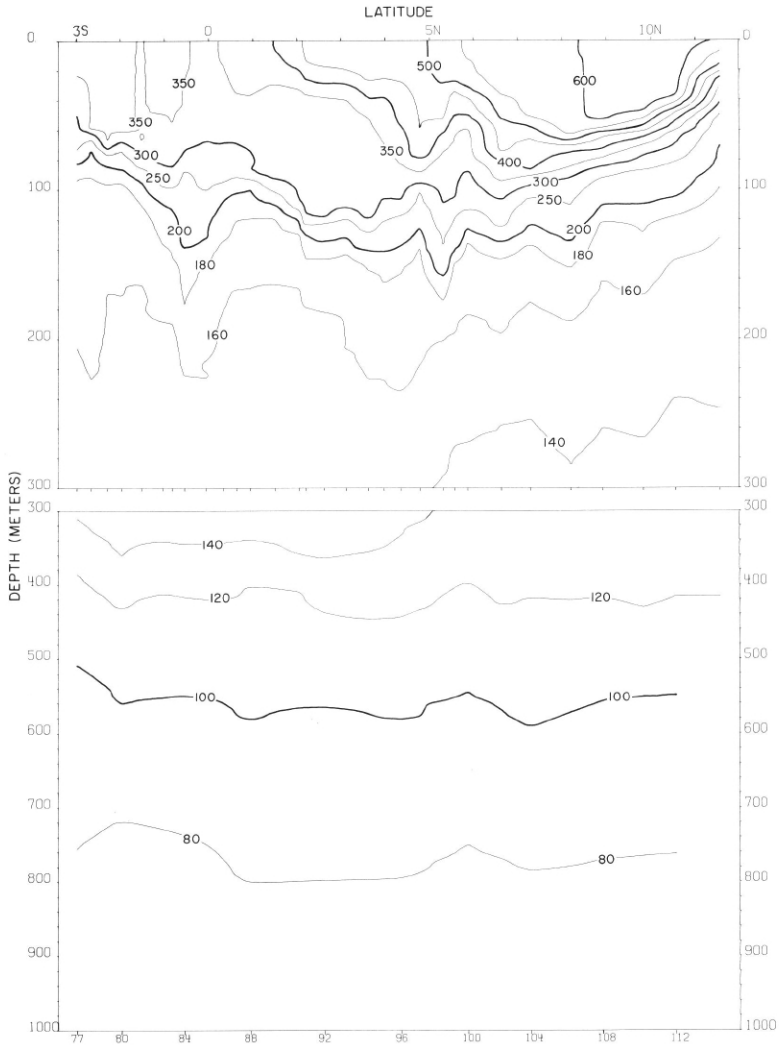

FIGURE 50-δ-v2.—Vertical distribution of thermosteric anomaly, δ_T, (cl./t.) along 112°10′ W., October 30-November 4, 1967.

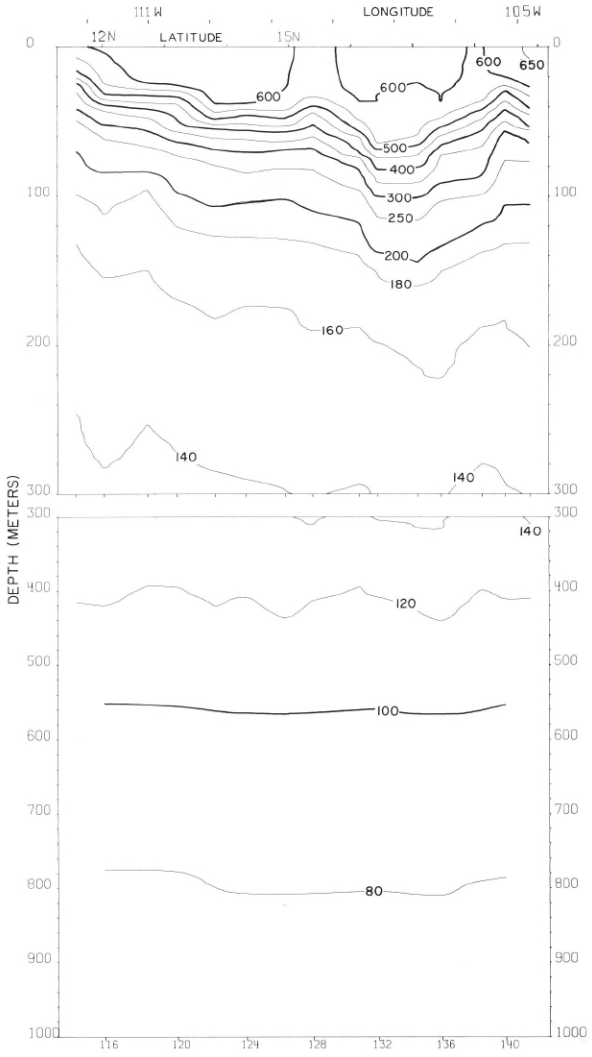

FIGURE 50-δ-v3.—Vertical distribution of thermosteric anomaly, δ_T, (cl./t.) along a section from 12° N., 112°10′ W. to Manzanillo, November 4-7, 1967.

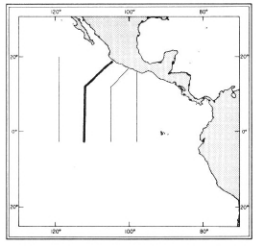

50-δ-v2.

50-δ-v3.

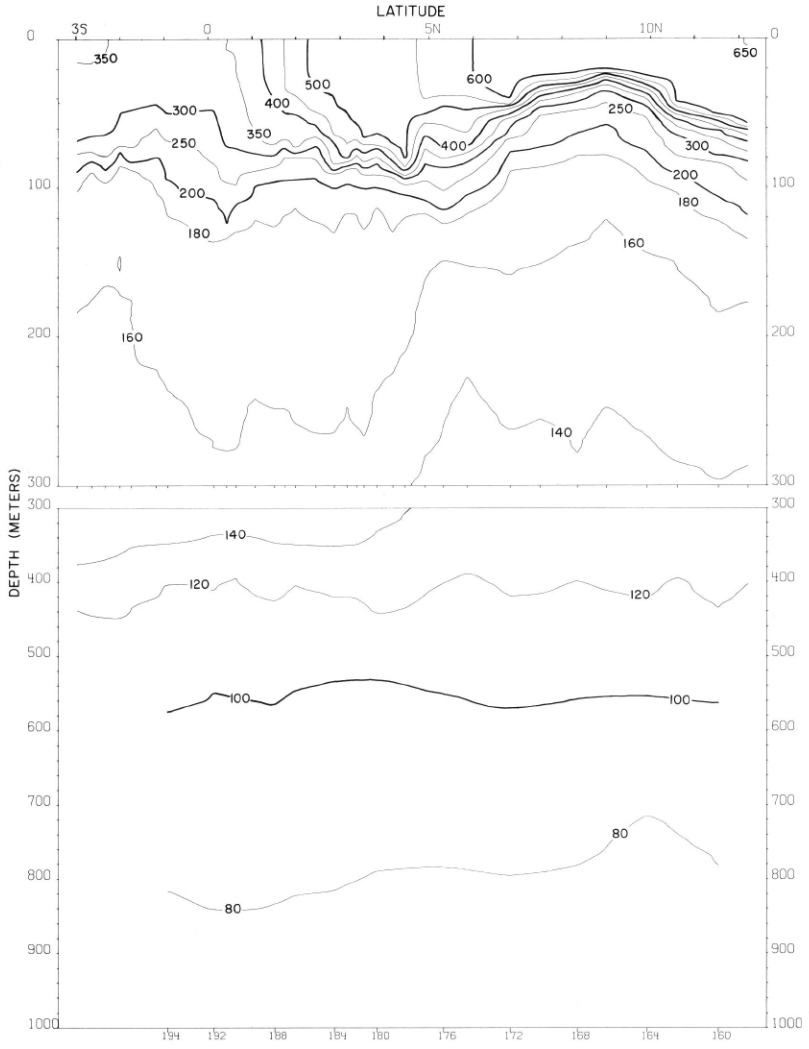

FIGURE 50-δ-v5.—Vertical distribution of thermosteric anomaly, δ_T, (cl./t.) along 105°10′ W., November 13-18, 1967.

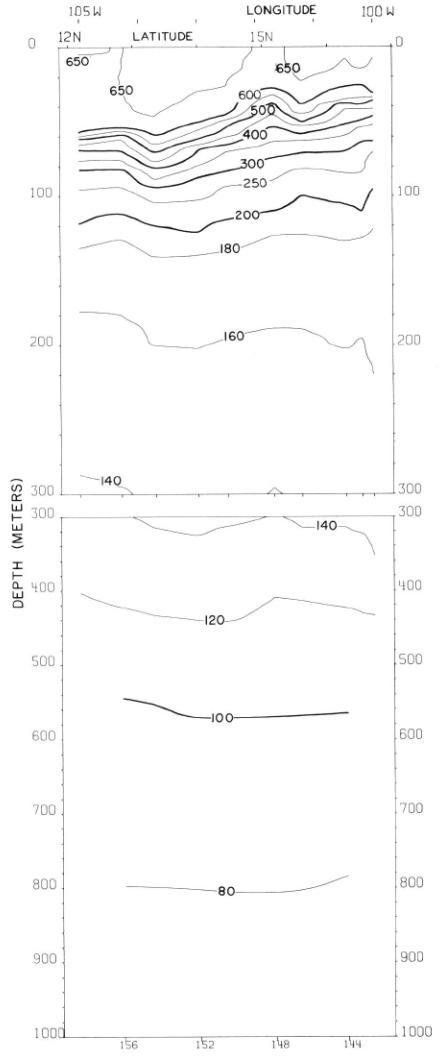

FIGURE 50-δ-v4.—Vertical distribution of thermosteric anomaly, δ_T, (cl./t.) along a section from Acapulco to 12° N., 105°10′ W., November 11-13, 1967.

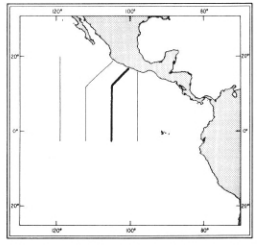

50-δ-v4.

50-δ-v5.

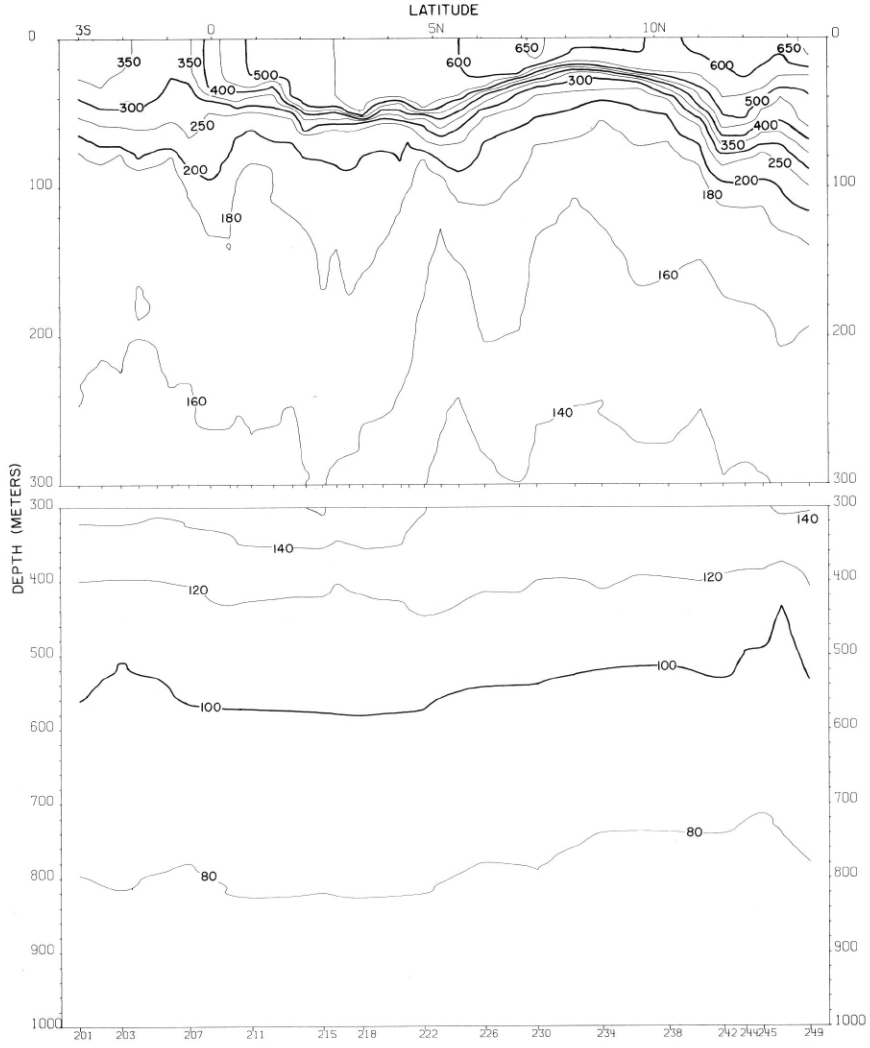

FIGURE 50-δ-v6.—Vertical distribution of thermosteric anomaly, δ_T, (cl./t.) along 98°10′ W., November 20-26, 1967.

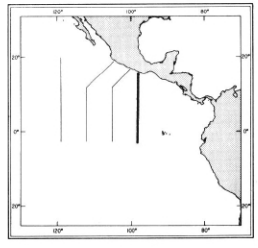

50-δ-v6.

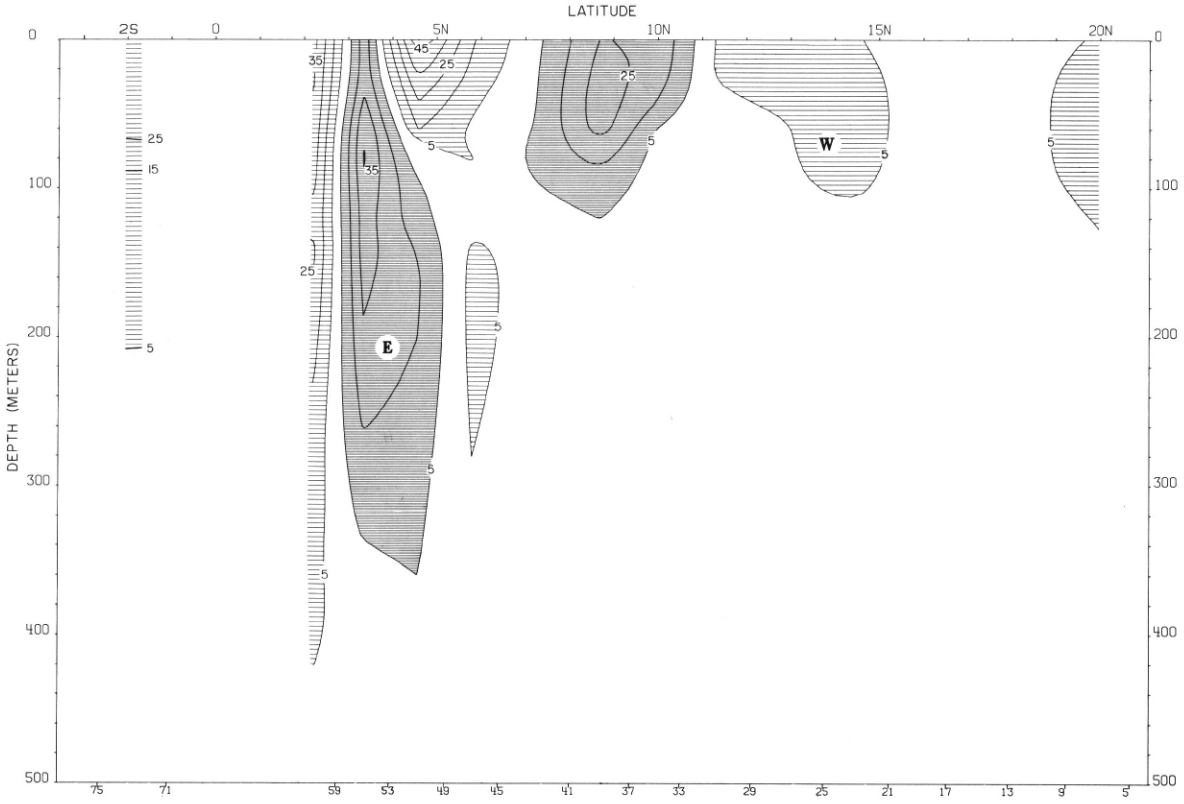

FIGURE 50-G-v1.—Vertical distribution of the zonal component of geostrophic velocity (cm./sec.), relative to 500 db., along 119°10′ W., October 20-29, 1967. Dark shading indicates eastward flow with a velocity greater than 5 cm./sec.; light shading indicates westward flow with a velocity greater than 5 cm./sec.

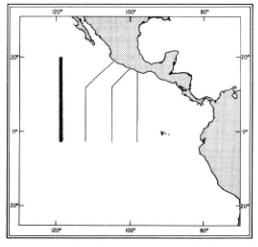

50-G-v1.

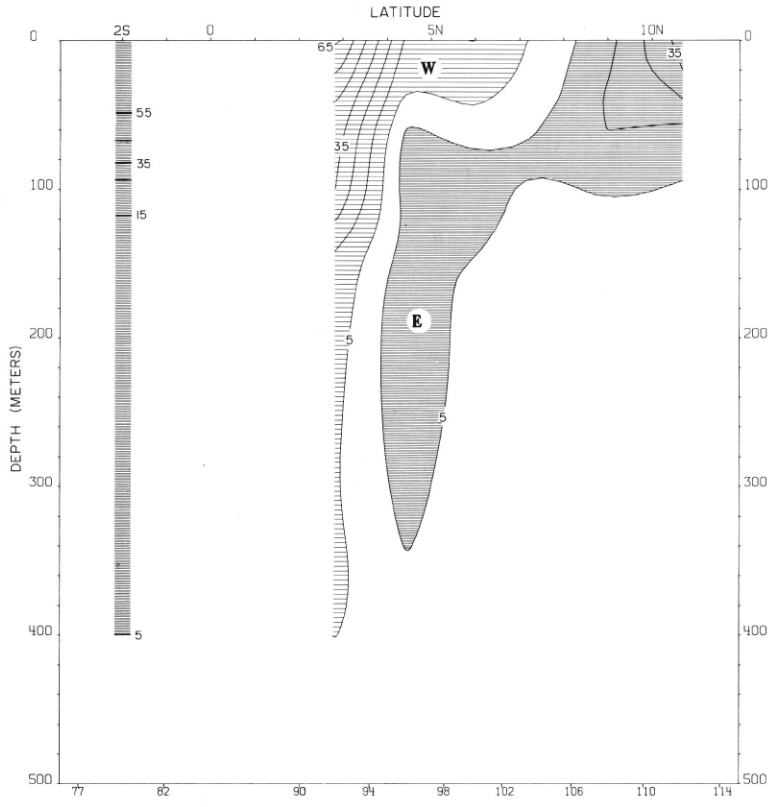

FIGURE 50-G-v2.—Vertical distribution of the zonal component of geostrophic velocity (cm./sec.), relative to 500 db., along 112°10′ W., October 30-November 4, 1967. Dark shading indicates eastward flow with a velocity greater than 5 cm./sec.; light shading indicates westward flow with a velocity greater than 5 cm./sec.

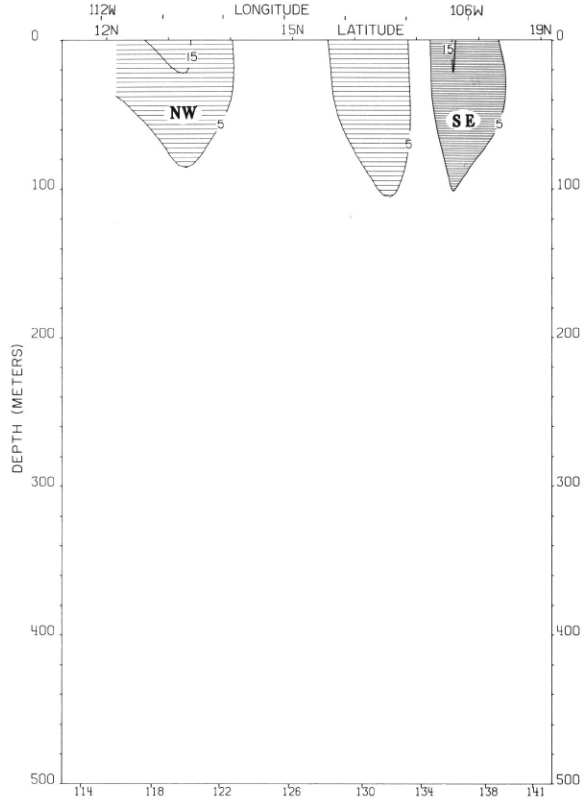

FIGURE 50-G-v3.—Vertical distribution of the component of geostrophic velocity (cm./sec.), relative to 500 db., normal to a section from 12° N., 112°10′ W. to Manzanillo, November 4-7, 1967. Dark shading indicates flow toward the southeast with a velocity greater than 5 cm./sec.; light shading indicates flow toward the northwest with a velocity greater than 5 cm./sec.

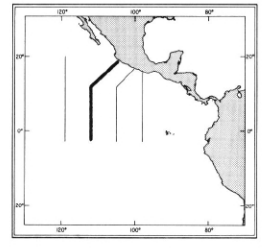

50-G-v2.

50-G-v3.

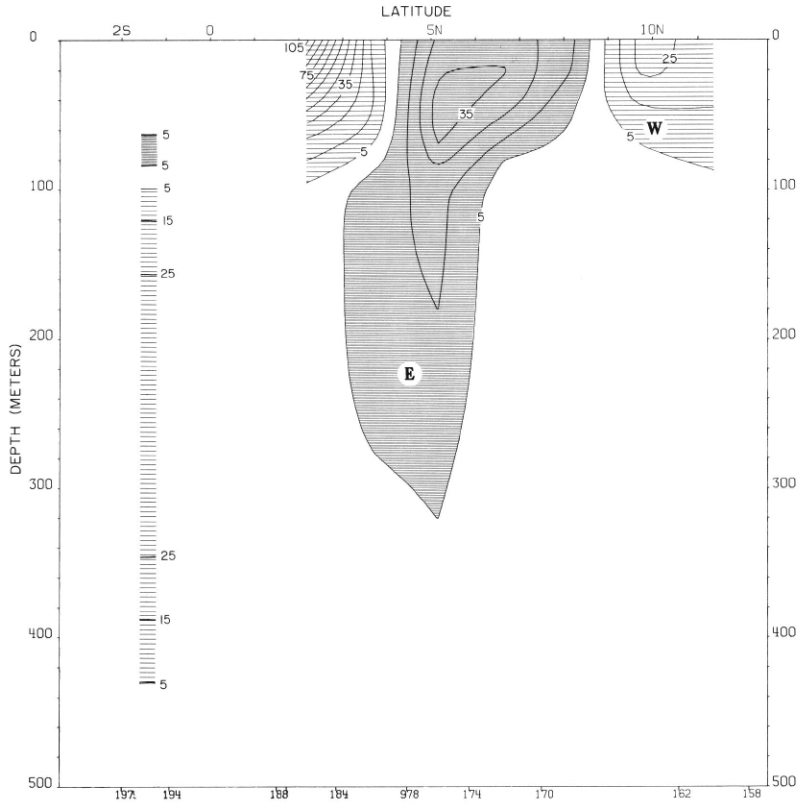

FIGURE 50-G-v5.—Vertical distribution of the zonal component of geostrophic velocity (cm./sec.), relative to 500 db., along 105° 10′ W., November 13-18, 1967. Dark shading indicates eastward flow with a velocity greater than 5 cm./sec.; light shading indicates westward flow with a velocity greater than 5 cm./sec.

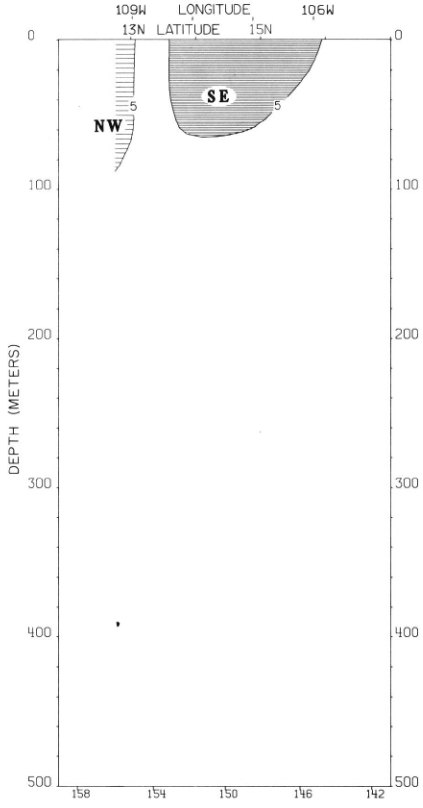

FIGURE 50-G-v4.—Vertical distribution of the component of geostrophic velocity (cm./sec.), relative to 500 db., normal to a section from Acapulco to 12° N., 105° 10′ W., November 11-13, 1967. Dark shading indicates flow toward the southeast with a velocity greater than 5 cm./sec.; light shading indicates flow toward the northwest with a velocity greater than 5 cm./sec.

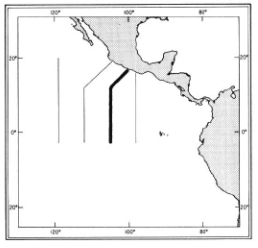

50-G-v4.

50-G-v5.

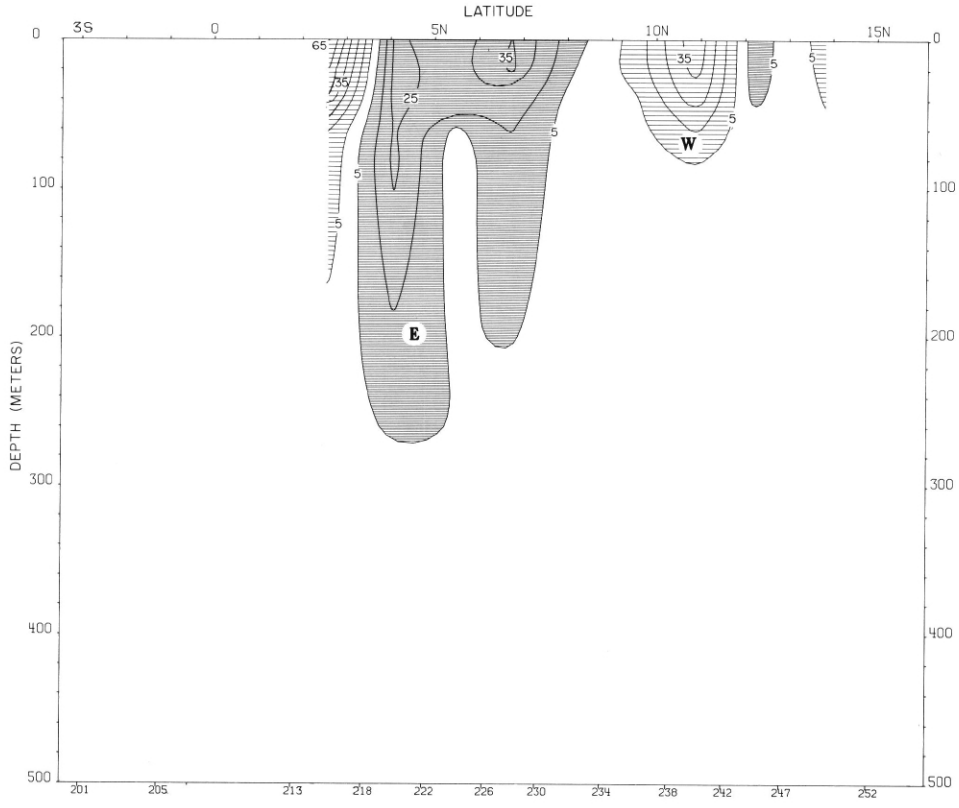

FIGURE 50-G-v6.—Vertical distribution of the zonal component of geostrophic velocity (cm./sec.), relative to 500 db., along 98°10′ W., November 20-26, 1967. Dark shading indicates eastward flow with a velocity greater than 5 cm./sec.; light shading indicates westward flow with a velocity greater than 5 cm./sec.

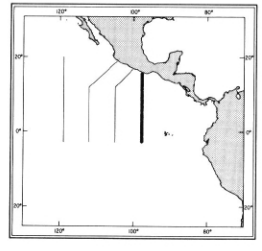

50-G-v6.

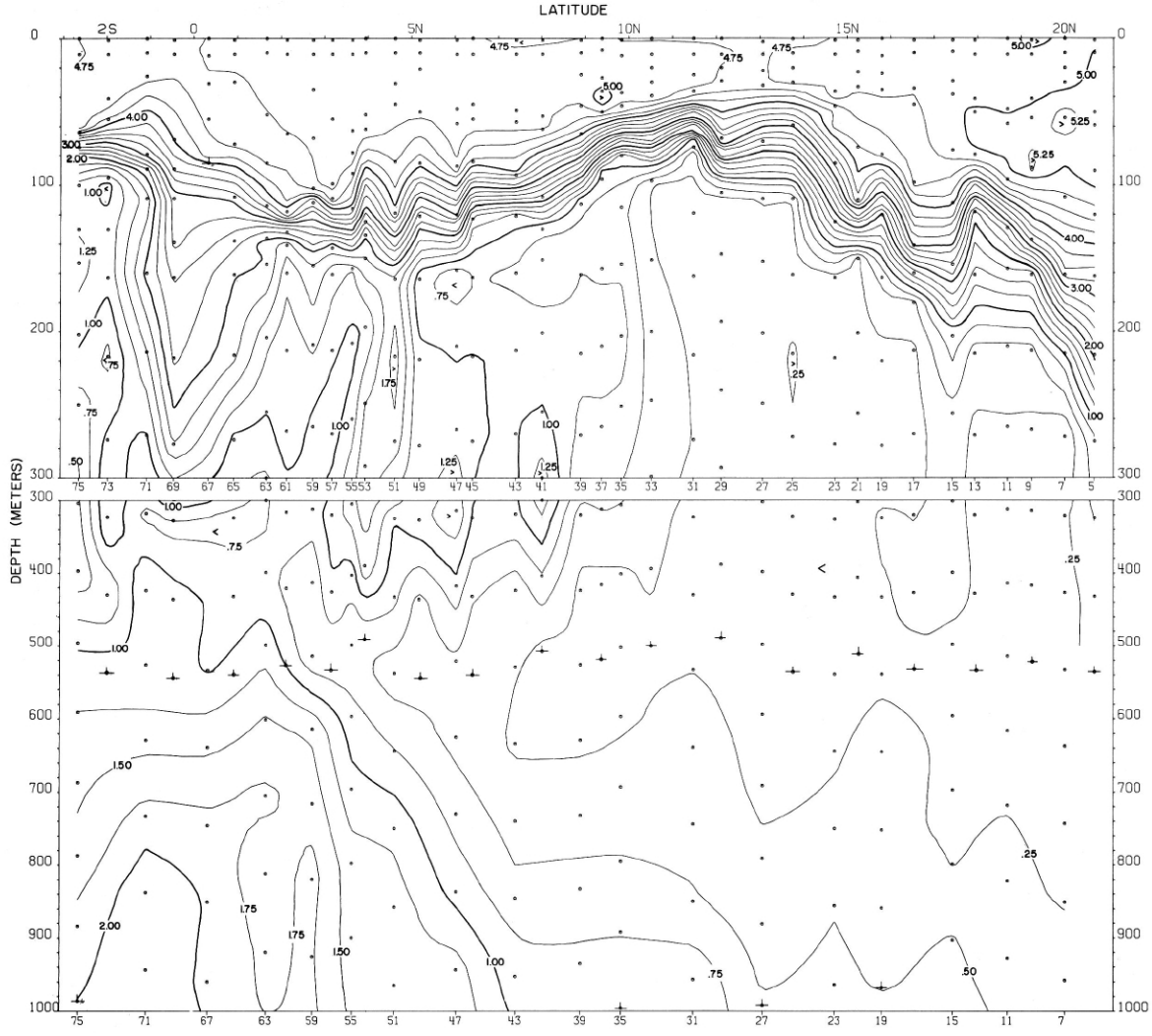

FIGURE 50-O₂-v1.—Vertical distribution of oxygen (ml./l.) along 119°10′ W., October 20-29, 1967.

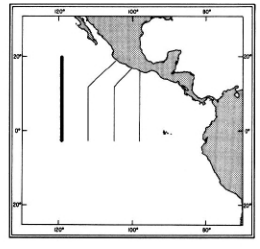

50-O₂-v1.

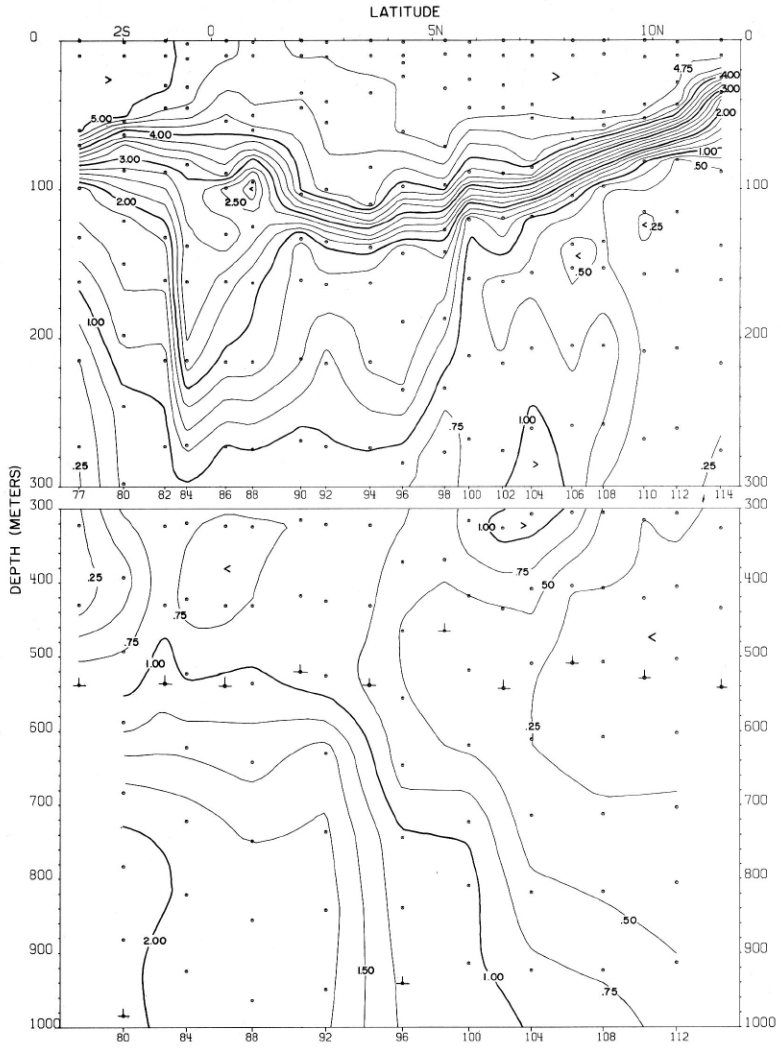

FIGURE 50-O_2-v2.—Vertical distribution of oxygen (ml./l.) along 112°10′ W., October 30-November 4, 1967.

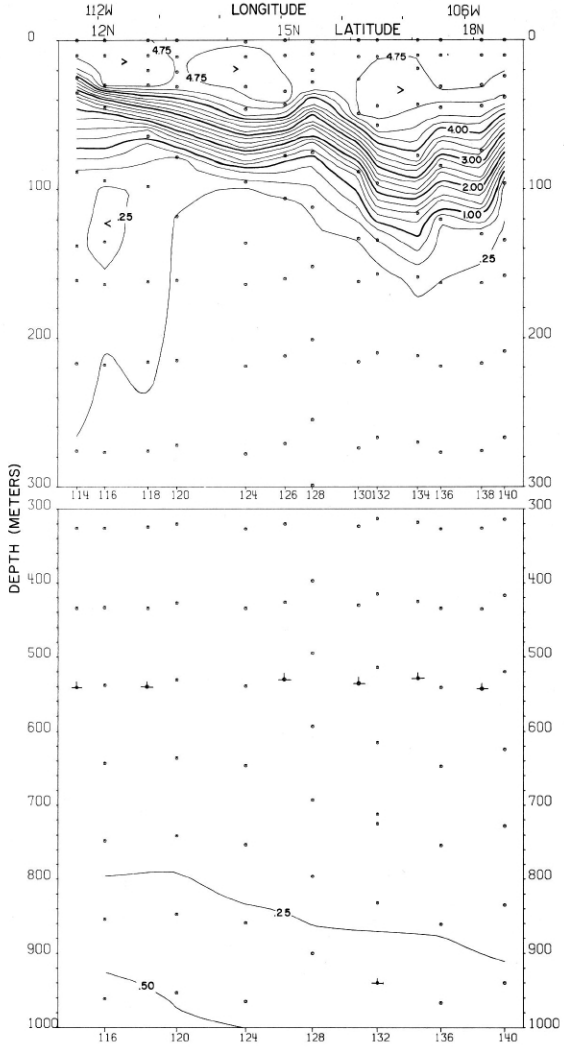

FIGURE 50-O_2-v3.—Vertical distribution of oxygen (ml./l.) along a section from 12° N., 112°10′ W. to Manzanillo, November 4-7, 1967.

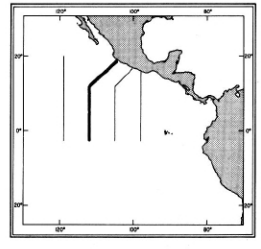

50-O_2-v2.

50-O_2-v3.

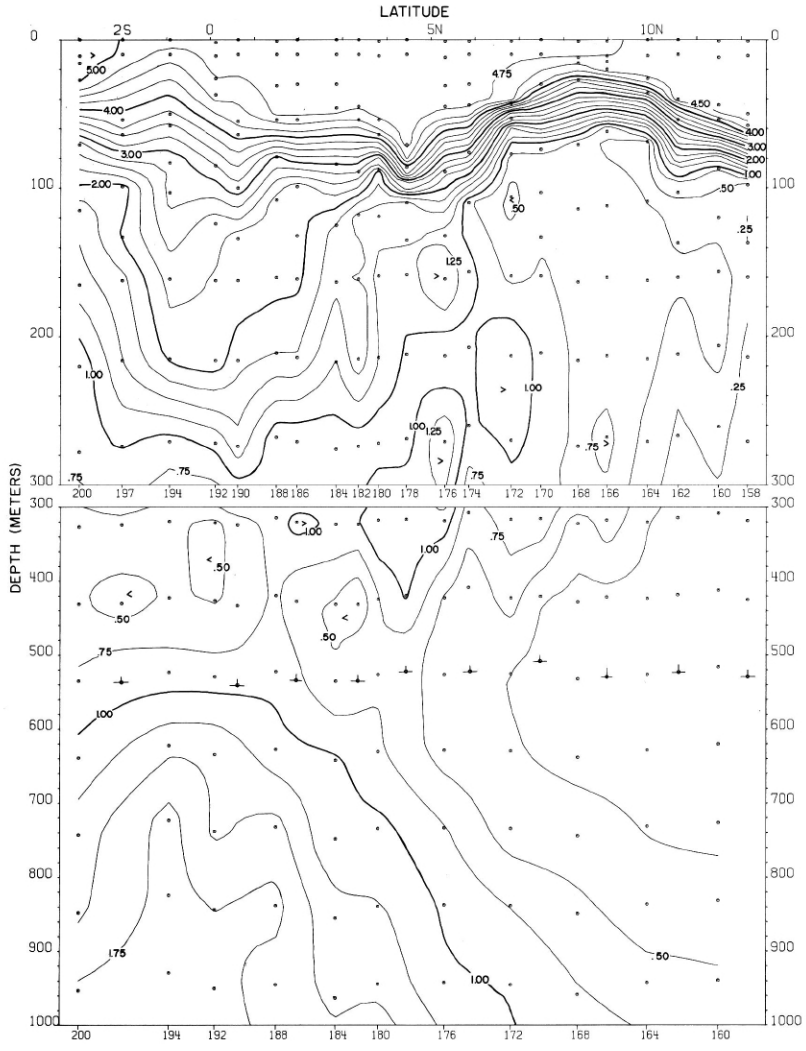

FIGURE 50-O₂-v5.—Vertical distribution of oxygen (ml./l.) along 105°10′ W., November 13-18, 1967.

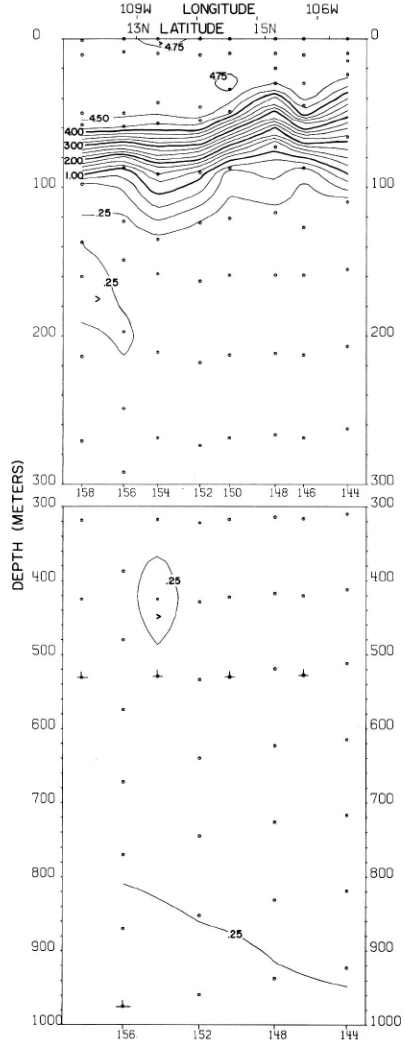

FIGURE 50-O₂-v4.—Vertical distribution of oxygen (ml./l.) along a section from Acapulco to 12° N., 105°10′ W., November 11-13, 1967.

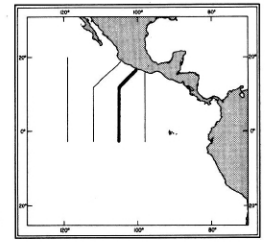

50-O₂-v4.

50-O₂-v5.

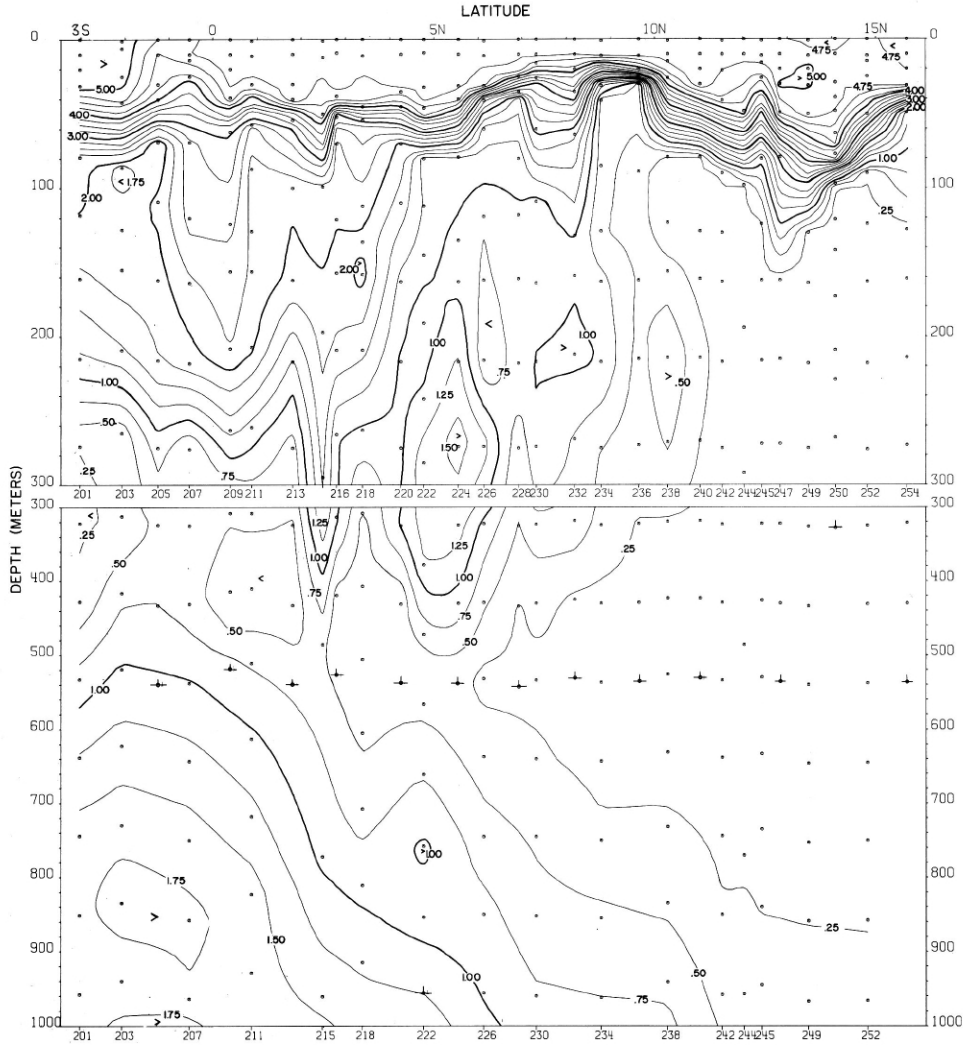

FIGURE 50-O_2-v6.—Vertical distribution of oxygen (ml./l.) along 98°10′ W., November 20-27, 1967.

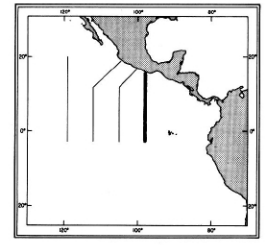

50-O_2-v6.

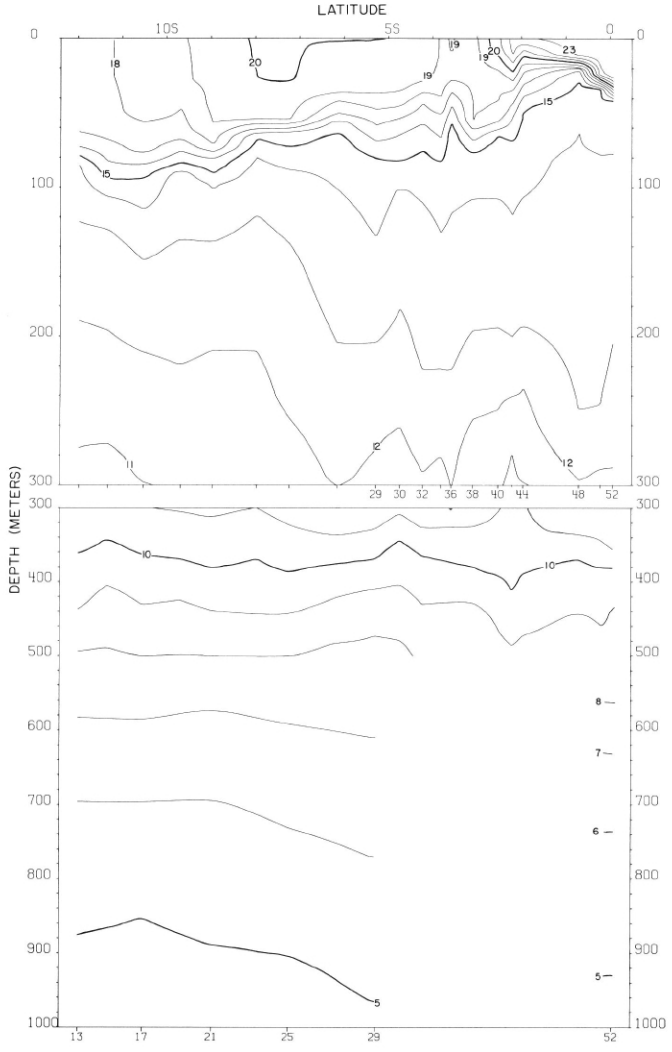

FIGURE OP-T-v2.—Vertical distribution of temperature (°C.) along 85° W., November 15-19, 1967.

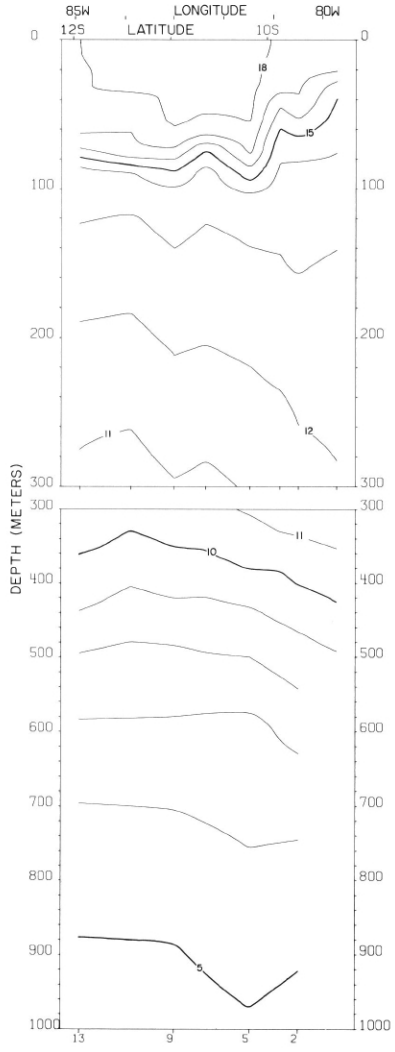

FIGURE OP-T-v1.—Vertical distribution of temperature (°C.) along a northeast-southwest section from the coast of Peru to 12° S., 85° W., November 14-15, 1967.

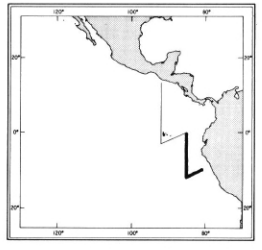

OP-T-v1.

OP-T-v2.

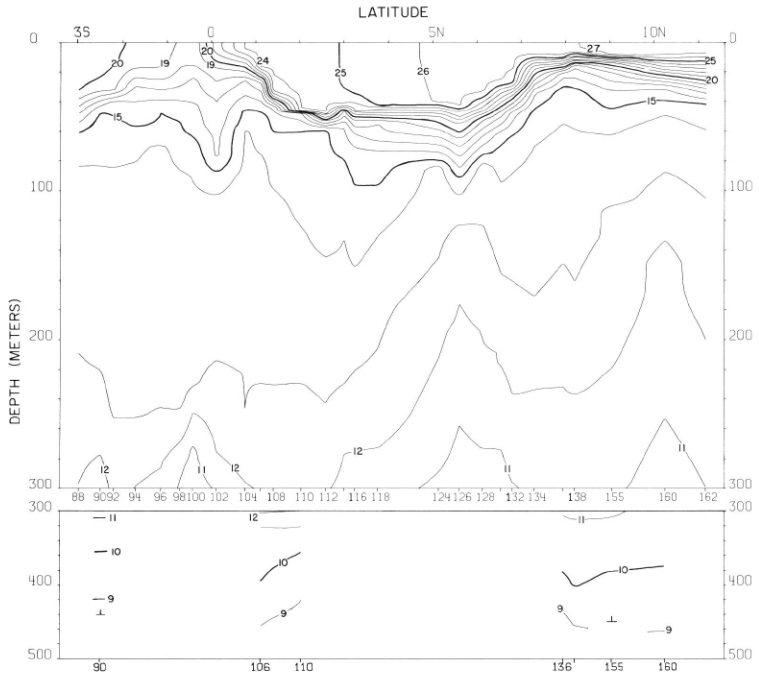

FIGURE OP-T-v4.—Vertical distribution of temperature (°C.) along 92° W., November 21-26, 1967.

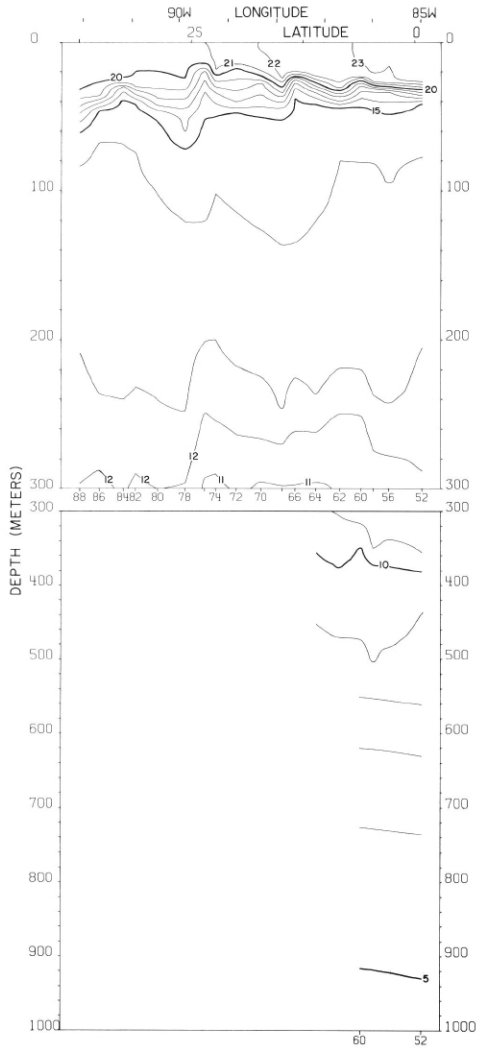

FIGURE OP-T-v3.—Vertical distribution of temperature (°C.) along a northeast-southwest section from the Equator at 85° W. to 3° S., 92° W., November 19-21, 1967.

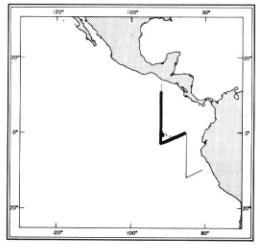

OP-T-v3.

OP-T-v4.

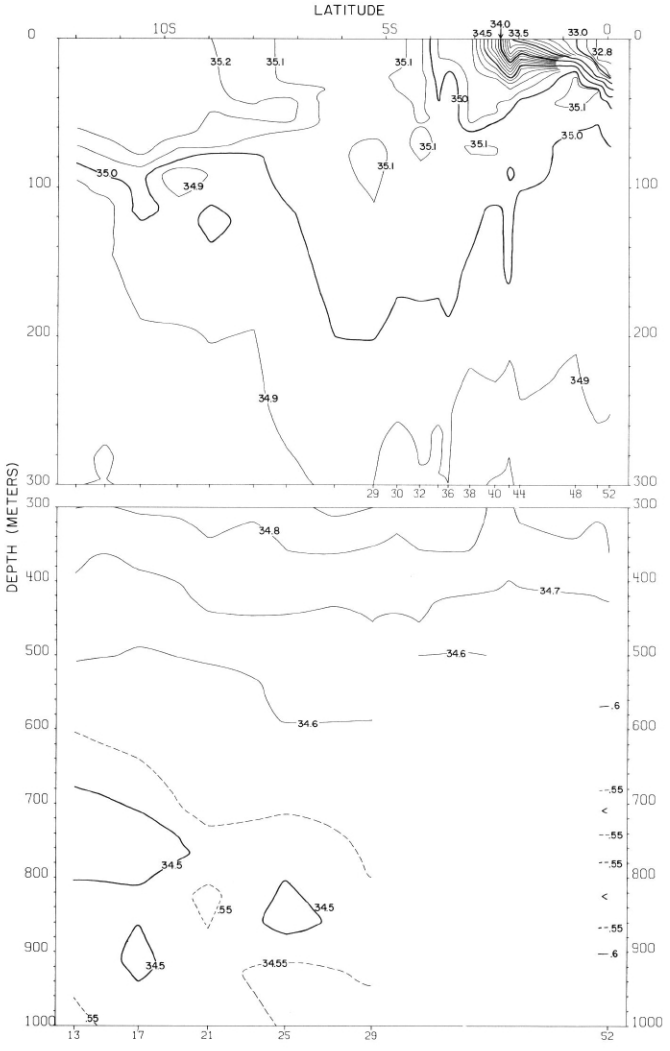

FIGURE OP-S-v2.—Vertical distribution of salinity (‰) along 85° W., November 15-19, 1967.

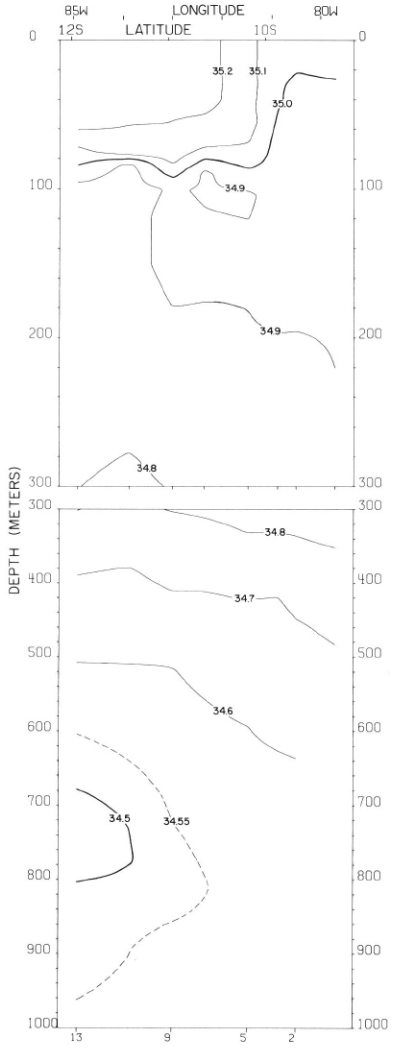

FIGURE OP-S-v1.—Vertical distribution of salinity (‰) along a northeast-southwest section from the coast of Peru to 12° S., 85° W., November 14-15, 1967.

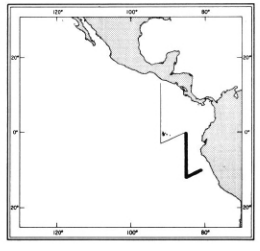

OP-S-v1.

OP-S-v2.

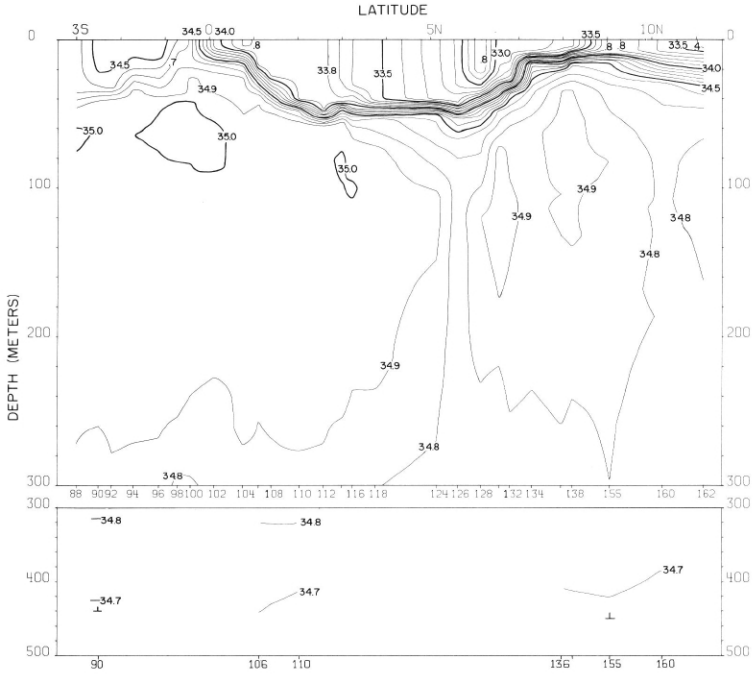

FIGURE OP-S-v4.—Vertical distribution of salinity (‰) along 92° W., November 21-26, 1967.

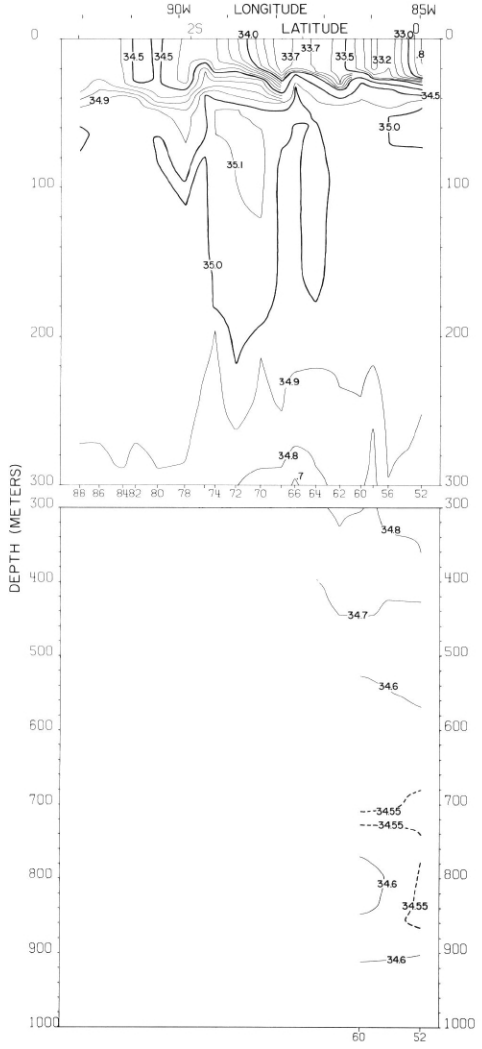

FIGURE OP-S-v3.—Vertical distribution of salinity (‰) along a northeast-southwest section from the Equator at 85° W. to 3° S., 92° W., November 19-21, 1967.

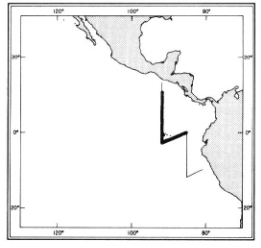

OP-S-v3.

OP-S-v4.

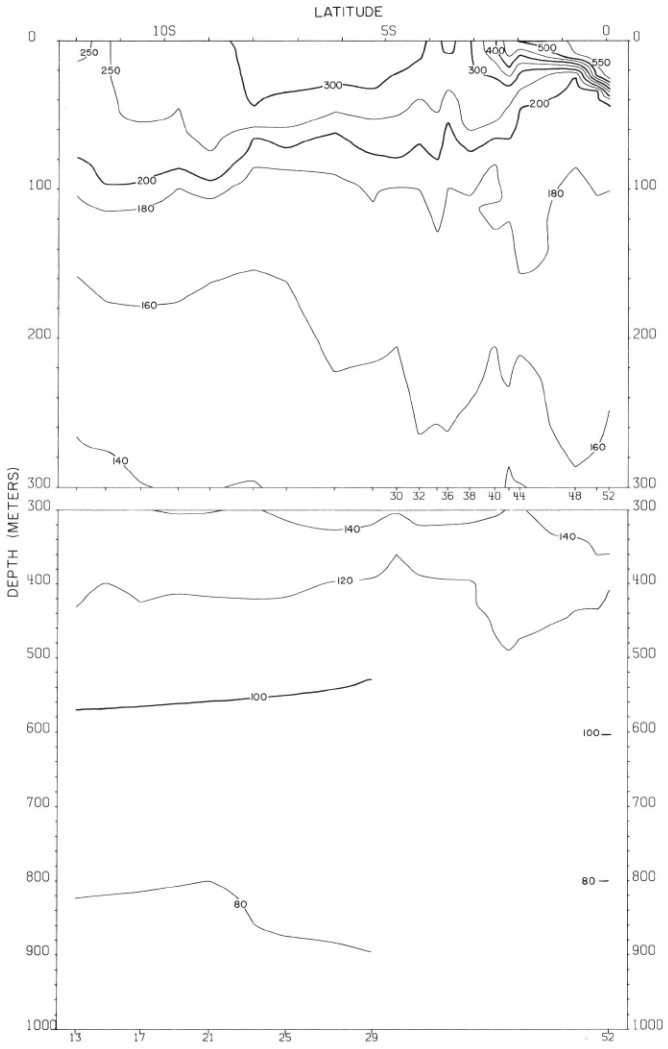

FIGURE OP-δ-v2.—Vertical distribution of thermosteric anomaly, δ_T, (cl./t.) along 85° W., November 15-19, 1967.

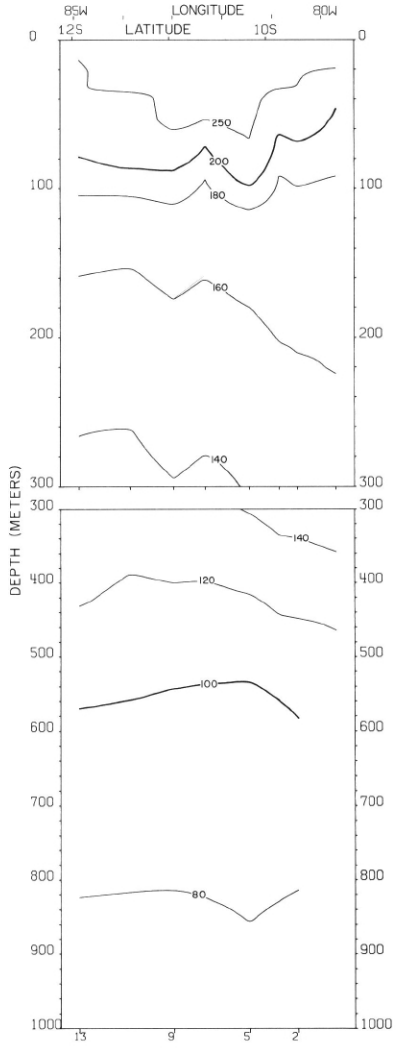

FIGURE OP-δ-v1.—Vertical distribution of thermosteric anomaly, δ_T, (cl./t.) along a northeast-southwest section from the coast of Peru to 12° S., 85° W., November 14-15, 1967.

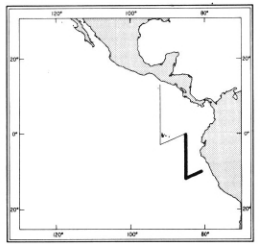

OP-δ-v1.

OP-δ-v2.

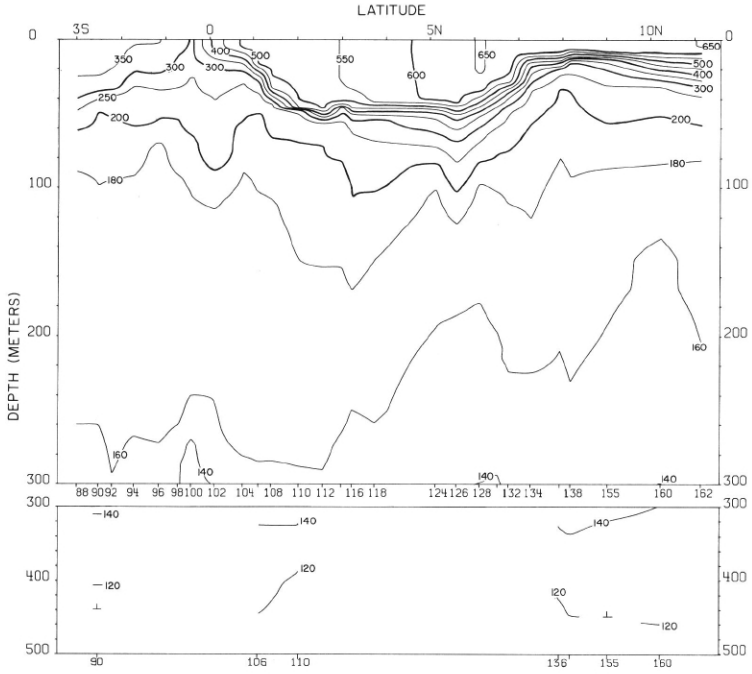

FIGURE OP-δ-v4.—Vertical distribution of thermosteric anomaly, δ_T, (cl./t.) along 92° W., November 21-26, 1967.

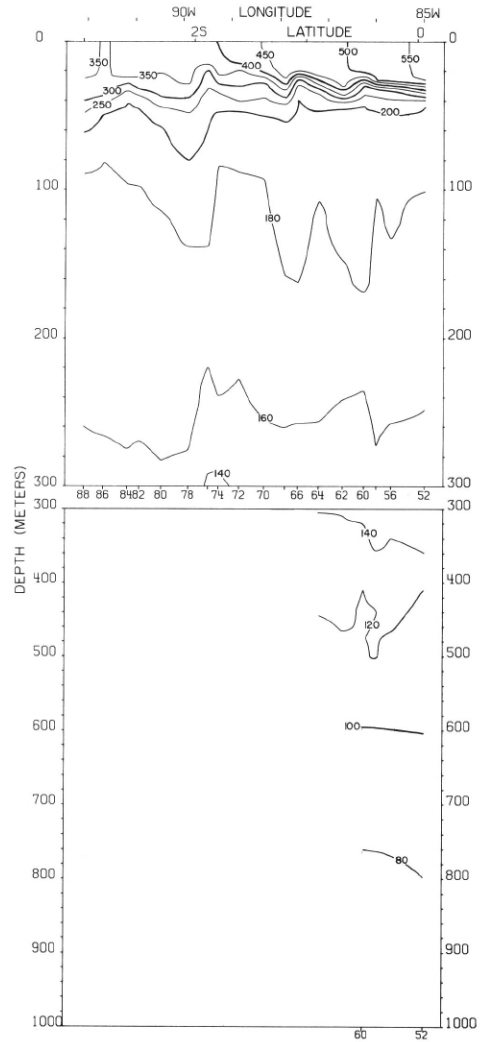

FIGURE OP-δ-v3.—Vertical distribution of thermosteric anomaly, δ_T, (cl./t.) along a northeast-southwest section from the Equator at 85° W. to 3° S., 92° W., November 19-21, 1967.

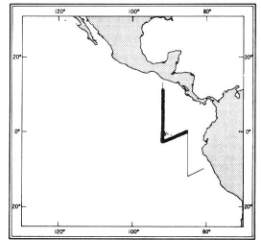

OP-δ-v3.

OP-δ-v4.

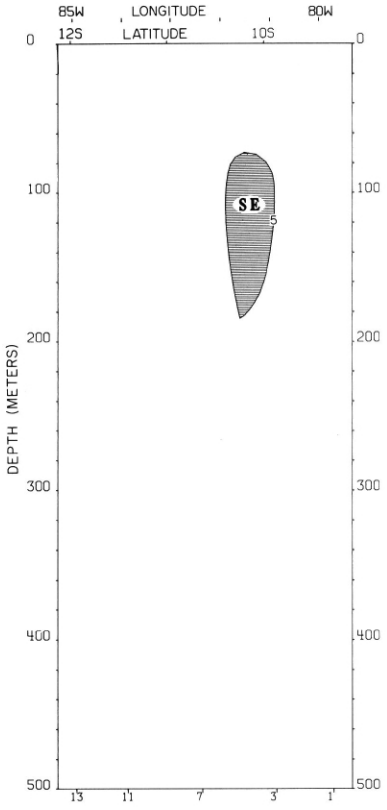

FIGURE OP-G-v1.—Vertical distribution of the component of geostrophic velocity (cm./sec.), relative to 500 db., normal to a northeast-southwest section from the coast of Peru to 12° S., 85° W., November 14-15, 1967. Dark shading indicates flow toward the southeast with a velocity greater than 5 cm./sec.

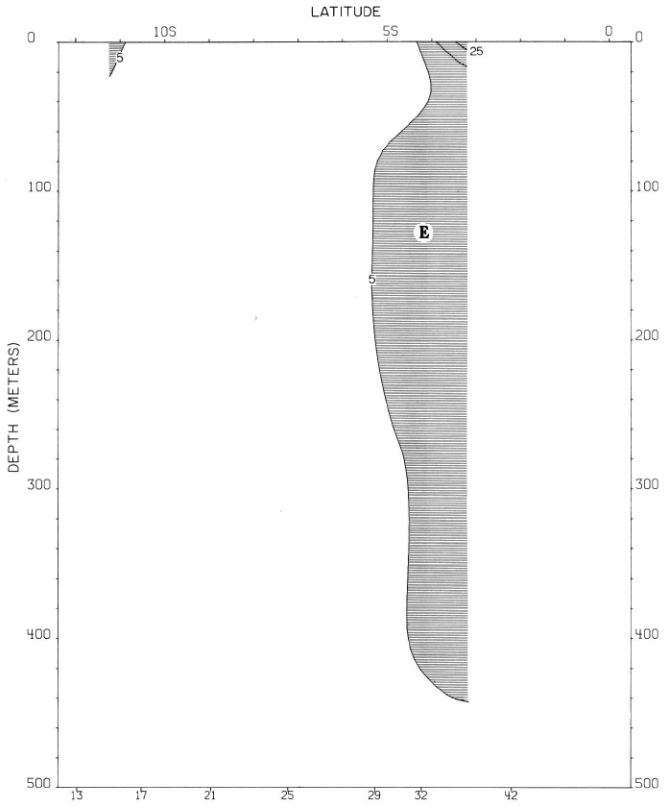

FIGURE OP-G-v2.—Vertical distribution of the zonal component of geostrophic velocity (cm./sec.), relative to 500 db., along 85° W., November 15-18, 1967. Dark shading indicates eastward flow with a velocity greater than 5 cm./sec.

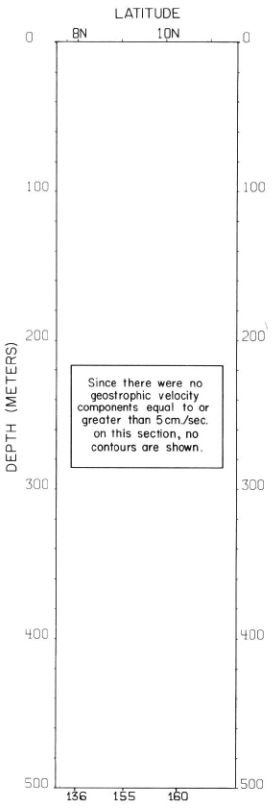

FIGURE OP-G-v4.—Vertical distribution of the zonal component of geostrophic velocity (cm./sec.), relative to 500 db., along 92° W., November 24-25, 1967. Since there were no geostrophic velocity components equal to or greater than 5 cm./sec. on this section, no contours are shown.

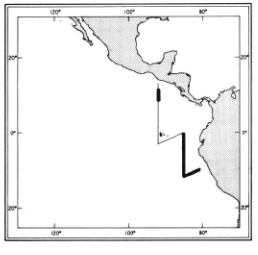

OP-G-v1.

OP-G-v2.

OP-G-v4.

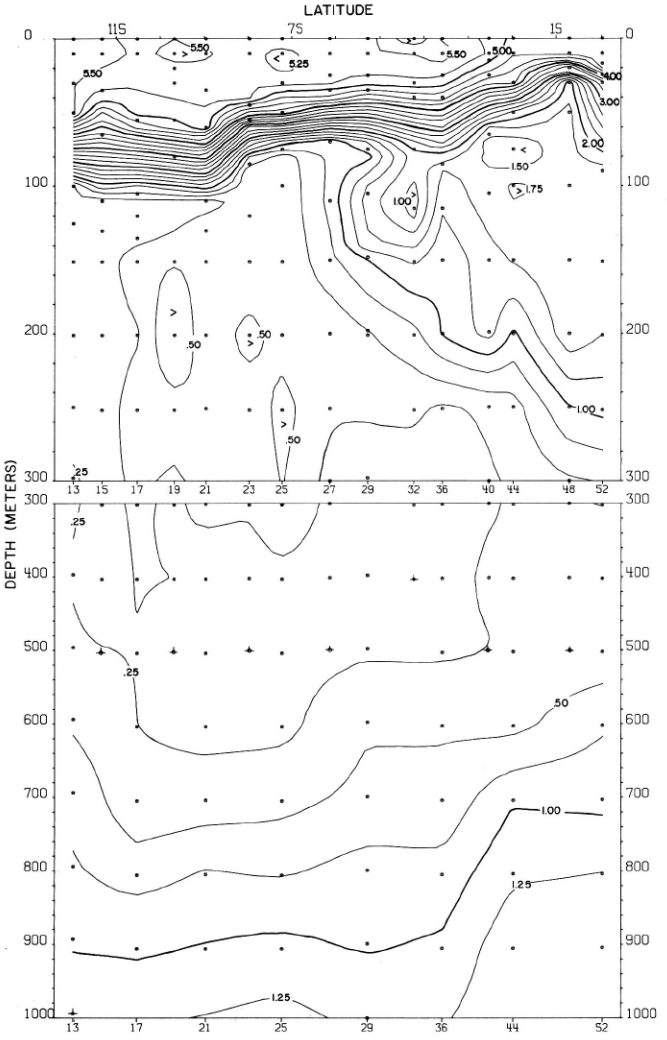

FIGURE OP-O₂-v2.—Vertical distribution of oxygen (ml./l.) along 85° W., November 15-19, 1967.

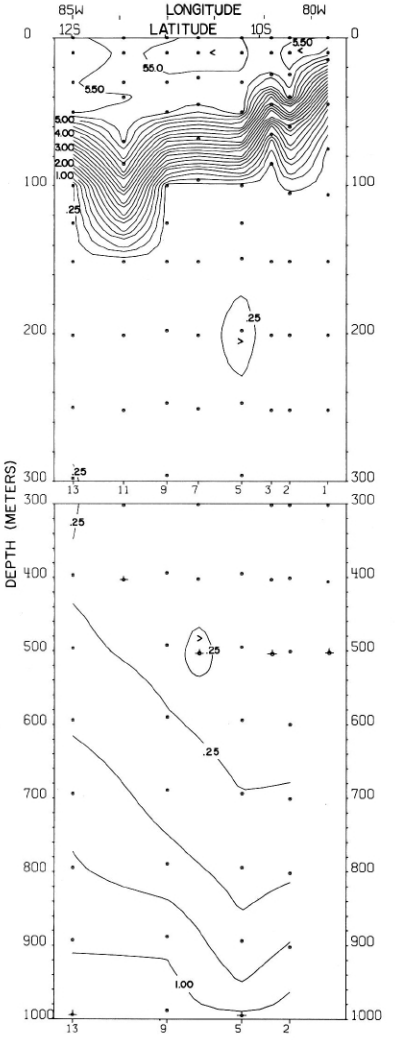

FIGURE OP-O₂-v1.—Vertical distribution of oxygen (ml./l.) along a northeast-southwest section from the coast of Peru to 12° S., 85° W., November 14-15, 1967.

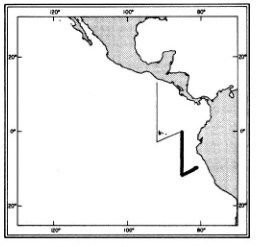

OP-O₂-v1.

OP-O₂-v2.

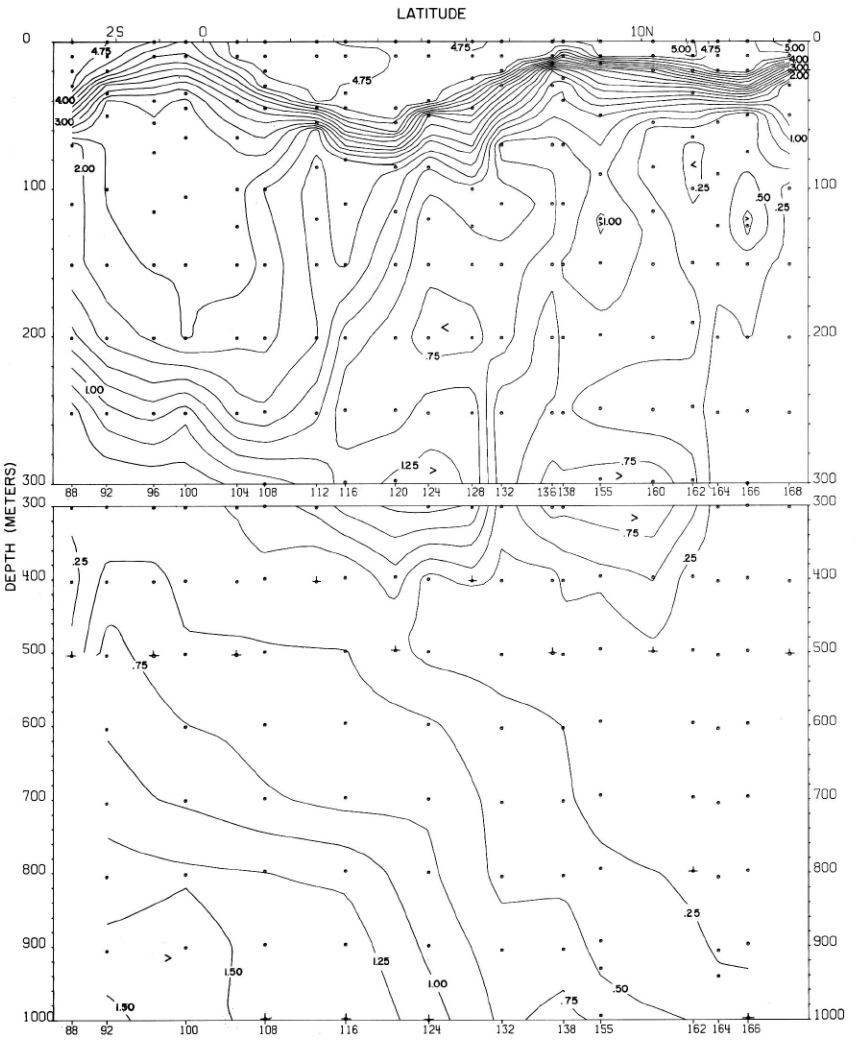

FIGURE OP-O₂-v4.—Vertical distribution of oxygen (ml./l.) along 92° W., November 21-26, 1967.

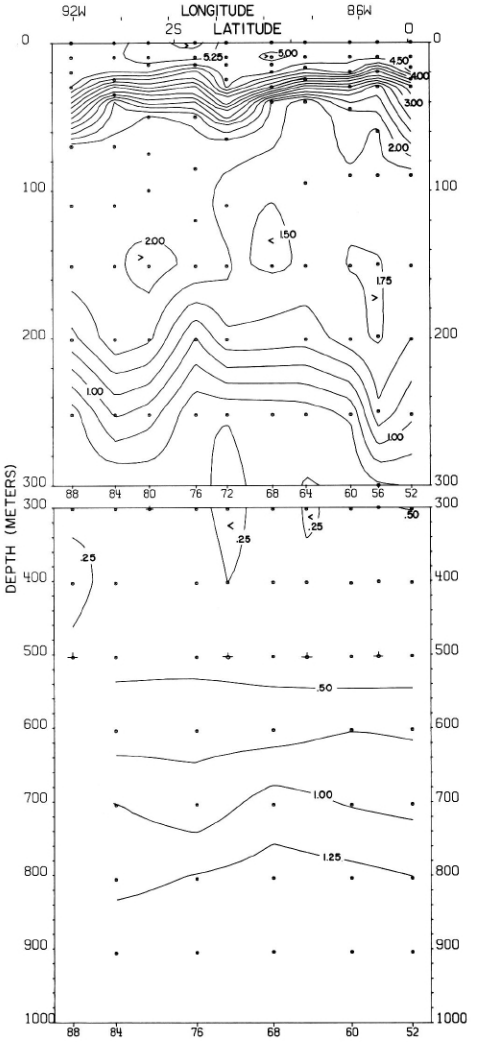

FIGURE OP-O₂-v3.—Vertical distribution of oxygen (ml./l.) along a northeast-southwest section from the Equator at 85° W. to 3° S., 92° W., November 19-21, 1967.

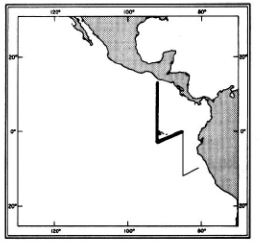

OP-O₂-v3.

OP-O₂-v4.

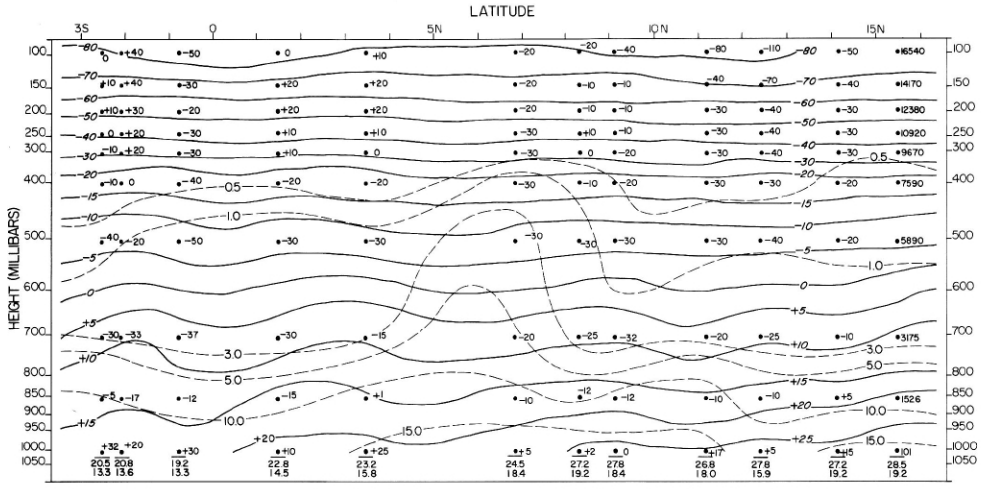

FIGURE OP-UA-v4.—Vertical section of the atmosphere along 92° W., November 21-28, 1967. Solid lines are isotherms of air temperature (°C.). Dashed lines are isopleths of mixing ratio of the air (g./kg.). Surface air temperature is plotted above surface mixing ratio and below a base line representing the surface pressure (mb.). The computed height (m.) of each standard pressure surface is plotted for the northernmost radiosonde station of the section. At other stations the difference of computed height minus the corresponding height at the northern station is shown at each standard level.

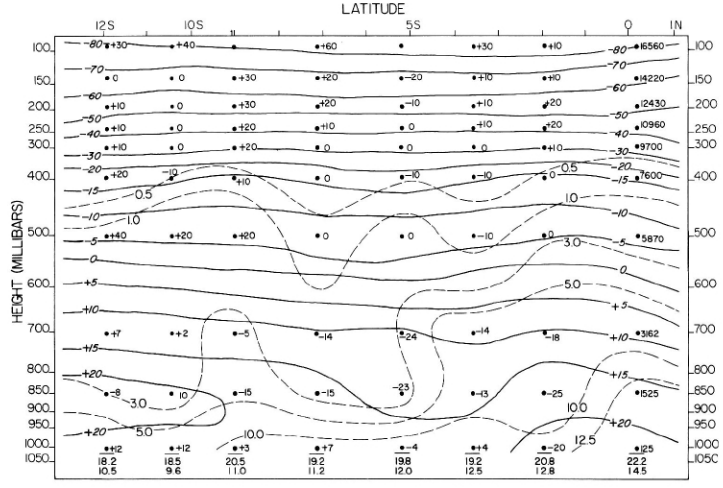

FIGURE OP-UA-v2.—Vertical section of the atmosphere along 85° W., November 16-21,1967. Solid lines are isotherms of air temperature (°C.). Dashed lines are isopleths of mixing ratio of the air (g./kg.). Surface air temperature is plotted above surface mixing ratio and below a base line representing the surface pressure (mb.). The computed height (m.) of each standard pressure surface is plotted for the northernmost radiosonde station of the section. At other stations the difference of computed height minus the corresponding height at the northern station is shown at each standard level.

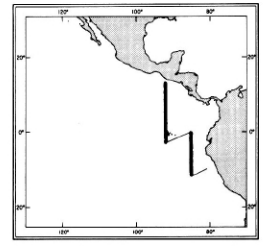

OP-UA-v2.

OP-UA-v4.

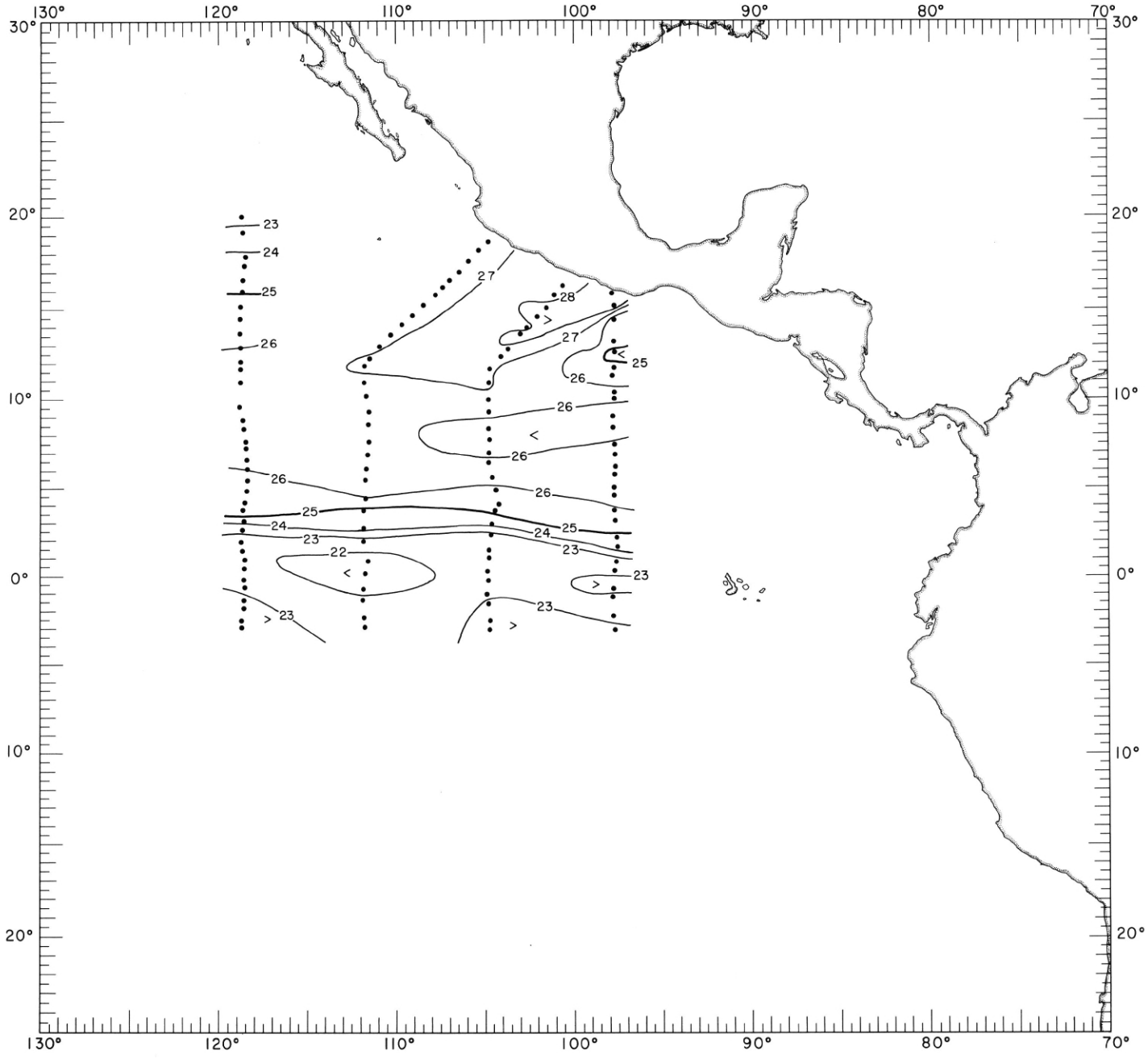

60-T-s.

FIGURE 60-T-s.—Temperature (°C.) at the sea surface, December 1967-January 1968. These contours are based on Nansen cast data.

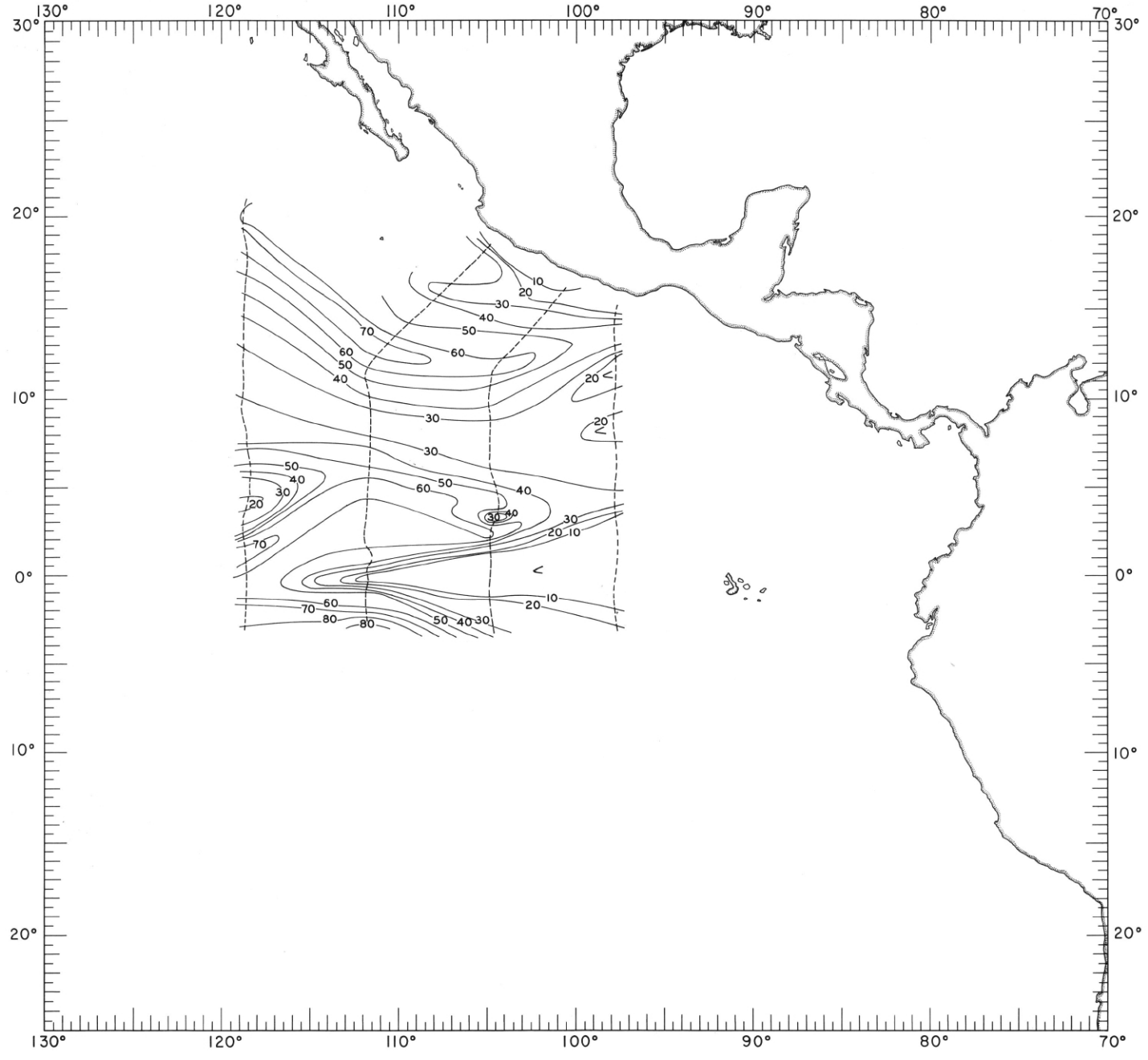

60-ML.

FIGURE 60-ML.—Thickness of the mixed layer in meters, December 1967-January 1968. Dashed lines indicate portions of the cruise track where such data were collected.

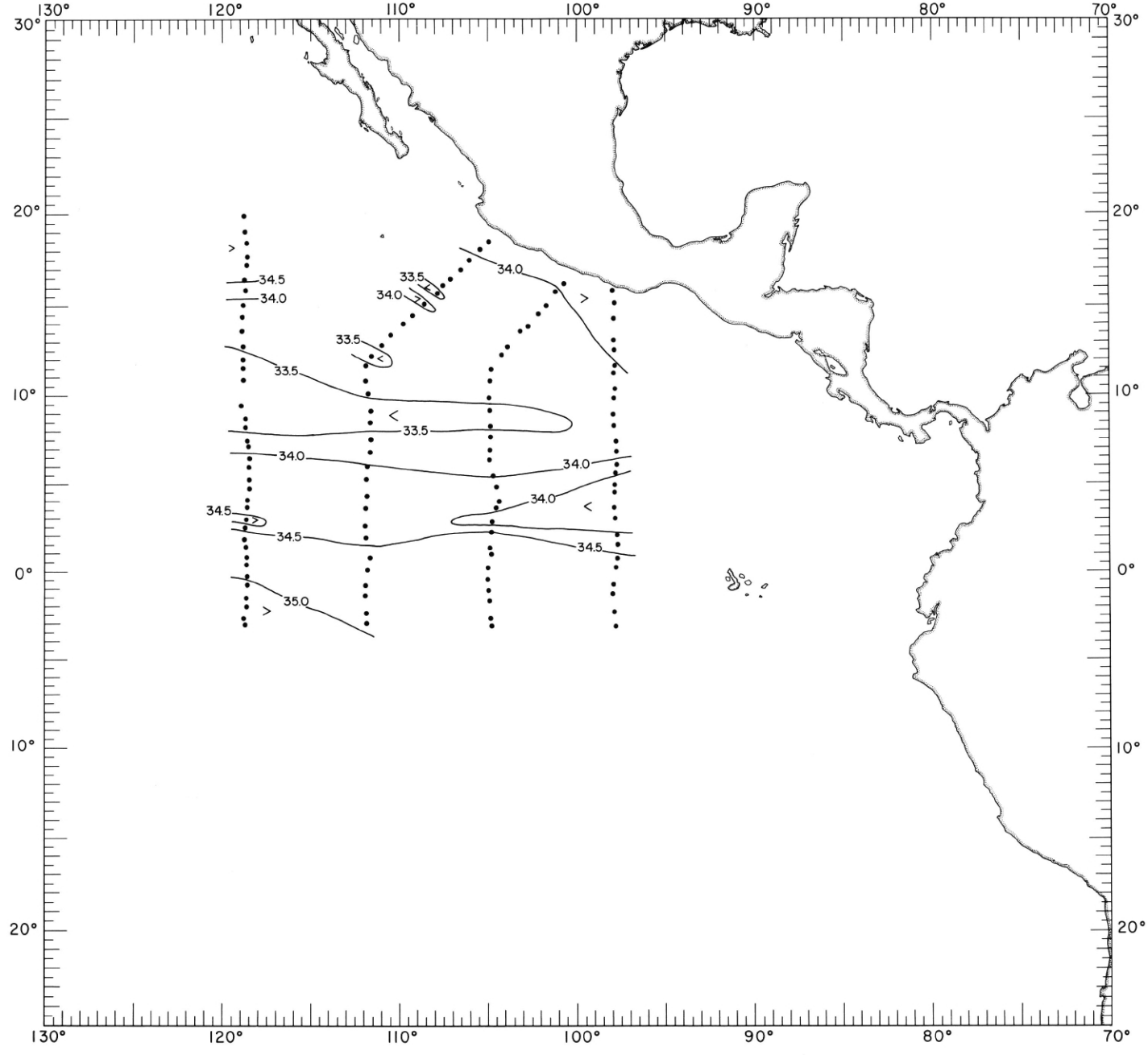

60-S-s.

FIGURE 60-S-s.—Salinity (‰) at the sea surface, December 1967-January 1968. The contours are based on Nansen cast data.

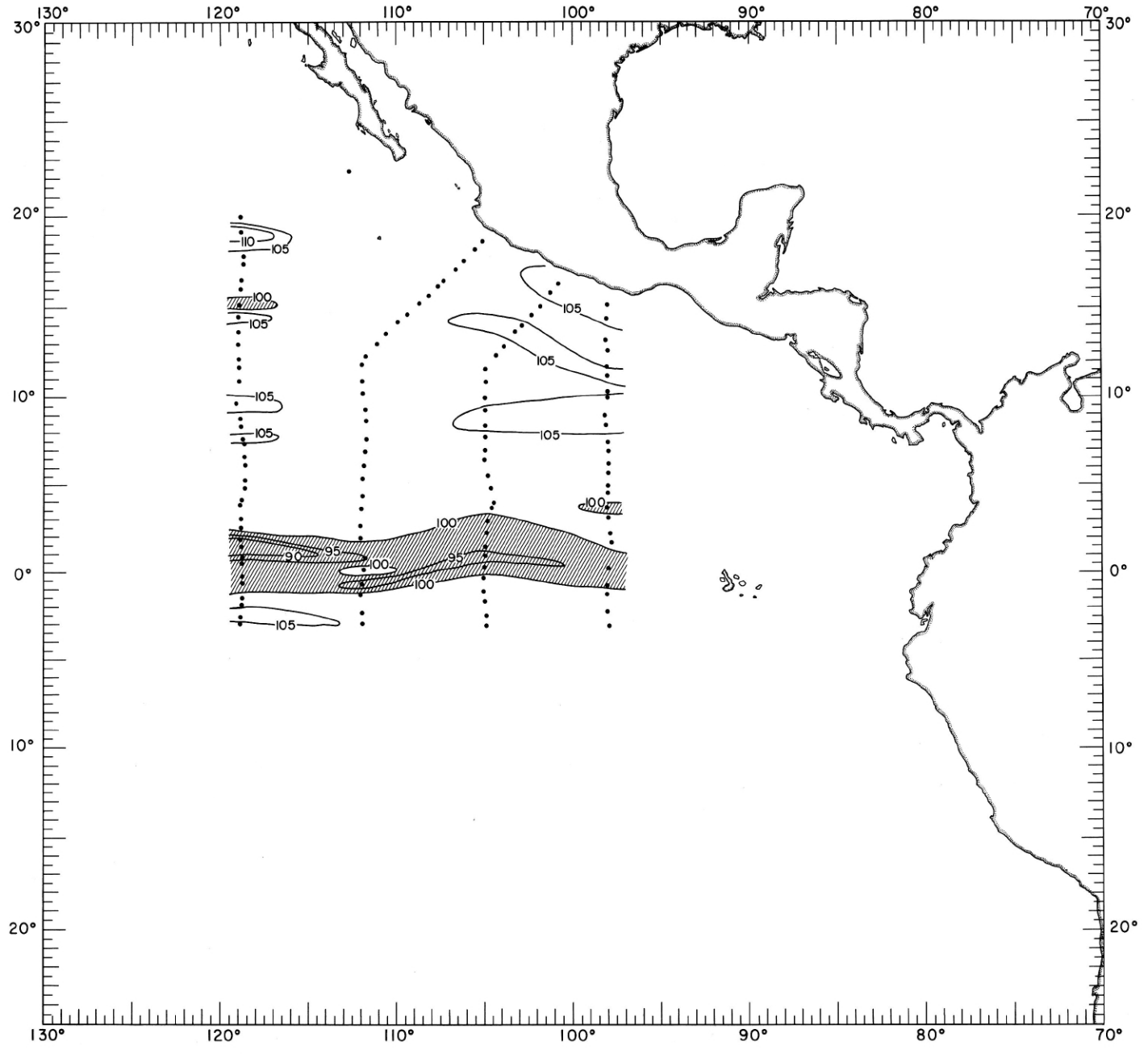

60-O_2Sa-10.

FIGURE 60-O_2Sa-10.—Oxygen saturation (%) at 10 meters, December 1967-January 1968. Areas with less than 100% saturation are shaded.

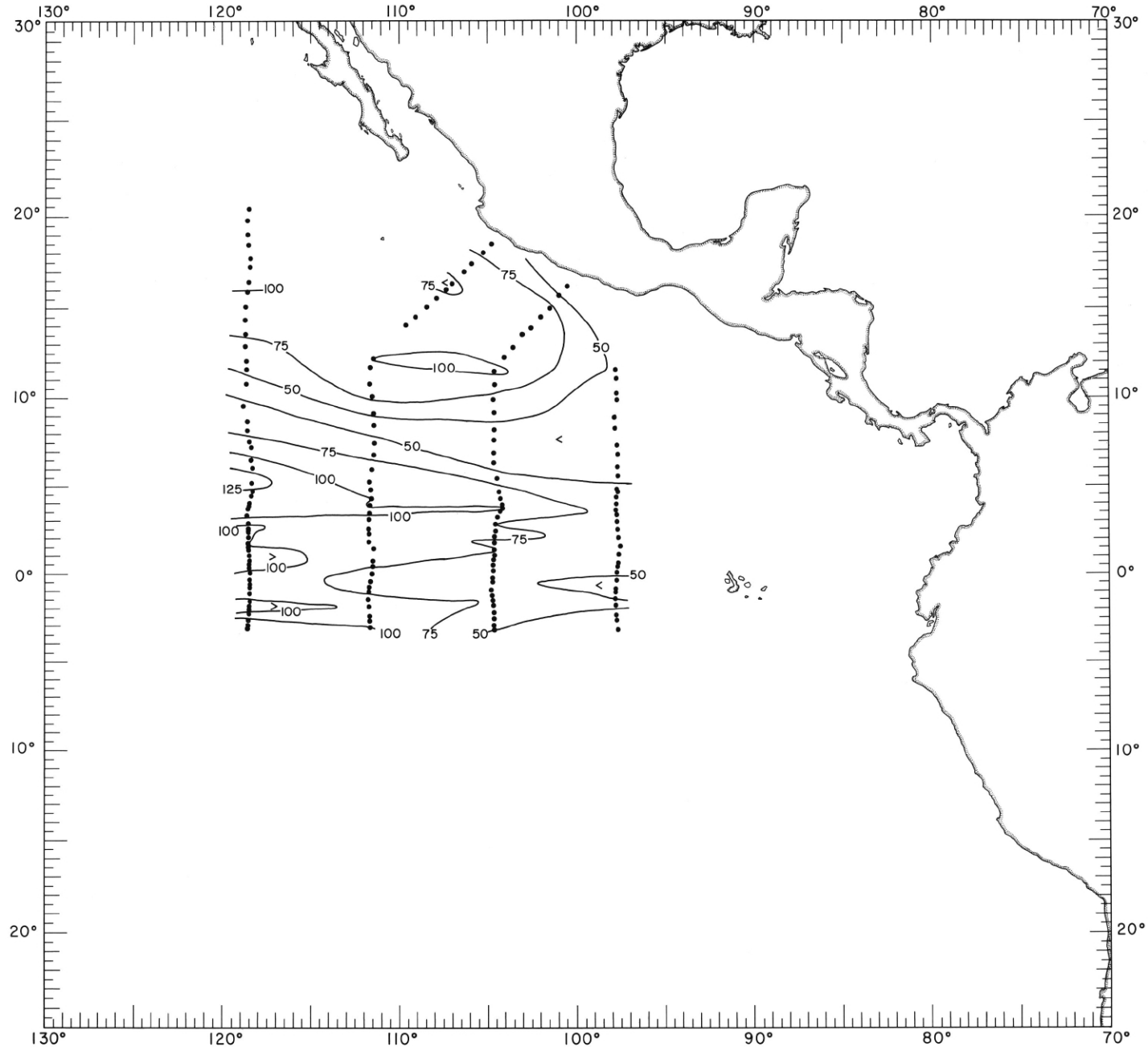

60-δ300-z.

FIGURE 60-δ300-z.—Depth (m.) of the surface where $\delta_T = 300$ cl./t., December 1967-January 1968.

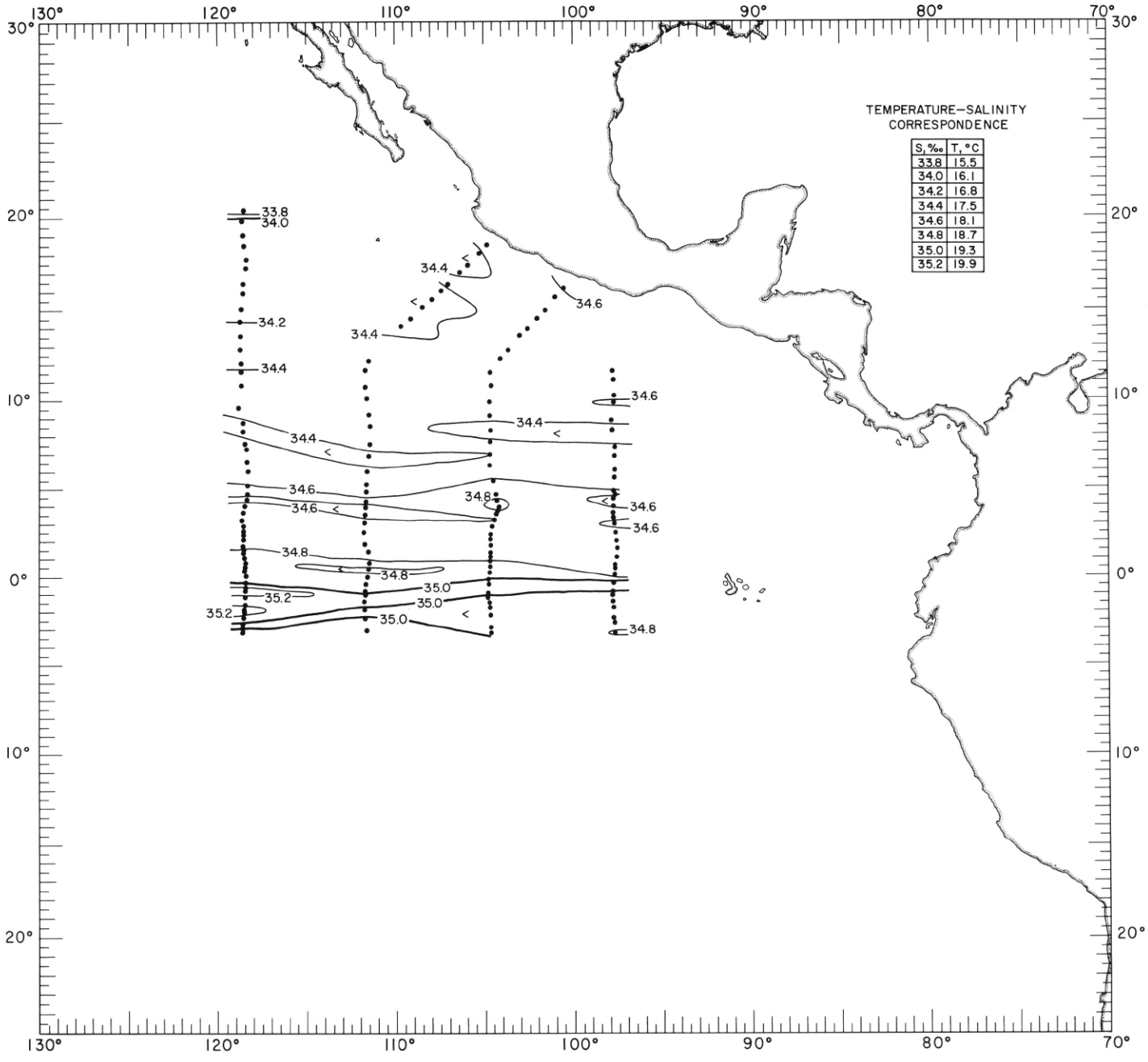

60-S-δ300.

FIGURE 60-S-δ300.—Salinity (‰) on the surface where $\delta_T = 300$ cl./t., December 1967-January 1968. The table shows the temperature corresponding to each isohaline on the chart.

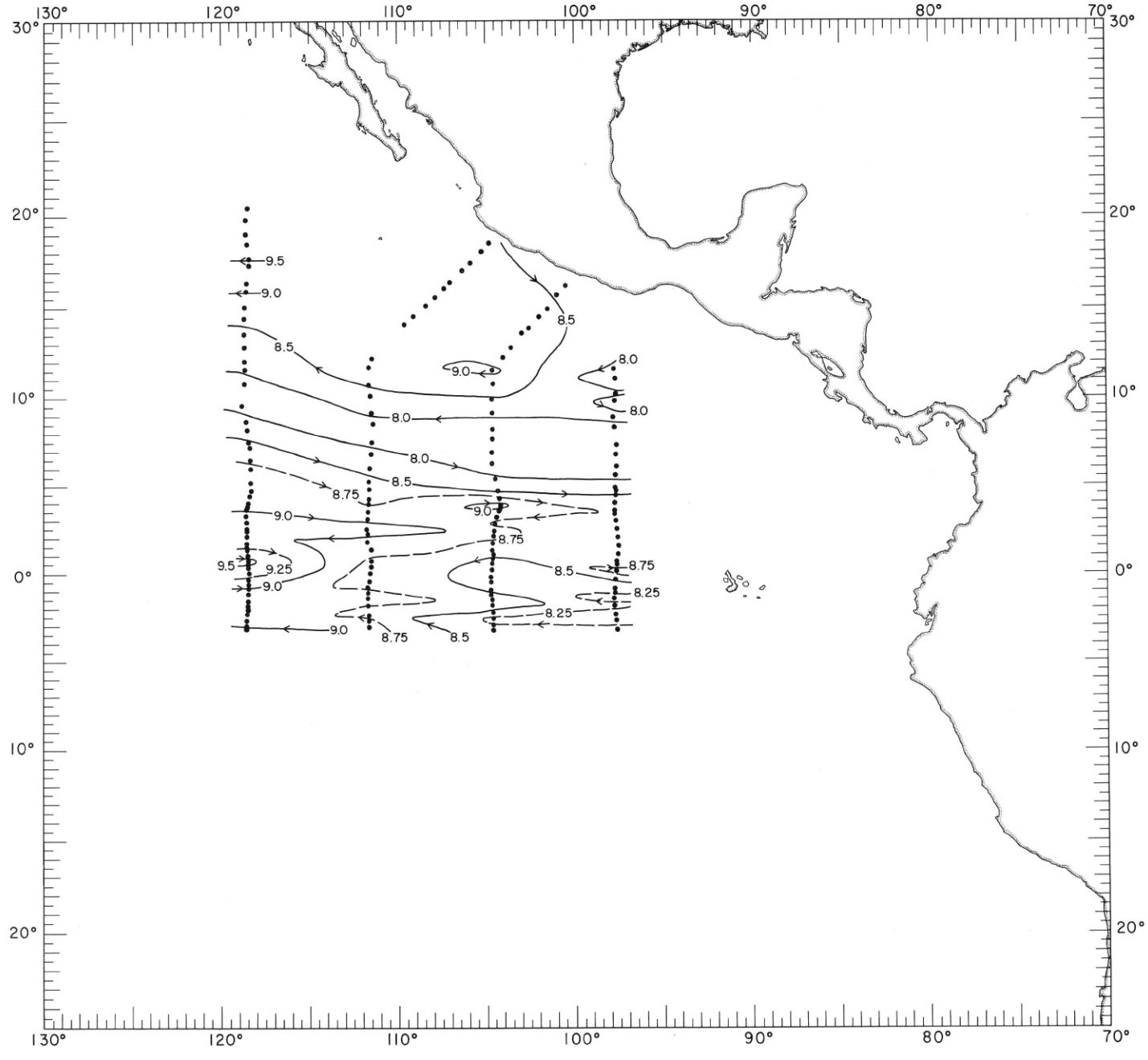

60-AP-δ300.

FIGURE 60-AP-δ300.—Acceleration potential (j./kg.), relative to 500 db., on the surface where $\delta_T = 300$ cl./t., December 1967-January 1968. For computing acceleration potential, thermosteric anomaly, δ_T, was used instead of specific volume anomaly, δ.

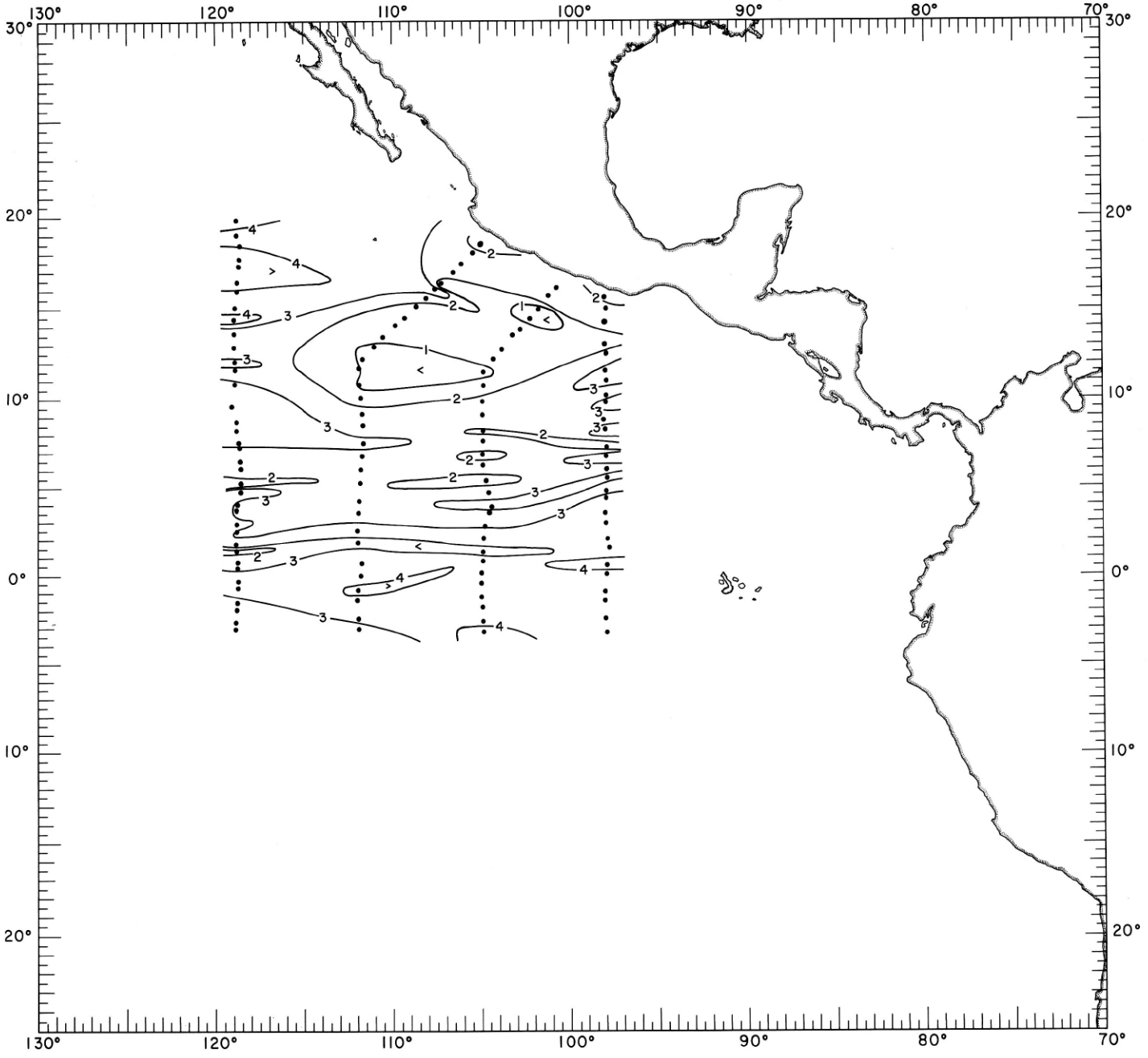

FIGURE 60-O_2-δ300.—Oxygen (ml./l.) on the surface where $\delta_T = 300$ cl./t., December 1967-January 1968.

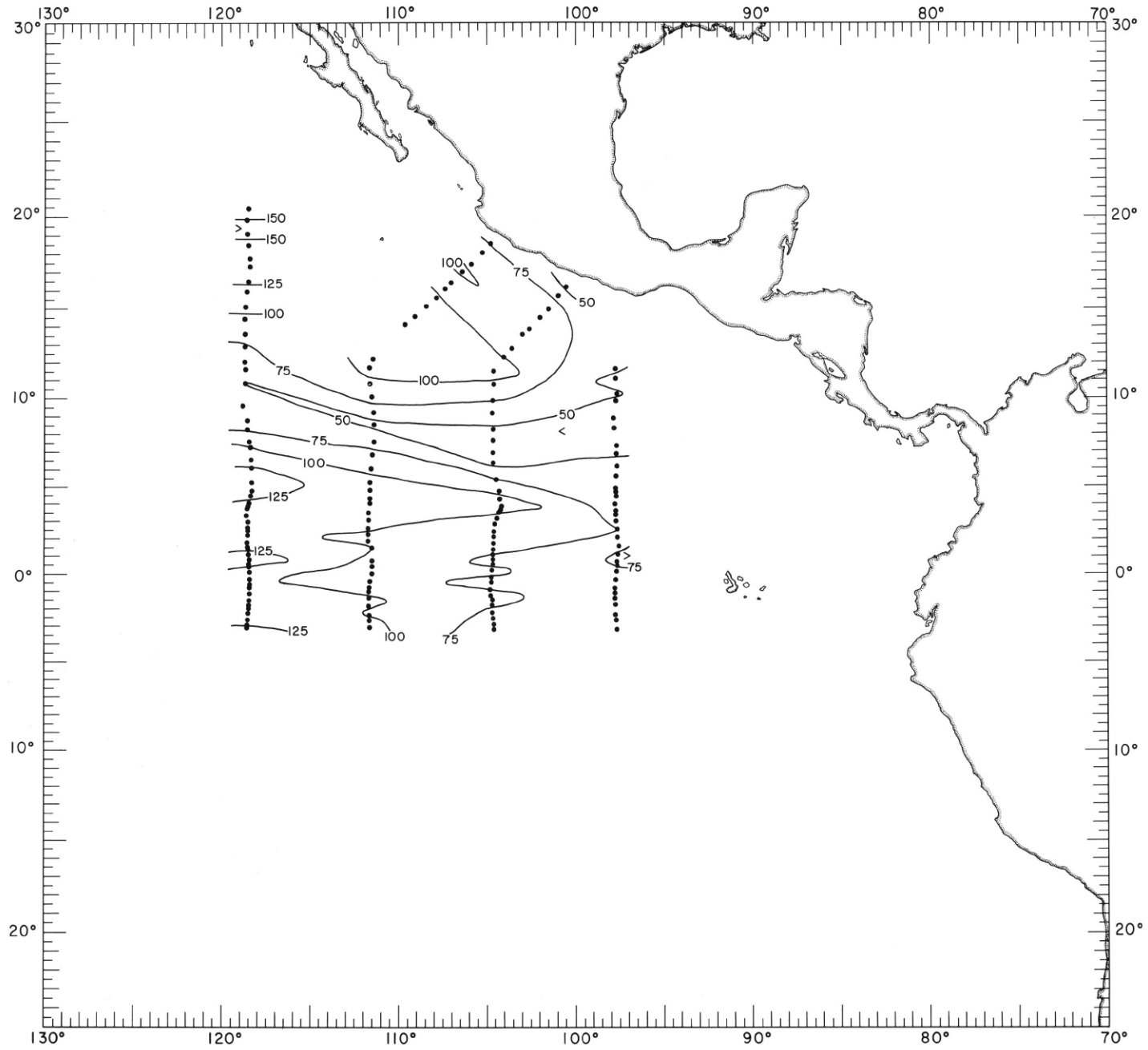

FIGURE 60-δ250-z.—Depth (m.) of the surface where $\delta_T = 250$ cl./t., December 1967-January 1968.

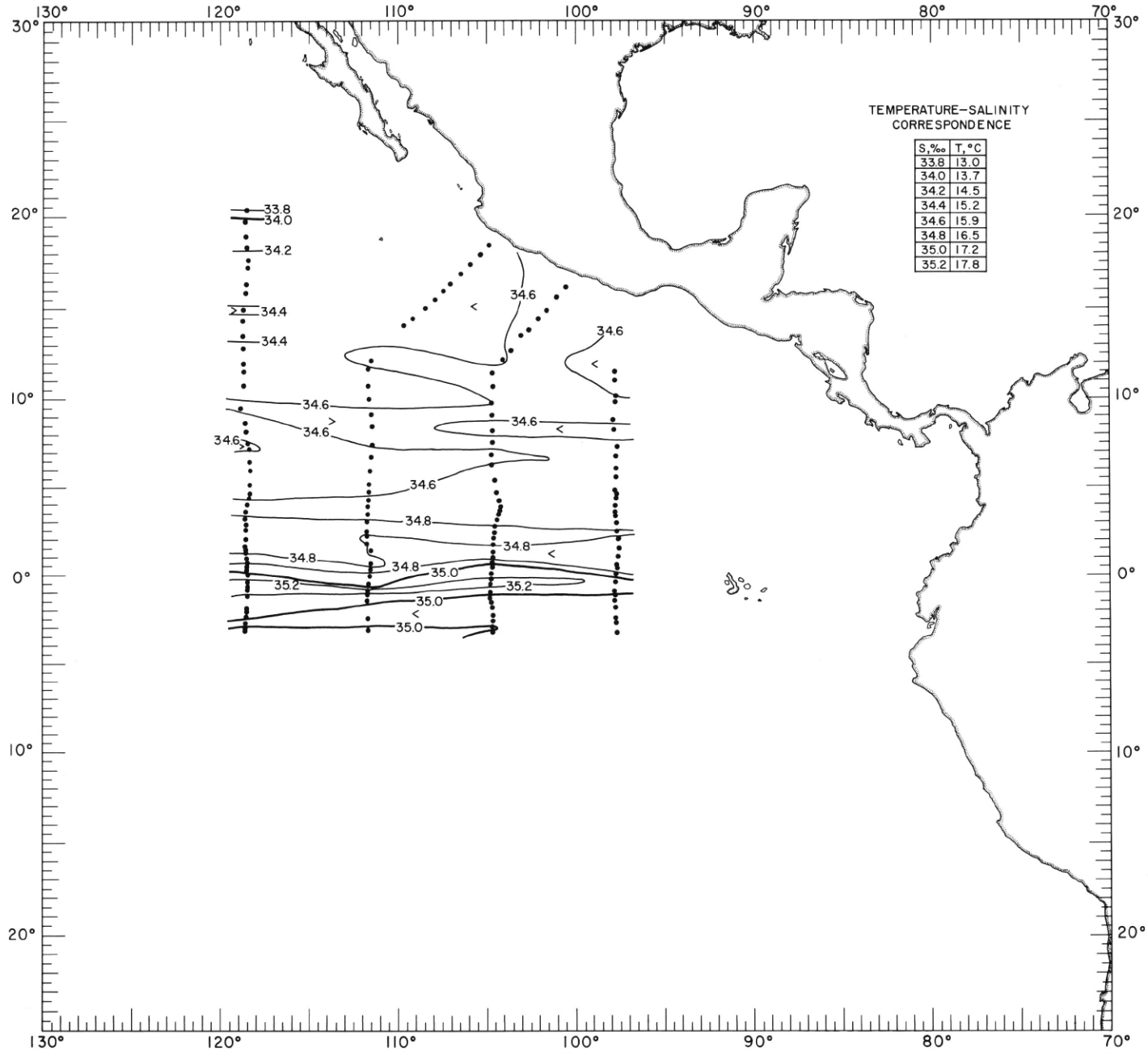

60-S-δ250.

FIGURE 60-S-δ250.—Salinity (‰) on the surface where $\delta_T = 250$ cl./t., December 1967-January 1968. The table shows the temperature corresponding to each isohaline on the chart.

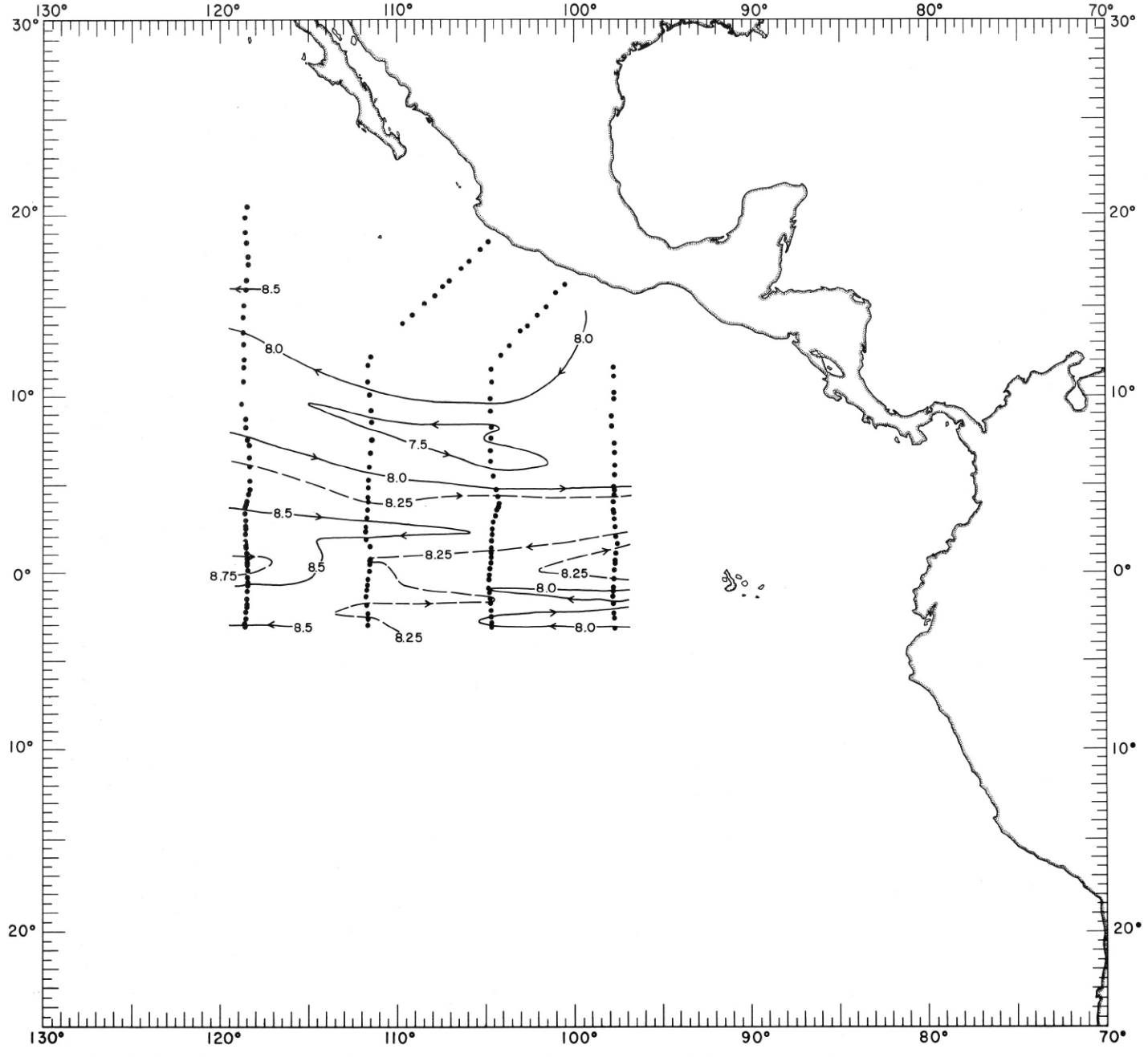

60-AP-δ250.

FIGURE 60-AP-δ250.—Acceleration potential (j./kg.), relative to 500 db., on the surface where $\delta_T = 250$ cl./t., December 1967-January 1968. For computing acceleration potential, thermosteric anomaly, δ_T, was used instead of specific volume anomaly, δ.

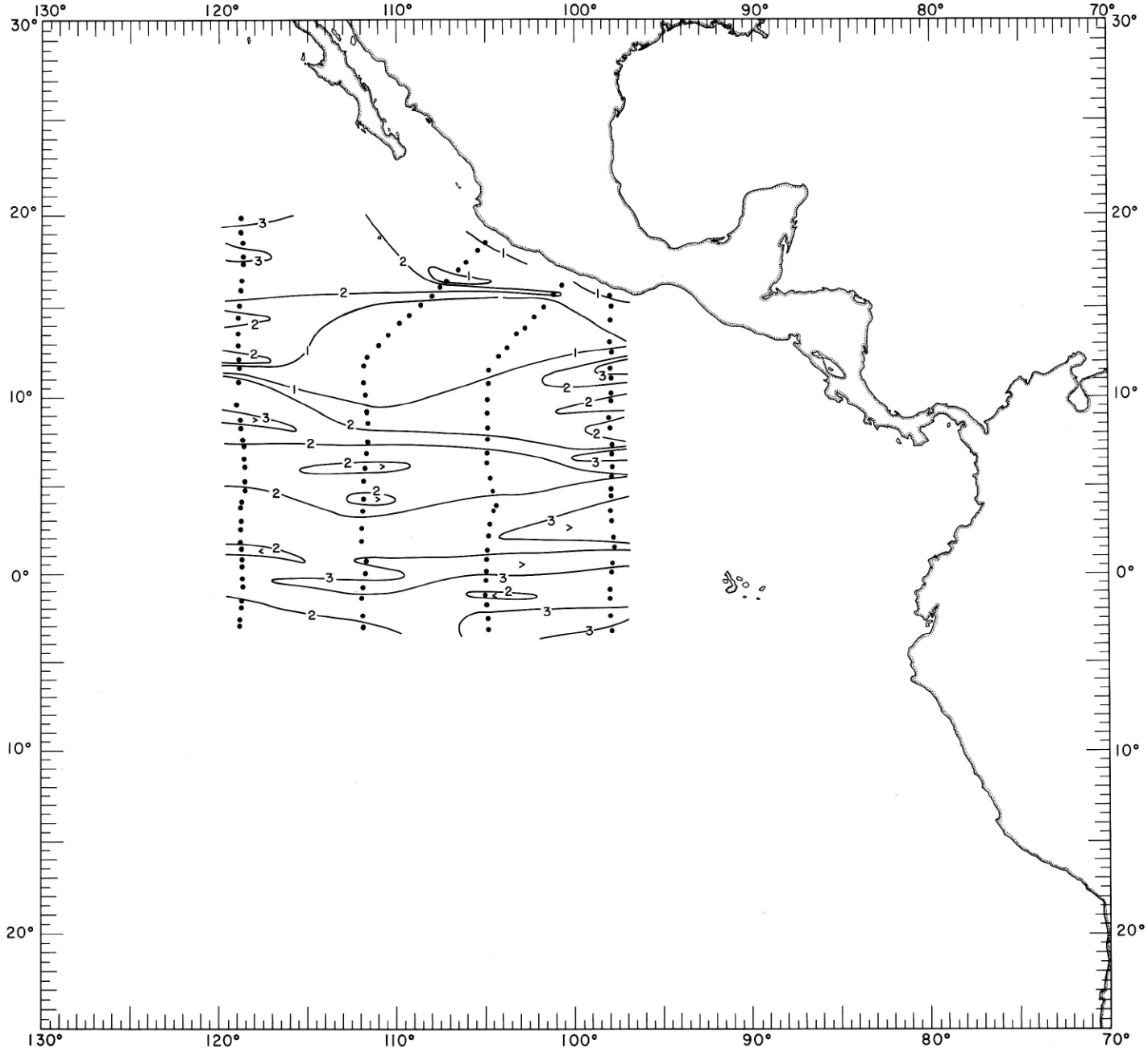

FIGURE 60-O_2-δ250.—Oxygen (ml./l.) on the surface where $\delta_T = 250$ cl./t., December 1967-January 1968.

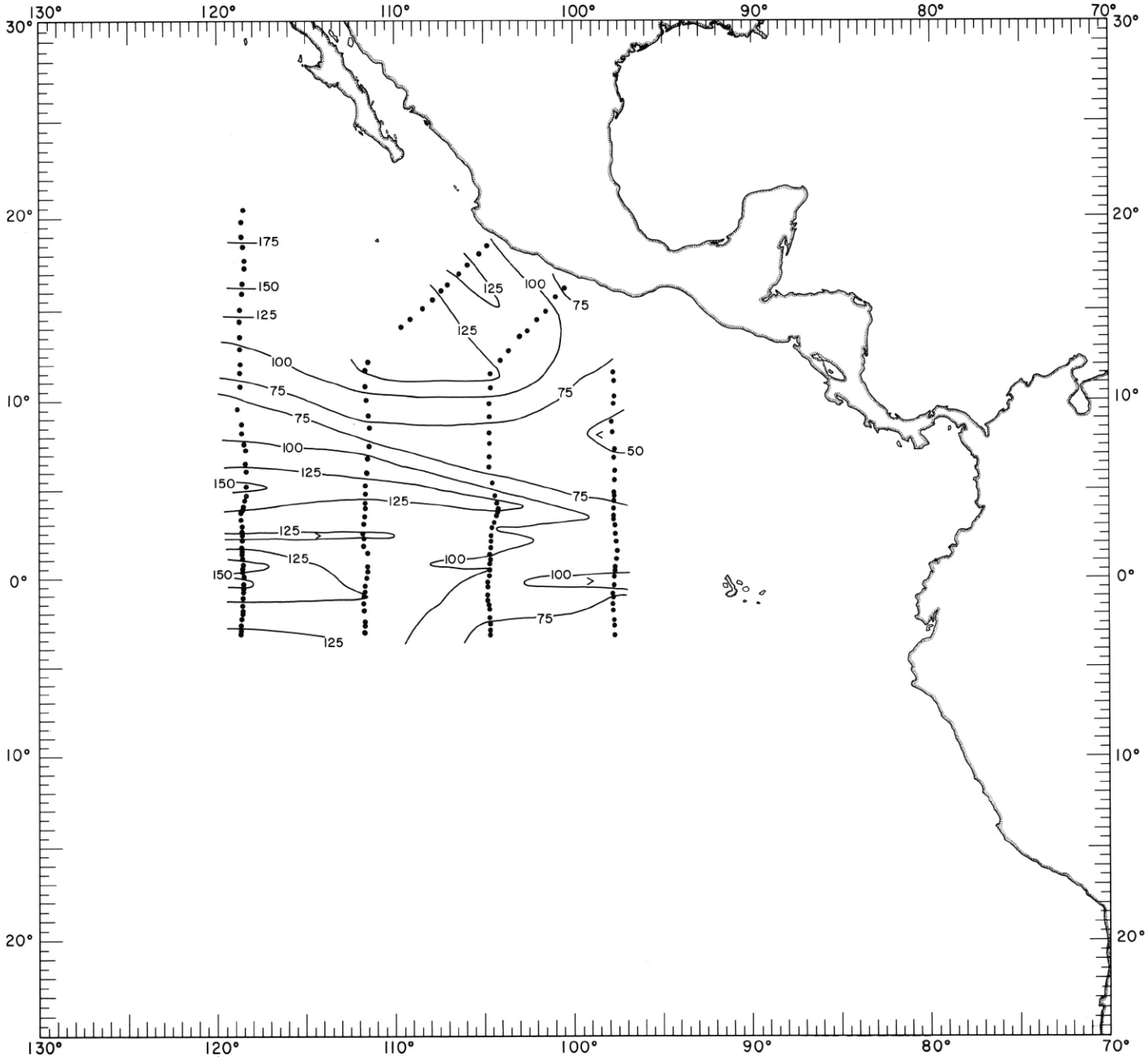

60-δ200-z.

FIGURE 60-δ200-z.—Depth (m.) of the surface where $\delta_T = 200$ cl./t., December 1967-January 1968.

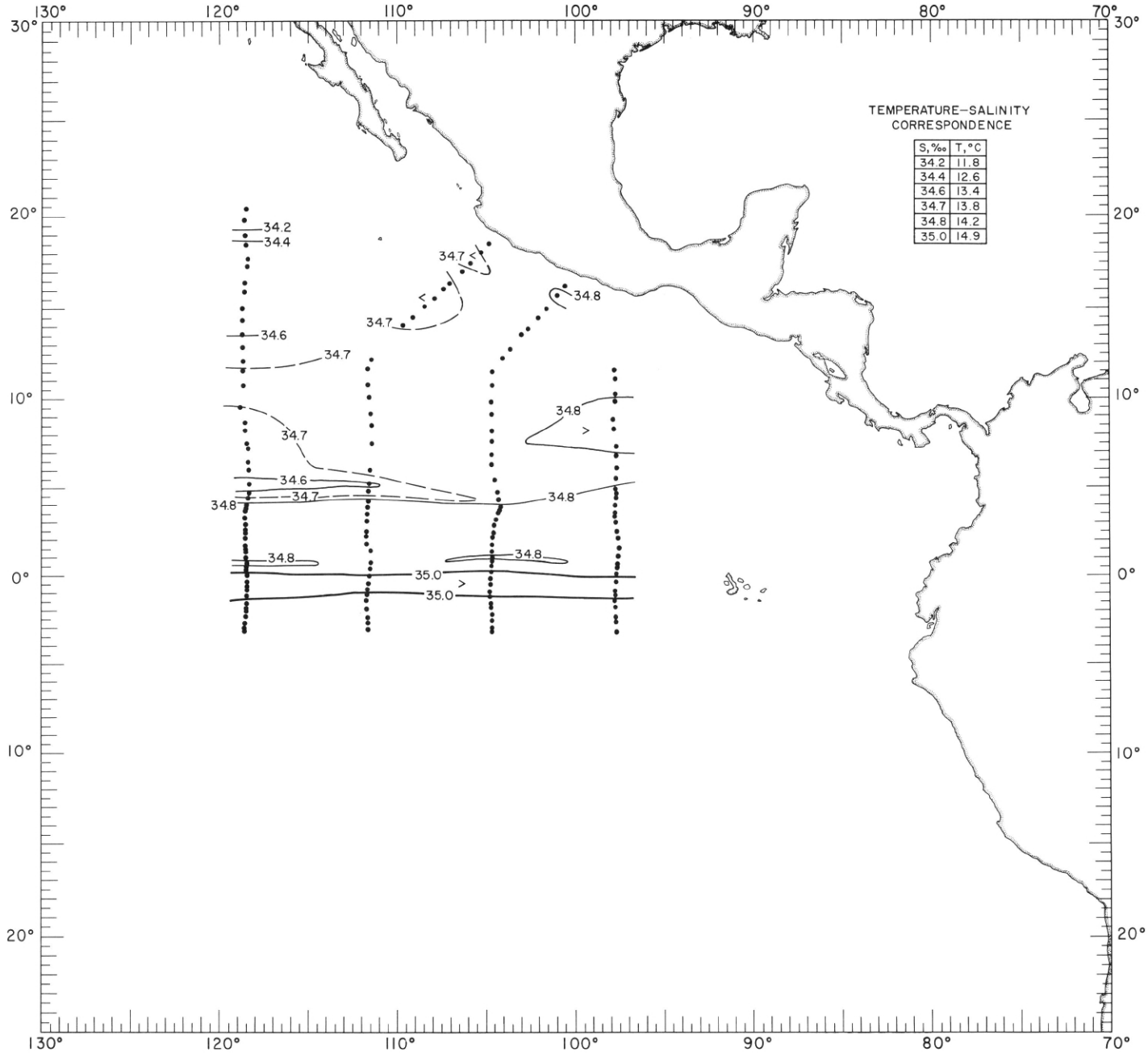

60-S-δ200.

FIGURE 60-S-δ200.—Salinity (‰) on the surface where $\delta_T = 200$ cl./t., December 1967-January 1968. The table shows the temperature corresponding to each isohaline on the chart.

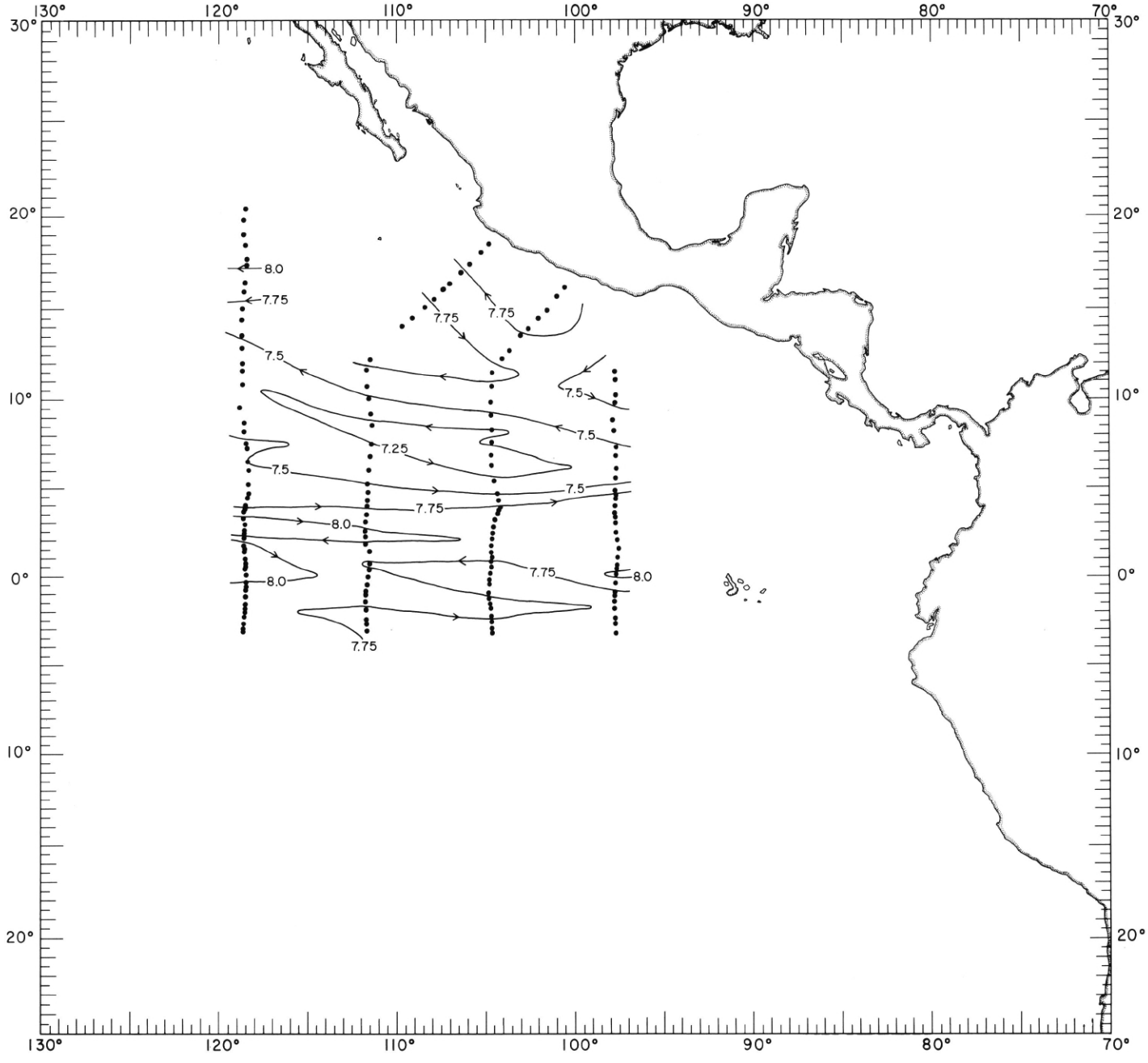

60-AP-δ200.

FIGURE 60-AP-δ200.—Acceleration potential (j./kg.), relative to 500 db., on the surface where $\delta_T = 200$ cl./t., December 1967-January 1968. For computing acceleration potential, thermosteric anomaly, δ_T, was used instead of specific volume anomaly, δ.

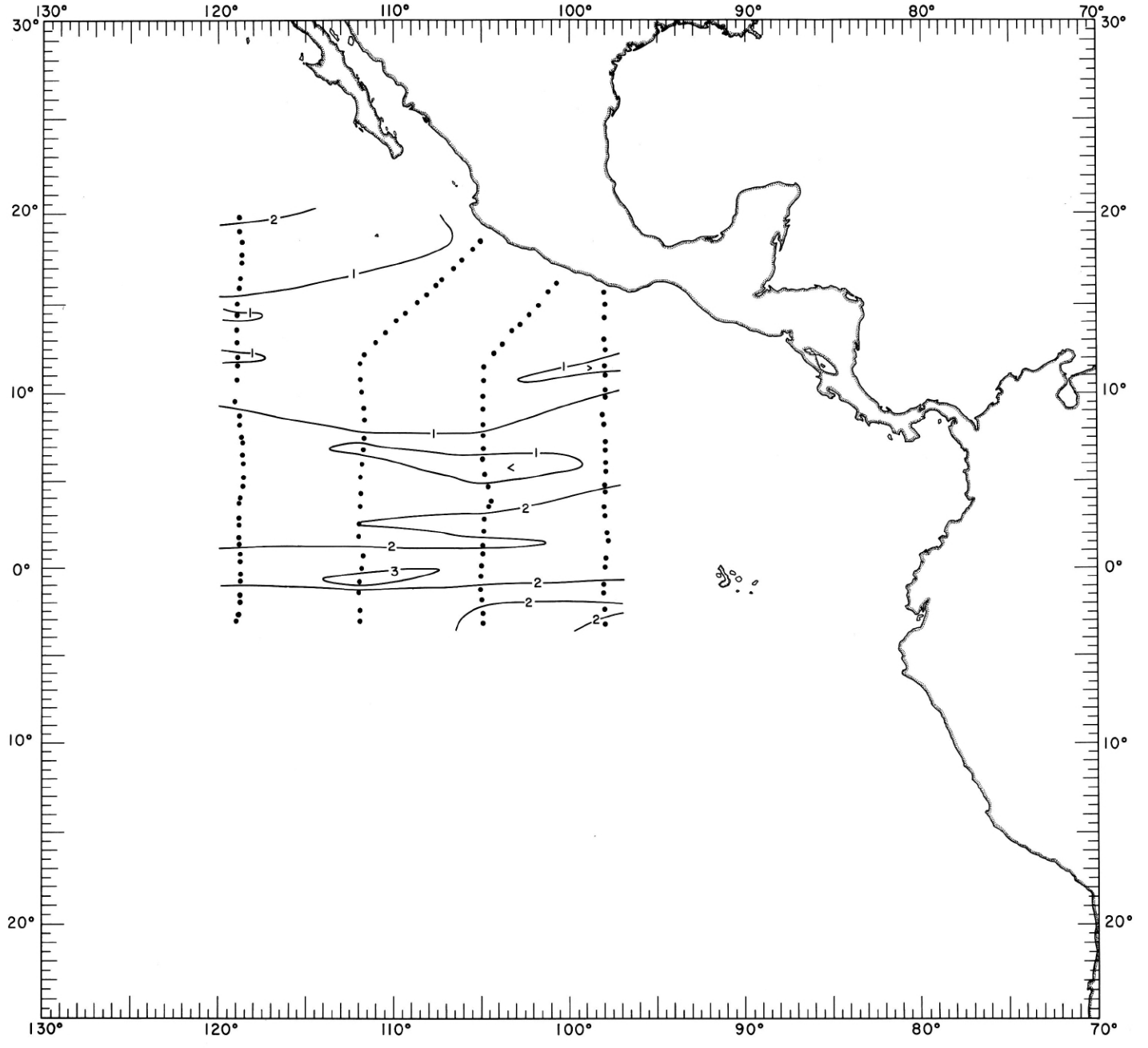

FIGURE 60-O_2-δ200.—Oxygen (ml./l.) on the surface where $\delta_T = 200$ cl./t., December 1967-January 1968.

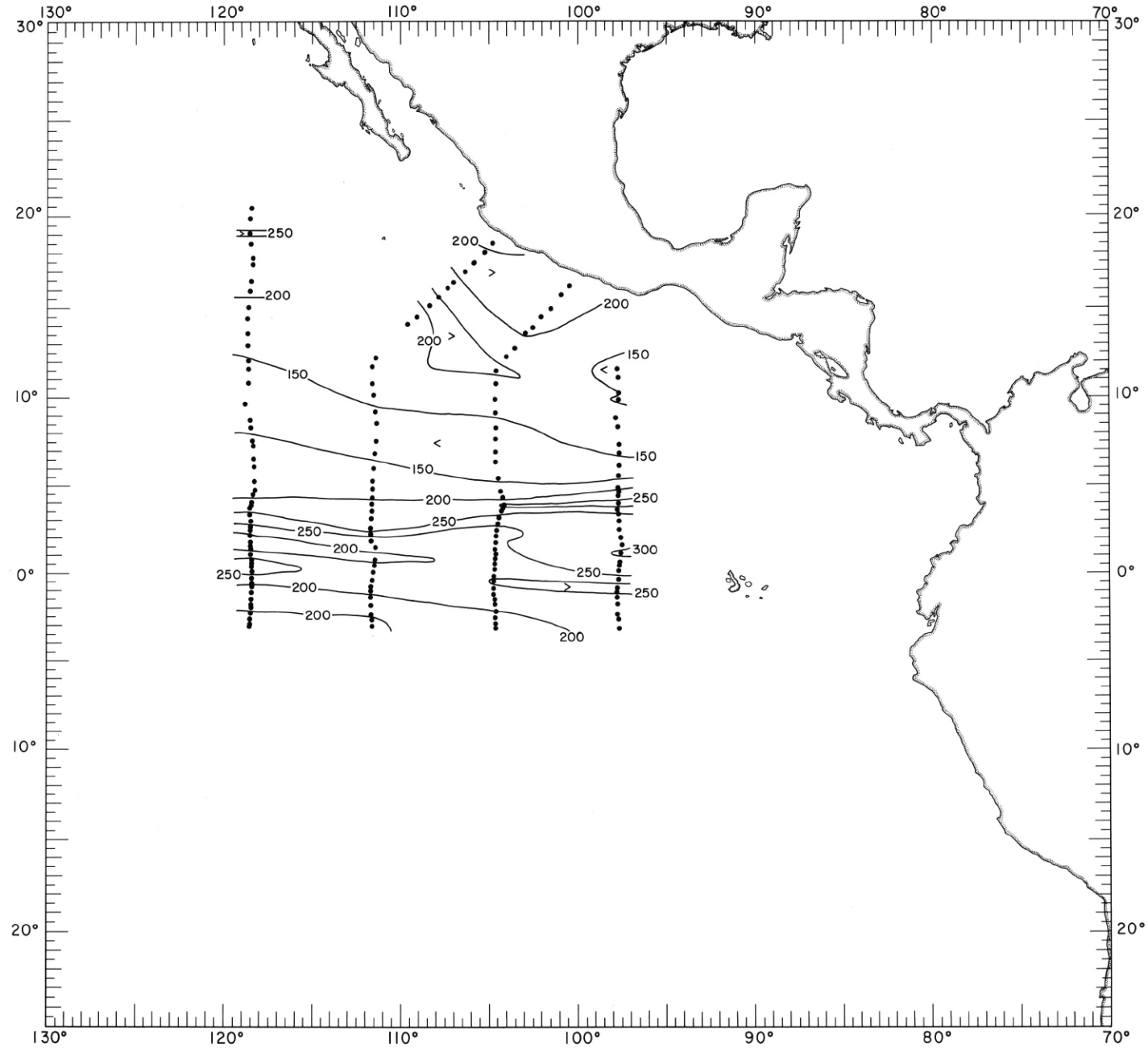

FIGURE 60-δ160-z.—Depth (m.) of the surface where $\delta_T = 160$ cl./t., December 1967-January 1968.

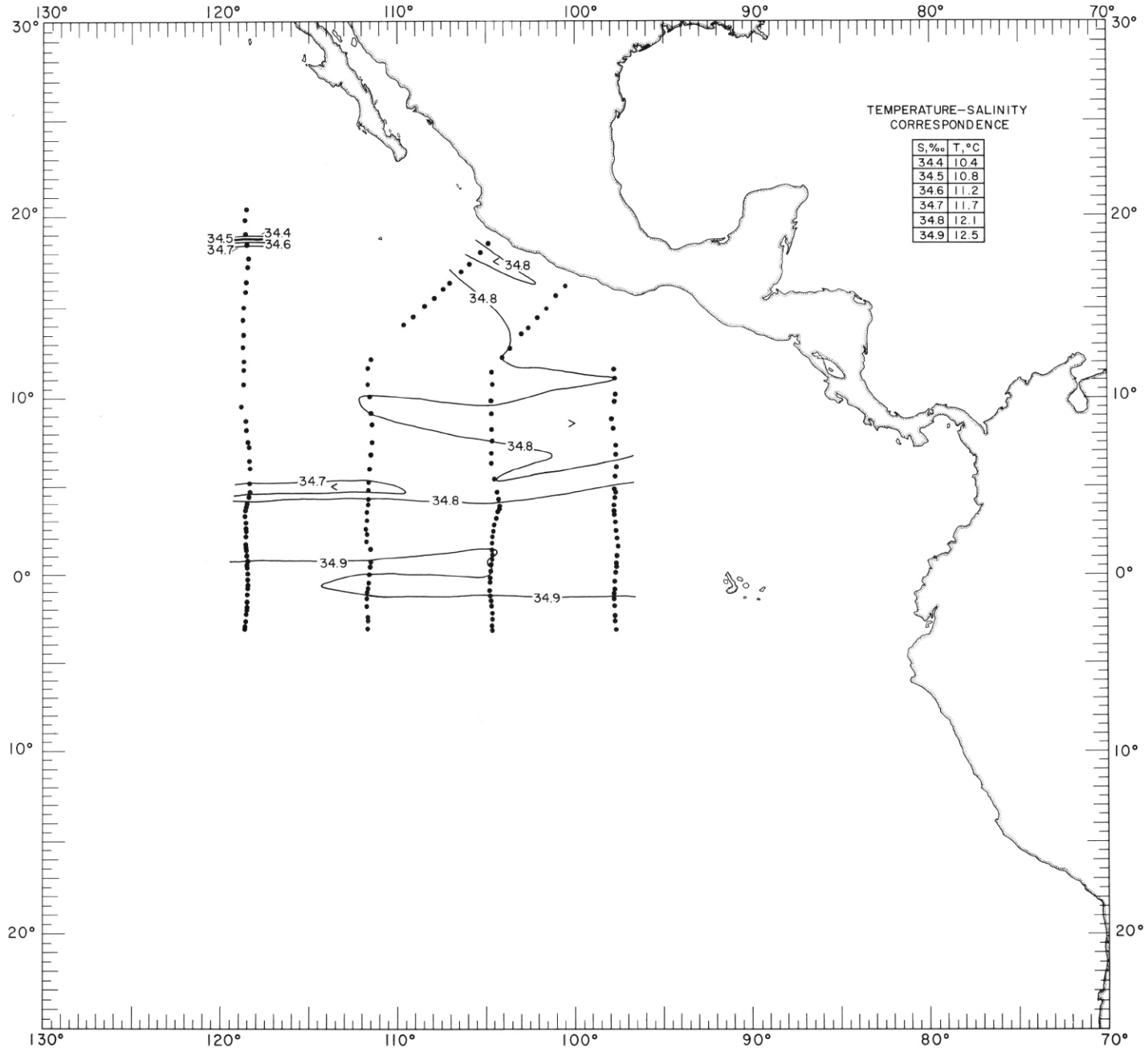

60-S-δ160.

FIGURE 60-S-δ160.—Salinity (‰) on the surface where $\delta_T = 160$ cl./t., December 1967-January 1968. The table shows the temperature corresponding to each isohaline on the chart.

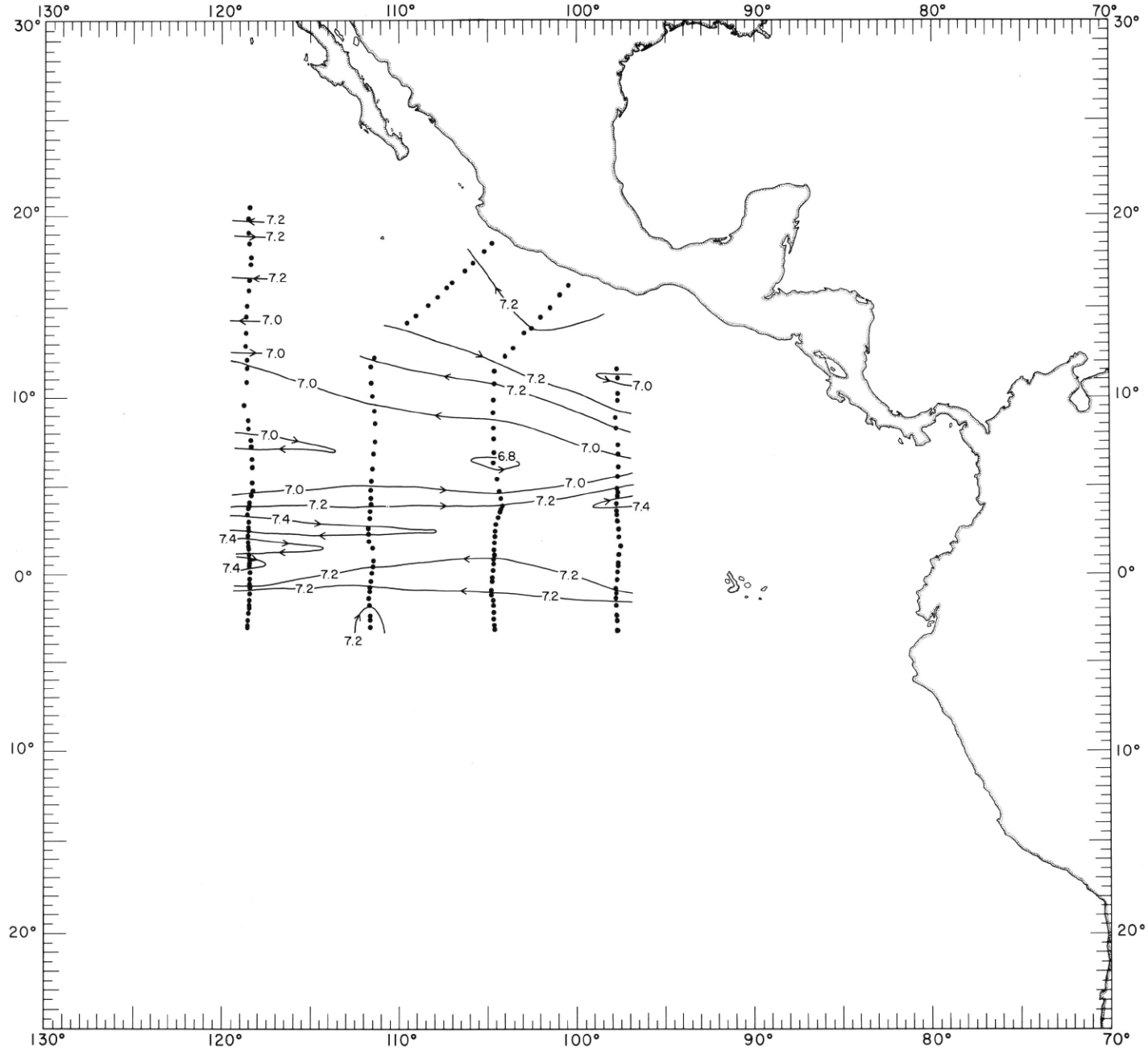

60-AP-δ160.

FIGURE 60-AP-δ160.—Acceleration potential (j./kg.), relative to 500 db., on the surface where $\delta_T = 160$ cl./t., December 1967-January 1968. For computing acceleration potential, thermosteric anomaly, δ_T, was used instead of specific volume anomaly, δ.

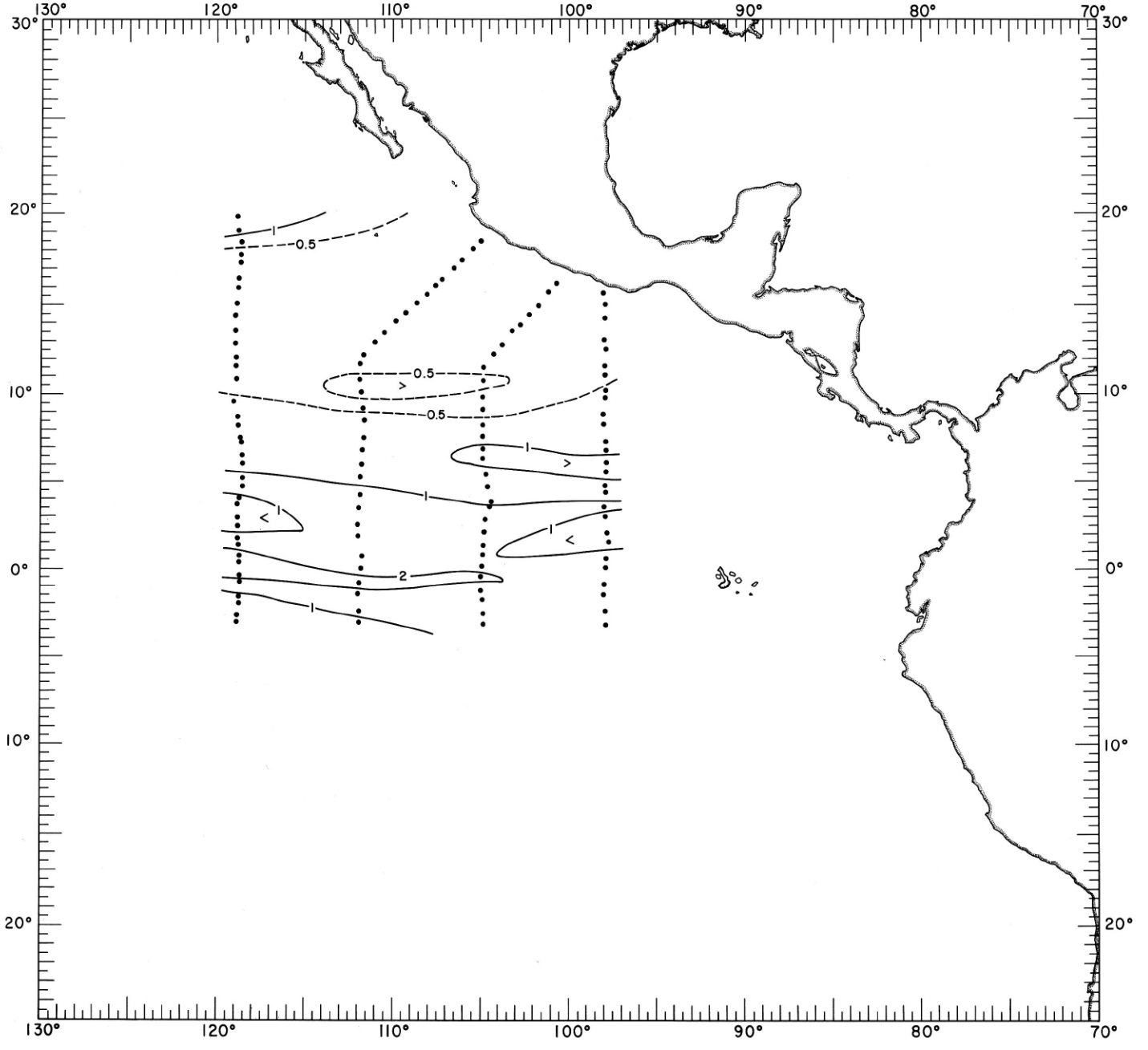

FIGURE 60-O_2-δ160.—Oxygen (ml./l.) on the surface where $\delta_T = 160$ cl./t., December 1967-January 1968.

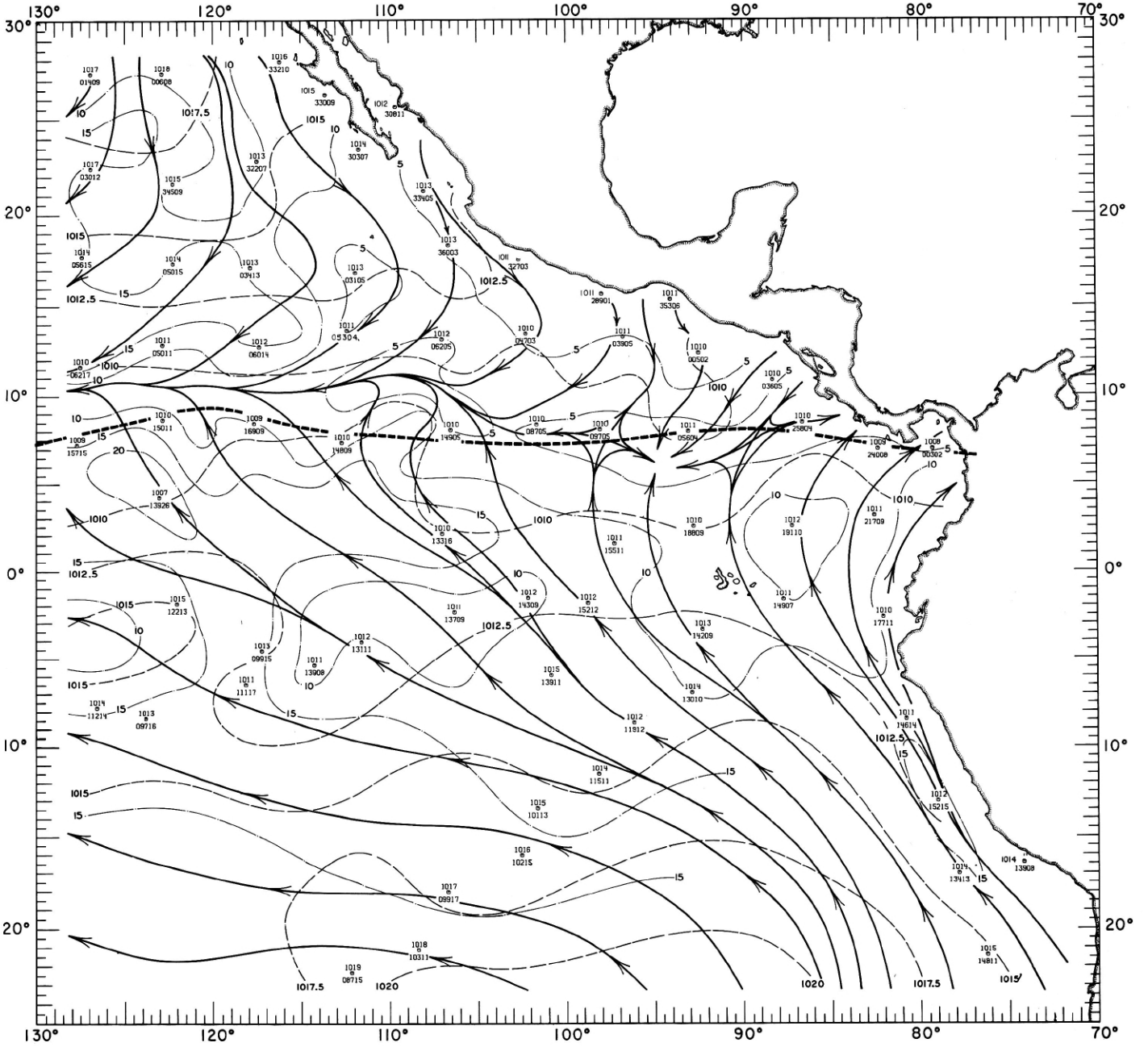

60-MW-1.

FIGURE 60-MW-1.—Analyses of the surface air pressure and surface winds from all available ship observations, averaged over 2-degree (latitude-longitude) squares for the period December 1-16, 1967. Heavy dashed lines are isobars. Solid lines are streamlines showing the mean resultant direction of wind flow. Light dash-dot lines are isotachs indicating mean resultant wind speed (kn.). Pressure (mb.) averaged for 5-degree squares is plotted above the mean position of the square, and resultant wind direction followed by speed (kn.) is plotted below. The monthly climatological position of the intertropical convergence zone is shown by a wide dashed band.

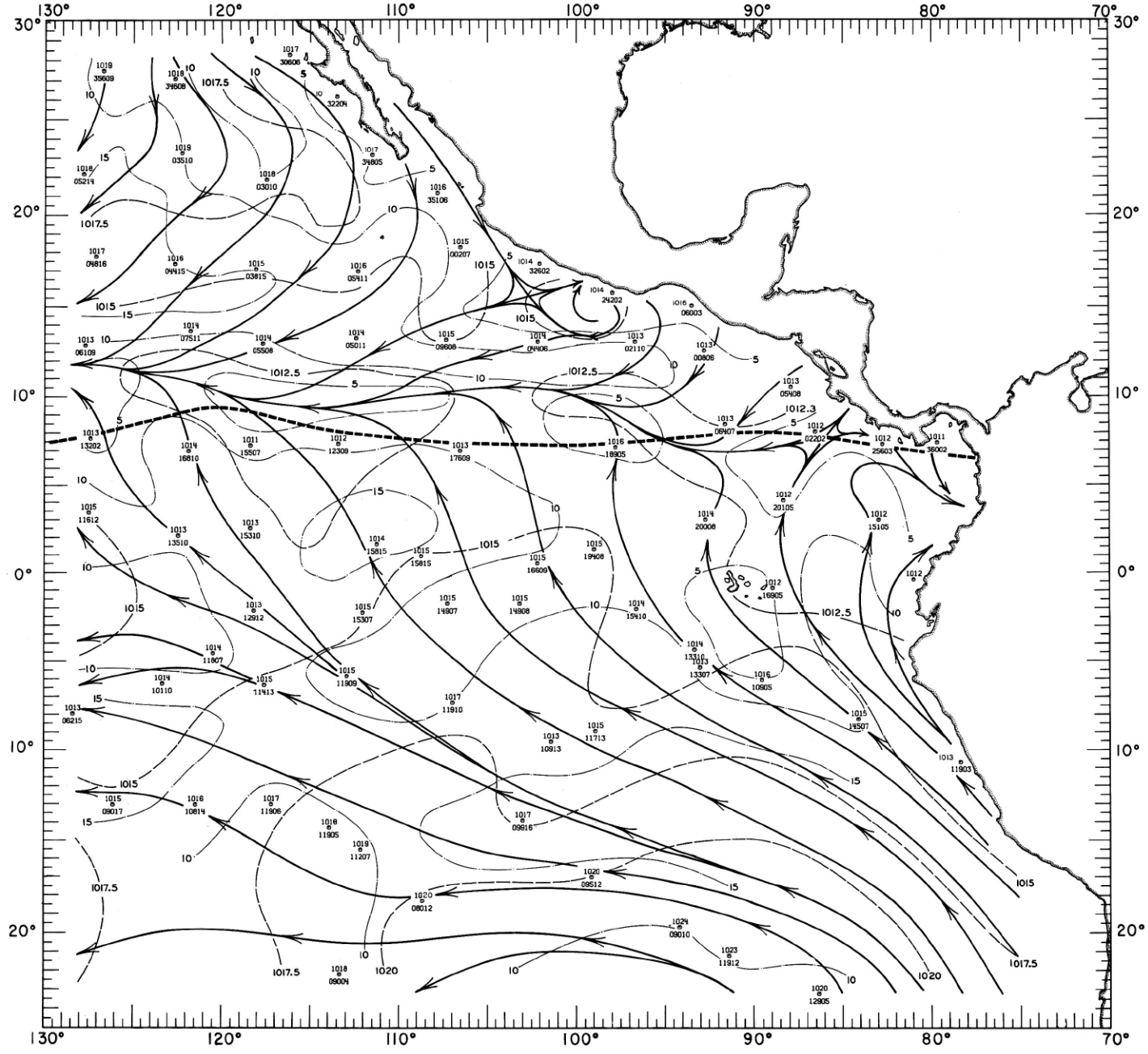

60-MW-2.

FIGURE 60-MW-2.—Analyses of the surface air pressure and surface winds from all available ship observations, averaged over 2-degree (latitude-longitude) squares for the period December 17-31, 1967. Heavy dashed lines are isobars. Solid lines are streamlines showing the mean resultant direction of wind flow. Light dash-dot lines are isotachs indicating mean resultant wind speed (kn.). Pressure (mb.) averaged for 5-degree squares is plotted above the mean position of the square, and resultant wind direction followed by speed (kn.) is plotted below. The monthly climatological position of the intertropical convergence zone is shown by a wide dashed band.

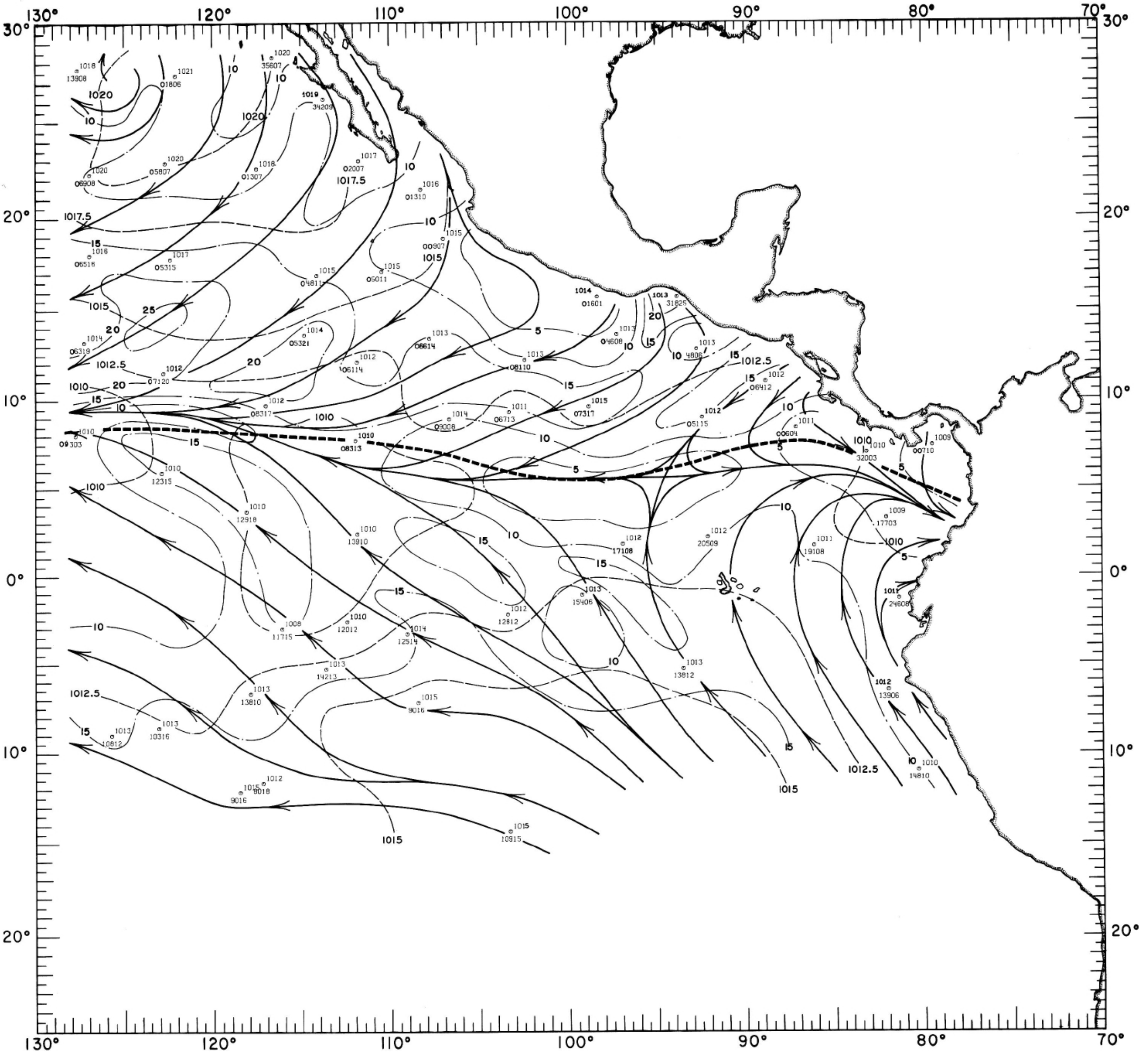

60-MW-3.

FIGURE 60-MW-3.—Analyses of the surface air pressure and surface winds from all available ship observations, averaged over 2-degree (latitude-longitude) squares for the period January 1-14, 1968. Heavy dashed lines are isobars. Solid lines are streamlines showing the mean resultant direction of wind flow. Light dash-dot lines are isotachs indicating mean resultant wind speed (kn.). Pressure (mb.) averaged for 5-degree squares is plotted above the mean position of the square, and resultant wind direction followed by speed (kn.) is plotted below. The monthly climatological position of the intertropical convergence zone is shown by a wide dashed band.

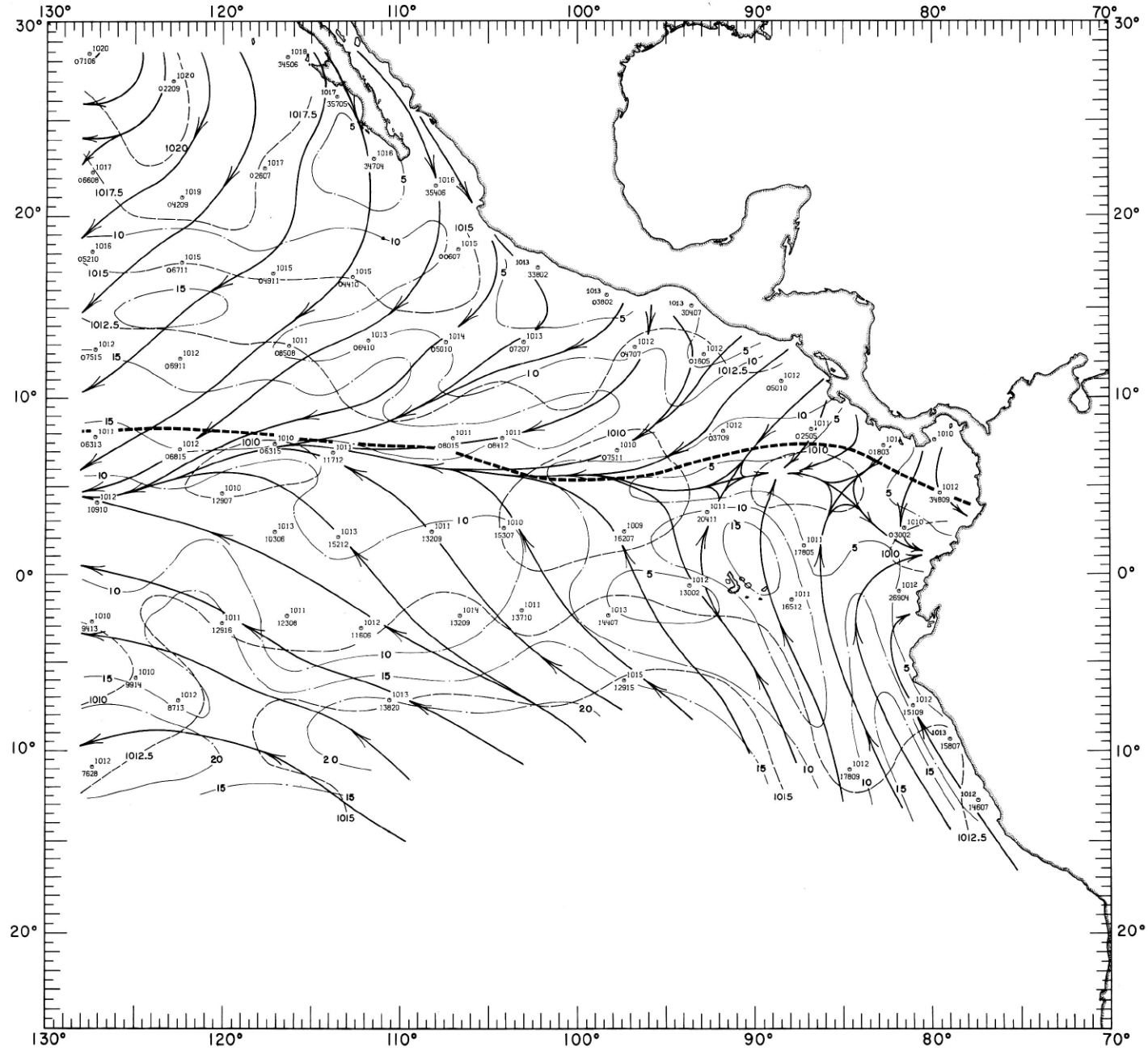

60-MW-4.

FIGURE 60-MW-4.—Analyses of the surface air pressure and surface winds from all available ship observations, averaged over 2-degree (latitude-longitude) squares for the period January 15-31, 1968. Heavy dashed lines are isobars. Solid lines are streamlines showing the mean resultant direction of wind flow. Light dash-dot lines are isotachs indicating mean resultant wind speed (kn.). Pressure (mb.) averaged for 5-degree squares is plotted above the mean position of the square, and resultant wind direction followed by speed (kn.) is plotted below. The monthly climatological position of the intertropical convergence zone is shown by a wide dashed band.

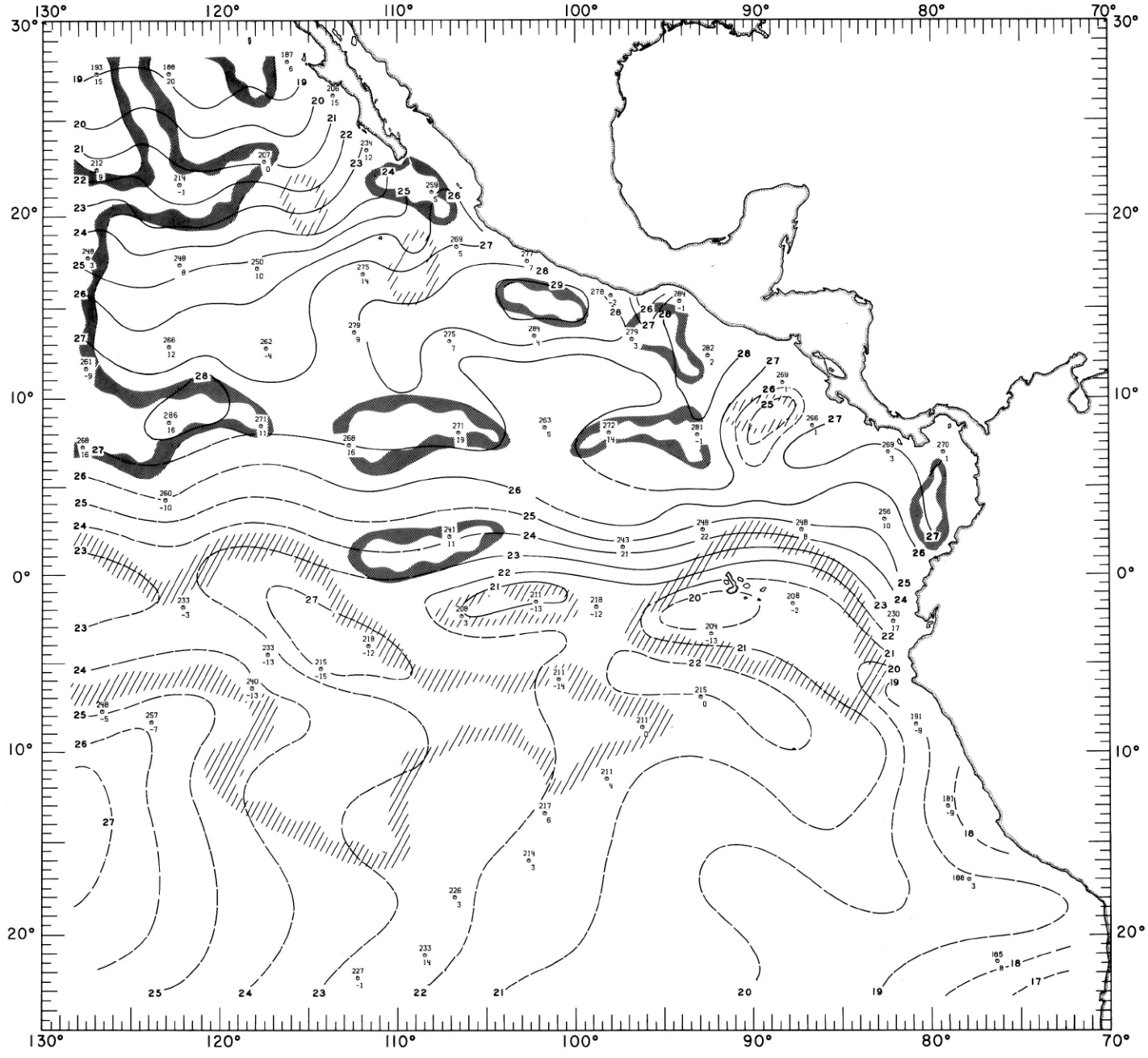

60-MT-1.

FIGURE 60-MT-1.—Analysis of sea surface temperatures based on averages for 2-degree (latitude-longitude) squares from all available ship observations for the period December 1-16, 1967. Solid lines are sea surface isotherms (°C.); the isotherms are dashed where data are sparse. Dark hatching outlines areas with positive temperature anomalies (computed from mean sea surface temperatures averaged over 22 years) greater than 1° C.; light hatching shows areas with negative anomalies greater than 1° C. Sea surface temperature (°C. x 10) averaged for 5-degree squares is plotted above the mean position of the square; sea temperature minus air temperature difference (°C. x 10) is plotted below the symbol.

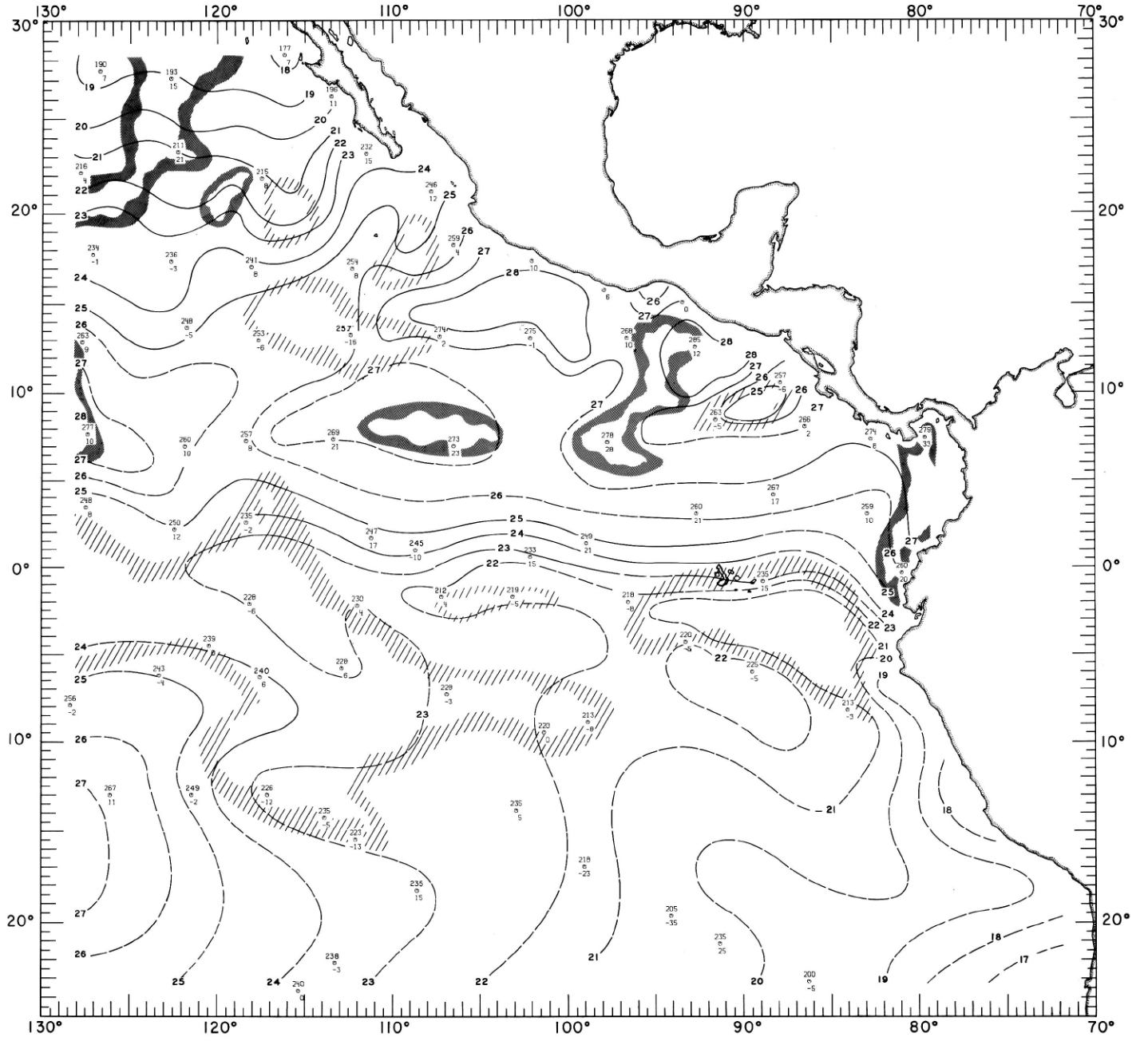

60-MT-2.

FIGURE 60-MT-2.—Analysis of sea surface temperatures based on averages for 2-degree (latitude-longitude) squares from all available ship observations for the period December 17-31, 1967. Solid lines are sea surface isotherms (°C.); the isotherms are dashed where data are sparse. Dark hatching outlines areas with positive temperature anomalies (computed from mean sea surface temperatures averaged over 22 years) greater than 1° C.; light hatching shows areas with negative anomalies greater than 1° C. Sea surface temperature (°C. x 10) averaged for 5-degree squares is plotted above the mean position of the square; sea temperature minus air temperature difference (°C. x 10) is plotted below the symbol.

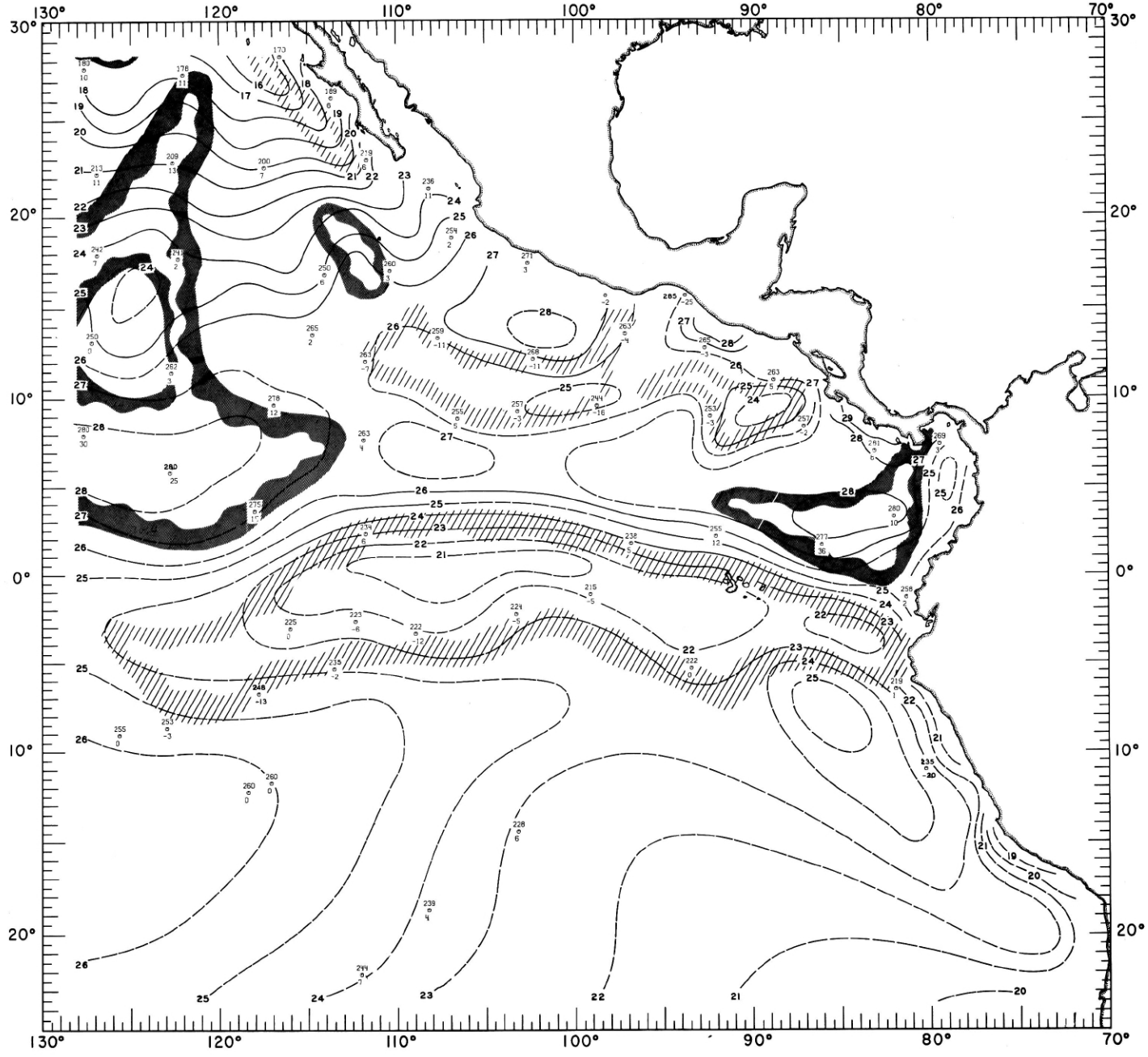

60-MT-3.

FIGURE 60-MT-3.—Analysis of sea surface temperatures based on averages for 2-degree (latitude-longitude) squares from all available ship observations for the period January 1-14, 1968. Solid lines are sea surface isotherms (°C.); the isotherms are dashed where data are sparse. Dark hatching outlines areas with positive temperature anomalies (computed from mean sea surface temperatures averaged over 22 years) greater than 1° C.; light hatching shows areas with negative anomalies greater than 1° C. Sea surface temperature (°C. x 10) averaged for 5-degree squares is plotted above the mean position of the square; sea temperature minus air temperature difference (°C. x 10) is plotted below the symbol.

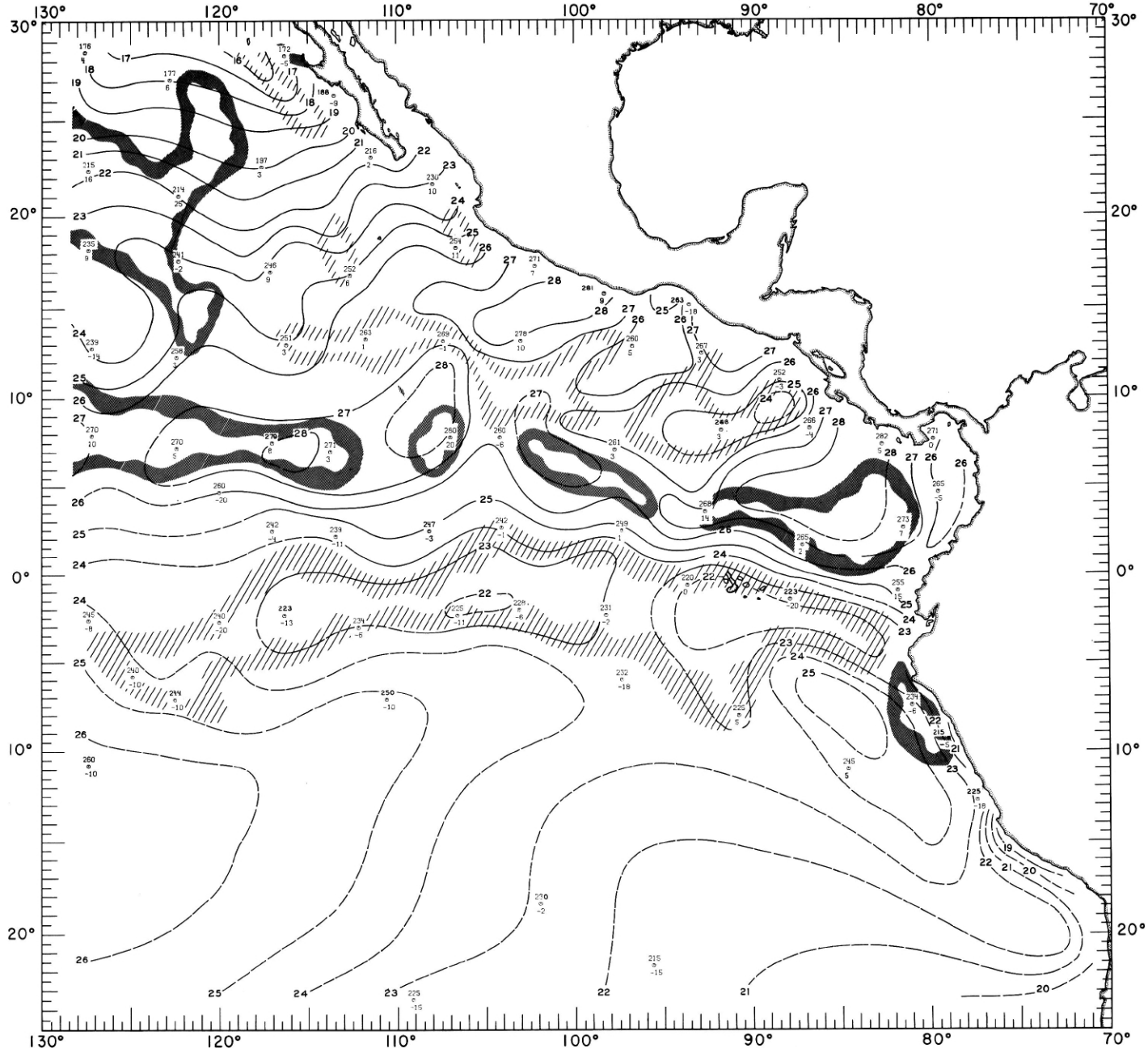

60-MT-4.

FIGURE 60-MT-4.—Analysis of sea surface temperatures based on averages for 2-degree (latitude-longitude) squares from all available ship observations for the period January 15-31, 1968. Solid lines are sea surface isotherms (°C.); the isotherms are dashed where data are sparse. Dark hatching outlines areas with positive temperature anomalies (computed from mean sea surface temperatures averaged over 22 years) greater than 1° C.; light hatching shows areas with negative anomalies greater than 1° C. Sea surface temperature (°C. x 10) averaged for 5-degree squares is plotted above the mean position of the square; sea temperature minus air temperature difference (°C. x 10) is plotted below the symbol.

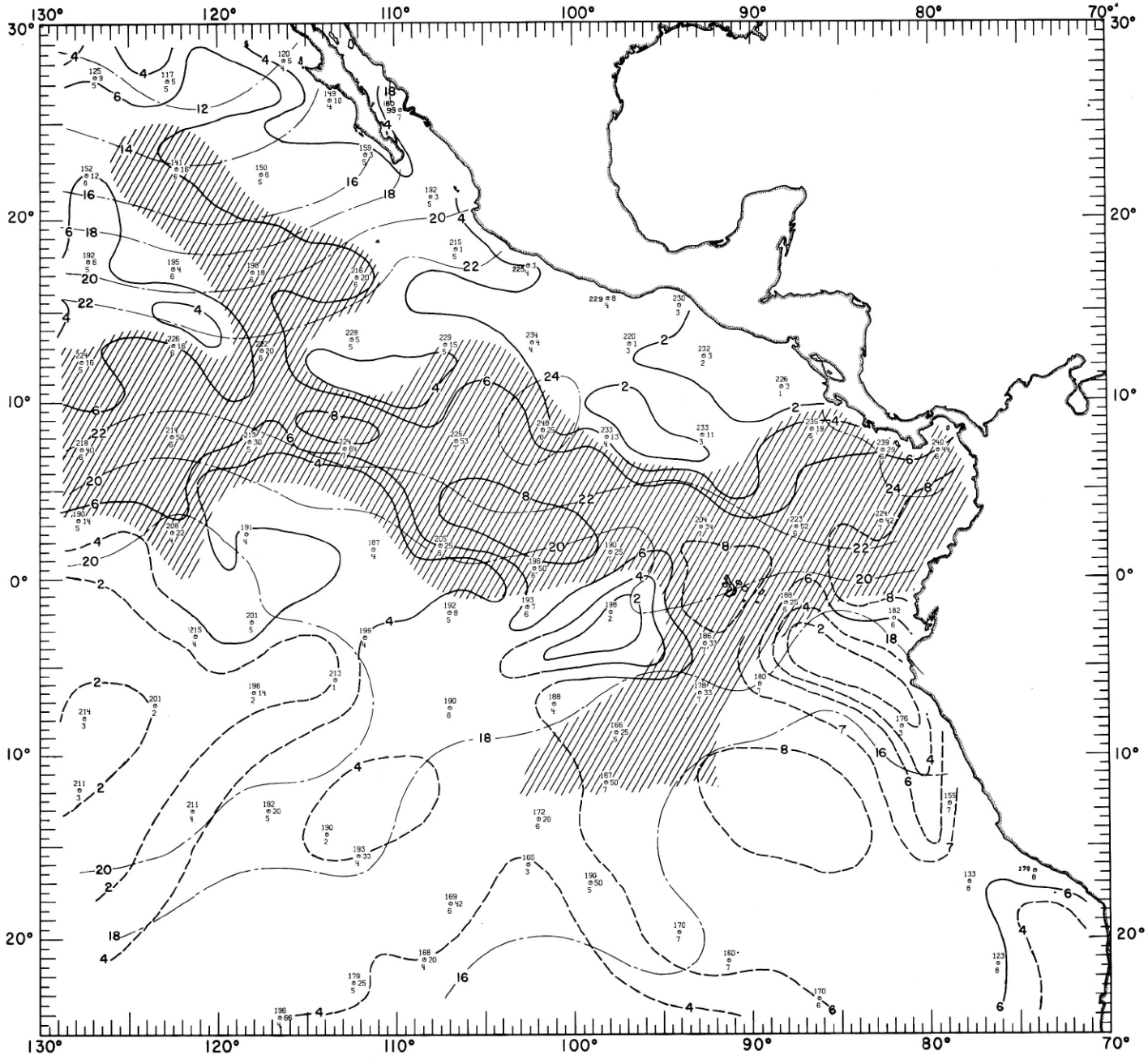

60-MC-1.

FIGURE 60-MC-1.—Analyses of the surface dew-point temperature of the air and total cloud cover based on 2-degree (latitude-longitude) averages from all available ship observations for the month of December 1967. Solid lines depict the monthly mean total cloud cover in oktas; the lines are dashed where data are sparse. Dash-dot lines are isotherms of the mean monthly dew-point temperature at 2-degree (C.) intervals. Areas where 15 percent or more of the ships reported rain of any type at or within sight of the ship are shaded. Dew-point temperature (°C. x 10) averaged for 5-degree squares is plotted above the mean position of the square, with total cloud cover (oktas) below the rainfall frequency (%) to the right of the symbol.

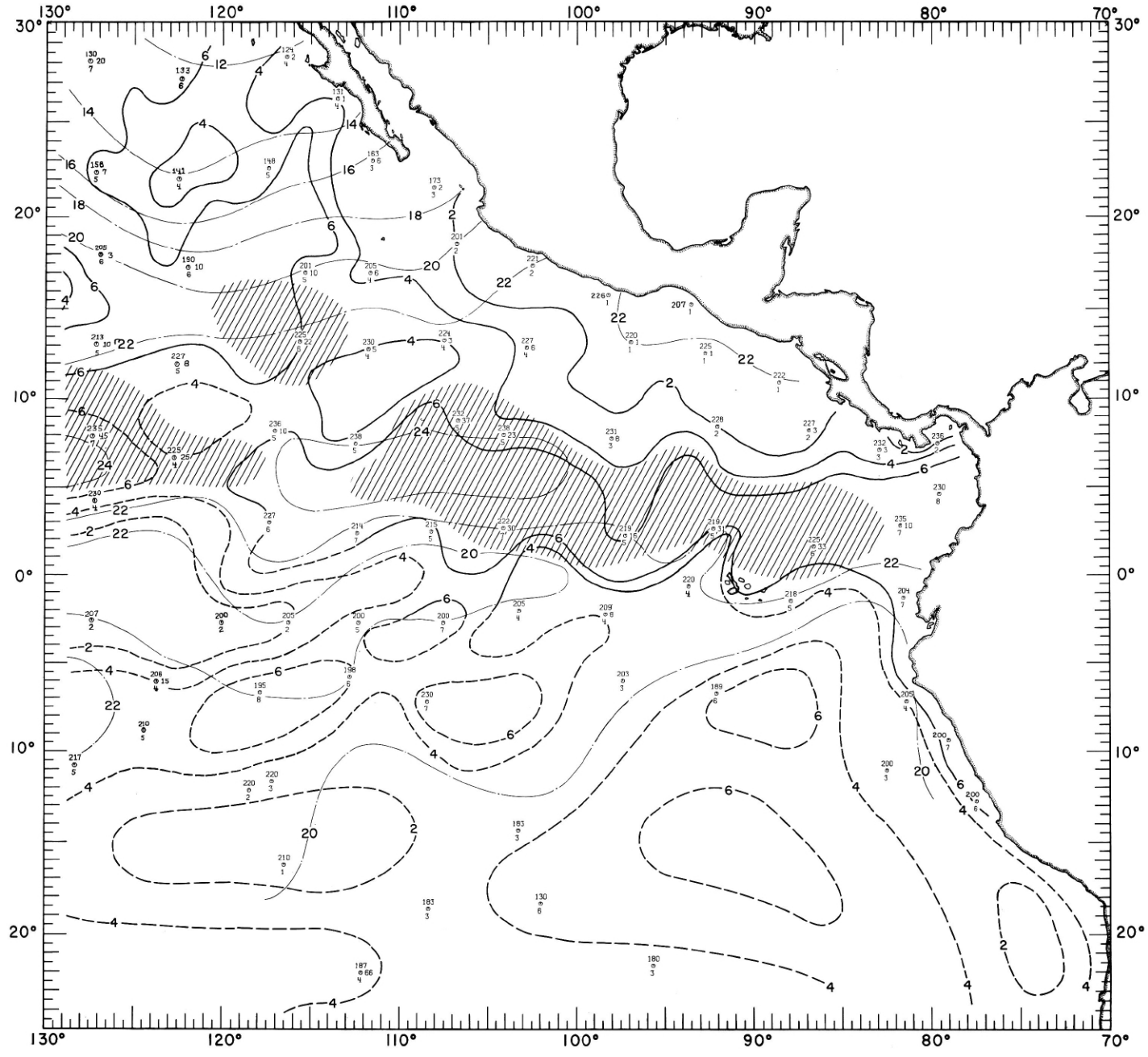

FIGURE 60-MC-2.—Analyses of the surface dew-point temperature of the air and total cloud cover based on 2-degree (latitude-longitude) averages from all available ship observations for the month of January 1968. Solid lines depict the monthly mean total cloud cover in oktas; the lines are dashed where data are sparse. Dash-dot lines are isotherms of the mean monthly dew-point temperature at 2-degree (C.) intervals. Areas where 15 percent or more of the ships reported rain of any type at or within sight of the ship are shaded. Dew-point temperature (°C. x 10) averaged for 5-degree squares is plotted above the mean position of the square, with total cloud cover (oktas) below the rainfall frequency (%) to the right of the symbol.

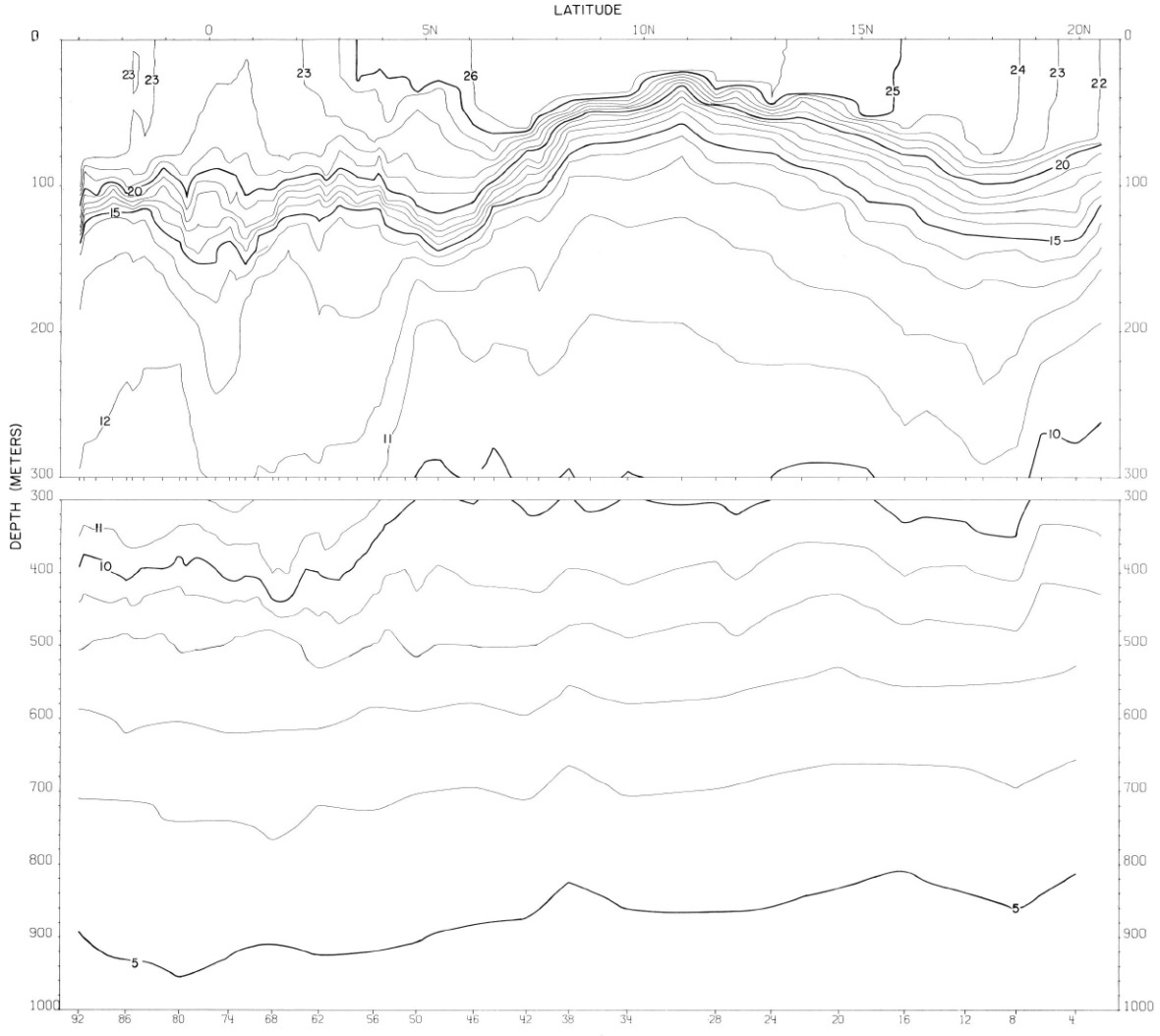

FIGURE 60-T-v1.—Vertical distribution of temperature (°C.) along 118°45′ W., December 21-31, 1967.

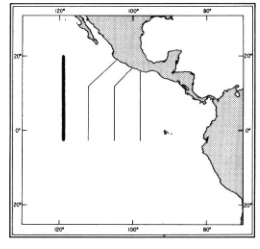

60-T-v1.

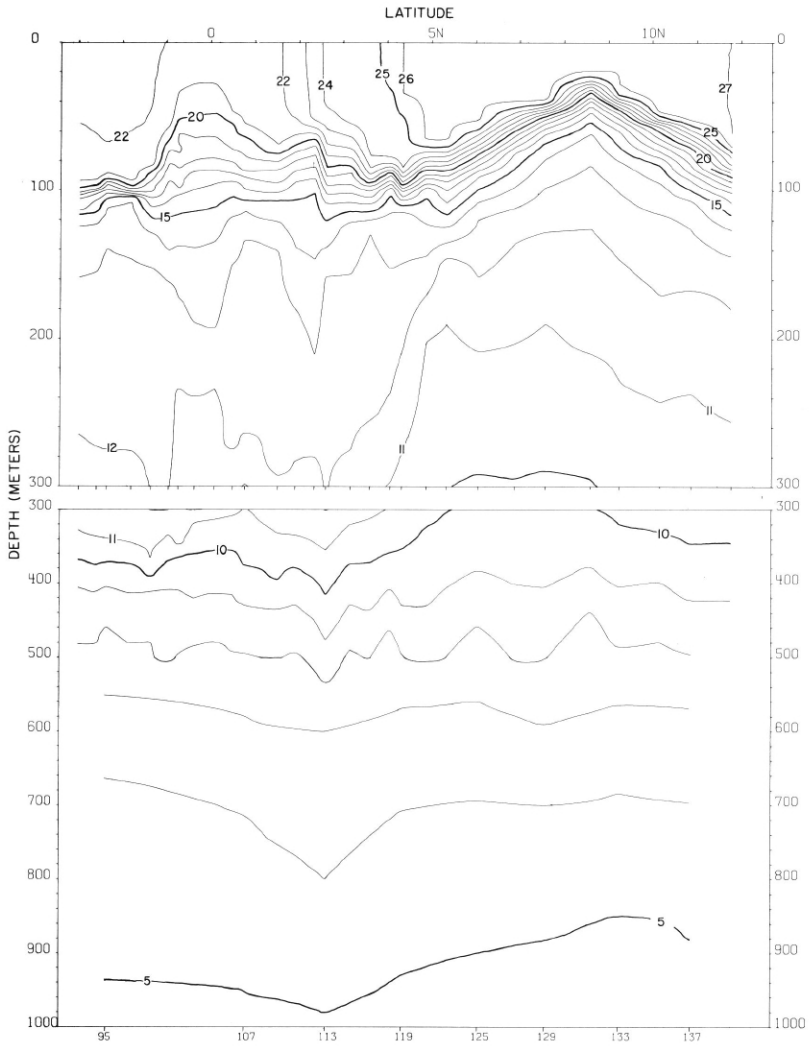

FIGURE 60-T-v2.—Vertical distribution of temperature (°C.) along 111°45′ W., January 2-6, 1968.

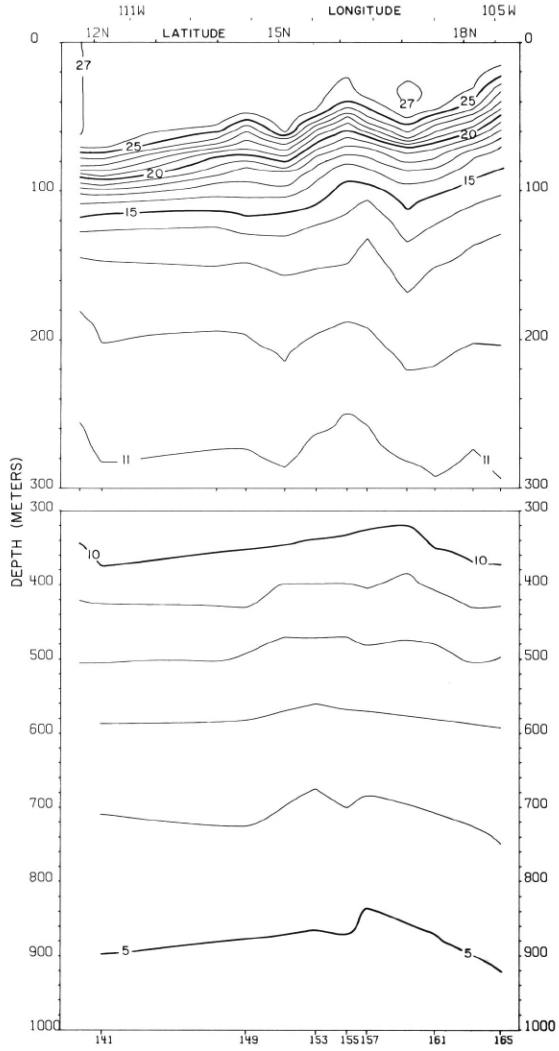

FIGURE 60-T-v3.—Vertical distribution of temperature (°C.) along a section from 12° N., 111°45′ W. to Manzanillo, January 6-9, 1968.

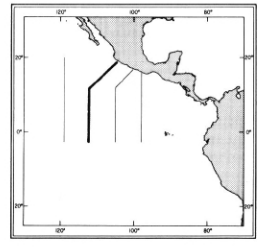

60-T-v2.

60-T-v3.

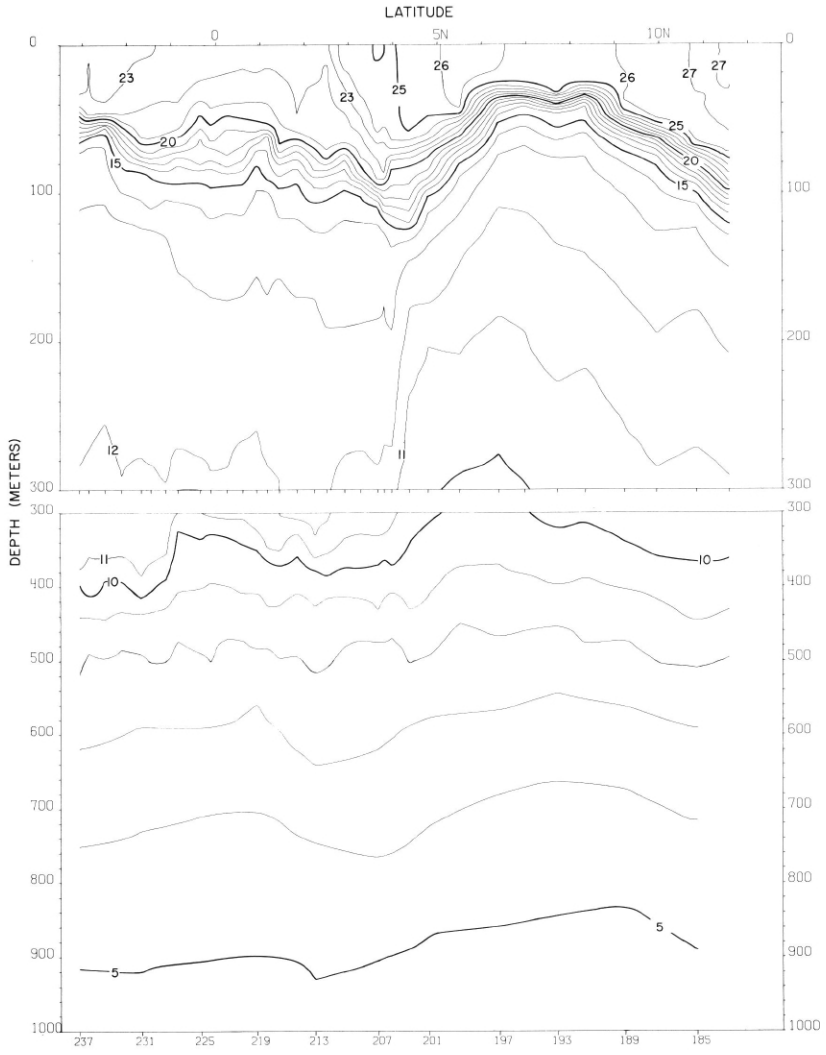

FIGURE 60-T-v5.—Vertical distribution of temperature (°C.) along 104°45′ W., January 15-21, 1968.

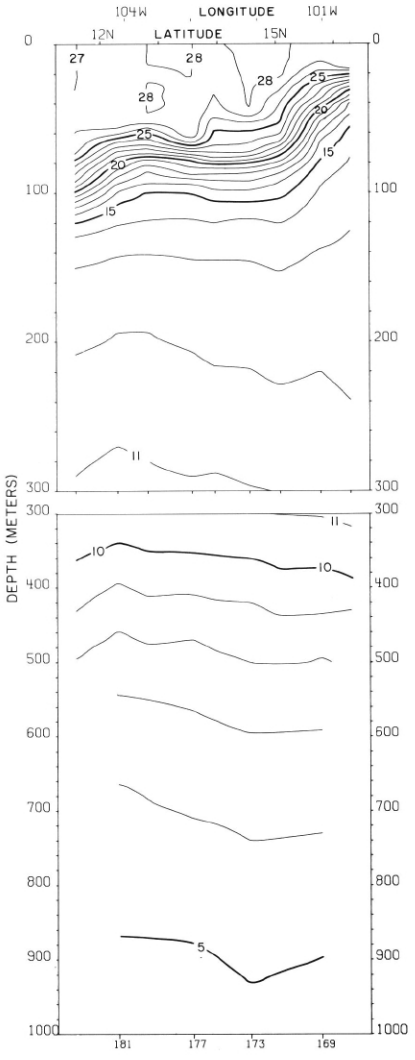

FIGURE 60-T-v4.—Vertical distribution of temperature (°C.) along a section from Acapulco to 12° N., 104°45′ W., January 13-15, 1968.

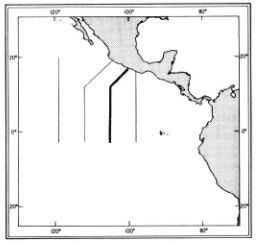

60-T-v4.

60-T-v5.

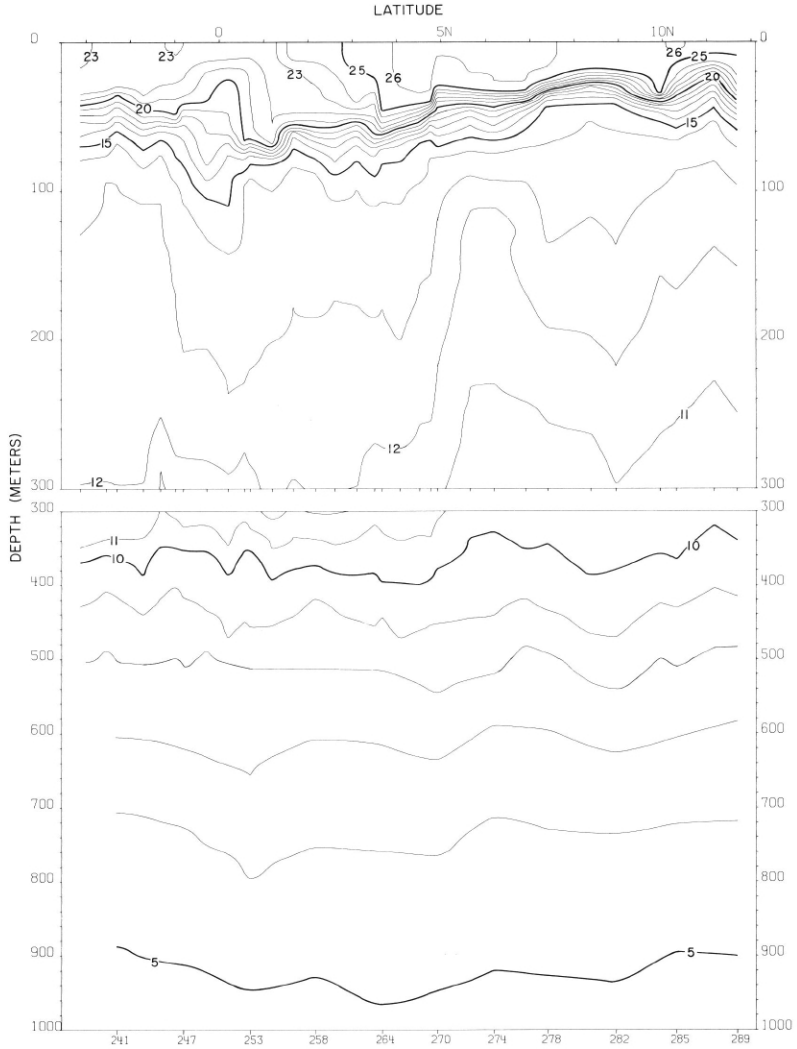

FIGURE 60-T-v6.—Vertical distribution of temperature (°C.) along 97°45′ W., January 22-28, 1968.

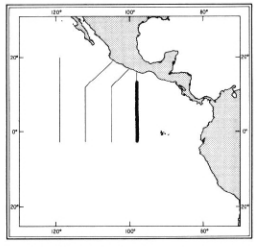

60-T-v6.

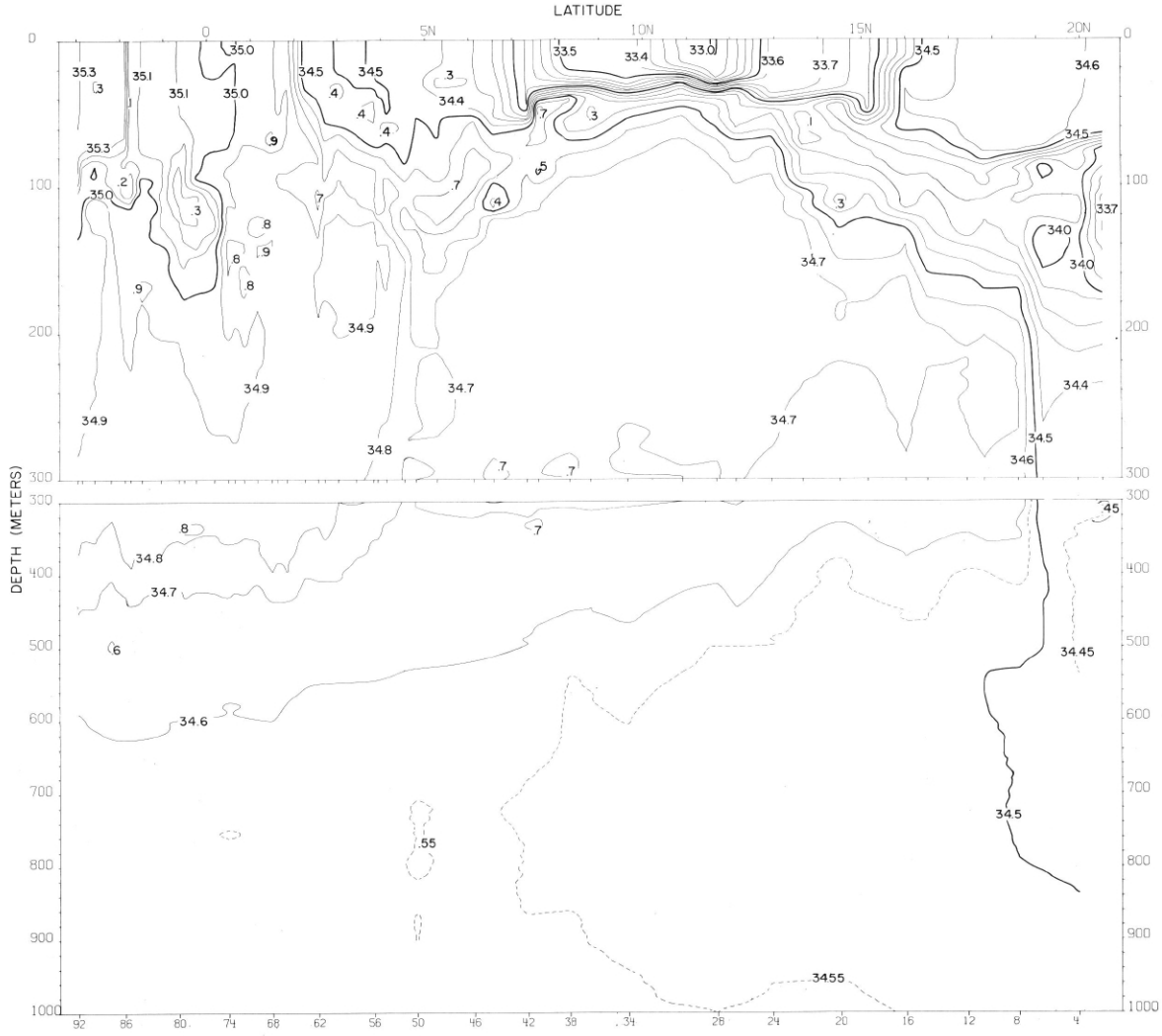

FIGURE 60-S-v1.—Vertical distribution of salinity (‰) along 118°45′ W., December 21-31, 1967.

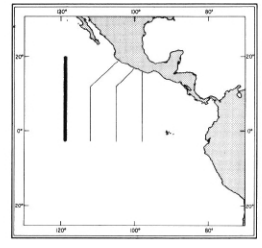

60-S-v1.

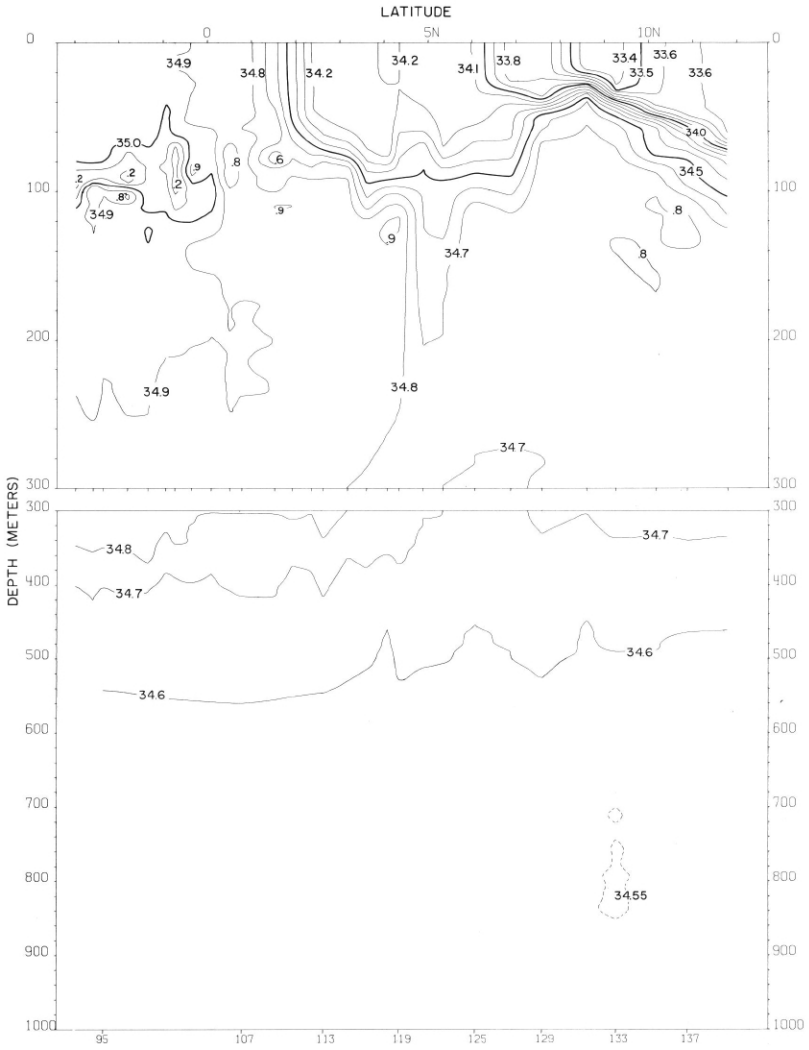

FIGURE 60-S-v2.—Vertical distribution of salinity (‰) along 111°45′ W., January 2-6, 1968.

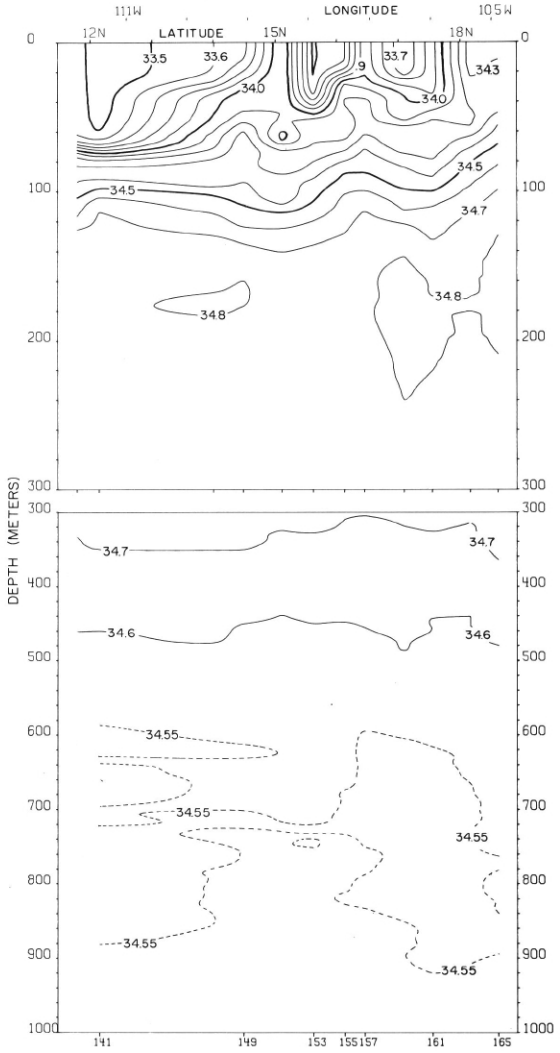

FIGURE 60-S-v3.—Vertical distribution of salinity (‰) along a section from 12° N., 111°45′ W. to Manzanillo, January 6-9, 1968.

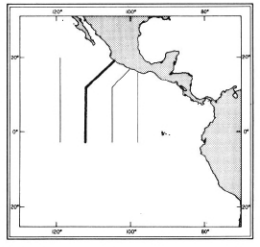

60-S-v2.

60-S-v3.

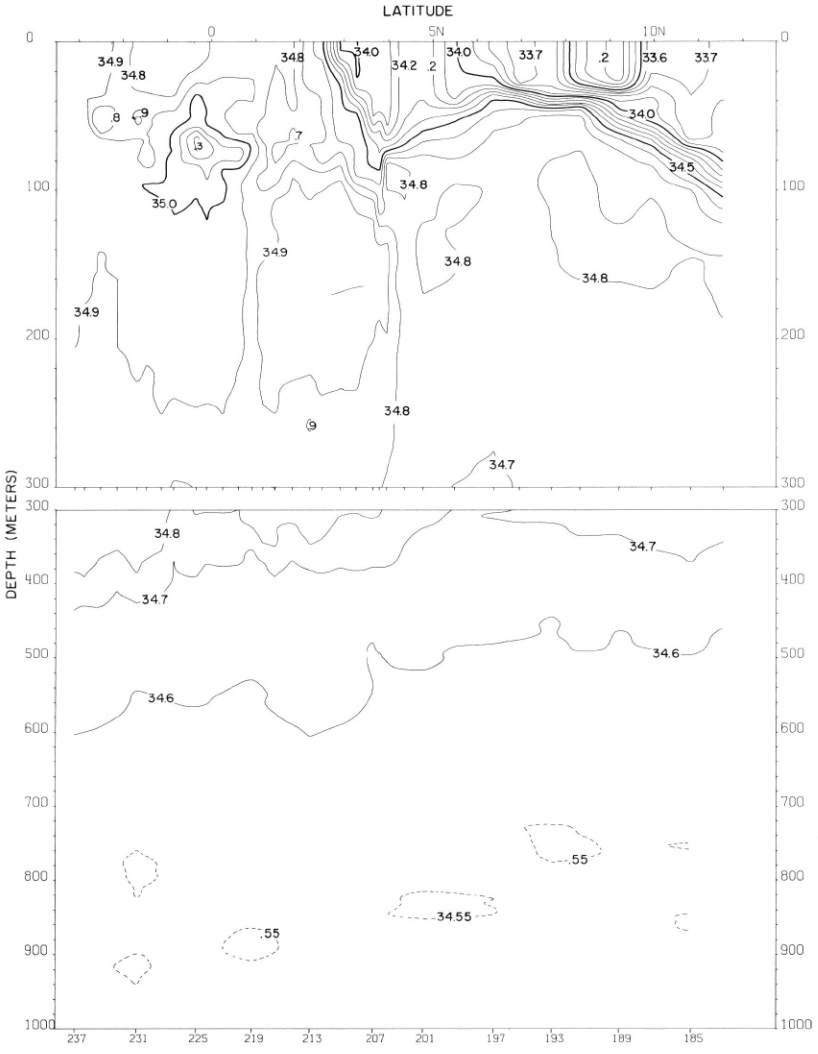

FIGURE 60-S-v5.—Vertical distribution of salinity (‰) along 104°45′ W., January 15-21, 1968.

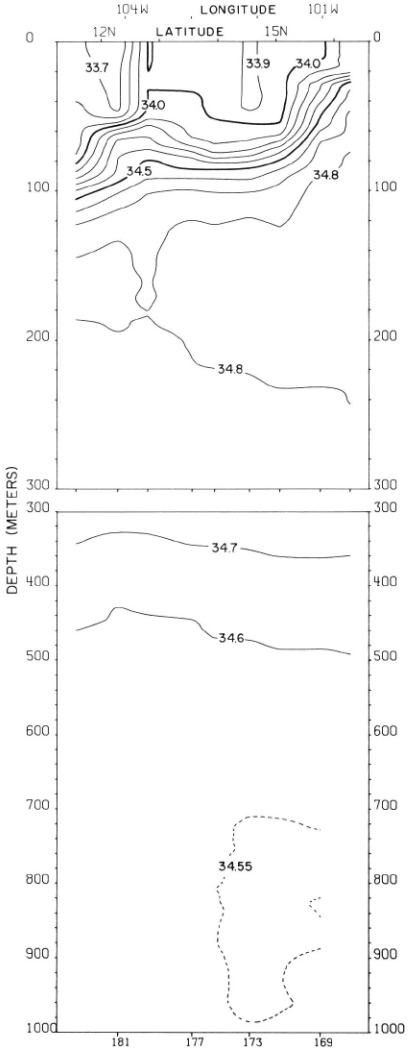

FIGURE 60-S-v4.—Vertical distribution of salinity (‰) along a section from Acapulco to 12° N., 104°45′ W., January 13-15, 1968.

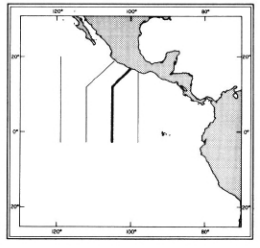

60-S-v4.

60-S-v5.

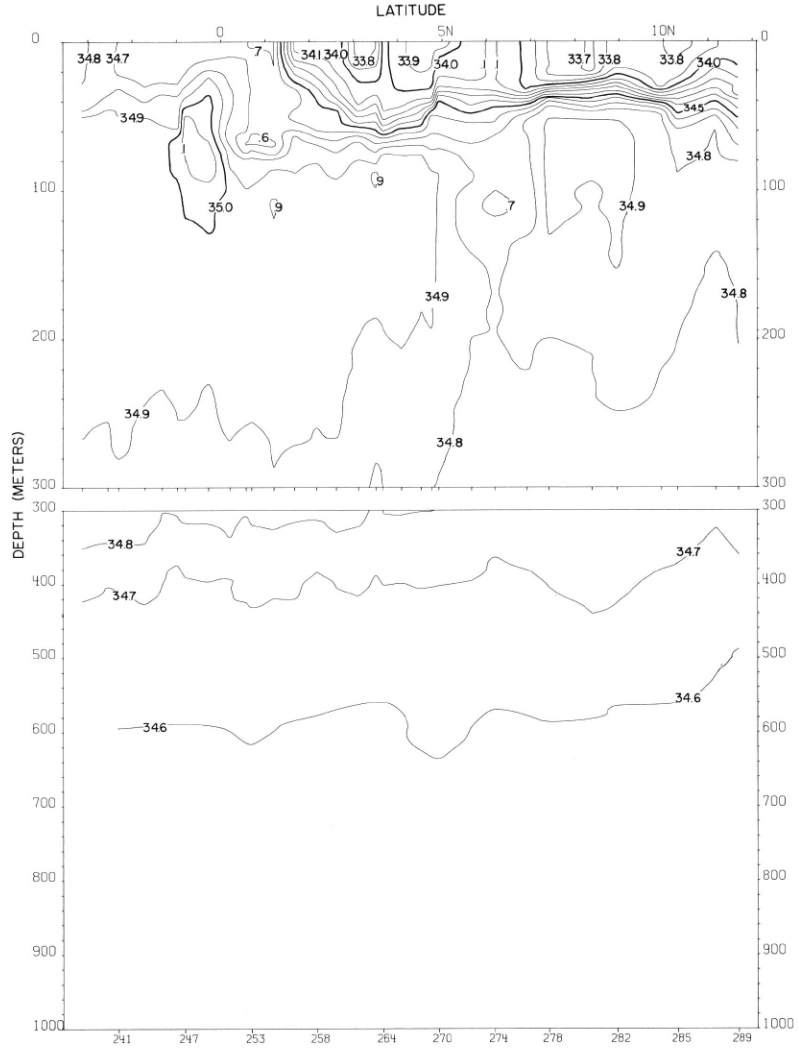

FIGURE 60-S-v6.—Vertical distribution of salinity (‰) along 97°45′ W., January 22-28, 1968.

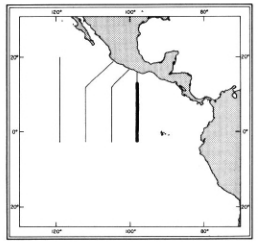

60-S-v6.

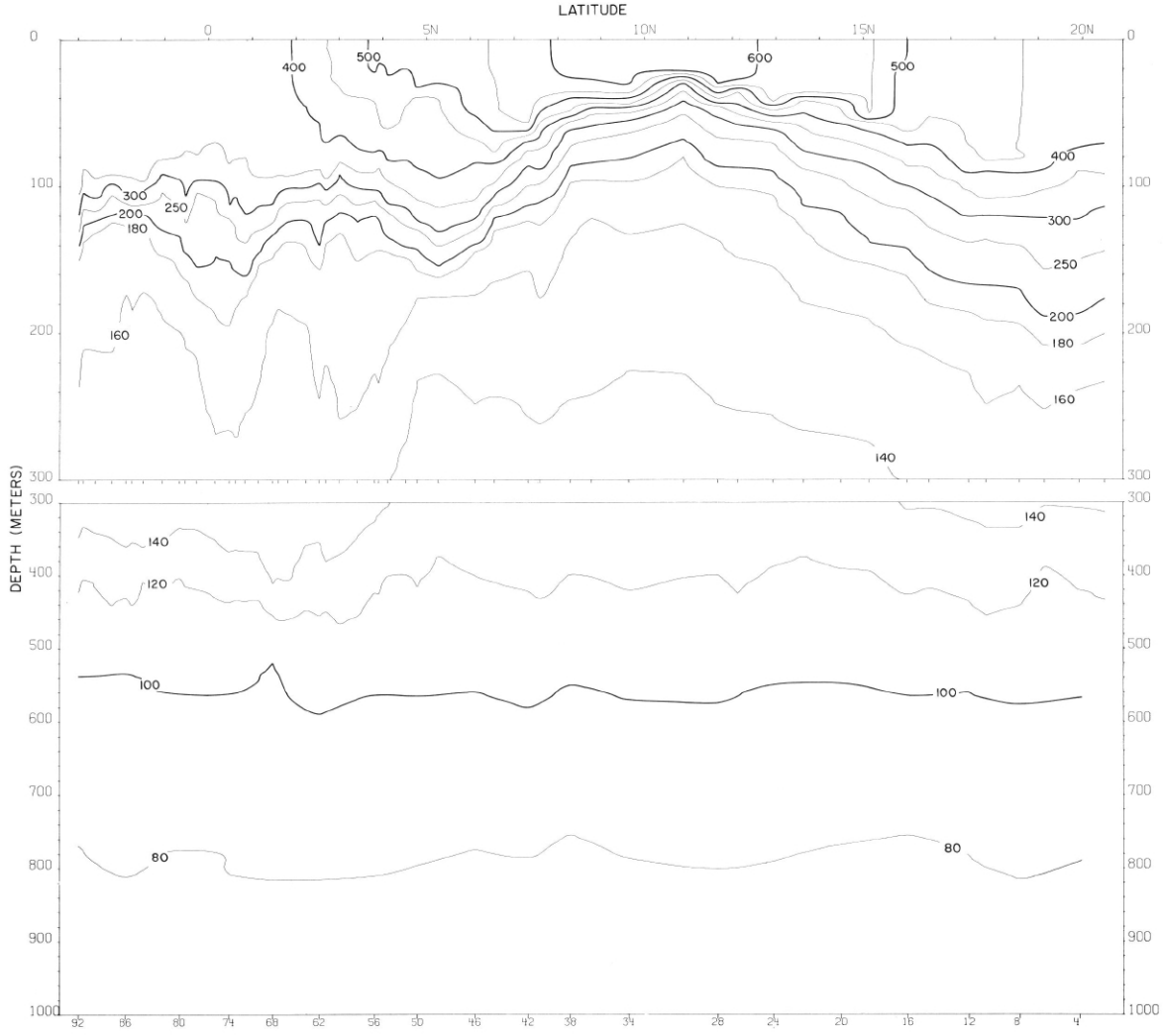

FIGURE 60-δ-v1.—Vertical distribution of thermosteric anomaly, δ_T, (cl./t.) along 118°45′ W., December 21-31, 1967.

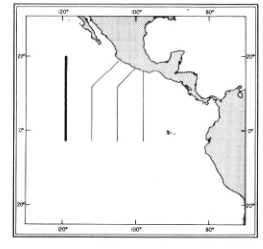

60-δ-v1.

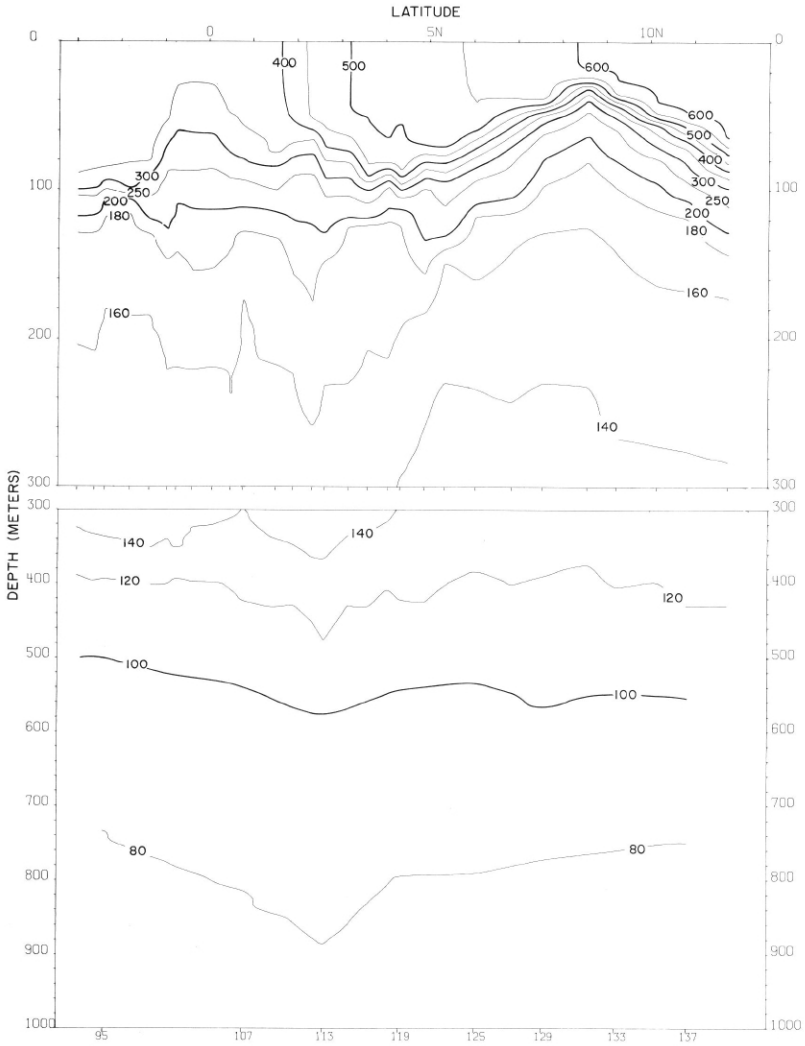

FIGURE 60-δ-v2.—Vertical distribution of thermosteric anomaly, δ_T, (cl./t.) along 111°45′ W., January 2-6, 1968.

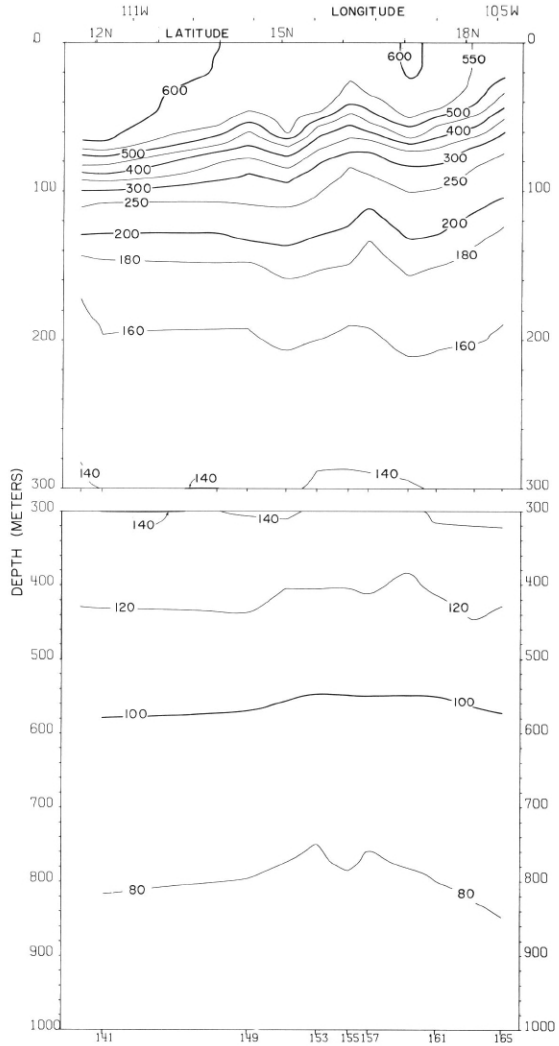

FIGURE 60-δ-v3.—Vertical distribution of thermosteric anomaly, δ_T, (cl./t.) along a section from 12° N., 111°45′ W. to Manzanillo, January 6-9, 1968.

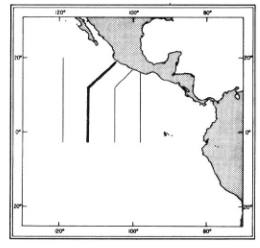

60-δ-v2.

60-δ-v3.

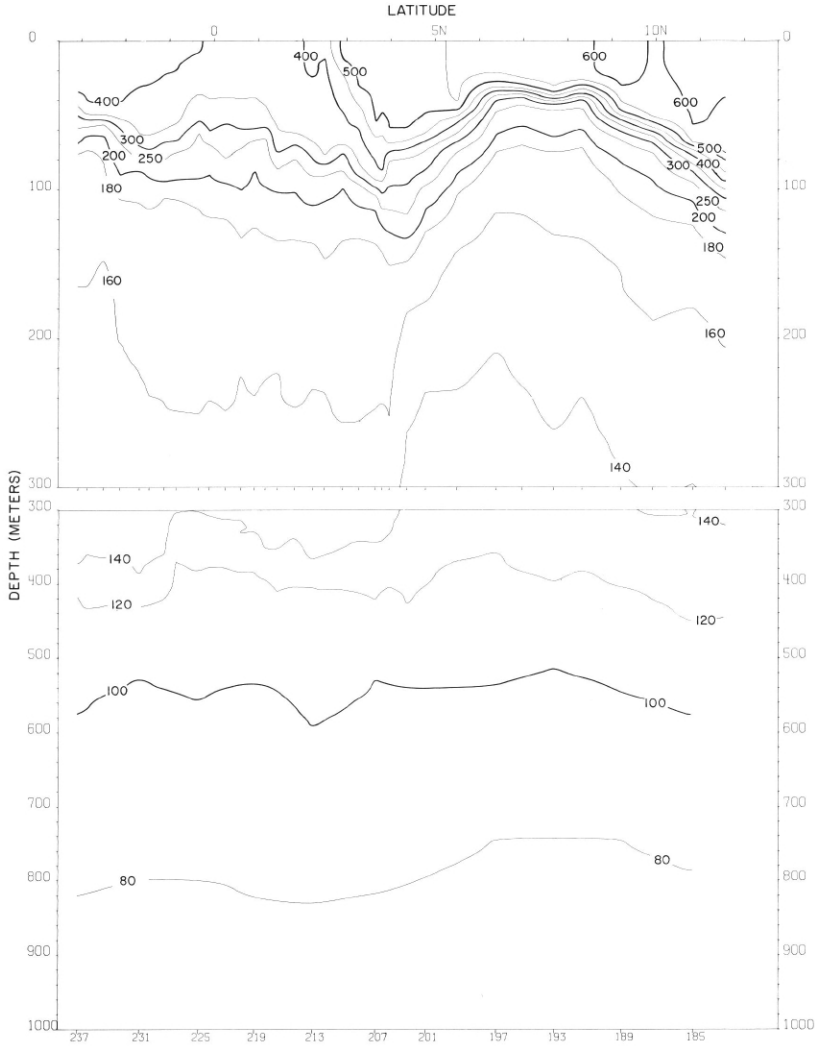

FIGURE 60-δ-v5.—Vertical distribution of thermosteric anomaly, δ_T, (cl./t.) along 104°45′ W., January 15-21, 1968.

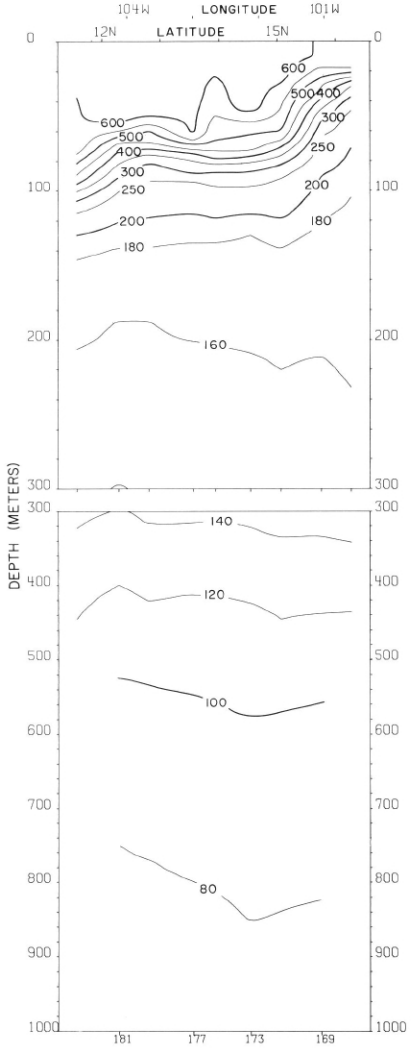

FIGURE 60-δ-v4.—Vertical distribution of thermosteric anomaly, δ_T, (cl./t.) along a section from Acapulco to 12° N., 104°45′ W., January 13-15, 1968.

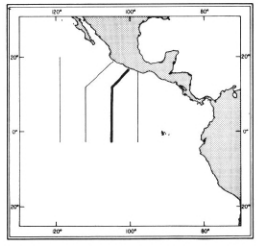

60-δ-v4.

60-δ-v5.

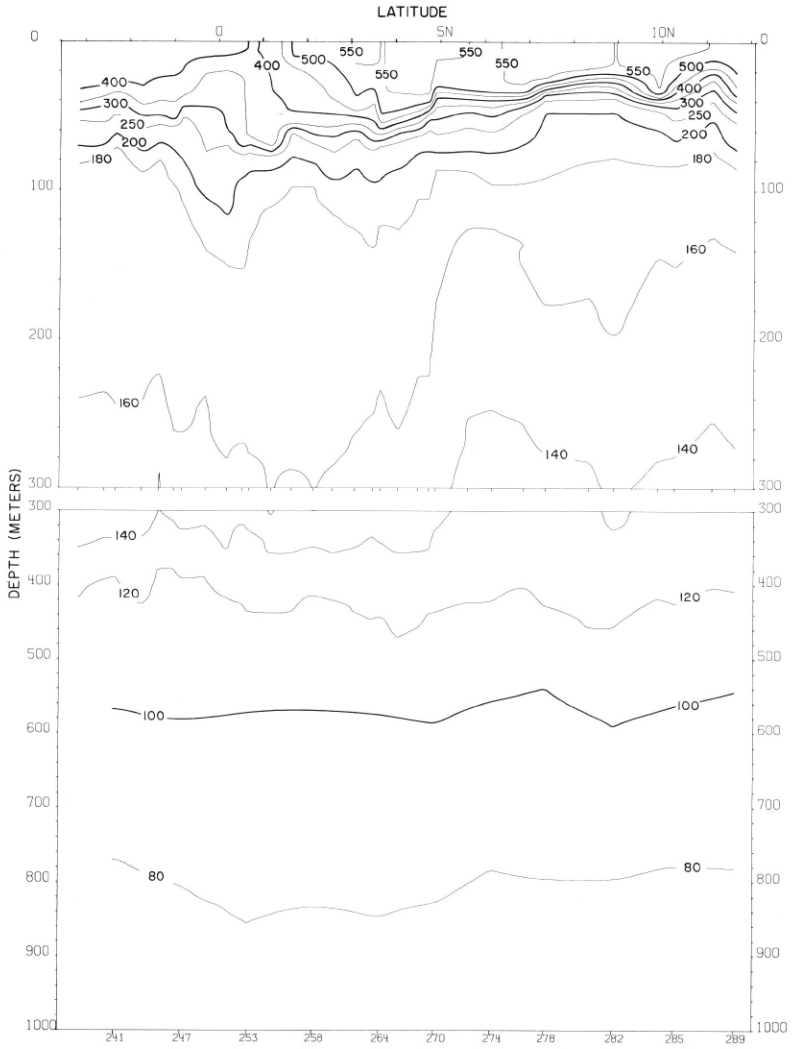

FIGURE 60-δ-v6.—Vertical distribution of thermosteric anomaly, δ_T, (cl./t.) along 97°45′ W., January 22-28, 1968.

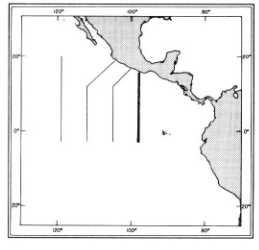

60-δ-v6.

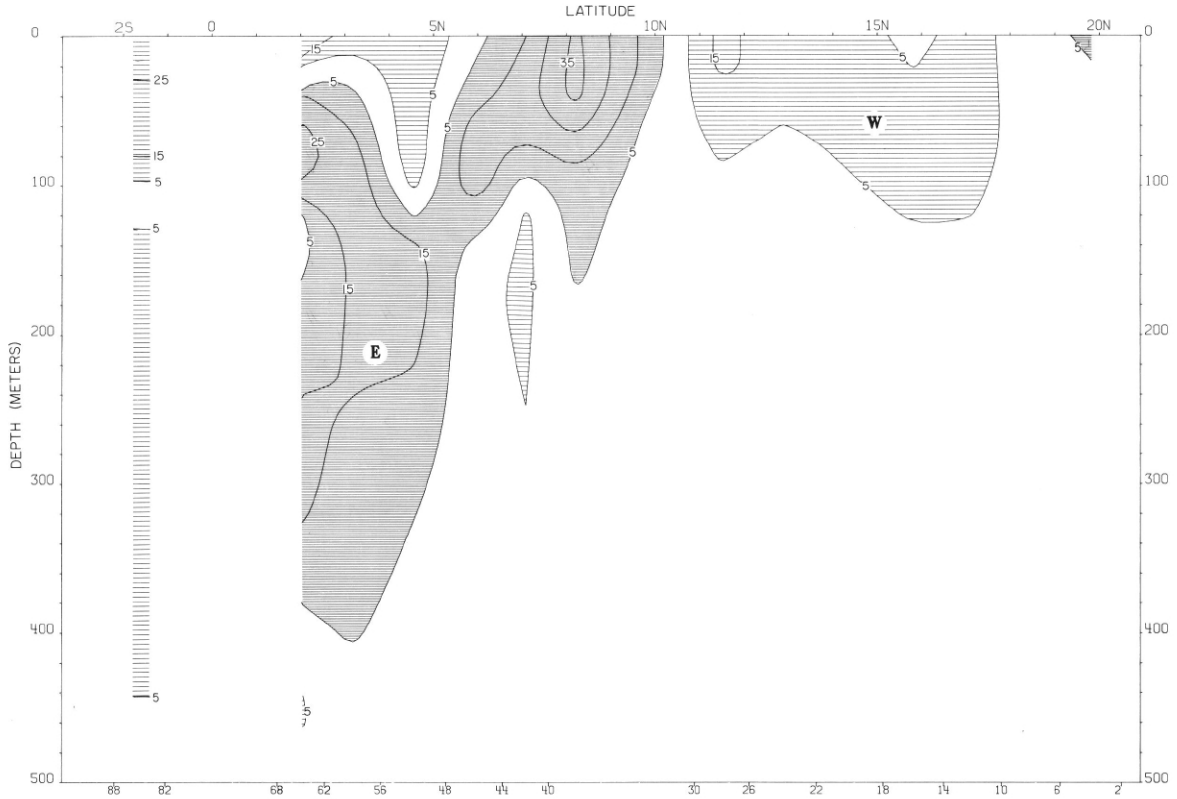

FIGURE 60-G-v1.—Vertical distribution of the zonal component of geostrophic velocity (cm./sec.), relative to 500 db., along 118°45′ W., December 21-31, 1967. Dark shading indicates eastward flow with a velocity greater than 5 cm./sec.; light shading indicates westward flow with a velocity greater than 5 cm./sec.

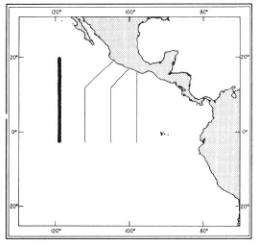

60-G-v1.

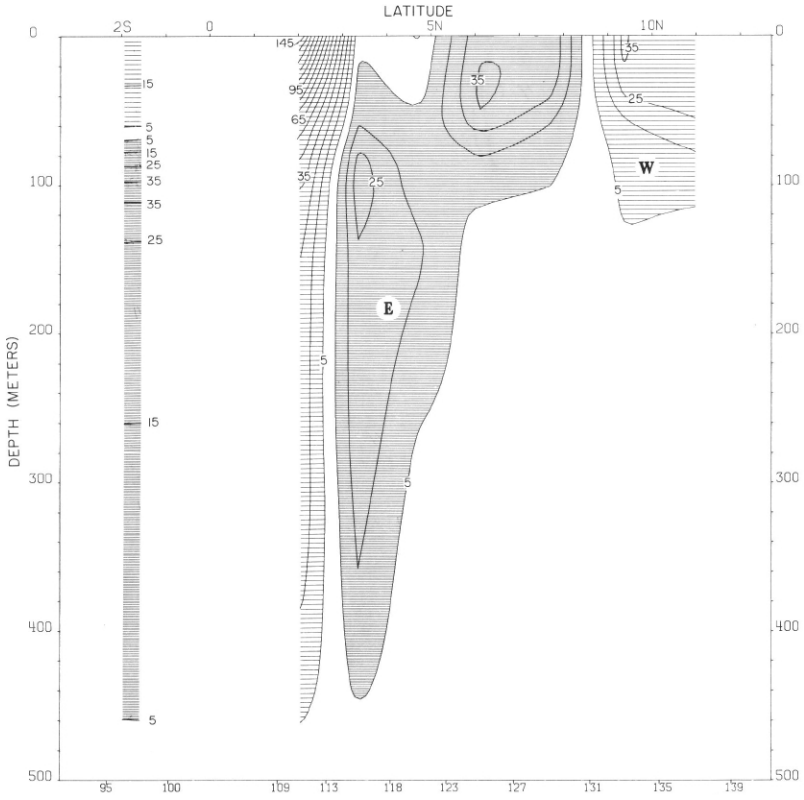

FIGURE 60-G-v2.—Vertical distribution of the zonal component of geostrophic velocity (cm./sec.), relative to 500 db., along 111°45′ W., January 2-6, 1968. Dark shading indicates eastward flow with a velocity greater than 5 cm./sec.; light shading indicates westward flow with a velocity greater than 5 cm./sec.

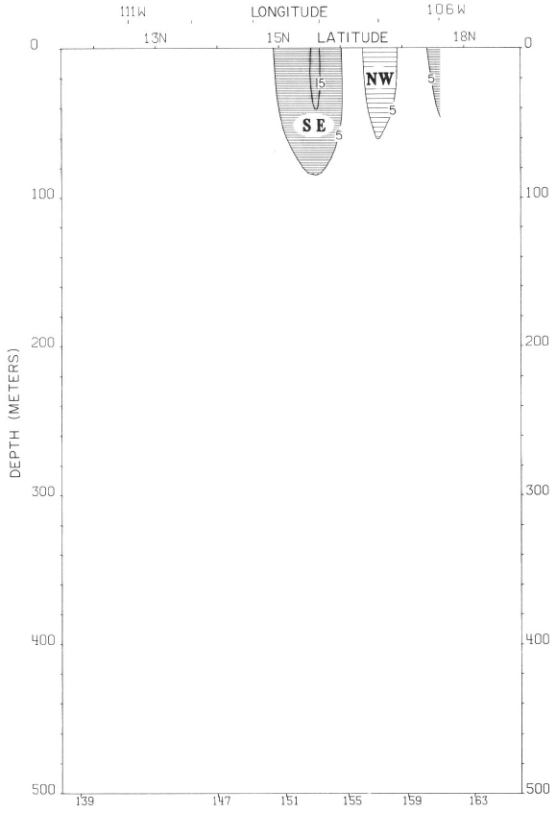

FIGURE 60-G-v3.—Vertical distribution of the component of geostrophic velocity (cm./sec.), relative to 500 db., normal to a section from 12° N., 111°45′ W. to Manzanillo, January 6-9, 1968. Dark shading indicates flow toward the southeast with a velocity greater than 5 cm./sec.; light shading indicates flow toward the northwest with a velocity greater than 5 cm./sec.

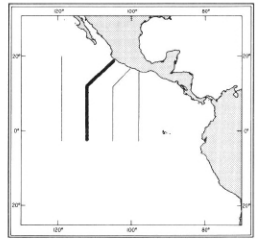

60-G-v2.

60-G-v3.

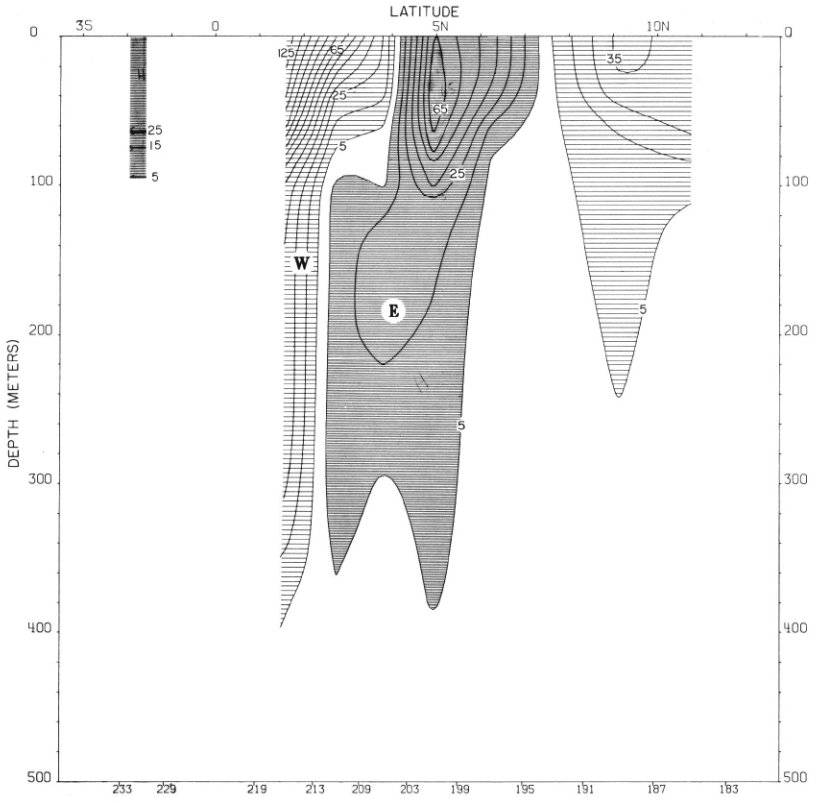

FIGURE 60-G-v5.—Vertical distribution of the zonal component of geostrophic velocity (cm./sec.), relative to 500 db., along 104°45′ W., January 15-21, 1968. Dark shading indicates eastward flow with a velocity greater than 5 cm./sec.; light shading indicates westward flow with a velocity greater than 5 cm./sec.

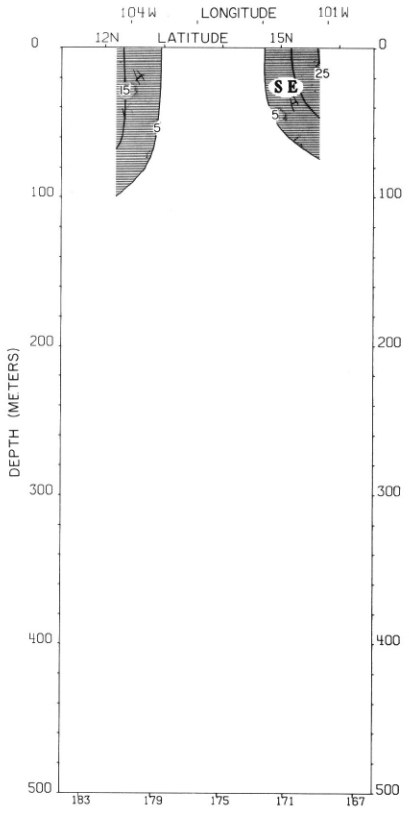

FIGURE 60-G-v4.—Vertical distribution of the component of geostrophic velocity (cm./sec.), relative to 500 db., normal to a section from Acapulco to 12° N., 104°45′ W., January 14-15, 1968. Dark shading indicates flow toward the southeast with a velocity greater than 5 cm./sec.

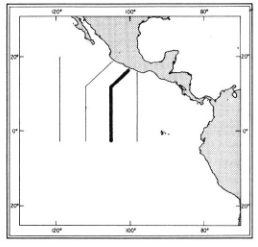

60-G-v4.

60-G-v5.

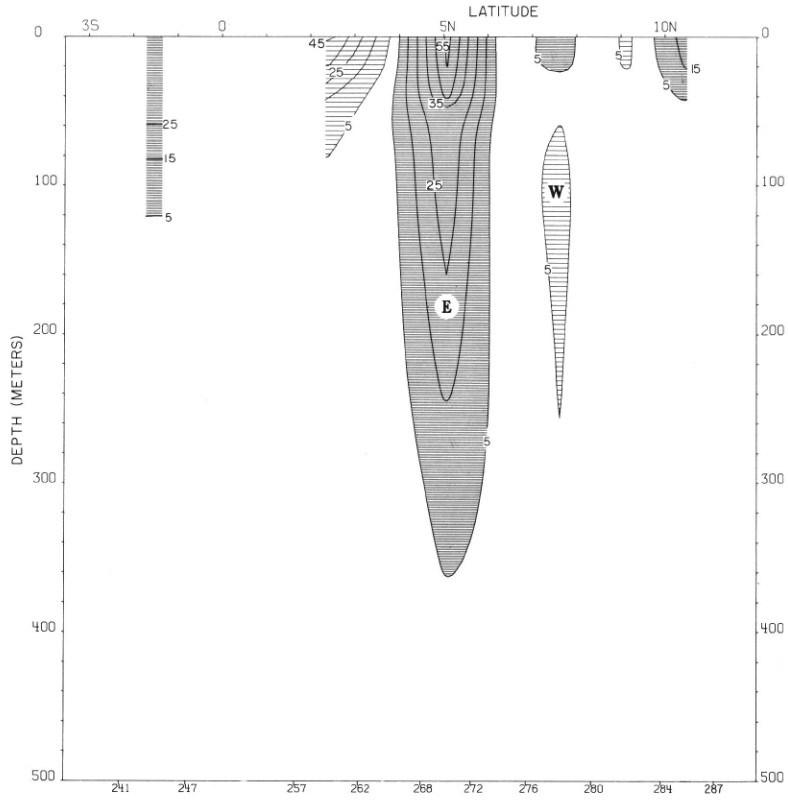

FIGURE 60-G-v6.—Vertical distribution of the zonal component of geostrophic velocity (cm./sec.), relative to 500 db., along 97°45′ W., January 22-28, 1968. Dark shading indicates eastward flow with a velocity greater than 5 cm./sec.; light shading indicates westward flow with a velocity greater than 5 cm./sec.

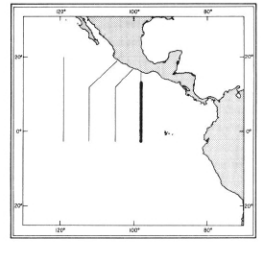

60-G-v6.

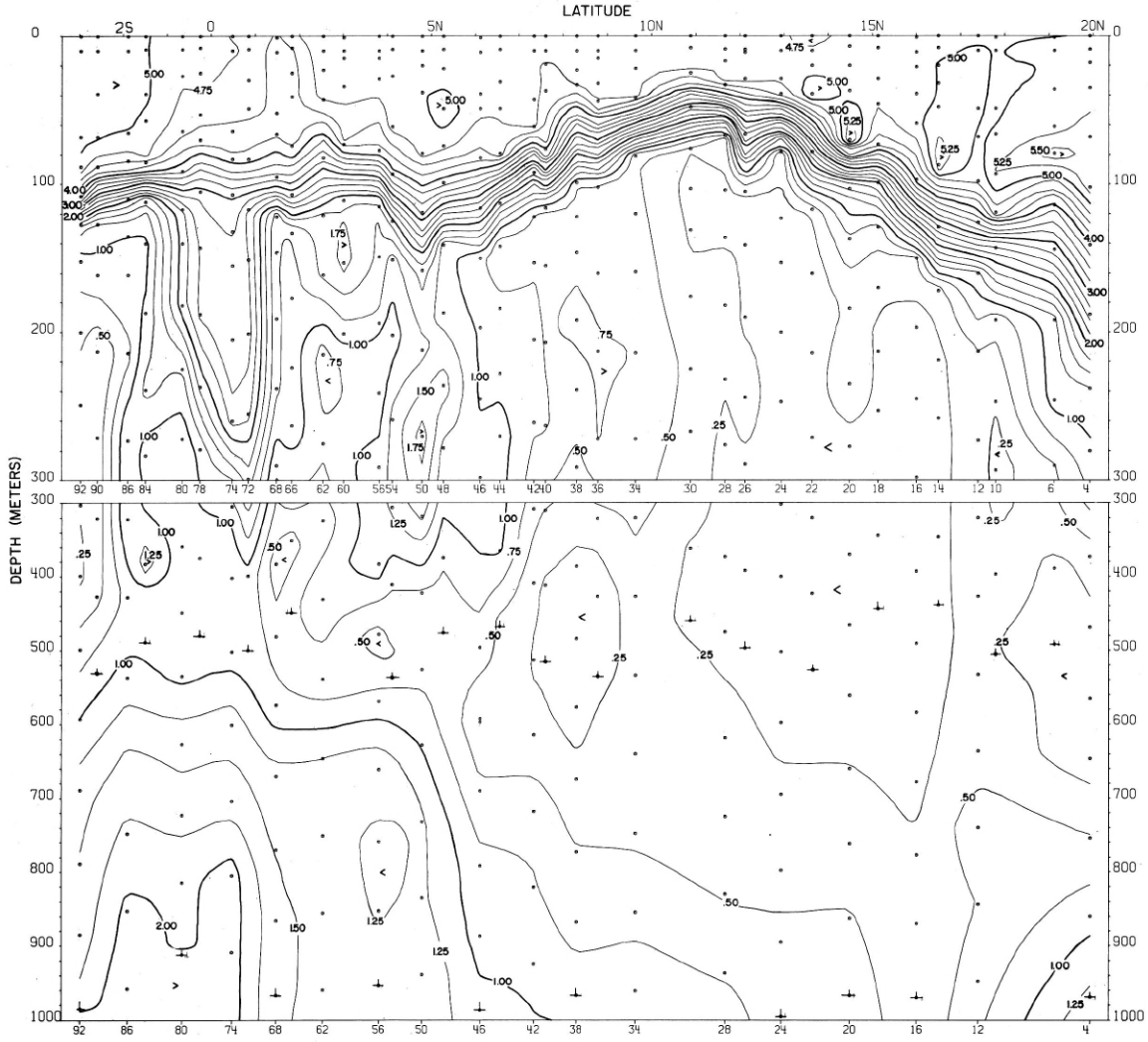

FIGURE 60-O_2-v1.—Vertical distribution of oxygen (ml./l.) along 118°45′ W., December 21-31, 1967.

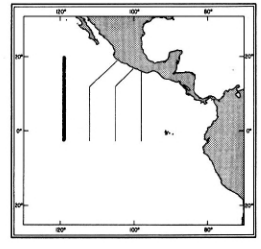

60-O_2-v1.

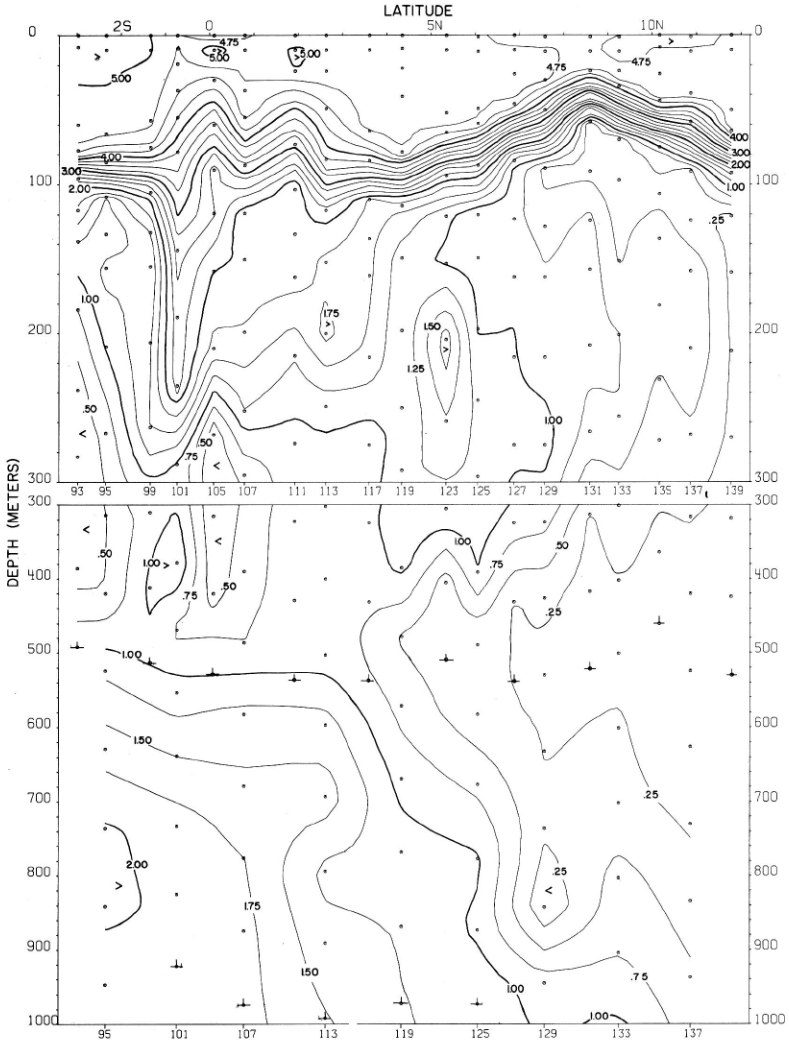

FIGURE 60-O_2-v2.—Vertical distribution of oxygen (ml./l.) along 111°45′ W., January 2-6, 1968.

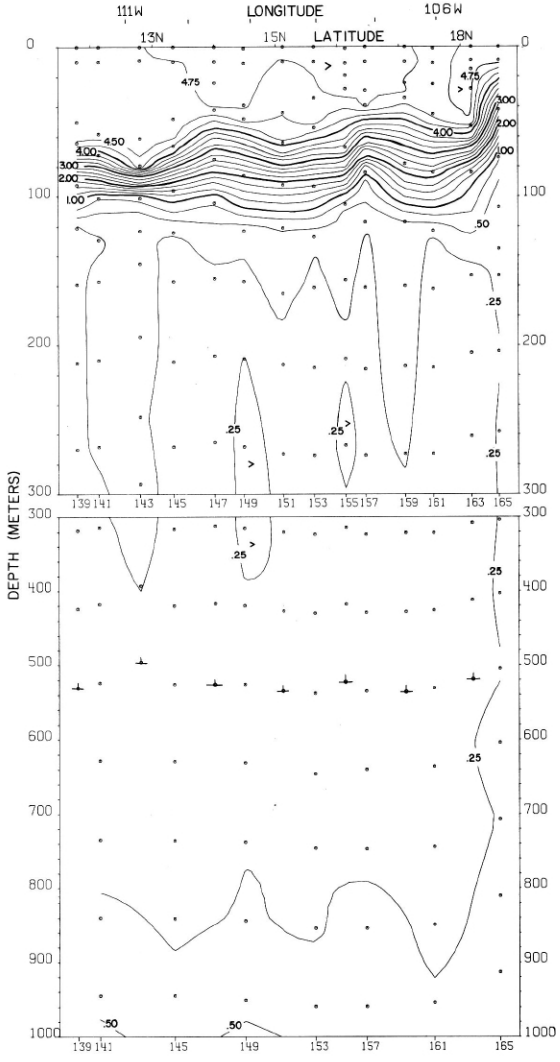

FIGURE 60-O_2-v3.—Vertical distribution of oxygen (ml./L) along a section from 12° N., 111°45′ W. to Manzanillo, January 6-9, 1968.

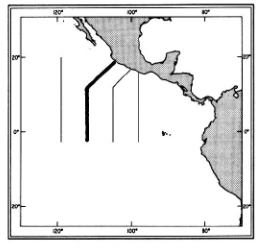

60-O_2-v2.

60-O_2-v3.

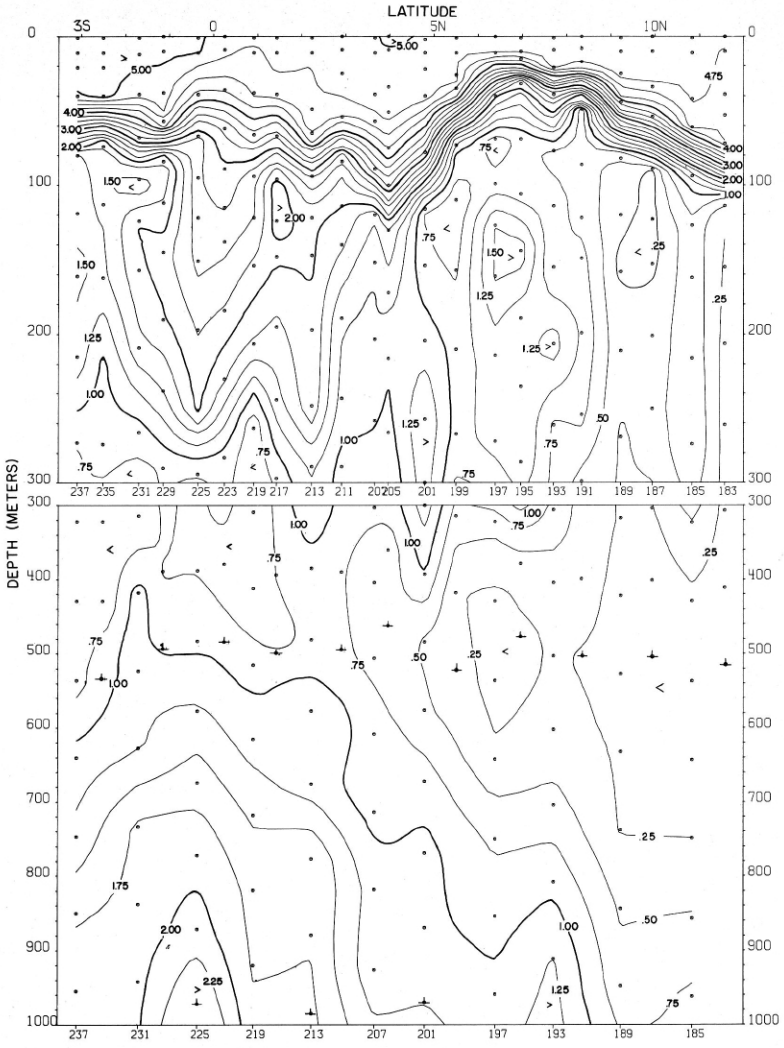

FIGURE 60-O₂-v5.—Vertical distribution of oxygen (ml./l.) along 104°45′ W., January 15-21, 1968.

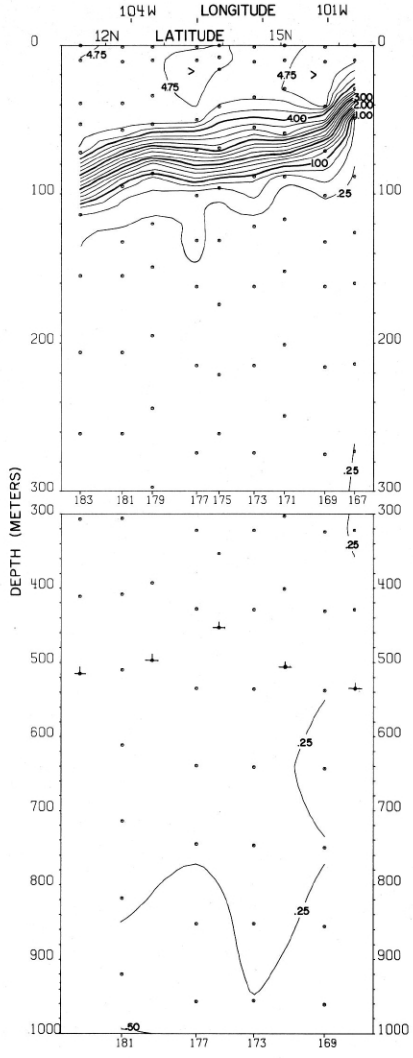

FIGURE 60-O₂-v4.—Vertical distribution of oxygen (ml./l.) along a section from Acapulco to 12° N., 104°45′ W., January 13-15, 1968.

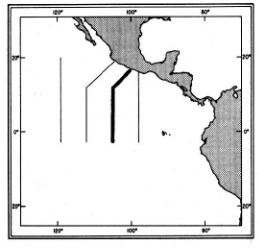

60-O₂-v4.

60-O₂-v5.

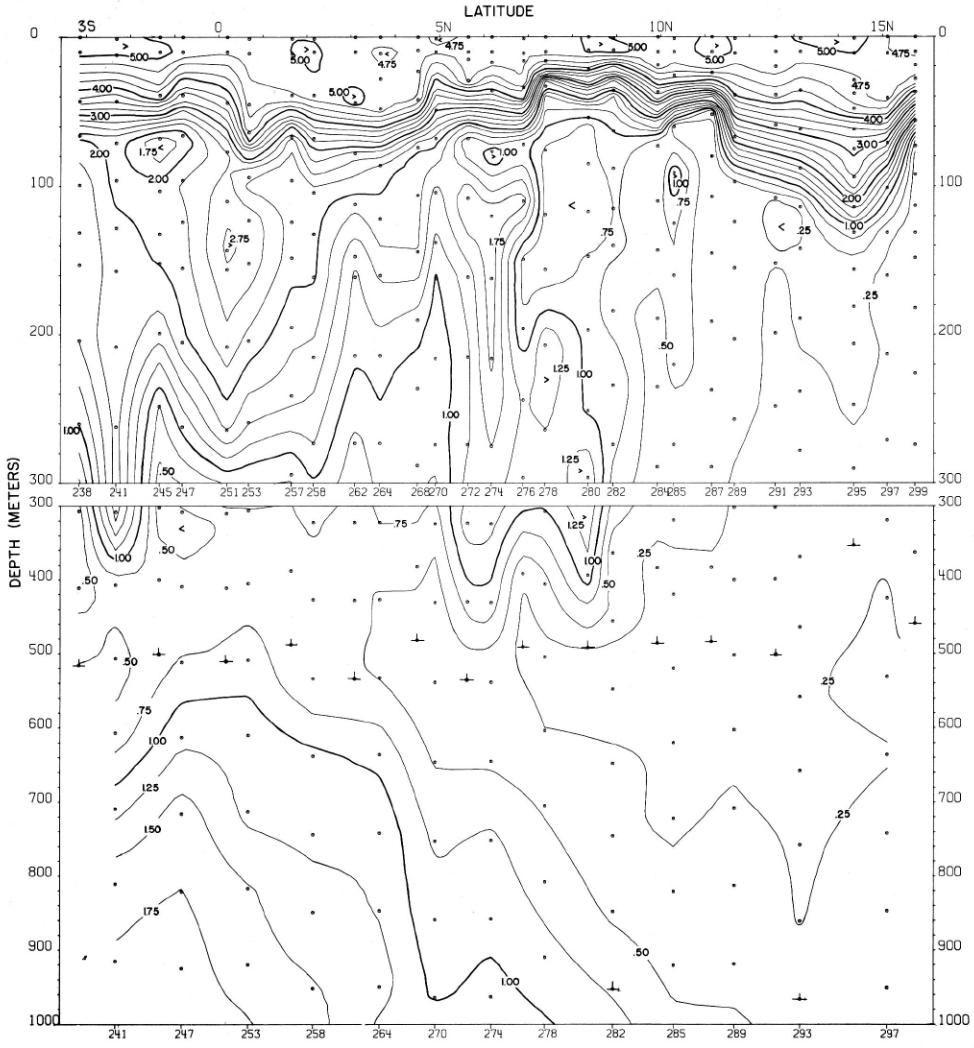

FIGURE 60-O2-v6.—Vertical distribution of oxygen (ml./l.) along 97°45′ W., January 22-29, 1968.

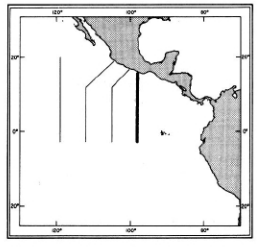

60-O2-v6.